The role of Huntingtin in innate immune cells

Grace Caitríona O'Regan
University College London

A thesis submitted in partial fulfilment of the requirements for the degree of Doctor of Philosophy from University College London
2019

Declaration

I, Grace O'Regan, confirm that the work presented in this thesis is my own original research. Where information has been derived from other sources, this has been clearly indicated in the text.

Acknowledgements

First and foremost I would like to thank my primary supervisor, Dr Ralph Andre, for his invaluable guidance and support throughout my PhD. Ralph, with your help I have become a better scientist and writer. I would never have made it this far without you, and I'm incredibly grateful to have had you as a supervisor, thank you.

To the rest of my supervisory team, I would also like to say thank you; Sarah, for always making me believe more was possible and inspiring me, and Jenny, for being the voice of reason and making sure I didn't try to do every possible experiment at once.

I would also like to thank the rest of the Tabrizi lab and extended members of the Huntington's disease centre at UCL, past and present. Thank you for your friendships and brilliant scientific minds; particularly in my final year, you all made PhD life much better.

I would also like to thank James Behagg. Truly I think the HDC would fall apart without you! Thank you for making sure all the important behind the scenes things were happening for my PhD, and for always being kind and endlessly helpful, not to mention donating blood for some of my experiments.

Outside of the HDC, I would particularly like to thank Matt and Pras. Pras for being the most chilled out PhD student I have ever met, and putting up with endless bothering from me, it's been fun. Matt, for being a kind and supportive friend, as well as the master of organised fun and bringing people together.

I would also like to thank Sue, trying to keep a whole department of scientific equipment in working order is no small task and we're so lucky to have had you looking after us.

To everyone who donated blood for my research, Andrew, Akshay, Felipe, Paul, James, Lauren, Pras, Laura, Marta and more, thank you so much. Giving blood is no one's favourite thing to do, and I really appreciate everyone who supported my work in this way.

To the Edinburgh crew, thank you for always being a wonderful escape from my PhD, and lifelong friends, you guys are the best.

To Eirik, my wonderful, supportive partner- I am eternally grateful to have had you by my side during this process. You made every day better, from the lowest lows to the highest highs, they were always improved with you around.

Mum and Dad, thank you for everything, for inspiring me and supporting me, before I knew that any of this could be possible.

Abstract

Huntington's disease (HD) is a devastating neurodegenerative disease. It is caused by the presence of an expanded trinucleotide CAG repeat in the *HTT* gene, resulting in expression of expanded polyglutamine-containing mutant HTT throughout the body. HD patients display a dysfunctional peripheral immune system up to sixteen years before disease onset. This is shown also in HD animal models, where immune system dysfunction is found both in the periphery and central nervous system (CNS).

The overall aim of this work is to determine the mechanism(s) by which mutant and wild type HTT regulate myeloid cell function and contribute to innate immune system dysregulation as a potential modifier of HD progression. Specifically, this thesis had two aims: firstly, to investigate the CNS component of the innate immune system in a human HD microglia-like cell model; and secondly, to assess the role of wild type HTT in peripheral innate immune cells.

To address the first aim, a unique cohort of human induced pluripotent stem cell lines from related individuals with varying HTT polyglutamine expansion lengths (22Q, 58Q, 69Q, 75Q) and an isogenic series of embryonic stem cell lines (30Q, 45Q and 81Q) were differentiated to microglia-like cells. Our results suggest that these HD microglia-like cells display subtle altered phenotypes compared to control microglia in a HTT polyglutamine length-dependent manner. To investigate the impact of these altered phenotypes on HD pathology, a series of conditioned media experiments were conducted to assess the effects of HD or control microglia-like cell-conditioned media from basal and stressed conditions on HD and control medium spiny neurons, and vice versa. Finally, to assess the performance of HD and control microglia-like cells in an environment closer to what would be found in the CNS, microglia-like cells were treated with CSF from HD and control individuals and their health and function assessed. This work represents the first assessment of human HD microglia *in vitro* and shows that human HD microglia-like cells are dysfunctional like their rodent counterparts and peripheral myeloid cells from HD patients.

For the second aim, glucan-encapsulated siRNA particles were used to lower HTT levels in non-HD primary human macrophages and a series of functional assessments were performed, comparing HTT-lowered and control cells. These

findings suggest a novel role for wild type HTT in the myeloid cells of the peripheral immune system, specifically in cytokine expression, phagocytosis and their response to cellular stress. Together, these results further elucidate the role of huntingtin in innate immune cells in health and disease.

Impact statement

Huntington's disease (HD) is a fatal, inherited neurodegenerative disease and the most common monogenic neurological condition in the developed world (Evans et al., 2013; Morrison et al., 2011). Individuals typically become symptomatic in the prime of life, with the average age at onset being just 40 years old (Myers, 2004).

This work focused on assessing the role of disease-associated, mutant (m)HTT and normal, wild-type (wt)HTT, in the innate immune system as a modifier of HD. To achieve this, a pluripotent stem cell (PSC) derived model of the CNS component of the innate immune system, microglia, was developed and characterised.

The production of a PSC-derived microglia model is particularly beneficial as it allows the study of a cell type that was previously very inaccessible for scientists. Previously the majority of research in human microglia was done using cells isolated post-mortem, with extremely limited availability. In this way, therapeutics may be tested in this human cell model as well as in animal models, as is currently the standard. The hope is that this will improve the translation of therapeutics across from animal models into humans, as the minutia of treating human cells can be investigated in this model prior to clinical testing. The use of PSCs has the further benefit of reducing the requirement for animals used in research, although animal products such as antibodies are still used. Additionally, this research has highlighted the benefits of using isogenic series of PSC lines to reduce the noise in data caused by genetic variability, allowing greater confidence in drawing conclusions from data.

This work shows that HD microglia-like cells are hyper reactive in their cytokine production as previously seen in animal models of HD, but it has also uncovered some not previously tested for before, specifically that human HD microglia-like

cells produce elevated levels of reactive oxygen species. This can now be assessed in animal models and optimised as a read out in the context of disease interventions. Furthermore, beyond the development and characterisation of a human HD microglial model, a conditioned-media co-culture paradigm was also established. This co-culture set-up can be used to identify interactions between various cell types relevant to HD, in order to identify druggable targets.

Finally, the investigation into the effects of wtHTT on the innate immune system were conducted on primary human macrophages and confirmed a role for wtHTT in pro-inflammatory cytokine expression. Follow up work should identify the cellular pathways through which wtHTT exerts these effects, which can then be targeted for the treatment of immune disorders such as rheumatoid arthritis.

Table of Contents

List of Figures

List of Tables

Abbreviations

2D two dimensional
2-ME 2-mercaptoethanol
3D three dimensional
3-NP 3-Nitropropionic acid
6-OHDA 6-hydroxydopamine
8-OHDG 8-Oxo-2'-deoxyguanosine
53BP1 TP53-binding protein 1
AAO age at onset
ACTB beta actin gene
AD Alzheimer's Disease
ALR AIM2-like receptor
AMPA α-amino-3-hydroxy-5-methyl-4-isoxazolepropionic acid
AIF1 Allograft inflammatory factor 1 gene (also known as IBA1)
ANOVA analysis of variance
AP1 Activator protein 1
ASO antisense oligonucleotide
ATP adenosine 5'-triphosphate
BAC bacterial artificial chromosome
BCA bicinchoninic acid
BDNF brain-derived neurotrophic factor
bFGF basic fibroblast growth factor
BMP-4 bone morphogenic protein 4
bp base pair
BSA bovine serum albumin
BV2 immortalised murine microglial cell line
C Celsius
C1QA complement c1q A chain
C5a Complement component 5a
CAA glutamine
CAG glutamine
Cas9 CRISPR associated protein 9
CB2 cannabinoid receptor type 2
CBP cAMP response element-binding protein-binding protein
CD cluster of differentiation
cDNA complementary deoxyribonucleic acid
CLR C-type lectin receptor
CNS central nervous system
COS7 fibroblast-like cell line derived from monkey kidney tissue
CRISPR a family of DNA sequences found within the genomes of prokaryotic organisms such as bacteria and archaea
CSE control standard endotoxin
CSF cerebrospinal fluid
CSF1 colony stimulating factor 1, also known as M-CSF
CSF2 colony stimulating factor 2, also known as GM-CSF
Ct threshold cycle
CTIP2 COUP-TF-interacting protein 2
CXCR C-X-C chemokine receptor

DAN 2,3 diaminonaphthalene
DAP12 DNAX activating protein of 12 kDa
DARP32 dopamine- and cAMP-regulated neuronal phosphoprotein
DCFDA 2′,7′-Dichlorodihydrofluorescein diacetate
ddCt delta-delta-Ct
ddH2O deionised distilled water
DHC dynein heavy chain gene
DMEM/F12 Dulbecco's Modified Eagle Medium/Nutrient Mixture F-12
DMSO Dimethyl sulfoxide
DNA deoxyribonucleic acid
DNase deoxyribonuclease
dNTP deoxyribonucleotide triphosphate
Dorsomorphin selective small molecule inhibitor of BMP signalling
DPBS Dulbecco's Phosphate-Buffered Saline
DSB double strand break
DSPQ downstream of the polyQ site
DTT dithiothreitol
E embryonic day
E8+ supplemented essential 8 media
EBs embryoid bodies
ECM extracellular matrix
EDTA ethylenediaminetetraacetic acid
e.g. for example
EGFP Enhanced green fluorescent protein
ELISA enzyme-linked immunosorbent assay
eNOS endothelial nitric oxide synthase
EP Endo-Porter
ER endoplasmic reticulum
ERK extracellular signal-regulated kinase
ESCs embryonic stem cells
ESET histone methyltransferase
Et al et alia
EU European Union
FACS fluorescence-activated cell sorting
FBS foetal bovine serum
FITC fluorescein isothiocyanate
Fix/Perm Fixation and Permeabilisation buffers
FLT3 ligand ligand for a receptor tyrosine kinase called FLT3
FOXP3 forkhead box P3
FSC forward scatter
g gram
GABA γ-aminobutyric acid
GABAergic pertaining to or affecting the neurotransmitter GABA
GAPDH Glyceraldehyde 3-phosphate dehydrogenase
GAS6 growth arrest specific 6
GC Guanine Cytosine
GeRP beta-1,3-D-glucan-encapsulated siRNA particle
GM-CSF granulocyte-macrophage colony-stimulating factor
GPR34 G protein–coupled receptor 34
GTPase large family of hydrolase enzymes that bind to the nucleotide guanosine triphosphate and hydrolyse it to guanosine diphosphate

GWAS Genome wide association study
h hour
H2AX Variant histone H2A
H3 Histone H3
H4 Histone H4
H2DCFDA chemically reduced form of 2',7'-dichlorodihydrofluorescein diacetate
HAP1 huntingtin-associated protein 1
HBSS Hank's Balanced Salt Solution
HCI high content imaging
HD Huntington's disease
HEAT huntingtin, elongation factor 3, the PR65/A subunit of protein phosphatase 2A and the lipid kinase Tor
HeLa immortal cell line isolated from cervical cancer
HEPES 4-(2-hydroxyethyl)-1-piperazineethanesulfonic acid
HIP huntingtin interacting protein
HIPPI synonym IFT57 intraflagellar transport 57
HSR heat shock response
HTT human huntingtin gene
HTT human huntingtin protein
Hdh murine huntingtin gene
IBA1 Ionized calcium binding adaptor molecule 1 gene (also known as AIF1)
i.e. id est
IF immunofluorescence
IFNγ interferon gamma
IFN$\alpha\beta$ interferon alpha beta
IκB inhibitor of kappa B
IKK IκB kinase
IL interleukin
iNOS inducible nitric oxide synthase
iPSC induced pluripotent stem cell
IRAK interleukin-1 receptor-associated kinase
IRF Interferon regulatory factor
IRK induced receptor-like kinase
IsoHD isogenic series of ESC lines created by Ooi et al., 2019.
IT15 interesting transcript 15
JAK janus kinase
kb kilo base pair
kDa kilodalton
KIF5A kinesin family member 5A gene
KMO kynurenine 3-monooxygenase
L litre
LDH lactate dehydrogenase
LDN selective BMP signaling inhibitor
LPS lipopolysaccharide
M molar
M1 classically activated macrophages/monocytes
M2 alternatively activated macrophages/monocytes
mM millimolar
mHTT mutant HTT
MACS magnetic-activated cell sorting
MAL MyD88 adapter-like

MAPK mitogen-activated protein kinase
M-CSF macrophage colony-stimulating factor also known as CSF1
MERTK MER proto-oncogene, tyrosine kinase
mHTT mutant HTT
MHC major histocompatibility complex
min minutes
miRNA micro-ribonucleic acid
ml millilitre
MMP matrix metalloproteinase
MPTP 1-methyl-4-phenyl-1,2,3,6-tetrahydropyridine
mRNA messenger ribonucleic acid
MSD Meso Scale Discovery
MSN medium spiny neurons
mTOR mechanistic target of rapamycin
MYB gene for protein named Transcriptional activator Myb
MYC v-myc avian myelocytomatosis viral oncogene homolog
MyD88 myeloid differentiation primary response gene 88
n number
N number
NFκB nuclear factor kappa-light-chain-enhancer of activated B cells
NLR NOD-like receptor
NMDA N-methyl-D-aspartate
Nm wavelength
nNOS neuronal nitric oxide synthase
NO nitric oxide
NOS nitric oxide synthase
NRSF Neuron-Restrictive Silencer Factor also known as REST
NSAIDs Non-steroidal anti-inflammatory drugs
NuMA Nuclear mitotic apparatus protein 1
OD optical density
P2RY12 purinergic receptor P2Y12
P38 MAPK P38 mitogen-activated protein kinases
P53 Tumor protein p53
P62 ubiquitin-binding protein p62
PAMP pathogen-associated molecular pattern
PBMC peripheral blood mononuclear cell
PBS phosphate-buffered saline
PCM1 Pericentriolar material 1 protein
PCR polymerase chain reaction
PD Parkinson’s Disease
PE phycoerythrin
Pen/Strep cocktail of penicillin and streptomycin
PFA paraformaldehyde
PolyQ polyglutamine
PRR pattern recognition receptor
PROS1 protein S gene
PSCs pluripotent stem cells
PSD post synaptic density
PU1 transcription factor encoded by SPI1 gene
PuroR puromycin resistant
Q glutamine

QC quality control
qPCR quantitative polymerase chain reaction
RAB Family of Ras-like small GTPases
REL v-rel avian reticuloendotheliosis viral oncogene homolog
REST RE1-silencing transcription factor also known as NRSF
RI ROCK inhibitor (Y-27632)
RIPA radioimmunoprecipitation assay
RISC RNA-induced silencing complex
RLR RIG-I like receptor
RNA ribonucleic acid
RNAi RNA interference
RNase ribonuclease
RNA-Seq RNA sequencing
RNS reactive nitrogen species
ROCK Rho-associated, coiled-coil containing protein kinase
ROS reactive oxygen species
RPMI Roswell Park Memorial Institute
rRNA ribosomal ribonucleic acid
RT-qPCR real time qPCR
RUES2 Rockefeller University Embryonic Stem cell line 2
RUNX1 gene name for RUNX Family Transcription Factor 1
s seconds
s421 serine position 421
SB431542 A specific inhibitor of TGF-β Receptor Kinase
SCF stem cell factor
SCR scrambled
SD standard deviation
SDS sodium dodecyl sulfate
SEM standard error of the mean
siRNA small interfering ribonucleic acid
SIN3A SIN3 Transcription Regulator Family Member A
SK-N-SH neuroblastoma cell line
SMAD a family of structurally similar proteins that are the main signal transducers for receptors of the transforming growth factor beta (TGF-B) superfamily
SNP single nucleotide polymorphism
SOD superoxide dismutase
SPI1 gene name for Transcription factor PU.1
SSC side scatter
ssRNA single-stranded ribonucleic acid
STAT signal transducers and activators of transcription
TALENs Transcription activator-like effector nucleases
TAE tris-acetate-EDTA
TBHP tert-Butyl hydroperoxide
TBP TATA-Box Binding Protein
TE tris-EDTA
TFC total functional capacity
TGF transforming growth factor
Th T helper cell
TLR toll-like receptor
TMEM119 Transmembrane Protein 119 gene

TNF tumour necrosis factor
TPO thrombopoietin
TRAF TNF receptor-associated factor
TRAM TRIF-related adaptor molecule
TREM2 triggering receptors expressed on myeloid cells 2 gene
TR-FRET time-resolved Förster energy transfer
TRIF TIR-domain-containing adapter-inducing interferon-β
TRK Tropomyosin receptor kinase
Tyr Tyrosine
UCL University College London
UHDRS unified Huntington's disease rating scale
UPS ubiquitin-proteasome system
US United States
USPQ upstream of the polyQ site
UTR untranslated region
VEGF Vascular endothelial growth factor
vs. versus
WT wild type
wtHTT wild type HTT
xg gravitational acceleration
YAC yeast artificial chromosome
ZFP Zinc Finger Protein

1. Chapter 1: Introduction

1.1. Huntington's disease

1.1.1. Clinical features

Huntington's disease (HD) is a fatal, inherited neurodegenerative disease and the most common monogenic neurological condition in the developed world (Evans et al., 2013; Morrison et al., 2011). The prevalence of HD varies up to ten-fold between different ethnicities; Caucasian populations generally show the highest prevalence, with approximately 9.71 cases per 100,000 people, whereas the prevalence in some Asian countries is as low as 0.42 cases per 100,000 (Rawlins et al., 2016). Individuals typically become symptomatic in the prime of life, with the average age at onset being just 40 years old (Myers, 2004). However, approximately 5-10% of cases have onset before 20 years of age and are classified as juvenile HD (Gonzalez-Alegre and Afifi, 2006; O. W. Quarrell et al., 2013; Ross et al., 2014).

HD is characterised by a triad of symptoms, with motor, cognitive and psychiatric function affected. The distinctive motor phenotype of uncontrolled "dancing" movements, or chorea, marks the definitive diagnostic onset of the disease in adult HD cases and patients have increasing difficulty controlling voluntary movements as the disease progresses. Cognitive deficits may include attentional deficits and problems with emotional recognition, and neuropsychiatric issues may comprise apathy, depression and blunted affect display. The clinical presentation of HD is complex, with considerable variability between patients, but cognitive and motor phenotypes do appear to progress together (Novak and Tabrizi, 2010). It is important to note that while the first signs of motor symptoms define the clinical onset of the disease, cognitive impairment and neuropsychiatric deterioration can occur much earlier, and have a significant impact on quality of life before clinical diagnosis (Bates et al., 2015; Rosas et al., 2008; Ross et al., 2014). This pre-manifest phase can last up to fifteen years; however, once motor symptoms begin, the median survival is eighteen years from diagnosis (Ross et al., 2014).

Juvenile HD has some overlap with the adult form in terms of clinical pathology, but there is a predominance of bradykinesia and dystonia rather than chorea and

a more frequent occurrence of myoclonus and epilepsy. At post-mortem, juvenile HD brains show much more widespread degeneration than their adult counterparts (O. W. Quarrell et al., 2013).

1.1.2. Genetics

HD is unique among the most common neurodegenerative diseases in that its underlying cause is definitive and well-known. Thanks to the efforts of the Huntington Disease Collaborative Research Group, the HD gene (*HTT*, encoding the huntingtin protein) was located on human chromosome 4 and the nature of the disease-causing mutation identified as an expanded CAG repeat at the N-terminus of the gene (The Huntington Disease Collaborative Research Group et al., 1993). The length of the expansion, encoded by CAG trinucleotide repeats, is variable within the population, with unaffected individuals carrying repeats of 6-35 units. Individuals carrying expansions greater than forty units in length invariably develop HD and in general longer repeat lengths lead to earlier onset of disease. Adult onset patients typically carry repeats of between 40-50 CAG units and juvenile HD patients typically carry mutations above 55 CAG units, but there are rare cases of juvenile onset HD with smaller mutation sizes (O. W. J. Quarrell et al., 2013). Interestingly, for each *HTT* CAG size there is a range of ages when patients may begin to show symptoms. This may be due to the influence of other modifying genetic factors, as well as environmental effects (Langbehn et al., 2010). Repeats in the intermediate range of 36-39 CAG units show reduced penetrance, with some individuals never being clinically diagnosed, while others develop HD (Bates et al., 2015). This has recently been partially explained by studies which found that the length of the uninterrupted repeat in these cases predicted onset, with longer pure CAG repeats causing earlier onset and those interrupted with CAA codons appearing protective (Lee et al., 2019; Wright et al., 2019).

1.1.3. Central nervous system (CNS) pathology

HD is characterised by progressive neurodegeneration, with an overall decrease in brain volume of 19% at death (Halliday et al., 1998). Specific regions are more heavily affected, however, most notably the GABAergic medium spiny neurons of the striatum where up to 95% are lost by end-stage disease, resulting in a 50% reduction of total striatal volume (Vonsattel, J.P., DiFiglia, 1998). This striatal loss

correlates with signs of motor impairment and is a key pathological correlate of disease progression (Guo et al., 2012). However, the reduction in brain volume in HD patients at post-mortem is not accounted for by striatal loss alone, and the cerebral cortex and hypothalamus are also known to be strongly affected (Halliday et al., 1998; Rosas et al., 2005). Pathology is not just confined to neuronal degeneration, however, as glial cells also appear to be affected (Shin et al., 2005). There is also significant white matter loss in HD patients, with deficiencies occurring at the very earliest stages of disease, particularly in the cortico-striatal tract (Novak et al., 2014; Phillips et al., 2014; Yi Teo et al., 2016). As well as this, there is pre-symptomatic and progressive accumulation of activated microglia, in response to pathological stimulation, and accompanying neuroinflammation in brain areas most affected by the disease (McColgan et al., 2017; Pavese et al., 2006; Sapp et al., 2001; Tai et al., 2007), as is observed in many other neurodegenerative diseases.

1.1.4. Pathology beyond the CNS

The neuropathology of HD is an obvious core part of the disease process and clearly correlates with the characteristic symptoms seen in patients. However, evidence points to this CNS pathology being accompanied by diverse peripheral phenotypes and pathologies, which is perhaps unsurprising given that HTT is expressed in all tissues of the body (Li et al., 1993; van der Burg et al., 2009).

Skeletal muscle wasting and weight loss are both prominent in HD patients and some animal models of HD (Goodman et al., 2008). The heart is also known to be affected, and heart failure is reported to be the second leading cause of death in HD (Lanska et al., 1988). Cardiac dysfunction is also found in mouse models of the disease (Mihm et al., 2007) and when mutant HTT (mHTT) is expressed only in the cardiomyocytes of wild-type mice, they develop heart failure (Pattison et al., 2008), suggesting that this peripheral phenotype occurs independently of events in the CNS. HTT is very highly expressed in the testis and while fertility is unaffected in patients with HD, there is clear pathology; and animal models of HD show considerable testicular atrophy (van der Burg et al., 2009; Van Raamsdonk et al., 2007). Some reports have also suggested that osteoporosis may be a part of the peripheral phenotype in HD, which increases in severity with increasing *HTT* CAG length However, it is unclear whether this is a secondary effect from

the immobility associated with the later stages of disease, a side-effect of the neuroleptic treatment, or a direct effect of the peripheral expression of mHTT (Bonelli et al., 2007; Goodman and Barker, 2011). These peripheral pathologies of HD are accompanied by dysfunction in the innate immune system which persists when its cells are isolated and tested *ex vivo*, suggesting cell autonomous dysfunction caused by the expression of mHTT alone (Björkqvist et al., 2008; Dalrymple et al., 2007; Kwan et al., 2012; Miller et al., 2016; Trager et al., 2014; Träger et al., 2015).

1.1.5. The HTT protein

The *HTT* gene is located at chromosome 4p16.3. It is a large multi-exon gene that can be alternately spliced to form a number of HTT protein isoforms (The Huntington Disease Collaborative Research Group et al., 1993).

1.1.5.1. Wild-type HTT

Wild-type HTT (wtHTT) is a large soluble protein of 348 kDa (Cattaneo et al., 2005). It is ubiquitously expressed in all cells and tissues, with highest expression levels in the CNS and the testes (Li et al., 1993). The CAG repeat, which is expanded in disease, is found in exon 1. It encodes an N-terminal polyglutamine sequence that forms a largely helical secondary structure, the exact conformation and stability of which is influenced by the surrounding protein regions. The function of this low-complexity region has not been fully elucidated but it is suggested that such regions aid in the modulation of protein-protein interactions (Xiao and Jeang, 1998), protein–nucleic acid interactions (Shen et al., 2004) and protein subcellular localisation (Salichs et al., 2009). HTT also contains a number of so-called HEAT (huntingtin, elongation factor 3, a subunit of protein phosphatase 2A and TOR1) repeats. These are tandem repeat sequences of roughly forty amino acids that are arranged in anti-parallel alpha-helices. The function of HEAT regions in proteins is unclear, but they may be important in chromosomal interactions and intracellular transport, as they have been shown to bind to chromatin and adhesins (Neuwald and Hirano, 2000; Shiga et al., 1996). Additionally, in the case of HTT, the transcription factor NF-κB is known to bind to these HEAT repeats (Neuwald and Hirano, 2000). The HEAT regions are interspersed in the gene with disordered regions (Figure 1.1), which are believed to be important for HTT's ability to interact with a large number of other

proteins (Harjes and Wanker, 2003; Tourette et al., 2014). The wtHTT protein appears to have a large interactome, suggestive of a role as a molecular scaffold, and indeed in *Drosophila* this sort of role for HTT as a scaffold for selective macroautophagy has been shown (Rui et al., 2015). Most recently cryo-electron microscopy was used to determine the structure of full-length human wtHTT in complex with HTT-associated protein 40 at an overall resolution of 4 Å. This confirmed that qtHTT is largely α-helical and consists of three major domains. The amino- and carboxy-terminal domains contain multiple HEAT repeats connected by a smaller bridge domain containing different types of tandem repeats (Guo et al., 2018).

Despite the abundant roles of wtHTT and protective effects of its expression, it is unlikely that the extensive pathology seen in HD is caused by a loss of normal HTT function alone. Particularly as the lethality of wtHTT knockout and conditional knockout models are rescued by expression of mHTT, suggesting the mutant form of the protein retains the essential functions of wtHTT in development (Leavitt et al., 2001). Additionally, patients homozygous for the HTT mutation are rare, but do not appear to have an earlier age of onset than heterozygotes, despite lacking wtHTT entirely, and while there is some evidence that their progression is more severe (Squitieri et al., 2003), larger scale studies have not found replicated this result (Cubo et al., 2019). This suggests it is more likely that disease pathogenesis arises primarily from a toxic gain of function by mHTT.

1.1.5.2. Mutant HTT

The CAG repeat of the HTT gene is found in exon 1, and encodes the N-terminal polyglutamine sequence. It is expanded in mHTT and this results in an unstable protein structure and changes to its conformation and structure that are key to its toxicity (Ross and Tabrizi, 2011). Currently, it is not possible to crystallise mHTT due to its instability. This means that in-depth structural analysis has not been possible. However, it has been suggested that the expansion increases the length of the random coil, facilitating aggregation and abnormal protein interactions (Kim et al., 2009).

The alpha-helical structure found in wtHTT is largely lost in the mutant form, with mHTT fragments instead forming a compact beta-sheet structure that is capable

of aggregation, the efficiency of which is highly dependent on the CAG repeat length (Chen et al., 2001; Ross and Tabrizi, 2011). On a cellular level, N-terminal mHTT fragments form inclusions in both the cytoplasm and the nucleus, whereas wtHTT maintains a cytoplasmic localisation exclusively, and does not form inclusions or aggregates in that manner (Vonsattel, J.P., DiFiglia, 1998).

Both the wild type and mutant forms of the HTT protein are known to undergo significant post-translational modification, including phosphorylation, SUMOylation, ubiquitination, acetylation and palmitoylation (Cong et al., 2011; Steffan et al., 2000; Thompson et al., 2009; Yanai et al., 2006). These modifications tend to occur in the disordered regions of the protein and affect physical properties of the protein such as half-life and the propensity to form aggregates. The HTT protein is also known to be cleaved by a number of proteolytic enzymes (Graham et al., 2006), resulting in a large number of fragments ranging in size. Of particularly note is the exon 1 fragment formed from mHTT, of approximately one hundred amino acids which is suggested to be particularly toxic (Bates et al., 2015; Ross and Tabrizi, 2011).

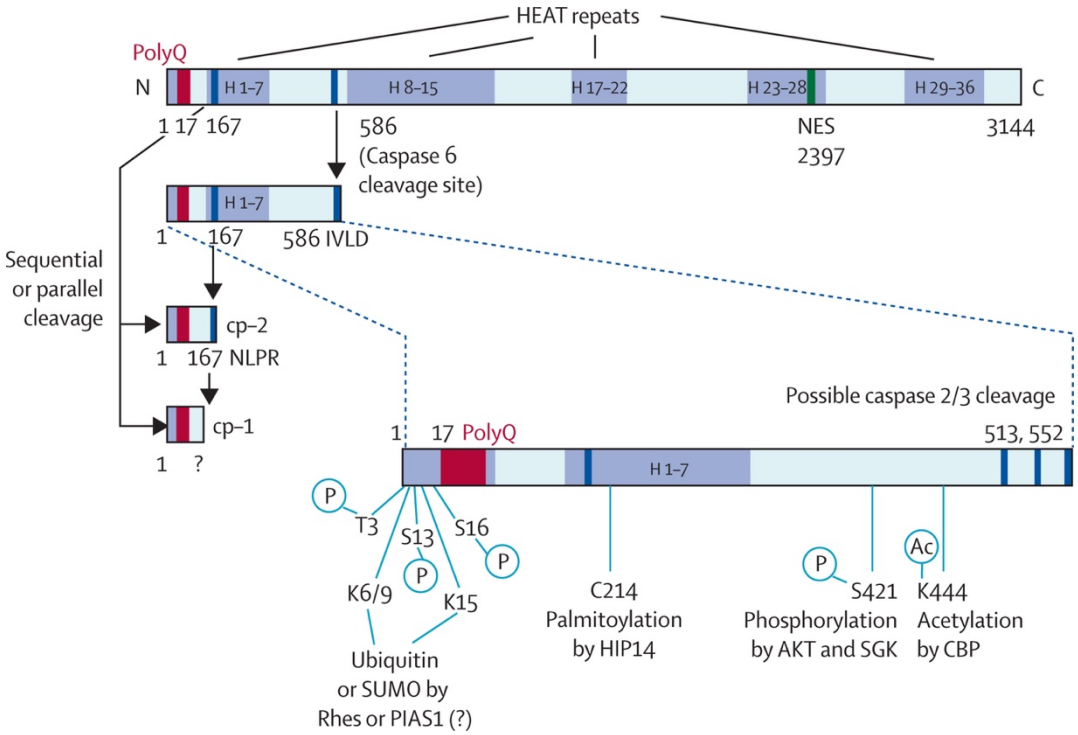

Figure 1.1. The huntingtin protein. The human HTT protein contains a number of HEAT repeat regions. A polyglutamine (polyQ) stretch is located at the N terminus, which is expanded in HD. Proteolytic cleavage by Caspase 6 results in the formation of toxic

N-terminal fragments such as cp-1 and cp-2. HTT is known to undergo many post translational modifications, such as acetylation (Ac), phosphorylation (P), and the addition of ubiquitin or small ubiquitin-like modifiers (SUMO). IVLD and NLPR are amino acid cleavage sequences. NES=nuclear export signal, PIAS1= Protein Inhibitor Of Activated STAT 1, HIP14= Huntingtin interacting protein 14, AKT= serine/threonine-specific protein kinase also known as Protein Kinase B. SGK= Serum/Glucocorticoid Regulated Kinase, CBP= CREB-binding protein. *Reprinted with permission from Ross and Tabrizi, 2011.*

1.1.5.3. Function

The exact function of wtHTT remains unclear. However, it is known to be essential for embryonic development, as HTT knockout is embryonic lethal in mice prior to CNS development (Duyao et al., 1995; Nasir et al., 1995). This is rescued by the expression of HTT in the extra-embryonic tissues, suggesting a role for HTT beyond the CNS during development (Dragatsis et al., 1998). Conditional knockout of HTT in neonates is lethal, but interestingly this is due to acute pancreatitis rather than any CNS pathology. Additionally, if the knockout occurs after four months of age it is non-lethal, suggesting a key developmental timing to the essential role of HTT (Wang et al., 2016).

Conditional HTT knockout adult mice exhibit increased CNS apoptosis (Zeitlin et al., 1995) and there is significant evidence that wtHTT is neuroprotective in HD, but also more generally in neurological conditions where cell death occurs (O'Kusky et al., 1999; Rigamonti et al., 2000; Zhang et al., 2003). For example, overexpression of wtHTT in HD mice leads to a reduction in striatal cell loss (Leavitt et al., 2006, 2001; Rigamonti et al., 2000).

The loss of wtHTT can also contribute to the HD phenotype in animal and cell models of the disease, with worsened motor phenotypes, survival rates and cell vulnerability in the absence of wtHTT (Van Raamsdonk et al., 2005; Zhang et al., 2003; Zuccato et al., 2003, 2001). Beyond HD, wtHTT is also protective, such as in a model of ischemia where mice expressing higher levels of wtHTT show a reduction in lesion size of 17% compared to their normal littermates. Additionally, wtHTT levels are reduced in mouse models of traumatic brain injury and spinal cord injury, which is blocked by administration of a broad caspase inhibitor, suggesting this depletion is due to HTT's role as a caspase substrate (Zhang et al., 2003).

Research to date has focused on the role of wtHTT in neurons, where possible roles for the protein in vesicular trafficking (Velier et al., 1998) and cellular trafficking of BDNF along microtubules (Gauthier et al., 2004) have been found. At a transcriptional level, wtHTT interacts with REST/NRSF to modulate the transcription of NRSF-controlled neuronal genes, which include BDNF (Zuccato et al., 2001). There is also evidence that wtHTT has a role in transporting NF-κB from the synapse to the nucleus, which is impaired by mHTT (Marcora and Kennedy, 2010). By comparison, little is known about the role of wtHTT in non-neuronal cells. However, recent work has suggested a novel role for wtHTT in the immune system, showing that lowering the levels of wtHTT results in a reduction in cytokine expression following stimulation with lipopolysaccharide (LPS) and interferon gamma (IFNγ) (Trager et al., 2014). Given the diversity of roles wtHTT has been shown to play in neuronal cells, it is possible that many more functions for wtHTT in other cell types remain to be uncovered.

Despite the abundant roles of wtHTT and the protective effects of its expression, as previously mentioned, it is unlikely that the extensive pathology seen in HD is caused solely or even largely by a loss of normal HTT function.

1.1.6. Experimental models of HD

1.1.6.1. Animal models

A wide variety of HD animals models have been developed, including *Drosophila*, rat, pig and sheep models (Baxa et al., 2013; Handley et al., 2016; Lewis and Smith, 2016; von Hörsten et al., 2003). The ability to study HD *in vivo* has been key to improving our understanding of the disease, and while no model perfectly recapitulates the human disease, each is useful for studying different aspects of the disease, and is complementary to work in human tissues to generate a full understanding of HD pathogenesis and progression.

Particularly frequently used have been rodent models of HD, where the most common models include: truncated N terminal fragment models, knock-in models using full-length HTT, and transgenic models using full-length HTT. See table 1.1. for a list of the most commonly used models. A more exhaustive list can be found in Pouladi et al., 2013 (Pouladi et al., 2013). Initial work relied on the use of transgenic fragment models of HD. For example, the R6/2 mouse model, in which

a fragment of the human HTT gene was inserted into the mouse genome, specifically the N-terminus, containing a CAG repeat expansion of 150 units (although larger expansions are commonly in use now) expressed using the *HTT* promoter (Mangiarini et al., 1996). Fragment models tend to have very severe disease phenotypes, with earlier onset and rapid progression, and are perhaps closer genetically and phenotypically to juvenile onset HD. Following on from these fragment models, a number of transgenic mouse models have been created that contain the full-length human *HTT* gene, such as the YAC128 and BACHD models. In each case, the full length gene is randomly inserted in the genome, with four or five copies present in addition to both alleles of the endogenous murine *HTT*, leading to high overall expression levels (Dagmar E. Ehrnhoefer et al., 2009). Knock-in mouse models also exist, which are perhaps the most similar to the human disease in terms of the genomic and protein expression of mHTT, where exon 1 of one allele of the mouse HTT gene is replaced with an expanded CAG construct, meaning the mutant allele is identical to the endogenous locus except for the exon 1 expansion and should be expressed at endogenous levels (Lin et al., 2001; Woodman et al., 2007). Two excitotoxic models of HD also exist, where intrastriatal injections of the endogenous metabolite quinolinic acid or systemic administration of 3-nitropropionic (3-NP), an inhibitor of the mitochondrial citric acid cycle, result in some of the biochemical, behavioural and pathological features of HD in rodents and non-human primates (Schwarcz et al., 1983). Finally, conditional models exist, whereby mHTT expression can be isolated to particular cell types, e.g. striatal cells only (Gu et al., 2007), through cross breeding mice where expression of a fragment of mHTT (Exon1), is driven by the endogenous ubiquitously-expressing Rosa26 promoter, and can only be switched on by Cre recombinase, with Cre recombinase expressing mice, where Cre expression is limited to particular cell types through the use of specific promoters e.g. the Nestin promoter, which drives pan neuronal Cre expression (Gu et al., 2005b, 2007). Collectively these murine models have been incredibly helpful in improving our understanding of HD, but it is important to note that therapies which have been successful in mouse models have failed when translated to human patients. This highlights the fact that animal models, while invaluable, do not fully recapitulate human disease; specifically the time frame and severity of disease, and so

perhaps should be used in tandem with human cell-based approaches. This understanding is what has driven the research contained in this thesis; to develop and characterise a human cell-based approach to support research into our understanding of Huntington's disease.

Table 1.1: Popular rodent models of HD

Model	**Transgene product**	**Promoter**	**CAG repeat length**	**mHTT expression**
R6/1 mice	67 amino acids of N-terminal fragment (human *HTT*)	1kb human *HTT* promoter	116	~x0.30
R6/2 mice	67 amino acids of N-terminal fragment (human *HTT*)	1kb human *HTT* promoter	150	~x0.75
HD51 rats	N-terminal fragment (22% of rat *Htt* gene)	Endogenous rat *Htt* promoter	51	<x1.00
HdhQ150 mice, HdhQ200 mice	Full-length chimeric human *HTT* exon 1:mouse *Htt*	Endogenous mouse *Htt* promoter	150, 200	x1.00
HdhQ111	Full-length chimeric human *HTT* exon 1:mouse *Htt*	Endogenous mouse *HTT* promoter	111	x1.00
zQ175 mice	Full-length chimeric human *HTT* exon 1:mouse *Htt*	Endogenous mouse *Htt* promoter	188	x1.00
YAC128 mice	Full-length human *HTT*	Human *HTT* promoter and	128	~x1.00

		regulatory elements (24kb upstream, 117kb downstream)		
BACHD mice	Full-length human *HTT*	Human *HTT* promoter and regulatory elements (20kb upstream, 50kb downstream)	97	~x1 (relative to expression of a full-length human HTT transgene containing 18 CAG repeats)
BACHD rats	Full-length human *HTT*	Human *HTT* promoter and regulatory elements	97	~x2.50-4.50

1.1.6.2. Cell models

A number of immortalised cell lines with CAG repeat knock-ins or over-expressing transgenic lines have been produced, either through isolation from malignant cancerous tissues, or through genetic modification of cells to be immortalised using viral methods or otherwise (Pérez-Severiano et al., 1998). These lines serve as an excellent resource, but due to being isolated from malignant tissue or the possibility of containing artefacts from becoming immortalised, results found in such models should be validated in other models (Park et al., 2008).

Primary human cells have been used extensively also, particularly from the most accessible tissues, such as fibroblasts, blood cells, and muscle cells. These cells

are then cultured *ex vivo* for experiments. The benefits of using cells direct from a patient are numerous; the expression level and CAG repeat size are as is found in the patient, and the epigenetic age of the cells is preserved. However, these samples can only be cultured for a limited period of time, are invasive to collect and rely on patients to be willing to donate. Additionally, cells may behave differently when isolated and *in vitro*, than they do when receiving environmental signals within a patient's system (Hawksworth, 1994; Park et al., 2008). It is on this background that pluripotent stem cells (PSCs) have been developed and their use adopted in labs around the world, with the gold standard being embryonic stem cells (ESCs), more recently joined by induced pluripotent stem cells (iPSCs).

iPSCs are produced through reprogramming of somatic cells, such as fibroblasts, through the introduction of specific transcription factors (Lowry et al., 2008; Takahashi et al., 2007; Yu et al., 2007). This is particularly useful for producing cell-based models of disease, where somatic cells from patients can be reprogrammed to a pluripotent state, while maintaining their genetic identity. Disease-specific iPSCs for a number of neurodegenerative disorders have been produced, including Parkinson's disease and Alzheimer's disease (Chang et al., 2019; H. Li et al., 2018; Yagi et al., 2011). This has also been applied in HD, with iPSC lines produced from HD patients and related controls. The benefit of these lines is the theoretically infinite source of patient material that they can produce, with the same polyQ length and expression level as the donor.

Embryonic Stem Cells (ESCs), on the other hand, are derived from donated blastocysts, either carrying specific disease mutations, or controls that can be edited using genome editing. In theory, a disease such as HD can be equally modelled by either iPSCs or ESCs (Halevy and Urbach, 2014).

Of additional benefit has been the production in recent years many differentiation protocols, such that it is possible to produce almost any cell type of interest from these starting materials (Abud et al., 2017; Arber et al., 2015; Van Wilgenburg et al., 2013). This is particularly useful in the cases of very inaccessible tissues and cell types such as those of the CNS.

However, as with any technique in its infancy, there are a number of caveats to the use of PSCs that are only now becoming apparent, as their use becomes

more widespread. For example, it has become apparent that the neurons produced from iPSCs may be more embryonic than previously expected, and that long maturation periods must be employed to generate even subtle disease relevant phenotypes, in the cases of diseases such as HD and AD, that have a later onset. There are some suggestions that these immature cell phenotypes and the reduced prevalence of disease pathology in iPSC-derived neurons, may be due to the reprogramming process which returns somatic cells to a pluripotent state, where the epigenetic clock becomes reset (Rando and Chang, 2012). This issue is being investigated by iPSC labs around the world currently, and the extent that this may caveat results is beginning to be understood. This issue may be circumvented through the use of direct-differentiation protocols, where somatic cells are directly differentiated into the desired cell type (e.g. cortical neurons), without the iPSC reprogramming procedure (Yoo et al., 2011). This method is also in its infancy, but appears to preserve the phenotypes of disease more effectively. Also, dependent on the reprogramming method used to create iPSCs, there is evidence of incomplete reprogramming, where iPSCs retain some "epigenetic memory" of the donor cell type (Bar-Nur et al., 2011; Kim et al., 2010; Ma et al., 2014).

HD is particularly tractable for production of an allelic series from control ESCs, as it is caused by a single gene, where a disease such as AD would be harder to model using ESCs. However, to create a disease model from control ESCs, genetic manipulation is required, for example using CRISPR-Cas9 technology. A number of research groups have now produced series of isogenic ESC lines with varying CAG lengths on identical genetic backgrounds, allowing for investigation of the effect of CAG length on phenotype without the presence any other genetic modifiers (An et al., 2014; Ooi et al., 2019; Ruzo et al., 2018). There are some caveats to this method, however, and it should be noted that off-target effects of CRISPR-Cas9 have now been suggested to be a relatively common occurrence when using this system, depending on the cell type used (Veres et al., 2014; Zhang et al., 2015) and so should be tested for and considered.

Another avenue for the production of HD ESC lines has been through the donation of embryos generated through IVF and screened for HD. Embryos

positive for the mutation may be donated to science for the production of HD ESC lines (Verlinsky et al., 2005).

Early research in the HD field using iPSC and ESC derived cell types has been of great interest, however the caveats of PSC use also apply in HD. For example, studies using iPSC-derived neurons particularly, failed to appreciate the impact of other genetic variation on the performance of the cells. For example, in a study with primary human immune cells, typically an N of 10 per group would be required. However, in some PSC-publications, a single HD line is used against a single control line for certain experiments, resulting in a significantly under powered study, with an associated high false discovery rate (Conforti et al., 2018).
However, with the correct number of repeats and controls in place, human iPSC and ESC-derived cell types can be a very promising model to use to investigate HD. This is particularly true for cell types such as microglia and neurons, where primary human cultures are difficult to obtain, and have a limited life time in culture; for such cell types, iPSCs and ESC derived versions provide a novel opportunity to address key research questions *in vitro*.

In summary, rodent models have been the research model of choice for many key discoveries and have been very useful in building our understanding of Huntington's disease. However, following 65 million years of evolutionary divergence, there are of course significant differences between rodent and human systems, in the CNS (Hodge et al., 2019), and also in the immune system, which form the focus of this thesis (Mestas and Hughes, 2004; Smith and Dragunow, 2014). Additionally, the failure of many therapeutics in human trials, that have been effective in rodents, emphasises that these differences are of consequence. For these reasons, human models should be pursued wherever possible, in parallel with *in vivo* animal research, to strengthen the case for results found in both. There is also a case for using immortalised cell lines for Huntington's and immune system research. However, given the possibilities of artefacts due to the immortalisation process, and possible genetic abnormalities in the cases of lines isolated from cancers, results found in such lines must be replicated in other models. This is particularly relevant for microglia, where recent studies have shown that microglia cell lines differ genetically and functionally from

primary microglia and *ex vivo* microglia (Butovsky et al., 2014; Das et al., 2016; Melief et al., 2016). Finally, primary human cells for the study of Huntington's disease carry many benefits; the use of the patient's own cells allows assessment of cells with the exact CAG length and HTT expression level of the patient. However, primary cells have a limited lifetime *in vitro*, and are challenging to obtain in large numbers. This is particularly true for the cells of the CNS, such as microglia, where cells can only be collected in low numbers post mortem, or following tissue resection for therapeutic reasons (tumour removal or epilepsy). For these reasons, this thesis has aimed to develop a human iPSC and ESC-derived model of Huntington's disease neurons and microglia. Human iPSC and ESC-derived neurons and microglia are a theoretically infinite resource for researchers, and in the case of HD, where lines are derived from HD patients, they express the polyQ at the size and expression level found in the donor patient.

1.1.7. Cellular pathogenesis of HD

1.1.7.1. HTT aggregation, fragmentation and accumulation

One neuropathological hallmark of HD is the accumulation of intracellular mHTT aggregates, and specifically, intranuclear aggregates, which sequester transcription factors, chaperone proteins, ubiquitin and wtHTT into them (Arrasate et al., 2004; Davies et al., 1997; DiFiglia et al., 1997; Steffan et al., 2000). In cell and animal models of HD, accumulation of these aggregates correlates with disease load (Becher et al., 1998; Sieradzan et al., 1999) and causes increased apoptotic cell death (Hackam et al., 2000). However in some models of HD, cells containing aggregates survive for longer than those without and suppression of aggregate formation increases toxicity (Arrasate et al., 2004; Choi et al., 2012). Indeed, the formation of aggregates may be a way for the cell to reduce the concentration of toxic species soluble in the cell and compartmentalise for improved cellular function. In fact, when aggregation is prevented in a fragment mouse model of HD, there is increased dysfunction of the ubiquitin proteasome system (UPS) (Ortega et al., 2010).

It is possible that mHTT has multiple toxic species with anything from soluble misfolded mHTT to protofibrils, fibrils, aggregation foci, compact beta-sheet structures potentially capable of toxicity (Bates, 2003; Rubinsztein and Carmichael, 2003). Full-length mHTT may be toxic in and of itself, but there is

clear evidence that that N-terminal exon 1 fragments of mHTT can be particularly toxic. Models expressing exon 1 alone show far more severe phenotypes than full-length models.

1.1.7.2. Dysregulated transcription

Transcriptional dysregulation is a central feature of pathogenesis in HD and one of the earliest signs of mHTT-induced dysfunction (Ryu et al., 2006). It is seen consistently in both patients and HD cell and animal models. There are several ways in which mHTT causes transcriptional dysregulation. Firstly, mHTT is capable of binding DNA directly and in this way regulates transcription and occupies gene promoters. This occurs in a polyQ length-dependent manner, with a longer expansion leading to increased binding (Benn et al., 2008).

Secondly, mHTT can indirectly affect transcription through influencing chromatin structure, thus affecting the accessibility of genes to transcription factors. In HD brains and R6/2 mice, histones H3 and H4 are hypo-acetylated and present in nuclear inclusions of mHTT. Moreover, HDAC inhibitors are found to improve some disease phenotypes of HD mice and *Drosophila* (Jia et al., 2016; Pallos et al., 2008; Steffan et al., 2001). Histone H3 (K9) is also found to be hyper-methylated in HD brains, with methylation a well-known mechanism for gene silencing. This is most likely caused by increased levels of ESET, a histone H3 (K9) methyltransferase whose expression is increased in HD patients and the R6/2 mouse model. Interestingly, treatment to reduce trimethylated H3 (K9) results in an amelioration of symptoms in the R6/2 mouse model (Labbadia et al., 2011; Ryu et al., 2006; Sadri-Vakili et al., 2007; Sadri-Vakili and Cha, 2006).

Finally, mHTT can affect transcription by directly interacting with transcription factors and their regulators. For example, mHTT is known to bind directly to CBP, which possesses histone-acetyltransferase activity, as well as TBP, p53, mSin3a and SP1, and can sequester them into inclusions. SP1 is bound by wtHTT also, but mHTT binds with a higher affinity and a downregulation of SP1 regulated genes is seen in HD (Ryu et al., 2006). mHTT is also known to directly interact with the IKK complex (Khoshnan et al., 2004), and significantly affects the activity of the NF-κB pathway, which is dysregulated in a number of different models of HD. For example, it has been found that resting human HD myeloid cells have upregulated expression of gene sets relating to NF-κB and significantly reduced

protein levels of the negative NF-κB regulator, IκB (Miller et al., 2016). This altered activity pattern has been suggested to be caused by mHTT binding to IKKγ, resulting in increased NF-κB activity, increased IκB degradation and subsequent NF-κB translocation (Trager et al., 2014). Additionally, in other models of HD, for example cultured cells expressing mHTT and striatal cells from HD transgenic mice, elevated NF-κB activity is seen (Takano and Gusella, 2002). mHTT exon 1 fragments alone can strongly increase NGF-induced NF-κB dependent gene expression (Khoshnan et al., 2004) and in slice culture genetic inhibition of NF-κB activity reduced mHTT exon 1 fragment induced toxicity (Smith et al., 2014; Träger et al., 2015).

1.1.7.3. Dysregulated proteostasis

Given the aggregation phenotype seen in HD, it seems clear that many cell types struggle to clear the mHTT protein, leading to increasing load in the cell and eventual formation of aggregates. This suggests dysfunction of protein clearance pathways and a great deal of evidence supports the idea of autophagy being dysfunctional in HD. HTT may ordinarily aid the autophagic processes; a function that is lost in the mutant form of the protein (Martin et al., 2015; Samaraweera et al., 2013; Steffan et al., 2000). Interestingly, in cell models of HD the UPS appears dysfunctional, but when tested *in vivo* this was not found, with mouse models only showing transient UPS dysfunction in response to acute expression of mHTT, with continued dysfunction only caused in the presence of aggregation inhibitors (Ortega et al., 2010). The heat shock response (HSR) pathway is also impaired in HD and while the presence of expanded HTT polyglutamine tracts in cells alone is insufficient to induce the HSR pathway, its presence does appear to inhibit the proper induction of the HSR in the presence of an additional stressor. In this way, cells have a reduced capacity to respond to stressors (Chafekar and Duennwald, 2012; Labbadia and Morimoto, 2013; San Gil et al., 2017).

1.1.7.4. Dysregulated mitochondrial function and bioenergetics

Mitochondrial dysfunction is also present in HD, with aberrant mitochondrial morphology seen in post mortem brain tissue and in *ex vivo* peripheral cells such as lymphoblasts (Gu et al., 1996; Squitieri et al., 2006). The performance of mitochondria in HD is also suggested to be impaired due to enzymatic changes and reductions in substrate availability, but it is likely that these impairments are

secondary to damage occurring elsewhere in the brain, rather than a primary event in the disease aetiology (Browne, 2008).

Oxidative stress is also found to occur in HD. There is evidence of abnormally increased levels of several markers of oxidative stress-induced damage in HD patients and models. For example, 8-OHDG, a biomarker of DNA oxidation, is significantly elevated in post mortem brain tissue (Browne et al., 2010), with a parallel increase is found in peripheral blood leukocytes (Chen et al., 2007). There is also evidence from *in vitro* cell work in HeLa, COS-7 and SK-N-SH cells, that the presence of mHTT itself results in elevated levels of reactive oxygen species (ROS) production in a polyQ-dependent manner (Wyttenbach et al., 2002), suggesting a cell autonomous mechanism. This increase in ROS production is linked to HTT polyQ length specifically, and can be induced without the presence of any surrounding exon1 sequence. In addition, ROS production and the formation of mHTT aggregates coincide in cells, both preceding toxicity and death. Blocking aggregation appeared to reduce ROS production in this model also (Hands et al., 2011). The mechanism by which mHTT causes ROS production is unknown, but it has been suggested that it occurs via inhibition of the proteasome (Wyttenbach et al., 2002).

Nitric oxide production is also found to be altered in HD. Nitric oxide synthase (NOS) can be either beneficial or detrimental in neurodegenerative disease. This is dependent on disease stage, the isoform of NOS involved, and the balance between nitrosative and oxidative stress. There are three isoforms of NOS; endothelial (eNOS), neuronal (nNOS) and inducible (iNOS). Endothelial and neuronal NOS are both constitutively expressed and have roles in homeostatic physiology, whereas iNOS is expressed in glial cells and only in response to stimulants (Deckel, 2001). Specifically, microglia express iNOS in response to LPS and IFNγ stimulation (Possel et al., 2000). NO has antioxidant properties in many cases (Wink et al., 1999). However, if the environment of the cell is rich in superoxides due to oxidative stress, NO species contribute to the formation of peroxynitrite, a neurotoxic by-product (Espey et al., 2000). In HD patient post mortem brain samples, nNOS mRNA and protein levels are reduced in the striatum, but not in the cortex (Norris et al., 1996), and the activity of nNOS is also reduced in R6/2 mice (Deckel et al., 2000).

In addition to this, peroxynitrite is increased in transgenic mouse models of HD (Browne et al., 1999; Deckel et al., 2000). In the 3-NP-induced model of HD, NO and peroxynitrite play a role in the neurodegeneration which follows 3-NP administration (Galpern et al., 1996; Nishino et al., 2000). In the quinolinic acid-induced model of HD, NOS activity is increased compared to controls and NOS inhibition is protective against the emergence of circling behaviour, a phenotype associated with neurodegeneration in the model (Pérez-Severiano et al., 1998). This suggests that nitrosative stress may play a role in HD pathology; however, this requires further confirmation in human HD cases.

1.1.7.5. Dysregulated cellular transport and trafficking

Dysregulated cellular transport and trafficking is also a known pathology in HD. For example, mHTT has been shown to interact with β-tubulin to disrupt protein transport post-Golgi and secretion (Smith et al., 2009). mHTT has also been shown to interfere with vesicle formation from recycling endosomes through altered interactions with RAB11 (Li et al., 2009). Most relevant for the striatal degeneration seen in HD patients, mHTT has been shown to have impaired ability to transport BDNF vesicles due to altered interactions with huntingtin-associated protein-1 (HAP1) and the p150Glued subunit of dynactin (Gauthier et al., 2004). Interestingly, the heterozygote mutants tested were as deficient as homozygous mutants, suggesting a dominant negative effect of the mutant form. This is particularly detrimental for striatal MSNs, which rely on BDNF for their survival, but do not produce it themselves (Li et al., 2009).

1.1.7.6. Non cell autonomous effects

It is important to acknowledge the role of cell-cell interactions in the production of HD pathology. Many publications have shown that expression of mHTT in some discrete cell types that are affected in HD, is insufficient to produce HD pathology. For example, in animal models of HD, expression of mHTT in cortical pyramidal neurons and glia alone were insufficient to produce HD pathology (Gu et al., 2005a). Expression of mHTT in striatal MSNs alone resulted in progressive and cell-autonomous accumulation of nuclear mHTT aggregates, but mice with this striatal degeneration alone failed to develop significant locomotor deficits and other stereotypical elements of striatal neuropathology such as gliosis usually associated with HD (Yang et al., 2007). Similarly, expression of mHTT in

microglial cells alone in mice resulted in a lack of disease phenotypes (Petkau et al., 2019). In a rodent model, expression of highly expanded mHTT in astrocytes has been shown to cause detrimental knock-on effects to the health of neurons, with the development of a neurological phenotype (Bradford et al., 2009), although not recapitulating all HD phenotypes. This highlights the importance of HTT expression throughout the cells of the brain, in the production of HD phenotypes and pathology. It has also been shown that HD patient brains and three different murine model types (R6/2, YAC128 and Hdh92 and Hdh111) have a higher level of excitotoxic Kynurenine 3-monooxygenase (KMO) pathway metabolites, suggesting dysfunction of the KMO pathway (Guidetti et al., 2006, 2004), further increasing the likelihood of excitotoxicity in the HD brain.

Co-culture experiments using *ex vivo* primary murine cells have shown that mHTT-expressing neurons are protected from glutamate toxicity when in the presence of wtHTT-expressing astrocytes compared to HD astrocytes (115-150Q). This may be due to an impaired ability of mHTT expressing astrocytes to clear synaptic glutamate, which can then result in excitotoxicity in neurons (Shin et al., 2005).

Studies in cell lines and *ex vivo* cells from murine models have shown that mHTT has an impaired ability to facilitate BDNF transport in comparison to wtHTT. This impairment may underlie the increased loss of MSNs in the striatum in HD, which are particularly vulnerable as they do not produce BDNF themselves and therefore require BDNF transport from the cortex for survival (Gauthier et al., 2004; Zuccato and Cattaneo, 2007). MSNs are also particularly vulnerable because of their high metabolic demands due to their high level of connectivity to the neocortex (Ehrlich, 2012). Taken together, these results highlight the importance of non-cell autonomous mechanisms in the accumulation and progression of pathology, with a myriad of dysfunctional cell types contributing to the complete phenotype seen in HD.

1.1.8. HD therapeutics

Current HD therapeutics are limited to treating the symptoms of HD, without addressing the underlying cause. Up until 2017, a total of 99 clinical trials were conducted investigating therapies to treat HD. The success rate of these trials has been very low, with just 3.5% of trials progressing to the next stage of testing

(McColgan and Tabrizi, 2018; Travessa et al., 2017). There is only one licensed drug for the treatment of HD, specifically, tetrabenazine, which aids in the control of chorea, but with some undesirable side effects (Kieburtz et al., 2018). In clinical practice, neuroleptics including olanzapine, respiridone and quetiapine are also commonly used to treat chorea (Kieburtz et al., 2018).

Outside of these existing symptom management options, a variety of drugs are under investigation as potential disease-modifying agents. These can be broadly classified into four categories. First, HTT-lowering therapies, either via RNA interference (RNAi), (Grondin et al., 2012; McBride et al., 2011; Stiles et al., 2012), anti-sense oligonucleotides (ASO) or zinc-finger protein (ZFP) methods (Evers et al., 2011; Garriga-Canut et al., 2012), which interact with the production of HTT protein at various points from transcription to translation to prevent pathology by lowering the level of mHTT in the system. The next area of investigation surrounds modulators of cellular homeostasis, such as chaperone enhancers (Sontag et al., 2013), autophagy enhancers and drugs that prevent aggregation (Labbadia et al., 2012; Renna et al., 2010). Thirdly, therapies to improve neurotrophic support to MSNs are being assessed (Simmons, 2017), either via TRK receptor agonists or delivery of BDNF and GDNF via viral or stem cell vehicles (Leschik et al., 2013). Finally, due to the improving understanding of the importance of glial cells in HD, the last category of therapeutics targets glial cell function such as Laquinimod, which targets inflammation, and CB2 agonists that target immune cell function (Bouchard et al., 2012; Comi et al., 2012).

1.2. The innate immune system

The innate immune system is the most evolutionarily ancient part of the immune system. It recognises invading pathogens or cellular damage and rapidly produces stereotyped responses to defend the integrity of the body (Janeway, 1989). The innate immune system has evolved to recognise specific pathogen-associated molecules that are highly conserved and essential for the pathogenicity and survival of invading pathogens. Importantly, these molecules are common to large groups of microorganisms, allowing the innate immune system to respond to a vast number of invading pathogens via recognition of a much smaller number of pathogenic protein signatures. These pathogenic protein signatures are known as pathogen associated molecular patterns (PAMPs) and

the receptors that recognise these PAMPs are known as pathogen recognition receptors (PRRs). Some of the best-known examples of PAMPs include bacterial lipopolysaccharide (LPS), peptidoglycans, bacterial DNA, double-stranded RNA and glucans. LPS, for example, is common to all gram negative bacteria and only bacteria produce it, making it an ideal PAMP for the innate immune system to recognise and react to (Janeway, 1989; Medzhitov and Janeway, 2000). PRRs can be split into a few families: Toll-like receptors (TLRs), Rig-I-like receptors (RLRs), Nod-like receptors (NLRs), AIM2-like receptors (ALRs) and C-type lectin receptors (CLRs). LPS is recognised by a member of the TLR family, TLR4 (Brubaker et al., 2015; Kumar et al., 2011). NLRs and TLRs can also sense non-infectious sterile tissue injury such as stroke or traumatic brain injury (Ransohoff and Brown, 2012).

The innate immune system works in tandem with the adaptive immune system, which consists of B and T lymphocytes, which carry out antibody responses and cell-mediated immune responses, respectively. Cell-mediated immune responses involve activated T cells reacting directly against an antigen that is presented to them to eliminate them, or may involve T cells signalling to the innate immune system's macrophages to phagocytose foreign material. Antibody responses are mediated by B cells, which produce and secrete antibodies which bind to foreign antigens, marking them for destruction by the innate immune system and also preventing them binding other cells of the body. Crucially, adaptive immune responses are slow to develop in response to a new pathogen, so it may take up to a week for the adaptive immune system's response to become effective in these cases. This is when the fast, stereotyped responses of the innate immune system are essential to keeping a new pathogen at bay. Importantly, the adaptive immune system remembers pathogens it has encountered before, so this lag only occurs when new pathogens enter the system (Alberts B, Johnson A, Lewis J, 2002; Medzhitov and Janeway, 1997).

1.2.1. Innate immune system signalling

Activation of PRRs results in a cascade of intracellular signalling in the innate immune system, leading to either rapid responses such as phagocytosis, autophagy (Deretic et al., 2013), cell death and cytokine processing (Lamkanfi and Dixit, 2014; Ransohoff and Brown, 2012), or slightly slower responses such

as the production and release of pro-inflammatory cytokines and interferon from the cell. These latter processes occur 24-48 hours after antigen recognition, signalling to the rest of the immune system to react to the invading pathogen (Brubaker et al., 2015).

TLRs are the best studied PRRs of the innate immune system. They were first discovered as orthologues to a receptor found in *Drosophila* and are considered to be the primary sensors of pathogens (Kumar et al., 2011). Once activated, they initiate intracellular signalling, via MyD88 primarily, but also via MYD88-adaptor-like protein (MAL), or TIR domain-containing adaptor protein inducing IFNβ (TRIF) and TRIF-related adaptor molecule (TRAM), which then interact with the NF-κB, ERK, AP1, IRK and p38 MAPK downstream pathways (Figure 1.2), resulting in initial upregulation of transcription of pro-inflammatory cytokines, such as IL-6, IL-8, TNFα, IL-1β and type 1 interferon (O'Neill et al., 2013). This upregulation is transient, peaking at 2-4 hours, before progressive repression of their expression after that. Other genes are induced at later time points, up to 24 hours after initial stimulation, and act in an autocrine manner to elicit secondary signalling cascades (Aung et al., 2006; Schroder, 2003).

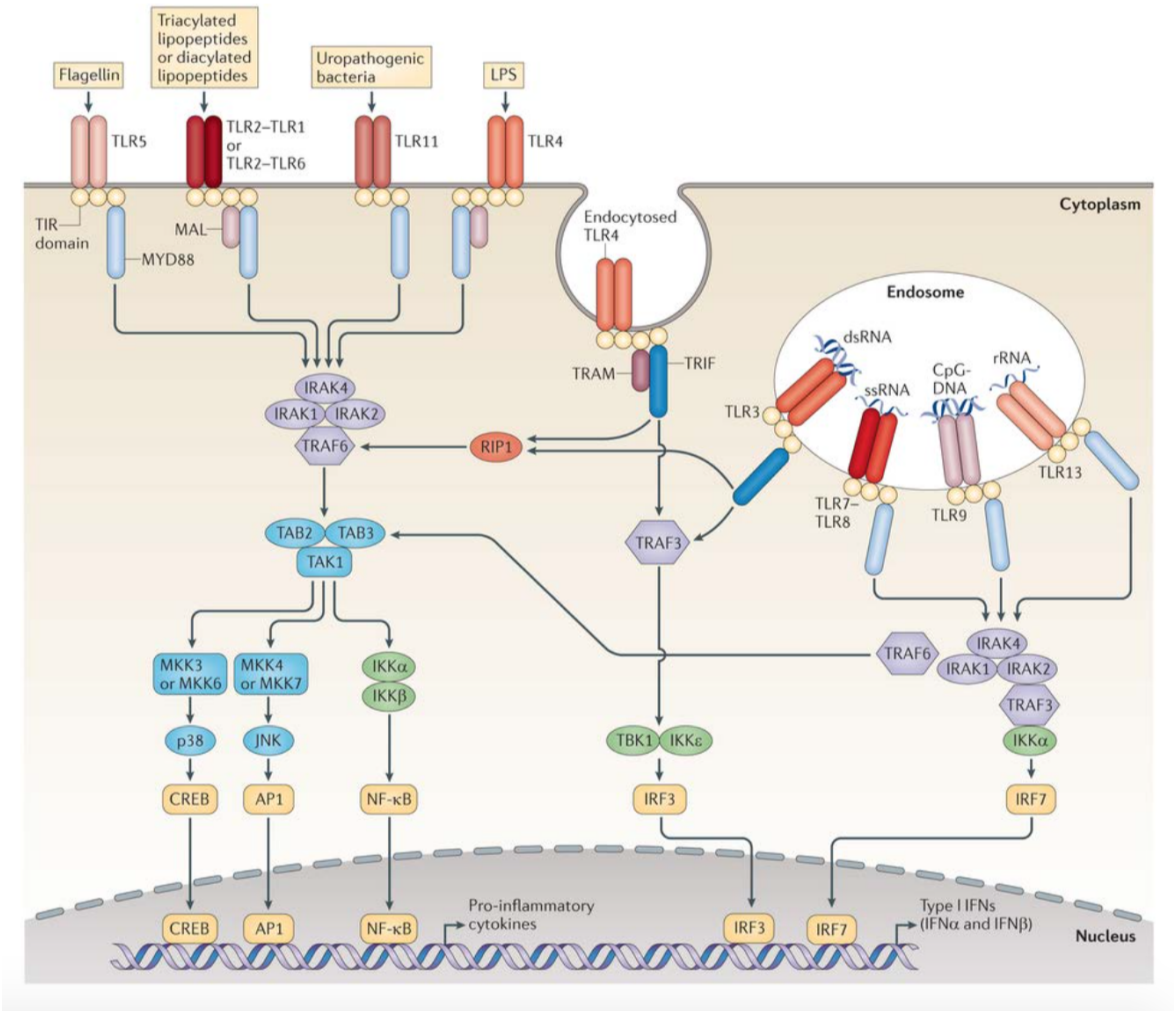

Figure 1.2. Mammalian Toll-like receptors. A summary of mammalian Toll-like receptor (TLR) signalling. TLRs are located at the cell surface or localised to the endosomes. TLR signalling is initiated by ligand-induced dimerization of receptors. Following this, TLRs engage with Toll-IL-1-resistance (TIR) domain-containing adaptor proteins, either MYD88, MAL, TRIF or TRAM (Myeloid differentiation primary-response protein 88, MYD88-adaptor-like protein, TIR domain-containing adaptor protein inducing IFNβ and TRIF-related adaptor molecule, respectively). This stimulates downstream signalling pathways involving IRAKs, TRAFs which in turn activate MAPKs and JNK and p38 leading to activation of transcription factors such as NF-κB, IRFs, CREB, AP1 (nuclear factor-κB, interferon-regulatory factors, cyclic AMP-responsive element-binding protein and activator protein 1, respectively). TLR signalling results in the induction of pro-inflammatory cytokine expression. dsRNA, double-stranded RNA; IKK, inhibitor of NF-κB kinase; LPS, lipopolysaccharide; MKK, MAP kinase kinase; RIP1, receptor-interacting protein 1; rRNA, ribosomal RNA; ssRNA, single-stranded RNA; TAB, TAK1-binding protein; TAK, TGFβ-activated kinase; TBK1, TANK-binding kinase 1.

Reprinted with permission from *"The history of Toll-like receptors — redefining innate immunity", 453-460, O'Neill et al., ©2013".*

1.2.2. Cells of the innate immune system

The innate immune system is made up of cells that can be split into two categories, myeloid or lymphoid, according to their developmental lineage (Gasteiger et al., 2017). Cells that develop from the myeloid lineage include granulocytes, monocytes, monocyte-derived macrophages, dendritic cells, and mast cells of the immune system. Cells that develop from the lymphoid lineage include B and T cells of the adaptive immune system (Janeway et al., 2001).

Tissue-resident macrophages such as alveolar and kidney macrophages, microglia, Kupffer cells and Langerhans cells (Haenseler et al., 2017; Hayden and Ghosh, 2011), also form part of the innate immune system, but come from a distinct lineage to myeloid or lymphoid cells (Ginhoux et al., 2013; Hoeffel and Ginhoux, 2015).

1.2.2.1. Monocytes

Monocytes make up 10% of total circulating white blood cells in humans (Auffray et al., 2009) and are replenished by pluripotent haematopoietic stem cells in the bone marrow. They are primary effector cells, with PRRs and chemokine receptors that mediate migration into tissues upon stimulation, where they differentiate further into dendritic cells and macrophages (Owen, 2012). They produce inflammatory cytokines and can phagocytose cells and toxic debris (Geissmann et al., 2010).

Human monocytes can be divided into three subtypes. Classical monocytes, which express CD14 at a high level and CD16 at a low level, are generally pro-inflammatory, but produce high levels of IL-10, an anti-inflammatory cytokine, and low levels of TNFα in response to LPS. They also preferentially express genes involved in wound healing. Non-classical monocytes express a lower level of CD14 but have a much higher expression of CD16. These monocytes have reduced phagocytic capacity and produce fewer reactive oxygen species (ROS). This subset releases IL-1β and TNFα in response to DNA or RNA particles, implicating them as a pathogenic agent in autoimmune diseases, such as rheumatoid arthritis. Intermediate monocytes express CD14 at a high level, as

well as CD16, and their numbers are consistently associated with human inflammatory disease (Yang et al., 2014; Ziegler-Heitbrock, 2007).

In human monocyte differentiation, it is accepted that classical monocytes expressing CD14 at a high level leave the bone marrow and differentiate into intermediate monocytes expressing both CD14 and CD16 at a high level and then sequentially differentiate into CD16 expressing non-classical monocytes in peripheral blood circulation. As such non-classical monocytes are considered a more mature cell type. It is likely that a spectrum of monocyte forms exists and that this three subset system is over-simplified, but it is helpful in the context of a brief summary (Yang et al., 2014).

1.2.2.2. Monocyte-derived macrophages and dendritic cells

Upon stimulation, monocytes migrate into tissues and differentiate into macrophages or dendritic cells. Macrophages express a broad range of PRRs that allow them to react to a diverse range of immune challenges. Typically, they respond by production of inflammatory cytokines and the induction of phagocytosis (Geissmann et al., 2010). Traditionally, macrophages have been classified as M1 and M2 subtypes, or classical and alternative, which echoes the subtype system used for monocytes. Again, it is a likely a spectrum exists of macrophages, from inflammatory classical macrophages to anti-inflammatory alternative macrophages, with intermediate subtypes prevalent (Martinez and Gordon, 2014). Dendritic cells also differentiate from circulating monocytes and form a diverse group of cells involved in the process of antigen presentation to lymphocytes, mediating the interactions between the innate and adaptive immune systems (Owen, 2012).

1.2.2.3. Tissue resident macrophages

Tissue-resident macrophages, which include the only CNS innate immune system cell type, microglia, come from a distinct developmental lineage, compared to monocyte-derived macrophages. It has become clear that tissue resident macrophages derive from an earlier wave of embryonic macrophage production and are MYB-independent but dependent on PU.1 and IRF8. Monocytes, and their differentiated macrophages, however, depend on MYB for their renewal (Ginhoux et al., 2010, 2013; Gomez Perdiguero et al., 2014; Hoeffel et al., 2015; Hoeffel and Ginhoux, 2015; Kierdorf et al., 2013; Palis et al., 1999).

Microglia are not readily replaced or replenished by other monocytes or macrophages from outside the brain, whereas some other tissue resident macrophages, which also originate from this earlier wave of embryonic macrophage production, can be partially or fully replaced by foetal liver or blood monocyte-derived macrophages in a tissue-specific manner (Bain et al., 2014; Calderon et al., 2015).

1.2.2.4. Microglia

1.2.2.4.1. Origin and roles of microglia in the CNS

Microglia, as previously mentioned, are tissue resident macrophages. They arise from primitive CD45+ CX3CR1- myeloid progenitors in the yolk sac, that differentiate to CD45+ CX3CR1+ microglial progenitors and travel into the brain before vascularisation and act as the resident immune cells of the brain. They make up 10-15% of the neuroglial population, which consists of astrocytes, oligodendrocytes and microglia (Nayak et al., 2014). The expression of the transcription factor PU.1 defines the microglia lineage, separating them from other tissue resident macrophages (Goldmann et al., 2016; Prasad et al., 2016). The majority of studies assessing microglial origin have been conducted in mouse models, in which microglia populate the CNS between E8.5 and E9.5; before astrocytes and oligodendrocytes emerge (Hoeffel et al., 2015; Minocha et al., 2017). Much less is known about the colonisation of microglia in the CNS in humans however (Petrik et al., 2013; Smith and Dragunow, 2014).

Expression of colony-stimulating factor 1 receptor (also called CD115) (Elmore et al., 2014), and the corresponding ligands M-CSF (CSF-1) and IL-34 (Solary and Droin, 2014), as well as GM-CSF are required for the maintenance and proliferation of microglia (Greter et al., 2012; Koguchi et al., 2003). Neuronal cells initially provide these factors, and later astrocytes also.

Microglia are necessary for normal brain development. They have a well-documented role in neuronal development, where they promote migration and differentiation of neural progenitors, neurogenesis, and oligodendrogenesis (Aarum et al., 2003; Paolicelli et al., 2011; Ueno et al., 2013). They have also been shown to contribute to the clearance of superfluous neurons during development and in adult neurogenesis (Cunningham et al., 2013; Marín-Teva et

al., 2012; Neumann et al., 2009). They also have been shown to regulate synaptogenesis, where DAP12 signalling in microglia is thought to be key to TrkB expression at the synapse and normal synaptic function, and to synaptic pruning; where microglia interact with and phagocytose excess synapses to remove them. This is thought to be mediated through deposition of microglial-associated proteins such as TREM2, fractalkine and complement proteins (Dalmau et al., 1998; Graeber et al., 2010; Hong et al., 2016b; Monier et al., 2006; Schafer and Stevens, 2010; Stevens et al., 2007; Tremblay et al., 2010). Interestingly, in mouse models of AD it has been shown that this synaptic pruning is aberrantly re-activated to cause synapse loss early in AD pathology (Hong et al., 2016a).

Microglia also have key roles in maintaining homeostasis in the brain. For example, microglia have been shown to play a role in maintaining synapses and synaptic plasticity through interactions with the synaptic cleft, dendritic spines and even astrocytic processes, to facilitate the process of synaptic maturation, pruning and elimination (Schafer and Stevens, 2015; Tremblay and Majewska, 2011). In this homeostatic role, at rest, microglia show a highly ramified morphology. Time-lapse imaging has revealed that microglia processes are highly motile, extending and retracting with brief static periods, to survey their environment looking for homeostatic disturbances (Davalos et al., 2005; Nimmerjahn et al., 2005; Wake et al., 2009). Microglia have also been shown to support the growth and maintenance of neural networks through the secretion of growth factors such as brain-derived neurotrophic factor, nerve growth factor and insulin-like growth factor (Elkabes et al., 1996; Ferrini and De Koninck, 2013; Li and Barres, 2018).

Microglia also have a key role in the injured brain. In response to injury, be it via bacterial infection, traumatic brain injury, ischemia or neurodegenerative disease, microglia shift activities, and may be termed “activated microglia”, switching from surveying their environment to responding to invading pathogens or damage signals from neurons; characteristically they adopt an amoeboid appearance. Reactive or activated microglia usually become phagocytic, engulfing necrotic cells and foreign material. Additionally, depending on the activating substance, microglia will release pro-inflammatory cytokines, reactive oxygen species, nitric oxide and quinolinic acid (Benarroch, 2013; Colton and Gilbert, 1987; Luheshi et

al., 2011; Nakagawa and Chiba, 2014), as in the case of bacterial infections (Hanisch et al., 2001; Häusler et al., 2002), or anti-inflammatory molecules such as IL-10 in response to apoptotic signalling (Hanisch et al., 2001; Häusler et al., 2002). This capacity to respond differently to a variety of stimulants highlights the complexity of microglial responses and their versatility as immune cells. Interestingly, it has been found that microglia will also respond differently to different concentrations of the same stimulant, for example, low doses of IFNγ illicit protective responses from microglia, such as downregulation of TNFα production (Butovsky et al., 2005), whereas higher doses of IFNγ result in cytotoxic responses (Butovsky et al., 2006).

Microglia have been shown to become increasingly inflammatory in the aged brain, with upregulation of major histocompatibility complex class II molecules, toll-like receptors and integrins. In this way, microglia in the aged brain can be considered "primed", and this phenomenon may contribute to the neuroinflammation seen in neurodegenerative diseases with adult onset, such as HD, AD and PD (Norden and Godbout, 2013).

1.2.2.4.2. Caveats to consider for microglial research to date

The majority of research into microglia thus far has been conducted in rodent models. There are many broad similarities between human and rodent microglia in terms of gene and protein expression, however, there are key inter-species differences, such as proliferation rate, NO production, TLR4 receptor expression and adhesive properties, among others (Mestas and Hughes, 2004; Smith and Dragunow, 2014). This reliance on rodent models in microglial research is in part due to the fact that research using primary human microglia is difficult to conduct. This is because primary human microglia are challenging to isolate and culture from post mortem brain samples, or from live patients; usually cultured following surgical resection of epileptic tissue or cancerous sites, and they can generally only be isolated in limited numbers (Radford et al., 2015; Schapansky et al., 2015). Also, given the sensitivity of microglia to their environment, microglia isolated from patients with neurological disorders or comorbidities may be activated, or in some way altered from their resting state.

Similarly, this sensitivity to their environment means that the results from work conducted on both human and rodent microglia *in vitro* and in isolation from other cell types must be considered with this sensitivity to their environment in mind. Indeed, studies have found that microglia isolated from tissue resections patients show marked transcriptional differences when assessed immediately *ex vivo* versus after *in vitro* culturing, with the authors concluding that transfer to a tissue culture environment causes rapid and extensive downregulation of microglia-specific genes (Gosselin et al., 2017).

It is clear, therefore, that there is a great need for the thorough assessment of human microglia to complement the large body of work conducted in rodent microglia, in order to identify and characterise the areas of function and dysfunction where human microglia differ to their rodent counterparts. Additionally, due to the difficulties of isolating and culturing primary human microglia, the opportunity that using microglial-like cells differentiated from human ESCs and iPSCs provides is enormous. This would allow assessment of human microglia in larger numbers, uninhibited by the challenges of primary human microglial work. However, it is important to bear in mind the limitations of *in vitro* work, as mentioned briefly above, and not to dismiss the importance of *in vivo* work. Scientists should consider repetition of results in *in vivo* models to verify findings where possible. The available methods of differentiating microglia-like cells are reviewed below.

1.2.2.4.3. PSC-derived microglia-like cells

At the beginning of this thesis, a number of microglial differentiation protocols were being published (Abud et al., 2017; Douvaras et al., 2017; Haenseler et al., 2017; Muffat et al., 2016; Pandya et al., 2017). Two of these were updated versions of earlier protocols for macrophages (Van Wilgenburg et al., 2013; Yanagimachi et al., 2013). To choose which protocols to use in this work, each protocol was assessed for the practical elements of yield, cost, time-required, whether the produced “microglia-like” cells were tested in co-culture, how reproducible the protocol was (number of lines tested in), requirements for specialist equipment (FACS, O2 changing incubators). They were also assessed for key scientific elements of the cells produced such as the expression of key microglial genes and proteins, the ability of the cells to produce cytokines,

phagocytose, respond to chemotactic stimuli, produce reactive oxygen species and show the morphological characteristics of human microglia, see Appendix 2, Table A2.1 for easy comparison of the results for each protocol.

To summarise each protocol briefly, Muffat et al., published a protocol to differentiate microglia-like cells in which they differentiated human ESCs and iPSCs into embryoid bodies (EB) of two main types: neuralised, dense EBs and cystic EBs. Cystic EBs were positive for markers of early yolk-sac myelogenesis, such as PU.1 after 14 days in culture. These YS-EBs were collected and re-plated for 30 days. At this point, semi-adherent round cells appeared that were highly phagocytic and highly motile. These semi-adherent round cells were cultured for further to produce microglia-like cells with mRNA expression similar to human foetal microglia, that are phagocytic, produce cytokines in response to LPS stimulation and migrate in response to chemotactic stimuli. However, the yield per starting cell was low. The authors tested this protocol in 20 iPSC and ESC lines, indicating good reproducibility (Muffat et al., 2016). This protocol was initially tested in this thesis, chosen as it was one of the first available, however repeated attempts could not produce microglia cells with the appropriate gene expression (data not shown).

Another protocol was published by Pandya et al. They differentiated human iPSCs into microglia-like cells through exposure to defined growth factors followed by co-culture with astrocytes. Briefly, iPSCs were exposed to a number of key growth factors through culturing with two different defined media across 14 days. After 14 days cells expressed CD34, CD45, and CD43, markers for myeloid progenitor cells. These cells were further co-cultured with human astrocytes in medium containing IL-3, granulocyte-macrophage colony-stimulating factor (GM-CSF) and macrophage colony-stimulating factor (M-CSF). Following 1-2 weeks in culture, these cells were considered to be “mature” by the authors. Gene expression showed that these microglia-like cells showed similar expression to human foetal microglia, and dendritic cells and macrophages. These cells were phagocytic, capable of producing cytokines in response to stimulation (LPS) and produced ROS,. These cells were not tested in a co-culture setting however, and the authors only tested two iPSC lines, so the reproducibility

of these results across different lines is not clear, and the yield per starting cell was low, limiting this protocol's utility in this thesis (Pandya et al., 2017).

At a similar time, Abud et al., in the lab of Matthew Blurton-Jones, also published protocol detailing a method to differentiate iPSCs into microglia. iPSCs were initially differentiated into CD43+ myeloid progenitors using defined medium and temporal exposure to low (5%) oxygen levels. The medium was then changed to serum-free microglia differentiation media containing M-CSF, IL-34, TGF-β1, and insulin. Finally, microglia-like cells were exposed to CD200 and CX3CL1 for 3 days to induce maturation. Gene expression analysis showed these microglia-like cells cluster with human fetal and adult primary microglia. The clustering with adult microglia is of particular note, as this was not achieved by any other protocol. These cells were also phagocytic, showed chemotactic responses and cytokine production. The yield per starting cell was also high, and the protocol has been testing in 10 iPSC lines (Abud et al., 2017). However, given the requirement for low oxygen incubators, it was not possible to test this protocol in this thesis.

Douvaras et al., also published a protocol in which ESCs and iPSCs were differentiated into microglia, building on previous work by Yanagimachi et al. This involved exposure to a plethora of key growth factors over 25 days, after which CD14+/CX3CR1+ cells were isolated and further cultured with GM-CSF and IL-34 to produce microglia-like cells. These cells also show a gene expression profile which mirrors that of human foetal microglia. These cells also show phagocytic activity, cytokine production and chemotactic responses, and the protocol was tested in 16 iPSC lines, showing good reproducibility. However they were not tested in co-culture, and the yield per starting cell was low which are weaknesses (Douvaras et al., 2017). The earlier version of this protocol was tested in this thesis, with an initial aim to differentiate human macrophages (Yanagimachi et al., 2013). However, following the publication of this updated protocol by Douvaras, we added the maturation step described here and tested the protocol for generation of microglia-like cells, and found the gene expression as described.

Finally, Haenseler et al., describe the simplest protocol to produce microglia-like cells from iPSCs, building on previous work by Van Wilgenburg et al. iPSCs were

grown into EBs, and after 3-4 weeks in culture embryonic tissue resident macrophage precursors emerged in the cell culture supernatant. These cells are MYB-independent primitive myeloid cells, which appear early in development and differentiate into a range of tissue-resident macrophage cells (such as alveolar and kidney macrophages, microglia, Kupffer cells, and Langerhans cells) hence being termed macrophage precursors (Buchrieser et al., 2017). These precursors were harvested and subsequently either co-cultured for 2 weeks with iPSC-derived cortical neurons or in neuronal-type media. This produced a high yield per starting cell of microglia-like cells that are phagocytic, produce cytokines when stimulated, respond to chemotactic stimuli, adopt a dynamic and ramified microglia-like morphology and have a transcriptional profile similar to human foetal microglia. It was tested in 28 iPSC and ESC lines, showing that it is highly reproducible (Haenseler et al., 2017; Yanagimachi et al., 2013). Although this protocol does not produce cells with an adult microglia transcriptomic signature it was chosen for testing in this thesis due to its ability to produce cells that possess many key microglial features and because it did not require specialist facilities such as FACS or low oxygen incubators, and as such was much easier to implement within the lab.

This assessment shows that while the yield and reproducibility of these different protocols varies somewhat, each of these approaches produces myeloid, or “microglia-like” cells that show the key functional capacities and transcriptional profiles of human microglia, albeit foetal human microglia.

As of yet, there is no consensus on the ideal methodology to generate PSC-derived microglia. To truly compare these protocols, direct comparative studies are necessary to identify the most reliable and reproducible method to produce microglia-like cells. Additionally, it must be noted these protocols, with the exception of Abud et al., produce microglia similar to human foetal microglia. While there is some evidence for effects of HD at such an early stage (Ruzo et al., 2018), symptom onset for the non-juvenile form is generally in mid-life and the strongest disease phenotypes at the cellular level are most likely to be seen in adult microglia. This is relevant for this thesis, where the microglia-like cells are more foetal in nature, so likely to show less significant changes in phenotype. In the future, direct reprogramming of somatic cells to microglia might tackle this

problem by avoiding the resetting of the genetic clock that occurs during iPSC generation. This retention of age associated transcriptomic signatures has been previously shown in neurons and oligodendrocytes (Das et al., 2016; Melief et al., 2016; Yoo et al., 2011).

1.2.2.4.4. Microglia in Huntington's disease

Microglia have previously been shown to be dysfunctional in rodent HD models and in post mortem and imaging assessments in human patients. This will be covered in detail in the sections below: 1.2.1.1-1.2.1.3, where the evidence for dysfunction of the innate immune system in HD, both peripherally and in the CNS is detailed. Briefly, HD microglia from rodent models have shown deficits in migration and elevated cytokine release in response to stimuli such as MMP3, compared to control animals (Connolly et al., 2016; Kwan et al., 2012). Additionally, there is significant evidence of early microglial accumulation in HD patient brains, as shown by imaging (Pavese et al., 2006; Politis et al., 2015, 2011; Tai et al., 2007), although there are caveats to the methods used to assess this (Choi et al., 2011; Owen and Matthews, 2011; Venneti et al., 2006). Finally, some post mortem investigations have shown microgliosis and complement production in HD patient brains (Sapp et al., 2001; Singhrao et al., 1999).

Due to this evidence of microglial dysfunction in HD, the microglial-like cells produced by the Haenseler et al., (updated Van Wigenburg protocol) and Douvaras et al., (updated Yanagimachi protocol), once confirmed to be "microglial-like" in their gene expression and capacity for cytokine production and phagocytosis, were further assessed for possible differences between lines carrying expanded CAGs of increasing sizes and control lines.

1.2.3. Neuroinflammation and neurodegenerative diseases

It is clear that the innate immune system in the CNS, particularly microglia, has a vital role in responding to immune challenges, providing rapid responses to a large variety of pathogens and triggering longer term responses from the adaptive immune system. With this in mind, the innate immune system has become a target for focused study in disease models, particularly neurodegenerative diseases, where neuroinflammation is a commonly found phenomenon (Heneka et al., 2014). Neuroinflammation can be particularly damaging in neurodegenerative disease, because unlike a pathogenic infection where

resolution is rapidly achieved and the invading pathogen removed, the underlying issue in neurodegenerative diseases cannot be rapidly resolved and the immune response and resultant damage is ongoing. This can result in chronic and pathological activation of the innate immune system in these cases, characterised by the accumulation of microglial cells, the appearance of dystrophic microglia and astrogliosis (Ellrichmann et al., 2013; Staal and Moller, 2014). Peripheral immune challenges can also exacerbate disease progression, which has been found in a number of neurodegenerative diseases (Lee et al., 2008; Murray et al., 2011; Nguyen, 2004).

In Parkinson's disease (PD), the second most common neurodegenerative disease after Alzheimer's disease (AD), patients present with a characteristic movement disorder, associated cognitive impairment, and progressive disability (Kim et al., 2000). Similar to HD, the substantia nigra is preferentially lost in PD. Interestingly, epidemiological studies have found long term use of anti-inflammatory agents, such as aspirin, reduces the risk of developing PD (Chen et al., 2005, 2003). In addition, studies in acute animal models of PD such as MPTP-induced PD (Kurkowska-Jastrzębska et al., 2004) and 6-OHDA-induced PD (Carrasco and Werner, 2002; Sánchez-Pernaute et al., 2004) have found that pre-treatment or concurrent treatment with anti-inflammatory drugs results in less severe dopamine depletion and reduced PD symptoms.

In normal rats, LPS injections into the substantia nigra, cortex and hippocampus result in neurodegeneration in the substantia nigra only. This was then repeated in primary cultures from the same areas, and the same pattern found, with dopaminergic neurons most strongly affected (Kim et al., 2000). Interestingly, the authors noted that microglial number were highest in the substantia nigra *in vivo* and *ex vivo*, although this may be as a result of innate higher suspectibility of these cells causing greater activation, migration and proliferation of microglia in that brain area, rather than the elevated levels of microglia directly contributing to the neuronal loss. The permanent loss of substantia nigra neurons following LPS injection was also found in additional studies, which suggested the LPS treatmented resulted in mitochondrial injury that led to neuronal death (Herrera et al., 2000; Hunter et al., 2017). Additionally, the pro-inflammatory cytokine TNFα is found to be elevated in the CSF of PD patients and in post-mortem brain

samples (Mogi et al., 1994). In animal models of PD, blocking TNFα signalling results in reduced neuronal loss and behavioural changes (Hunot et al., 1999; McCoy et al., 2008). Taken together, these data point to neuroinflammation affecting disease pathology in PD.

Another progressive neurodegenerative disease where neuroinflammation has been heavily implicated is AD. AD is the most common neurodegenerative disease in the world, characterised by memory loss, cognitive impairment and impairment in daily living (Ferri et al., 2005; Lobo et al., 2000; Qiu et al., 2009). Pathologically, it can be characterised by the build-up of extracellular amyloid plaques and intraneuronal tangles composed primarily of tau protein (Perl, 2010). Interestingly, early research showed that reactive phagocytic microglia were associated with these amyloid plaques (Carpenter et al., 1993; McGeer et al., 1988; Perlmutter et al., 1992), and so a great deal of research has been conducted to understand the role of microglia in this AD pathology (Wyss-Coray and Rogers, 2012). Eliminating microglia in mouse models of AD does not seem to effect plaque size, but in one study there were some signs of improved behavioural performance following elimination of microglia (Dagher et al., 2015). More recently, research has shown that microglia show aberrant reactivation of the pruning activity of early brain development in early AD, leading to the synapse loss associated with the early stages of disease (Hong et al., 2016a). This highlights a mechanism by which microglia directly affect AD pathology. Epidemiological studies suggest anti-inflammatory drugs reduce the risk of late-onset AD with the duration of use being particularly important (Szekely et al., 2007; Vlad et al., 2008). Furthermore, perhaps the most convincing data for a role of the immune system in AD has come from a number of genome wide association studies, which have implicated microglia-related genes including TREM2 and CD33 (Bertram et al., 2008; Guerreiro et al., 2012; Hollingworth et al., 2011; Jonsson et al., 2013; Lambert et al., 2013, 2009; Naj et al., 2011) as risk factors for AD.

1.3. HTT and the innate immune system

1.3.1. Dysfunction of the innate immune system in HD

1.3.1.1. Evidence from rodent models

A number of studies suggest activation of the immune system in HD, as well as the presence of altered immune responses very early on in the disease, prior even to the onset of noticeable symptoms (Ellrichmann et al., 2013). Patients show elevated inflammatory cytokine levels in their peripheral blood and cerebrospinal fluid (CSF) up to 16 years before disease onset and post-mortem analysis of HD brain tissue shows elevated levels of inflammatory cytokine mRNA (Björkqvist et al., 2008). Moreover, a hyper-reactive phenotype of monocytes and macrophages has been consistently found across human and mouse models, with elevated responses to immune stimuli such as LPS or CSE (Björkqvist et al., 2008; Connolly et al., 2016; Trager et al., 2014). Specifically, the expression of pro-inflammatory cytokines such as IL-6, IL-1β, and IL-8 seem to be consistently elevated. Most recently, research by Connolly et al., 2016 in YAC128 mice found that primary microglia cultured *ex vivo* differentially express IL-12, IL-10, IL1-β, IL-2, IL-4 and IL-5 in response to treatment with LPS, CSE or MMP3, compared to YAC18 mice and wild type mice, with no change at the mRNA level for these cytokines. This is particularly physiologically relevant as elevated MMP3 levels have been found in HD CSF samples (Connolly et al., 2016). Another interesting finding from this research was the existence of regional differences in microglia, which were maintained when assessed *ex vivo*. Specifically, microglia were harvested from various brain areas and their cytokine profile was assessed. Microglia from all brain areas except those isolated from the hippocampus were hyper-reactive.

Interestingly, in primary rodent neuronal cultures transfected with exon 1 mHTT, wtHTT-expressing microglia migrated towards neurons expressing mHTT, and positioned themselves along irregular neurites. However, they did not localise with mHTT inclusions, or exacerbate pathology. Additionally, prior to the emergence of neuronal pathology in this model, the wtHTT-expressing microglia upregulated IBA1, and with the emergence of neurodegeneration an increase in the production of IL-6 and complement component 1q was found, suggesting the

microglia show localised pro-inflammatory cytokine production in response to neurodegeneration even when expressing wtHTT alone (Kraft et al., 2012).

Investigations also uncovered a migration deficit in response to ATP and C5a, in microglia isolated from both mouse models compared to their wild type littermates, when assessed *ex vivo* using a Boyden chamber assay (Kwan et al., 2012). This deficit was additionally found in patient monocytes and macrophages assessed *ex vivo*. As well as this, a more general deficit in motility was shown, with deficits in extension and retraction of processes, as well as actin remodelling.

1.3.1.2. Evidence from post-mortem human studies

This work in mouse models is complemented by a number of studies conducted using human HD patients either post-mortem or via non-invasive imaging. One such study looked at post-mortem brain samples from HD patients, and assessed various brain areas for the expression of key cytokines at the mRNA level. In this study, *IL-6* expression was found to be upregulated in the striatum, cortex and even the cerebellum, which is thought to be largely spared from neuropathology in HD. *IL-8* was elevated in the striatum and cortex alone, and *MM9* mRNA was only detectable in HD samples. *IL-10*, an anti-inflammatory cytokine, was also upregulated in the striatum and has previously been found to be elevated in patient plasma too, suggesting efforts by the immune system to dampen down the hyper reactivity found in the disease state (Björkqvist et al., 2008; Silvestroni et al., 2009). It is important to note, however, that this study had a small sample size, and that qPCR has some caveats to its use, with some transcripts degrading more rapidly in samples, and during qPCR itself some transcripts can be preferentially replicated according to their GC nucleotide content.

Other post-mortem studies found marked astrogliosis and microgliosis in multiple brain areas in HD samples, but not in controls (Sapp et al., 2001; Singhrao et al., 1999). Sapp et al., 2001, did this by staining for thymosin beta-4, a marker for microglia reactivity and found that reactive microglia occurred in all stages of pathology, and accumulated in density with increasing pathology; Singhrao et al., 1999, found that the expression of multiple components of the complement pathway were upregulated in microglia from HD brains compared to controls.

1.3.1.3. Evidence from imaging studies in humans

The results from these post-mortem studies have been accompanied by non-invasive imaging studies, to assess microglia activation in pre-symptomatic gene carriers as well as manifest HD patients. Pavese et al., 2006, found a significant increase in activated microglia in the striatum, as assessed by [11C](R)-PK11195 binding. [11C](R)-PK11195 binds specifically and selectively to the peripheral benzodiazepine receptor (PBR) also known as translocator protein (TSPO), which is expressed by both microglia and astrocytes, with a greater contribution from microglia, although this remains a source of debate (Mangiarini et al., 1996). TSPO ligands have been shown to modulate functions consistent with microglial activation and as such, [11C](R)-PK11195 binding has been used as a marker of brain injury and inflammation. However this method is limited by poor signal to background ratio, making quantification challenging, and the contribution of astrocytes to the signals seen should be considered (Choi et al., 2011; Owen and Matthews, 2011). That being said, this method showed that microglial activity level assessed in this way was correlated with disease severity in HD, which itself was measured by assessing the striatal binding of [11C]raclopride, a marker of dopamine D2 receptor binding and thus a proxy for GABAergic cell function in the region, as well as the Unified Huntington's Disease Rating Scale score and the patient's CAG index. Also detected were significant increases in microglia activation in cortical regions including prefrontal cortex and anterior cingulate (Pavese et al., 2006).

A similar study made volumetric measures of HD brains using structural MRI, as well as the same functional measures using PET for D2/D3 receptor binding ([11C]raclopride) and activation of microglia ([11C](R)-PK11195) in HD brains. This was used to investigate the structure and function of individual brain regions and estimate regional networks known to be linked to key psychiatric, cognitive and motor symptoms in HD. In this way, the authors were able identify a close association between levels of microglial activation and clinical scales of disease severity and measures of daily living. Perhaps most interestingly, in the case of pre-manifest HD gene carriers, a correlation between microglial activation and the predicted probability of HD onset in the next five years was found (Politis et al., 2011), which was confirmed by another study (Tai et al., 2007). In a follow up study, the authors were able to find a correlation between increased microglial

activation in the cortical, basal ganglia and thalamic brain regions with elevated plasma levels of pro-inflammatory cytokines such as IL-1β , IL-6, IL-8 and TNFα in pre-symptomatic gene carriers predicted to be more than ten years from disease onset (Politis et al., 2015).

This fits with previous work in the peripheral immune system that found elevated cytokine levels in pre-manifest gene carriers, the likely source of which being the innate immune cells of the periphery, monocytes and macrophages. These cells, when isolated from pre-manifest gene carriers as well as manifest HD patients show a hyper-reactive phenotype, producing elevated levels of pro-inflammatory cytokines when assessed *ex vivo,* which is corrected upon *HTT*-lowering treatment (Trager et al., 2014). RNA sequencing of primary monocytes from manifest HD patients and controls sought to begin to investigate the underlying mechanism of this hyper-reactive phenotype, and intriguingly found that HD monocytes appear to be "primed" for immune reactions, with elevated mRNA expression levels of a number of key inflammatory cytokines under baseline conditions (Miller et al., 2016). This is in line with work conducted using the BV2 microglial cell line transfected with wtHTT or mHTT, which found that expression of mHTT promotes autonomous microglial activation through increased expression and activity of the myeloid lineage-determining factors, PU.1 and C/EBPs. These factors prime certain enhancers and promoters for binding by signal-induced transcription factors such as NF-κB. This was linked with elevated gene expression levels of pro-inflammatory cytokines *in vivo*. Additionally, when BV2 cells were co-cultured with mouse ESC-derived neurons, only those expressing mHTT increased neuronal apoptotic activity. Additional studies using primary human myeloid cells isolated from whole blood samples found that the load of mHTT fragments in these cells increases with disease load, as measured by levels of caudate atrophy (Weiss et al., 2012).

1.3.1.4. Evidence against targeting the immune system in HD

Finally, some *in vivo* mouse work published recently has cast doubt over the therapeutic benefits of targeting the innate immune system in HD and particularly microglia. Petkau et al., 2019, found that knocking out mHTT expression in microglia alone in the BACHD mouse model while maintaining mHTT expression in the rest of the CNS, appeared to successfully reduce elevated IL-6 expression

when assessed *ex vivo*, but did not rescue any of the phenotypes associated with HD. Additionally, when mHTT was knocked out in all CNS cell types except microglia, there was a significant rescue of body weight, rotarod performance and striatal volume (Petkau et al., 2019). While this research has some caveats, it does suggest that while HD microglia appear to be functionally altered compared to control microglia, this is insufficient alone to alter disease progression. This may be due to the relatively low percentage of microglia in the brain. In humans, microglia comprise approximately 10% of the number of cells in the CNS and are relatively small, (Jinno et al., 2007). Therefore, a reduction of mHTT in this small population may not alter the overall mHTT load in the brain to any great degree, meaning a sufficiently toxic environment can still develop, allowing neuronal pathology to progress whilst also causing wtHTT-expressing microglia to become dystrophic. Microglia are highly reactive cells, and so the impact of the environment that microglia are in, cannot be underestimated.

Crucially, recent single-cell RNA sequencing studies in mice have called into question the level of HTT expression in microglia. One such study, conducted in 41 mice, analysed the RNA expression in 76,000 individual microglia in mice during development, in old age and following brain injury. They identified nine clusters of microglia types and one monocyte/macrophage cluster. While it was not highlighted in their paper, the results for HTT expression can be found using their website and search function (http://www.microgliasinglecell.com/). This showed a sporadic pattern of HTT expression, with the majority of cells showing no expression at all (Hammond et al., 2019). Another study also conducted single cell RNA sequencing in adult mice only, profiling 690,000 cells (Saunders et al., 2018). Again, the expression level of HTT was not mentioned in their paper, however the authors have developed an interactive online software to allow their results to be searched (http://dropviz.org/). Searching for HTT in this software should that HTT is expressed in microglia (Microglia_Macrophage_C1qb or Microglia_Macrophag_Tmem119-Mrc1). With the highest levels in the thalamus, then increasingly less in the frontal cortex, cerebellum, globus pallidum, posterior cortex, substantia nigra, hippocampus and striatum, in that order. However, neurons did appear to show higher levels of expression. This fits with work completed in three murine models of HD and post mortem HD patient samples which have shown that only 0-2% of microglia have HTT inclusions (Jansen et

al., 2017). Altogether, this calls into question the validity of targeting mHTT in microglia, and suggests that the altered phenotypes in HD microglia shown thus far may be due to non-cell autonomous effects. Future studies should regularly assess HTT expression levels in microglia. Unfortunately this was not considered in this thesis, and is a weakness of the experiments included here.

Another study, conducted in the R6/2 model of HD, found numbers of microglia are significantly lower in the R6/2 model at the end stage of disease compared to controls. To try and alleviate this, a program of regular low dose LPS injections was implemented to increase microglial numbers. An increase in microglial numbers was induced, and correlated with an increased life span in these LPS-treated mice (Lee et al., 2018). However, it is worth noting that in HD patients an increase of microglia is seen that correlates with disease progression, so this result may not be applicable to the human disease.

1.3.1.5. Possible mechanisms underlying immune dysfunction in HD

Based on all the above research, a number of theories exist as to the mechanism underlying the immune dysfunction that is seen in HD. One theory is that aberrant NF-κB pathway activation occurs due to the presence of mHTT, leading to elevated immune responses. Trager et al., 2014, found that translocation of RELA (p65) to the nucleus occurred in a greater proportion of HD monocytes *ex vivo* compared to control samples, when stimulated with LPS, and that this translocation lasted longer in HD samples. Combined with findings in BV2 cells, this suggests that the presence of mHTT interacts with the NF-κB pathway at some level, to increase activity and also slow the resolution of responses to stimuli (Crotti et al., 2014).

In addition, there is significant evidence suggesting that the presence of mHTT alters ROS production in a polyQ-dependent manner (Wyttenbach et al., 2002). Interestingly, ROS have been shown to have a significant impact on the activation of the NF-κB pathway. For example, exogenously added hydrogen peroxide causes phosphorylation of IκBα on Tyr42 or other tyrosine residues and subsequent degradation of IκBα and activation of NF-κB pathway (Takada et al., 2003). There is also evidence that this activation of the pathway by ROS is through a distinct mechanism from how it is triggered by pro-inflammatory cytokines or antigens (Schoonbroodt et al., 2000). In this way, it may be possible

that mHTT interacts with the NF-κB pathway directly, and also through affecting ROS production.

1.3.2. Wild-type HTT in the innate immune system

In general, HD research has focused on the effects of mHTT, rather than wtHTT, and as such, there is not yet a clear picture of the role of wtHTT in the immune system. However, we do know that *HTT*-lowering via siRNA treatment of control *ex vivo* human macrophages results in a reduction in cytokine expression (Träger et al., 2014), which suggests a role for wtHTT in cytokine expression. Research into HTT's interacting partners more generally has suggested roles in transcription, RNA splicing, endocytosis, vesicular trafficking, and cellular homeostasis, as well as having anti-apoptotic effects. Additionally, the strength of some of these interactions is altered by the presence of the expanded polyQ (Harjes and Wanker, 2003). It may be through these interacting partners that wtHTT effects cytokine expression, but further research is required to assess these possibilities.

1.3.3. Pharmacological interventions targeting the innate immune system in HD

Several pharmacological interventions have been tested in mouse models of HD, with disease-modifying effects seen. For example, peripherally administered cannabinoid receptor 2 (CB2) agonist caused suppression of motor deficits and CNS inflammation in transgenic mice, whilst extending their life span. Interestingly, the application of a peripherally restricted CB2 antagonist blocked these effects, despite the presence of the agonist in the CNS (Bouchard et al., 2012). This points to a peripherally-restricted effector mechanism. Additionally, manipulating the KMO pathway of tryptophan degradation in peripheral immune cells results in extended lifespan of HD mice, with prevention of synaptic loss and a reduction in microglial activation. Interestingly, the modifying drug cannot cross the blood brain barrier so effects are due to peripheral manipulation alone (Zwilling et al., 2011). However, blood brain barrier leakage has been shown to exist in HD patients, with infiltration of peripheral immune system macrophages into the CNS. Indeed, it was recently shown that right caudate leakage correlates with HD progression, and although this does not show any causation it may be worth exploring further to see if cross-talk and CNS-infiltration plays a role in

progression and should therefore be considered when investigating therapeutic avenues (Drouin-Ouellet et al., 2015).

Some studies have found anti-inflammatory agents such as minocycline to be protective, effectively delaying mortality in the R6/2 model of HD (Chen et al., 2000), but this has not been replicated in other transgenic models of HD or with other anti-inflammatory drugs (Mievis et al., 2007; Norflus et al., 2004; Smith et al., 2003). Additionally, clinical trials with minocycline in HD patients showed only minimal improvement and even decline in cognitive performance in some cases (Cudkowicz, 2010). Laquinimod, another immunomodulatory agent which has shown some efficacy in cell models of HD, was also recently found to be ineffective in a clinical trial for HD (Kieburtz et al., 2018).

1.3.4. Targeting the immune system therapeutically in HD

There is considerable evidence in favour of targeting proinflammatory processes with an anti-inflammatory agent to treat neurodegenerative diseases, as previously described, with long term use of NSAIDs has been shown to reduce the risk of PD and AD (Heneka et al., 2014; Lucin and Wyss-Coray, 2009). However, the innate immune system, and the immune system generally, are incredibly complex, with many interacting signalling pathways. In this way, targeting specific aberrant proinflammatory cytokine levels as seen in HD, could have unforeseen negative effects. This has been the case in AD therapeutics research, where levels of IL-10, an anti-inflammatory cytokine, were increased in a mouse model of AD to combat neuroinflammation. Unfortunately, this caused suppression of microglial phagocytosis of amyloid beta, a concomitant increase in amyloid plaque accumulation, as well as a worsening of the memory impairment seen in the model (Chakrabarty et al., 2015).

A general dampening down of the immune system in HD may not, therefore, yield entirely positive therapeutic outputs. Rather, we will have to elucidate the underpinnings of the dysfunction seen in HD and discover more specific targets, to allow us to inhibit the damaging, negative impacts of the dysfunctional immune response, without impairing the protective effects of the immune system that have been seen in HD generally.

1.4. PhD aims and objectives

The overall aim of this work is to determine the mechanism(s) by which mutant and wild type HTT regulate myeloid cell function and contribute to innate immune system dysregulation as a potential modifier of HD progression.

More specifically, my work had two main aims:

1. To investigate the effects of mHTT on both the peripheral and CNS components of the innate immune system; monocytes and macrophages, and microglia, respectively.
2. To assess the functional role of wtHTT in peripheral innate immune cells.

The objectives of my work were:

1. Establish and characterise a human PSC-derived HD monocyte and macrophage cell model
2. Establish and characterise a human PSC-derived HD microglial cell model.
3. Investigate the effects of knockdown of wtHTT on human macrophages' function and biology.

2 Chapter 2: Materials and methods

2.1 Subject recruitment and classification

All experiments with human samples were performed in accordance with the Declaration of Helsinki and approved by the University College London (UCL)/UCL Hospitals Joint Research Ethics Committee (LREC 03/N008). All subjects provided informed written consent prior to sample donation or tissue biopsy. Blood samples were taken from control subjects recruited from staff and students at the UCL Institute of Neurology, in accordance with the study's ethics approval. Subjects with potential inflammatory or infective conditions were excluded from the study, as were subjects on immunomodulatory medications. Skin biopsies were taken from subjects recruited through the Huntington's disease clinic at the National Hospital for Neurology and Neurosurgery, London.

2.2 Isolation of blood monocytes

Whole blood samples were collected using BD Vacutainer® Cell Preparation Tubes containing polyester gel and a density gradient liquid that allows for isolation of PBMCs through a single centrifugation step at 1000 x*g* for 30 min, with the brake turned to "slow" for deceleration. The PBMC layer was then aspirated from the upper interface into a fresh sample tube using a sterile plastic Pasteur pipette. The sample was topped up to 30 ml with ice-cold sterile PBS and then centrifuged at 350 x*g* for 15 min, and the supernatant discarded.

To select for monocytes alone, cells were resuspended in 280 µl MACS buffer (PBS, 1% bovine serum albumin (BSA), 2 mM EDTA) and 60 µl CD14 microbeads (Miltenyi Biotec) and incubated at 4 °C for 15 min. The cells-beads mix was then centrifuged at 350 x*g* for 5 min before being resuspended in 1 ml MACS buffer. Magnetic cell sorting was carried out by placing MACS columns (Miltenyi Biotec) in a magnetic field and pre-washing with 500µl MACS buffer, before adding each cell suspension to an individual, labelled column. Once the cell suspension had passed through the column, the columns were washed with a total of 4 ml MACS buffer. Magnetically labelled cells were collected by removing the columns from the magnetic field and plunging 2.5 ml MACS buffer through the column twice using a plunger. The sample was topped up to 10 ml with MACS buffer and the isolated monocytes were counted using a Neubauer

counting chamber before being seeded on appropriate plates at an experiment-dependent density for downstream experiments.

2.3 Primary human monocyte and macrophage cell culture

Culture of primary human immune cells was carried out in a Containment Level 2 laboratory using strict aseptic technique. A tissue culture hood with a laminar flow unit was used for all procedures, including preparation of culture media and reconstitution of reagents. All reagents and plastics used for tissue culture were bought pre-sterilised and only opened within the tissue culture hood. All cells were cultured in an incubator set to 37 °C with 5% CO_2. Primary human immune cells were cultured in R10 media (RPMI 1640 supplemented with 10% FBS, 2 mM L-glutamine, 50 units/ml penicillin and 50 µg/ml streptomycin).

Monocyte-derived macrophages were obtained by adding 20 ng/ml GM-CSF (Cell Guidance Systems) to the monocyte culture media for six days to induce differentiation. The media was changed after three days to provide the cells with fresh media and GM-CSF for the final three days of the differentiation process. Monocytes treated with GM-CSF exhibited a macrophage phenotype after six days in culture.

2.4 iPSC and ESC cell culture

2.4.1 Generation of HD family iPSC lines

Induced PSCs were generated from fibroblasts in skin biopsies taken from three siblings with juvenile HD and carrying *HTT* mutations with polyQ (glutamine) lengths 58, 69 and 75 respectively, and their unaffected parent with a 22 polyQ, as a non-disease control. Two adjacent 3 mm punch biopsies taken from each subject's forearm were cut into squares of 0.5-1mm^2 and placed epidermis side up into one well of a 6-well plate containing two drops of pre-warmed fibroblast medium (DMEM with glutamax, 4.5 g/L glucose and 1 mM pyruvate (Gibco), 10% foetal bovine serum, 50 U/ml penicillin, 50 µg/ml streptomycin, 2.5 ml/L amphotericin, 2.5 ml/L amphotericin). A sterile coverslip was placed over the pieces of tissue to help them adhere to the plate and a further 2 ml pre-warmed medium added to the well, ensuring not to dislodge the coverslip. Following incubation at 37 °C, 5% CO_2 for one week, the media was changed. After this, cells were media changed every 3-4 days and passaged when required using

0.05% Trypsin-EDTA, re-seeding each time at $1x10^4$ cells/cm^2. During expansion of the cultures, cells were frozen down at passages three, four and five for storage in liquid nitrogen until required. The cells were used to generate iPSCs by Sendai virus reprogramming using the CytoTune-iPS 2.0 Sendai reprogramming kit (Thermo Fisher). These were verified by the expression of pluripotency markers, differentiation into all germ layers using a self-organisation assay, karyotyping, Sanger sequencing to confirm the CAG repeat length and confirmation of the absence of exogenous Sendai virus. Regular karyotyping and CAG sizing were not repeated after this point, however, which is a weakness of this approach. Three different clones of iPSCs were generated from each subject. These lines will be referred to as the "HD family lines" throughout this thesis. At a later time point, iPSCs from a patient carrying 125Q were generated in the same manner.

2.4.2 Generation of IsoHD ESC lines

An isogenic allelic ESC series was generated by the Pouladi group at Singapore University and shared with the Tabrizi lab. The method for generating these lines is described in their recent publication (Ooi et al., 2019). Briefly, H9 hESCs were chosen as the parental cell type to incorporate increasing CAG repeat lengths in exon 1 of HTT. To facilitate gene modifications in the CAG tract of HTT, two pairs of transcription activator-like effector nucleases (TALENs), which cleave either upstream (USPQ) or downstream (DSPQ) of the CAG repeat tract, were generated. DSPQ TALENs were more active than USPQ TALENs.

Donor DNA was constructed using a previously published strategy (Xu et al., 2017) and comprised homology arms carrying 30, 45, or 81 polyQ (glutamine) repeats in exon 1 of HTT. The homology arms flanked a piggyBac selection cassette that contains genes encoding EGFP, puromycin resistance (puroR), and thymidine kinase. DSPQ TALENs and donor DNA were transfected into H9 hESCs, and triple-antibiotic selection used to select for successful transformed cells. Monoallelic knock-in of the expanded polyQ tract in all clones was confirmed by PCR. To eliminate potential confounding effects of the selection cassettes, targeted hESCs were transfected with excision-only PiggyBac transposase plasmid, and removal of the selection cassette was validated by PCR. Overall, the resultant allelic panel contains heterozygous hESCs with a high CAG allele of 30, 45, and 81 repeats in exon 1 of HTT (encoding HTT protein

with a corresponding number of polyQs), referred to as “IsoHD cells” (Ooi et al., 2019).

2.4.3 Origins of other PSC lines

An additional, unrelated control iPSC line was used in experiments, carrying a 15 polyQ repeat, generated from a male donor, age-matched to the juvenile HD donors, gifted to the Tabrizi group by the Houlden lab at UCL. An additional control line (20Q) was generated by the Brivanlou group and gifted to the Tabrizi lab. Briefly, they combined CRISPR/Cas9 technology with ePiggyBac transposition to edit the genome of the RUES2 hESC line at the HD gene, reinserting the normal 20Q repeat into the control line to account for the effects of the gene editing process itself (Ruzo et al., 2018).

2.4.4 Culture of PSCs

Culture of iPSCs and ESCs was carried out in a Containment Level 2 laboratory using strict aseptic technique. A tissue culture hood with a laminar flow unit was used for all procedures, including preparation of culture media and reconstitution of reagents. All reagents and plastics used for tissue culture were bought pre-sterilised and only opened within the tissue culture hood. All cells were cultured in an incubator set to 37 °C with 5% CO_2. All non-differentiating cells were cultured on Nunc™ cell-culture treated multidishes coated with Geltrex LDEV-Free reduced growth factor basement membrane matrix at a dilution of 1:100, and in Essential 8 media (E8+; Gibco) unless otherwise stated.

Upon reaching ~85% confluency, PSC cultures were split at a 1:6 ratio, or less if required, using either EDTA (0.5 mM; Thermo Fisher Scientific) or TrypLE™ Express Enzyme phenol red (1x; Thermo Fisher Scientific), depending on the downstream experiment. In all cases, the media from the confluent wells was removed, and the well washed with D-PBS, then EDTA or TryPLE was added and incubated for 3-4 min at 37 °C. Following the incubation period, the EDTA was removed and the cells removed from the well by gentle trituration with the appropriate media, before seeding in a fresh, coated-plate at the appropriate density. When TryPLE was used, cells were triturated in the TryPLE itself, before collection in a fresh falcon tube and dilution 1:10 with DPBS. This suspension was centrifuged at 350 xg for 5 min, and the cell pellet resuspended in the appropriate media and plated at the required density.

To store PSC stocks, cells were washed with D-PBS and then harvested using EDTA (0.5 mM) as described in the above section, prior to collection in freezing media (E8+ containing 10% DMSO). Approximately 1 ml of cell suspension (from one well of a six well plate) was added per labelled cryovial, which was placed quickly into a Mr Frosty vessel and frozen overnight in a -80°C freezer prior to transfer to a liquid nitrogen tank for long term storage.

To thaw these frozen stocks of PSCs, vials of the desired genotype were removed from liquid nitrogen storage and thawed quickly by immersion in a 37 °C water bath without submerging the cap. The thawed cell suspension was then transferred gently to a fresh 15 ml conical tube, before room temperature media was slowly added in a dropwise fashion to reduce the osmotic shock to the cells while diluting out the DMSO in the freezing media. The cell suspension was then centrifuged at 200 xg for 5 min, and the resulting supernatant aspirated and discarded. The cell pellet was then resuspended in E8+ media containing ROCK inhibitor (Y27632, Sigma; 1:1000) and plated at the required density and gently placed in a 37 °C, 5% CO_2 incubator to settle overnight. The following day the media was replaced by E8+ media without ROCK inhibitor. The spent media was then replaced daily until the cells reached approximately 85% confluency.

2.5 Differentiation of PSC-derived microglia-like cells

2.5.1 The ‘Yanagimachi method’

The Yanagimachi et al., protocol consisted of five sequential steps. On day 0, primitive streak cells were induced from undifferentiated PSCs through treatment with bone morphogenetic protein 4 (BMP4) at 80 ng/ml in E8+ media. In the second step, on day 4 of the protocol, these cells were differentiated into KDR+ CD34+ hemangioblast-like hematopoietic progenitors using StemPro 34 supplemented media (Gibco) containing 2 mM Glutamax with vascular endothelial growth factor (VEGF) at 80 ng/ml, basic fibroblast growth factor (bFGF) at 25 ng/ml and stem cell factor (SCF) at 100 ng/ml. These hematopoietic progenitors were then committed towards initial myeloid differentiation in step three on day 6, using a cocktail of cytokines consisting of SCF at 50 ng/ml, interleukin 3 (IL-3) at 50 ng/ml, thrombopoietin (TPO) at 5 ng/ml, macrophage colony-stimulating factor (M-CSF, also known as colony stimulating factor 1, CSF1) at 50 ng/ml and FMS-like tyrosine kinase 3 ligand (Flt-3 ligand) at 50 ng/ml

in supplemented StemPro34 containing 2 mM Glutamax. These cells were then differentiated further into the myeloid lineage in step four, using a similar cocktail of Flt3 ligand (50ng/ml), granulocyte-macrophage colony-stimulating factor (GM-CSF, or colony stimulating factor 2, CSF2) at 25 ng/ml and M-CSF at 50 ng/ml from day 13-15 onwards, producing tissue resident macrophages. Importantly, the original protocol describes these cells as monocytic-lineage cells, yet subsequently were shown to be tissue-resident macrophages (Douvaras et al., 2017).

These tissue resident macrophage cells were isolated using CD14 microbeads (Miltenyi Biotec), as described in section 2.2. Finally, when an experiment required matured tissue resident macrophages, a fifth step was added, which involved CD14+ cells being cultured in RPMI-1640 medium (Sigma) supplemented with 10% foetal bovine serum (FBS) and M-CSF (100ng/mL, Cell Guidance Systems) for seven days with a media change at day four.

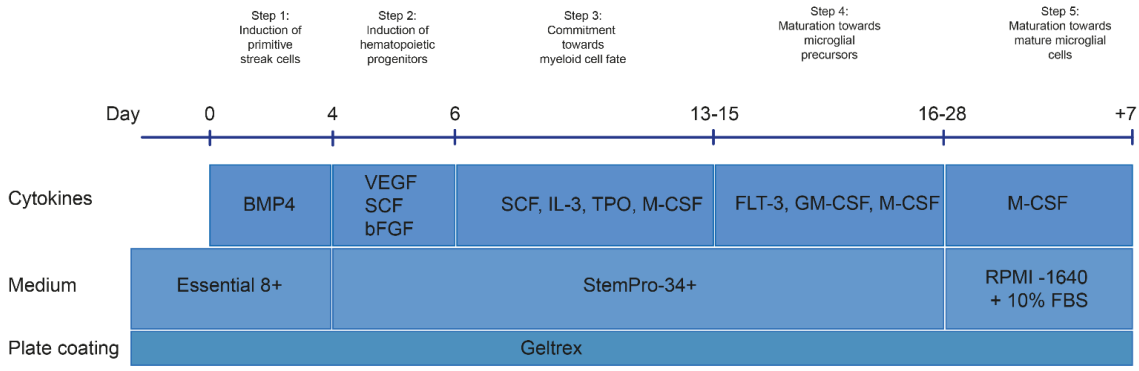

Figure 2.1 The Yanagimachi et al., 2013 protocol. Step 1: Primitive streak cells were induced from undifferentiated ESCs/iPSCs. Step 2: Cells were differentiated into hemangioblast-like hematopoietic progenitors. Step 3: Cells were committed towards initial myeloid differentiation. Step 4: Cells were differentiated into “monocytes” as described by the original paper, now referred to as “microglial precursors” defined as cells expressing CD14 and CX3CR1. Where more “mature” cells were required, harvested precursors were then cultured for a week in media supplemented with M-CSF to promote differentiation towards a further differentiated state.

2.5.2 The ‘Haenseler method’ (adapted Van Wilgenburg)

Microglia-like cells were differentiated according to a published protocol by Van Wilgenburg et al., 2013, and an adapted version used by Haenseler et al., 2017. Briefly, the protocol involves two major steps. First, embryoid bodies were formed by seeding 10,000 cells/well in a round-bottomed 96 well Corning Costar ultra-low attachment dish in the appropriate media (E8+ media with 50 ng/ml BMP-4 (Peprotech), 50 ng/ml VEGF (Cell Guidance Systems), 20 ng/ml SCF (Cell Guidance Systems) and 10 mM ROCK Inhibitor (Y27632, Sigma), followed by a brief centrifugation (3 min at 800 xg) to collect the cells at the bottom of each well. The embryoid bodies were collected five days later, and harvested into appropriate sized flasks (Thermo) with approximately 150 EBs per T175 flask in microglial differentiation media, consisting of X-vivo media (Lonza) supplemented 2 mM L-glutamine, 50 units/ml penicillin and 50 µg/ml streptomycin and 100 ng/ml M-CSF (Cell Guidance Systems), 25 ng/ml IL-3 (Cell Guidance Systems) and 2-mercaptoethanol at 1:1000 from 50 mM stock (Gibco). These EBs were then media changed weekly, with harvesting of tissue-macrophage precursors, so-called as they are MYB-independent primitive myeloid cells, which appear early in development and differentiate into a range of tissue-resident macrophage cells (such as alveolar and kidney macrophages, microglia, Kupffer cells, and Langerhans cells) (Buchrieser et al., 2017) from three weeks post EB harvesting. Harvested precursors were then cultured for two weeks in microglial maturation media, consisting of DMEM/F12 supplemented with 2 mM L-glutamine, 50 units/ml penicillin and 50 µg/ml streptomycin and 100 ng/ml GM-CSF (Cell Guidance Systems) and 100 ng/ml IL-34 (R&D Systems) to promote further differentiation. All plates for maturation, other than Cell Carrier-96 (Perkin Elmer), were Primaria.

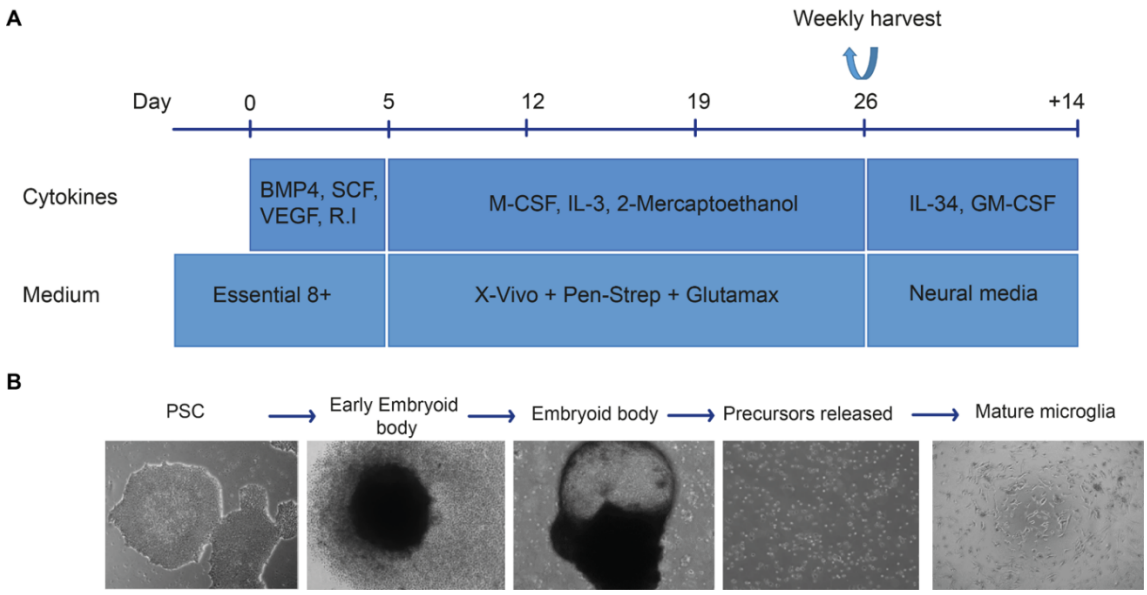

Figure 2.2: The Haenseler (adapted Van Wilgenburg) protocol. A) A graphical summary of the protocol, including the timeline of differentiation, and the media and cytokines used to progressively differentiate PSCs to microglia-like cells. **B**) Bright field images of cells at each stage of the protocol, from PSC stage to microglia-like cells.

2.6 Differentiation of PSC-derived MSNs

PSCs were cultured on Geltrex (1:100, Gibco) according to the manufacturer's instructions. Cells were differentiated to neuronal cultures containing MSNs using a protocol adapted from Arber et al., 2015 with several modifications. Briefly, this involved neural induction of PSCs at the appropriate confluency through the addition of N2B27pre medium (DMEM/F12 and Neurobasal media in a 2:1 ratio, with N2 supplement and B27 supplement without vitamin A, and 2 mM L-glutamine) supplemented with 100 nM LDN193189, 10 µM SB431542 and 200 nM dorsomorphin. Passage 1 was conducted between day 9-12 after neural induction. Cells were split 2:3 onto fibronectin-coated (Millipore) 12-well plates (Thermo Nunc) in N2B27pre medium supplemented with ROCK inhibitor (Y27632, Sigma) and activin A (PeproTech). Twenty four hours later, the 1 ml of media on the cells was removed and replaced with 1.5 ml N2B27pre medium with activin A, without ROCK inhibitor. Thereafter, cells received a 50% media change every other day to gradually dilute out the ROCK inhibitor. At day 19-22 following neural induction, passage 2 was conducted. Cultures were dissociated with EDTA, and re-plated onto poly-D-lysine and laminin-coated 6-well plates (Thermo

Nunc), resulting in a split ratio of 1:3. At day 28-30 of differentiation, cells were dissociated and plated for imaging. CellCarrier-96 well plates (Perkin Elmer) were pre-coated with Geltrex (1:100 diluted in cold DMEM:F12) at 37 °C for at least one hour prior to use, but no longer than 24 h in advance. After aspirating off the spent media, room temperature Accutase (0.5 ml per well) was applied directly to cells, and incubated at 37 °C for 10 min. Cells were dissociated to near single cell suspension by trituration using a P1000 pipette. Cells were washed by centrifugation through 10 ml PBS at 280-300 xg for 3 mins. The supernatant was discarded and the cell pellet resuspended in 1 ml N2B27 post medium. Cells were counted and seeded at 30,000 per well in 200 µl N2B27 Post (DMEM/F12 and Neurobasal media in a 2:1 ratio, with N2 supplement and B27 supplement with vitamin A, and 2mM L-glutamine). After 48 hours the wells received a half media change. Every other day after this, half the culture medium was changed until day 36 when the cultures are considered to be sufficiently mature to conduct experiments.

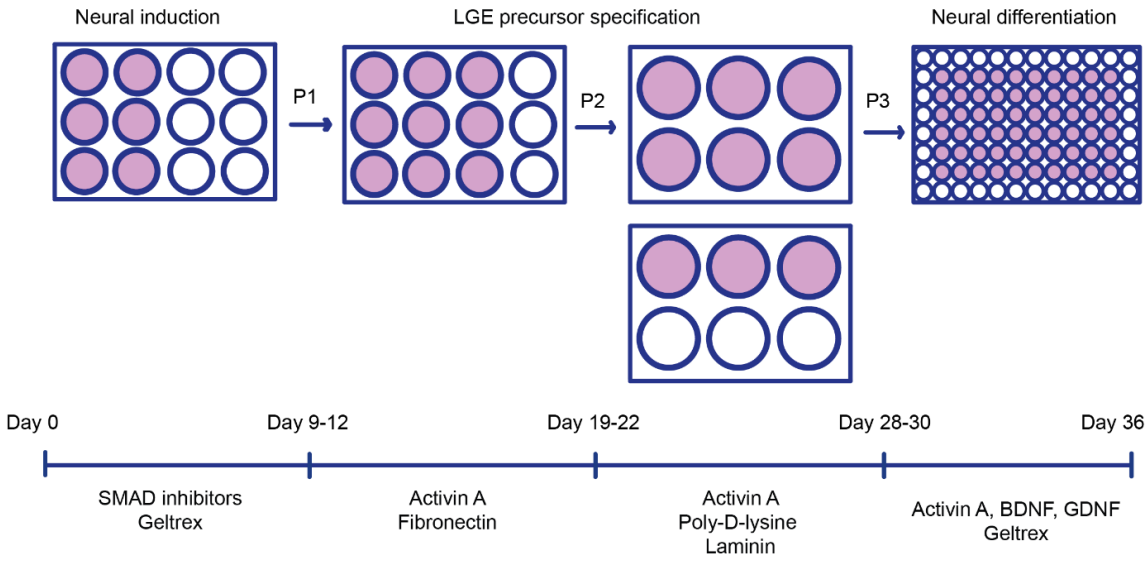

Figure 2.3: The protocol used to differentiate MSN-enriched neuronal cultures based on Arber et al., 2015. Differentiation of PSCs to MSN-enriched neuronal cultures took place over 36 days, with four different differentiation media used and three passage steps to progressively differentiate the cells towards a neuronal fate, at a final density suitable for high content imaging (HCI). BDNF=

brain-derived neurotrophic factor, GDNF= glial cell-derived neurotrophic factor, LGE= lateral ganglionic eminence, P= passage.

2.7 Conditioned media and CSF treatments of PSC-derived cells

2.7.1 Treatment of microglia-like cells with MSN conditioned media

MSN media was harvested from day 36 PSC-derived MSN cultures. Baseline and stressed samples were collected by either harvesting media 24 h following a media change, or 24 h following a heat treatment of 45 min at 42 °C. Harvested media was immediately snap frozen on dry ice and stored at -80 °C until use. Frozen media samples were then placed on ice at 4 °C overnight to thaw and diluted 1:2 with unconditioned microglia media before use. Control media conditions were unconditioned microglia media, and unconditioned MSN media diluted 1:2 with unconditioned microglia media.

On day zero of the experiment, microglia-like cells were media changed into these various media treatments following their fourteen day maturation period. At least 10-12 wells of a 96 well dish were used for each media treatment. On day two, the wells received a media change of the appropriate media type. Finally, on day five, 50 µl of media from each well was harvested and assessed by LDH assay as described in section 2.12.1, and the cells fixed before staining for IBA1 and Caspase 3. These plates were then imaged and analysed using the Opera Phenix high content imaging (HCI) platform (section 2.10).

2.7.2 Treatment of microglia with CSF

CSF harvested from HD patients and controls, kindly provided by Dr Ed Wild, was collected according to the published protocol for the HD-CSF study (Lauren M Byrne et al., 2018b). Briefly, lumbar punctures were carried out between 9 and 10.30 am, after 12 h fasting, samples were collected on ice and processed within 30 min of collection by centrifugation and freezing using standard kits containing polypropylene plasticware supplied by the HDClarity study. CSF samples were thawed on ice for 4 h prior to use. For ROS assessments, microglia-like cells were incubated in CSF samples diluted 1:2 in Assay buffer. For LDH assessment and HCI screening, CSF samples were diluted 1:2 in microglia media.

2.7.3 Treatment of MSNs with microglia-like cells-conditioned media

Microglia media was harvested from microglia-like cells kept in culture for 14 days to develop characteristics such as expression of key microglial genes and proteins, and develop functional capacities such as phagocytosis and cytokine production. Baseline and stimulated samples were collected either 24 h after a media change, or 24 h after treatment with 2 µg/ml LPS and 10 ng/ml IFNγ. These samples were immediately snap frozen and stored at -80 °C until use. Frozen media samples were then placed on ice at 4 °C overnight to thaw and diluted 1:2 with unconditioned MSN media before use. The control media condition was unconditioned MSN media.

On day zero of the experiment, MSNs were media changed into these various media treatments, at day 36 of their differentiation protocol. Twelve wells of a 96 well dish were used for each media treatment. On day two, the wells received a half media change of the appropriate media type. Finally on day five, the cells fixed before staining for H2AX, Caspase 3, DARP32, CTIP2 and nestin. These plates were then imaged using the Opera Phenix HCI platform (section 2.10).

2.8 GeRP-mediated *HTT*-lowering

β-1,3-D-glucan-encapsulated siRNA particles (GeRPs) were synthesised according to a previously published method (Soto et al., 2012). Macrophages were transfected with GeRP particles on day three of the differentiation protocol. GeRPs containing the appropriate siRNA (either targeting *HTT*, or a scrambled siRNA sequence as a control, see table 2.1 for sequences) were added to the cells at a 10:1 particle to cell ratio, then incubated for 24 h before being removed by a complete media change.

Table 2.1: siRNA sequences used in HTT knock-down experiments

Primer		Sequence
anti-HTT siRNA	Guide strand	5’- pUUCAUCAGCUUUUCCAGGGUC-3’
	Passenger strand	5’ -CCCUGGAAAAGCUGAUGACGG -3’
scrambled siRNA	Guide strand	5’-pUUUCGAAGUACUCAGCGUGAG-3’
	Passenger strand	5’-CACGCUGAGUACUUCGAACUU-3’

2.9 Gene expression analysis

2.9.1 RNA extraction

RNA for all experiments was isolated using either the RNeasy Mini Kit or RNeasy Mini Kit Plus (Qiagen). Cells were either lysed in Buffer RLT or Buffer RLT plus (350 µl for < $5x10^6$ cells, 600 µl for ≤ $1x10^7$ cells). If harvested in RLT Plus, the samples were then added to gDNA Eliminator spin columns and centrifuged at 8,000 xg for 30 sec. The column was then discarded and the flow through diluted in an equal volume of 70% ethanol (diluted in ddH2O) to precipitate the RNA. If harvested in Buffer RLT, the samples were just diluted with an equal volume of 70% ethanol. Samples were then added to RNeasy spin columns and centrifuged at 8,000 xg for 15 sec to bind the RNA to the column membrane. Samples in Buffer RLT were washed once with 350 µl Buffer RW1 by centrifuging at 8,000 xg for 15 sec, before RNase-free DNase solution (Qiagen) was made up by adding 70 µl Buffer RDD to 10 µl DNase stock solution (reconstituted in ddH2O). Eighty microlitres of this solution was added directly to the column membrane and the samples were incubated for 15 min at room temperature to digest genomic DNA. The columns were then washed again with 350 µl Buffer RW1. Samples in Buffer RLT Plus did not require this DNase step due to the use of gDNA elimination spin columns earlier in the protocol. As such, they were washed with 700 µl Buffer RW1 at once.

The columns were then washed twice with 500 µl Buffer RPE by centrifuging at 8,000 xg for 15 sec and 2 min, respectively. The columns were then dried by centrifuging at 8,000 xg for 1 min in a fresh collection tube, before the RNA was eluted by adding 15-50 µl RNase-free water, depending on the concentration required, directly to the column membrane and centrifuging at 8,000 xg for 1 min. If higher concentrations of RNA were required, the RNA elution was re-added to the column membrane and centrifuged again. The RNA concentration in each sample was measured using an ND-1000 Spectrophotometer (NanoDrop). RNA was stored at -20 °C.

2.9.2 cDNA conversion

Superscript III reverse transcriptase (Thermo fisher Scientific) was used to reverse transcribe RNA to cDNA. RNA (100-200 ng) was diluted in 10 µl RNase-

free water before 1 µl random primers (3 µg/µl) and 1 µl dNTPs (10 mM of each) were added. The mix was heated to 65 °C for 5 min and briefly incubated on ice before adding 4 µl 5X first-strand buffer, 2 µl 0.1 M DTT and 1 µl RNaseOUT recombinant ribonuclease inhibitor (40 units/µl) and incubating at room temperature for 2 min. One microlitre (200 units) SuperScript III reverse transcriptase was then added. Reverse transcription was carried out by incubating the reaction mix at 50 °C for 60 min. The reaction was terminated by incubating at 70 °C for 15 min. cDNA was stored at -20 °C.

2.9.3 Quantitative PCR

SYBR® Green PCR Master Mix (Thermo Fisher Scientific) was used for quantitative PCR (qPCR) analysis of mRNA expression. First, 12.5 µl SYBR® Green PCR Master Mix, 10.75 µl H2O, 0.75 µl of 10 µM primers solution (final concentration 300 nM; supplied by Sigma; see Table 2.2) and 1 µl (5 ng) cDNA were mixed in MicroAmp Fast Optical 96-Well Reaction Plates (Thermo Fisher Scientific) to give a final reaction volume of 25 µl. The plates were covered with MicroAmp optical adhesive film (Thermo Fisher Scientific) and centrifuged at 300 xg for 10 sec to collect the reaction mix at the bottom of each well, before being run on a 7500 Fast Real-Time PCR System (Thermo Fisher Scientific) using 7500 Software or on a QuantStudio5 machine (Applied Biosystems by Thermo Fisher Scientific) using QuantStudio™ Design & Analysis Software v1.4.3. The following PCR cycling conditions were used: 95 °C for 10 min, followed by forty cycles of 95 °C for 15 sec and 60 °C for 1 min. A melting curve of 60-95 °C was also run when new primers were tested to exclude the possibility of primer-dimer formation. All reactions were run in either duplicate or triplicate. Endogenous reference genes (*ACTB* and *GAPDH*) were also run in order to normalise the cycle threshold (Ct) values of genes of interest between samples.

Quantitative PCR data was analysed using Applied Biosystems 7500 Software or QuantStudio™ Design & Analysis Software v1.4.3. These software packages were both used to determine the baseline and Ct values of each sample, before the Ct value of each gene of interest was normalised by subtracting the mean Ct value of the reference genes for the same sample. Relative gene expression was then calculated by setting one condition as standard and using the following formula: relative gene expression = 2delta Ct (sample 1 – sample 2). Delta Ct is

defined as the expression of the gene of interest, normalised to that of the mean of the reference genes. Delta delta Ct is defined as the difference between the delta Ct values of the experimental sample and the control sample.

Table 2.2: Primers used for qPCR

Primer target	Forward Primer	Reverse Primer
C1QA	GTGACACATGCTCTAAGAAG	GACTCTTAAGCACTGGATTG
GAS6	CGAAGAAACTCAAGAAGCAG	AGACCTTGATCTCCATTAGG
GPR34	GAAGACAATGAGAAGTCATACC	TGTTGCTGAGAAGTTTTGTG
PROS1	AAAGATGTGGATGAATGCTC	TCACATTCAAAATCTCCTGG
MERTK	AGGACTTCCTCACTTTACTAAG	TGAACCCAGAAAATGTTGAC
P2RY12	AAGAGCACTCAAGACTTTAC	GGGTTTGAATGTATCCAGTAAG
TMEM119	AGTCCTGTACGCCAAGGAAC	GCAGCAACAGAAGGATGAGG
TREM2	TCTGAGAGCTTCGAGGATGC	GGGGATTTCTCCTTCAAGA
CD93	CAGAATGCGGCAGACAGTTA	TTCAGCAGTCTGTCCCAGGT
CX3CR1	GGCAGACTTGGATTTCAGGA	GGGAACTGATCCATGGTGAA
CD14	ATTTGGTGGCAGGAGATCAA	GGCTTCCAGGCTTCACACT
HTT	AGTGATTGTTGCTATGGAGCGG	GCTGCTGGTTGGACAGAAACTC
GAPDH	AACAGCGACACCCACTCCT	CATACCAGGAAATGAGCTTGACAA
ACTB	AAGGCCAACCGTGAAAAGAT	GTGGTACGACCAGAGGCATAC

IL-6	TACCCCCAGGAGAAGATTCC	AGTGCCTCTTTGCTGCTTTC
IL-8	GAGACAGCAGAGCACACAAG	TGCACCTTCACACAGAGCT
IL-1β	CTCAAGTGTCTGAAGCAGCC	GCACTTCATCTGTTTAGGGCC
TNFα	CCTCAGCCTCTTCTCCTTCC	AGATGATCTGACTGCCTGGG

2.10 High content immunofluorescence imaging

Microglia-like cell cultures were seeded at 25,000 cells/well in CellCarrier-96 plates (Perkin Elmer) and cultured for 14 days. MSN cultures were seeded at 30,000 cells/ well in CellCarrier-96 plates (Perkin Elmer) and matured until day 36 of the differentiation protocol. Following experimental procedures, cells were fixed gently with 10% formalin solution (containing 4% paraformaldehyde) for 15 min at room temperature and then washed sequentially into PBS while maintaining a sufficient level of liquid in the wells to cover the fixed cells at all times. Cells were then permeabilised with 0.2% Triton X-100 for 15 min at room temperature. Blocking solution containing 10% donkey or goat serum and 10% BSA in PBS was then applied for 1 h at room temperature. Primary antibodies were added in PBS with 1% BSA and incubated overnight at 4 °C. After four washes, secondary antibodies were added at a dilution of 1:1000 and incubated for 1 h in the dark at room temperature. After two further PBS wash steps, Hoechstt diluted to 1 µg/ml in PBS was added for 5 min at room temperature, protected from light. Cells were washed twice more in PBS then finally changed into PBS containing 0.02% sodium azide. The plates sealed and stored at 4 °C in the dark until imaged. Prior to imaging the volumes of liquid inside each well was reduced to 100 µl. The primary antibodies used for experiments are listed in Appendix 3.

All plates were imaged within fourteen days of staining, using the Perkin Elmer Opera Phenix HCS system, with twenty pre-set fields of view captured per well. A minimum of six replicate wells were imaged and analysed per experiment. A 40x air NA 0.6 objective was used and binning was set at two. Channels for Hoecshtt, 488, 568 and 647 were selected, the power set to 100% and separated

where appropriate to prevent cross-talk. Heights and gain settings for imaging were kept constant for each channel and each antibody combination. Images were then analysed using Perkin Elmer's Columbus image analysis software.
Assessment of MSN cultures was conducted as follows: nuclei were identified and categorised by the intensity and area of Hoechstt staining and the software's Find Nuclei function (Figure 2.4, B); βIII-tubulin+ cells and Caspase 3+ cells were detected using the Find Cytoplasm function (Figure 2.4, C and F, respectively); DARPP32+ and nestin+ cells were identified using the Find Cells function (Figure 2.4, D and H, respectively); CTIP2+ cells were determined by thresholding of staining in the nucleus (Figure 2.4, E); and H2AX puncta were identified using the Find Spots function (Figure 2.4, G).

Assessment of microglia-like cell cultures was conducted as follows: nuclei were identified and categorised by the intensity and area of Hoechstt staining and the software's Find Nuclei function, (Figure 2.5, B). PU1+ and TMEM119+ cells were identified by thresholding of staining in the nucleus (Figure 2.5, C and E, respectively). IBA1+ cells and TREM2+ cells were identified using the Find Cytoplasm function (Figure 2.5, D and F). Caspase 3+ cells were identified using the Find Cytoplasm function, method shown in MSNs (Figure 2.4, F). It is notable that additional TMEM119 staining is visible outside of the nucleus as would be expected, however given the co-existence of high intensity of nuclear staining, and the relative ease of quantification of nuclear stains, cells were assessed based on their nuclear TMEM119 staining only.

Appropriate population outputs and formula outputs were selected for Define Results, see Appendix 1 for details, to allow the calculation of the culture composition. This was then downloaded and exported to Microsoft Excel before statistical analysis using GraphPad Prism 6.07. Graphs were produced using GraphPad Prism 6.07 and then exported to Adobe Illustrator for the production of figures.

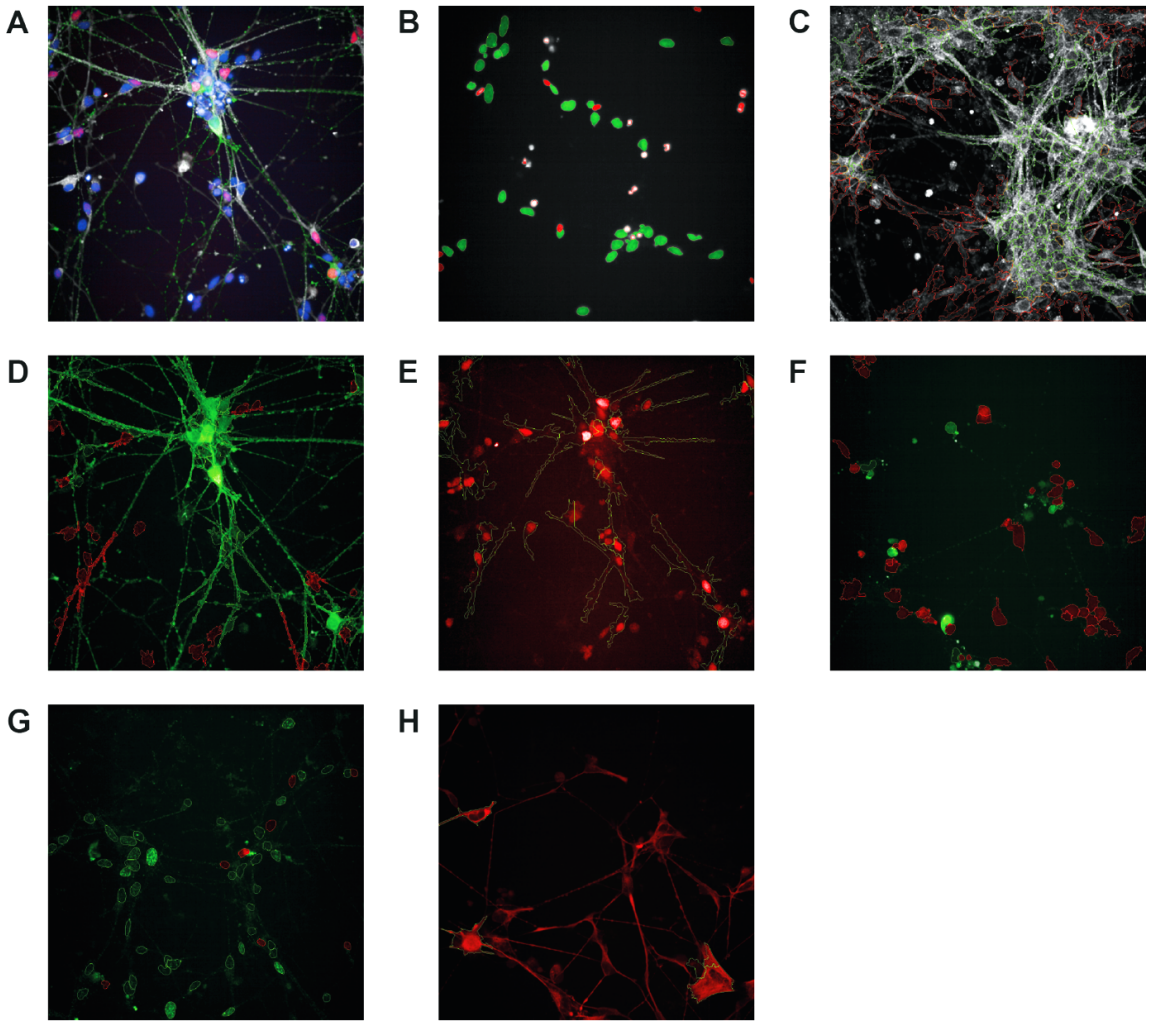

Figure 2.4: Example images of high content imaging analysis conducted using Columbus software for neurons. Columbus software was used to analyse all immunofluorescent images of MSNs. All MSNs cultures were assessed after day 36 of differentiation, when cultures are considered mature. **A**) An example image of an MSN culture, with DARP32 (green), CTIP2 (red), βIII-tubulin (white) and Hoechstt staining (blue). **B**) Nuclei were identified and categorised as viable (highlighted in green) or non-viable (highlighted in red) by means of the intensity and area of Hoeschtt staining and the software's Find Nuclei function. **C**) βIII-tubulin+ cells were identified using the Find Cytoplasm function on the viable nuclei population, and selected according to staining intensity. Selected cells are shown with a green border, discarded cells are shown with a red border. **D**) DARP32+ cells were identified using the Find Cells function on the Viable nuclei population, and selected according to staining intensity. Selected cells are shown in green, discarded cells are shown in red. **E**) CTIP2+ cells were identified by thresholding of staining in the nucleus of the viable nuclei

population. Selected cells are shown with a green border around the cell. **F**) Caspase 3+ cells were identified using the Find Cytoplasm function on the viable nuclei population and selected according to staining intensity. Selected cells are shown in green, discarded cells are shaded in red. **G**) Cell nuclei containing greater than ten H2ax spots were identified using the Find Spots function on the viable nuclei population, and a threshold of greater than ten spots set. Selected cells are shown with a green border, discarded cells are shown in red. **H**) Nestin+ cells were identified using the Find Cells function on the viable nuclei population and selected according to staining intensity. Selected cells are shown with a green border. Details of the antibodies used are provided in Appendix 3. The exact detection and analysis parameters for each metric are provided in Appendix 1.

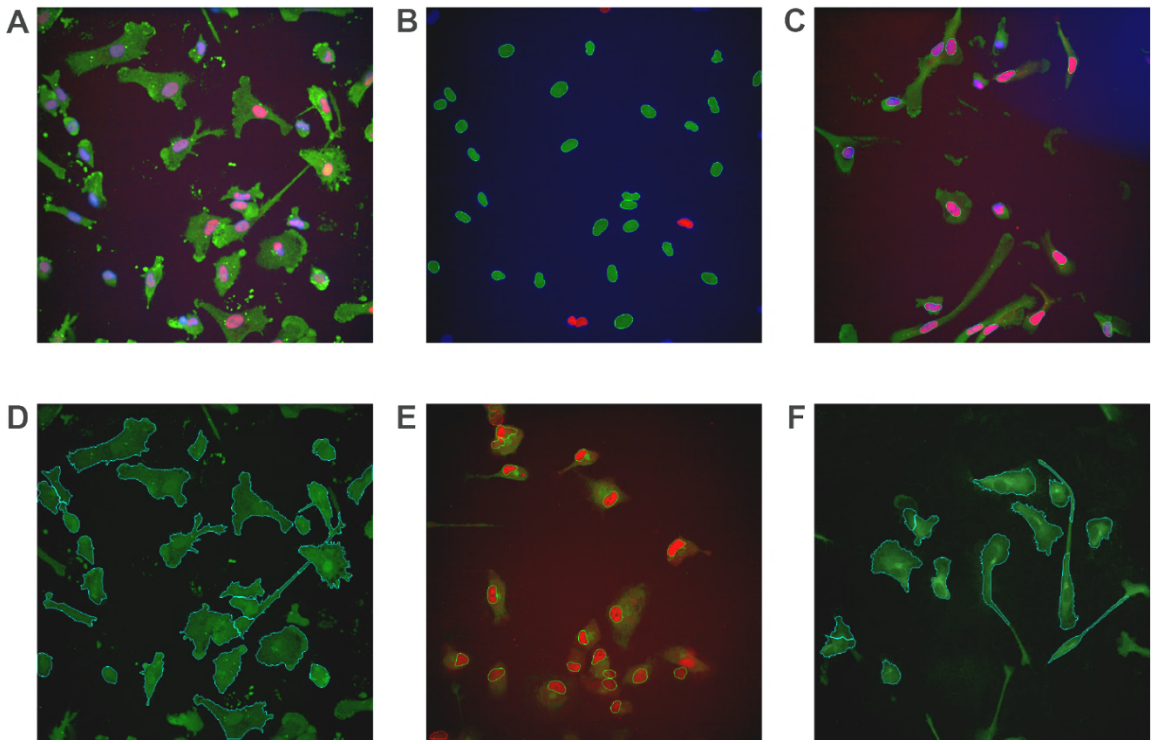

Figure 2.5: Example images of high content imaging analysis conducted using Columbus software for microglia-like cells. Columbus software was used to analyse all immunofluorescent images of microglia-like cells. All microglia-like cell cultures were cultured *in vitro* for 14 days and assessed for markers of microglial identity as follows. **A**) An example image of a microglia-like cell culture, with IBA1 (green), PU1 (red) and Hoechstt staining. **B**) Nuclei were identified and categorised as viable (highlighted in green) or non-viable (highlighted in red) by means of the intensity and area of Hoeschtt staining and the software's Find Nuclei function. **C**) PU1 staining was identified by thresholding of staining in the nucleus of the previously identified Viable nuclei population, cells expressing PU1 over the expected threshold have a green border around the nucleus. **D**) IBA1+ cells were identified using the Find Cytoplasm function on the Viable nuclei population, and selected according to staining intensity. Selected cells are shown with a turquoise border. **E**) TMEM119 staining was identified by thresholding of staining in the nucleus of the Viable nuclei population. Selected cells are shown with a green border around the nucleus, those not meeting the selection criteria are shown with a red border around the nucleus. **F**) TREM2 staining was identified using the Find Cytoplasm function on the Viable nuclei population and selected according to staining

intensity, selected cells are shown with a turquoise border. Details of the antibodies used are provided in Appendix 3. The exact detection and analysis parameters for each metric are provided in Appendix 1.

2.11 Imaging flow cytometry

Cell were scraped from their culture plate in ice cold PBS and pelleted by centrifugation at 350 x*g* for 5 min. Pelleted cells were then fixed for 15 min at 4 °C with shaking, before permeabilisation for 10 min at 4 °C with shaking. This was completed using the eBioscience intracellular Fix/Perm solutions (Invitrogen). The cells were then incubated in permeabilisation buffer with anti-NFκB p65 XP ® antibody at 1:200 (Cell Signaling Technology) for 60 min at 4 °C with shaking. Following this, cells were washed twice in FACS buffer (PBS with 1% BSA, 0.02% sodium azide) by centrifugation at 350 xg for 5 min followed by removal of the supernatant and resuspension in fresh FACS buffer. This was done very gently to avoid excess sample loss. Cells were then incubated in FACS buffer with F(ab')2-Donkey anti-rabbit IgG (H+L) PE-conjugated secondary antibody (eBioscience) at 1:100 for 30 min at 4 °C with shaking. After this, cells were washed twice in FACS buffer, then incubated in 1 µg/ml Hoechstt 33342 for 5 min and then washed once before being resuspended in approximately 50 µl for analysis. Single-stained samples were also generated to assess the need for compensation between fluorescent channels.

Samples were run on the ImageStreamX analyser (Amnis) and analysed using IDEAS software version 6.2. Gating was done to isolate in-focus, single cells, double-stained for p65 and Hoechstt, and the nuclear localisation wizard in the software allowed gating for translocation events where the p65 stain significantly co-localised with Hoechstt. This allowed calculation of the percentage of total cells with p65 translocated to the nucleus.

2.12 Cell viability assays

2.12.1 LDH assay

Cellular LDH (lactate dehydrogenase) levels were analysed using the CytoTox 96® non-radioactive cytotoxicity assay (Promega) kit. Prior to use assay buffer was thawed and warmed to room temperature, kept protected from light. Twelve millilitres of assay buffer was then added to a bottle of substrate mix and gently

shaken to mix and dissolve to form the CytoTox 96® Reagent. Cell populations to be analysed were seeded at 100,000 cells/well in a 96-well plate (Thermo) and cultured for the appropriate amount of time as per the specific protocol. Experimental wells were treated with 20 ng/ml bafilomycin A1 for 9 h or 2.5 mM hydrogen peroxide for 1 h prior to assessment, while control wells containing untreated cells were prepared to assess baseline viability, and control wells with media only were also prepared to obtain a measurement for background chemiluminescence. Maximum LDH release controls were also performed for each well, to allow interpretation of the level of LDH in experimental and control conditions as a percentage of maximum LDH for that well, in order to control for cell number variability. After the treatment period, 50 µl aliquots from all test and control wells were transferred to a fresh 96-well flat clear bottom plate. To obtain maximum LDH release values for each well, all wells were then treated with 10 µl of 10x lysis solution (per 100 µl original volume) for 45 min. Fifty microliter aliquots from the maximum release wells were then also transferred to the fresh 96-well flat clear bottom plate. To each sample aliquot, 50 µl of the CytoTox 96® Reagent was added, and the plate incubated at room temperature for 30 min, protected from light. Fifty microlitres of stop solution was then added to each well, any large bubbles popped, and the absorbance read at 490 nm within 1 h of adding the stop solution.

The results were analysed using the following formula, with values corrected for background absorbance levels:

Percent cytotoxicity = 100 × (Experimental LDH Release (OD490)/Maximum LDH Release (OD490))

For every experiment there were untreated control wells included, to assess baseline levels of viability in each cell population.

2.12.2 ATP assay

Cellular ATP levels were analysed using the CellTiter-Glo® Luminescent Cell Viability Assay (Promega). Prior to use the CellTiter-Glo® Buffer was thawed and equilibrated to room temperature along with the CellTiter-Glo® Substrate. After the Cell-Titer-Glo® Buffer had thawed, 12 ml was transferred into the CellTiter-Glo® Substrate bottle to reconstitute the lyophilised enzyme/substrate mixture; this mixture is the CellTiter-Glo® Reagent, and was mixed to ensure a

homogenous solution. Cell populations to be analysed were cultured in 96-well plates; with experimental cultures treated with 20 ng/ml bafilomycin A1 in 100 µl media for 20 h prior to assessment, while control wells containing untreated cells were prepared to assess baseline viability, and control wells with media only were also prepared to obtain a measurement for background luminescence. After the treatment period, the plate and its contents were equilibrated at room temperature for 30 min, before CellTiter-Glo® Reagent equal to the volume of media (100 µl) was added to each well. The plate was placed on a shaker for 2 min to induce cell lysis, and then incubated at room temperature for 10 min to stabilise the luminescent signal. The contents of the plate were then transferred to a fresh opaque-walled white 96-well plate (Greiner Bio-One), before luminescence was measured using an Infinite® 200 PRO microplate reader (Tecan). The results were analysed by setting one condition as standard and converting the experimental sample readings to a percentage of its ATP levels.

2.12.3 Annexin assay

Apoptosis and necrosis were assessed using the RealTime-Glo™ annexin V apoptosis and necrosis assay (Promega) according to the manufacturer's instructions. Briefly, microglia precursors were seeded at 10,000 cells/well in white flat bottom 96-well plates (Corning) and cultured for 14 days to become microglia-like cells. The cells were then treated with 50 µl of either bafilomycin A1 or hydrogen peroxide at 2x the desired final concentration, bafilomycin A1 at 80 ng/ml for a final concentration of 40 ng/ml, and hydrogen peroxide at 16 mM for a final concentration of 8 mM. To this, 50 µl of 2x detection reagent (containing 2x Annexin Nanobit substrate, 2x calcium chloride, 2x necrosis detection agent and 2x annexin V-SmBiT and 2x annexin V-LgBiT, supplied by the manufacturer and combined immediately prior to use) was added. The final concentrations of the toxins and detection reagent were therefore at 1x. The plate was then mixed for 30 sec at 500-700 rpm on a plate shaker, before incubation at 37 °C in 5% CO_2. Luminescence and fluorescence measures (485 excitation/525 emission) were then recorded recorded at 0 h (baseline), 2 h, 5 h, 7 h, 9 h and 24 h using the Infinite® 200 PRO microplate reader (Tecan).

2.13 Phagocytosis assay

Cells were seeded at 100,000 cells/well of a Cell Carrier-96 plate (Perkin Elmer) and cultured *in vitro* according to each specific protocol. Cultured cells were transferred into serum-free media overnight to stimulate phagocytosis. Before the assay, cells were washed three times with PBS and then incubated with HBSS containing calcium and magnesium and 20 mM HEPES for 1 h. Control wells were prepared to allow determination of background fluorescence in a no-cell context. pHrodo™ *Zymosan A* green or *E. coli* red fluorescent BioParticles® were thawed and the lyophilised product suspended in HBSS before brief vortexing. The suspension was then sonicated for a total of 5 min, in 30 sec bursts, with 30 sec rest periods between. After 1 h, the HBSS buffer was replaced with 100 µl of pHrodo™ BioParticles® fluorescent particles suspension. Cells were incubated at 37 °C for 2-3 h to allow phagocytosis and acidification to reach its maximum. All experimental, control and no-cell control wells were then scanned using an Infinite® 200 PRO microplate reader (Tecan) at the appropriate settings according to the excitation and emission maxima given (509/533 nm or 560/585 nm for *Zymosan A* green and *E. coli* red respectively.)

To assess the phagocytosis response to HTT knockdown, the percentage effect can be calculated as a fraction of the net positive control phagocytosis as follows:

% Effect = Net experimental phagocytosis × 100% Net positive control phagocytosis.

2.14 BCA assay

The Pierce BCA protein assay kit (Thermo Fisher Scientific) was according to manufacturer's instructions. Briefly, cell lysates were diluted appropriately with RIPA buffer and protease inhibitors (cOmplete™ Mini EDTA-free tablets, Sigma) depending on total cell number, while BSA standards were diluted in RIPA buffer according to the manufacturer's instructions. Standards and lysates were added to separate wells of a clear 96-well plate (Greiner), before working solution (made up of a 50:1 ratio of BCA Reagent A and BCA Reagent B) was added to each well. Each sample was analysed in duplicate. The plate was then incubated at 37 °C for 30 min, after which Infinite® 200 PRO microplate reader (Tecan) was used to measure the absorbance signal intensity at 562 nm. Analysis was carried out by using the BSA standards to create a standard curve for comparison.

2.15 Multiplex ELISA

Cytokine profiling was carried out using V-PLEX Assay Kits from MesoScale Discovery (MSD).

Cells were treated with either 2 µg/ml LPS and 10 ng/ml IFNγ or placed in fresh media only for 24 h. The supernatants were collected, and the cells washed once with sterile PBS and lysed in 60 µl radioimmunoprecipitation assay (RIPA) buffer supplemented with a protease inhibitor cocktail (cOmplete™ Mini EDTA-free tablets, Sigma) to provide protein values for cytokine normalisation using bicinchoninic acid (BCA) assays. The supernatants were analysed for cytokine production using the V-PLEX Proinflammatory Panel 1 (Human) Kit (IL-10, IL-1β, IL-6, IL-8, and TNFα for all experiments and IL-12p70 for experiments on primary macrophages only). The MSD plate was washed three times in PBS containing 0.05 % Tween (PBS-T) before the addition of any samples. Depending on the cell type and experimental condition, 50 µl of undiluted, 1:2, 1:5, 1:50 or 1:300 diluted samples were added to the MSD plate and incubated with vigorous shaking for 2 h at room temperature, or at 4 °C overnight. MSD Diluent 2 was used to dilute samples for the multiplex assays. Eight standards of known concentration were also added to the plates by carrying out serial fourfold dilutions of the Calibrator Blend included in each kit, according to the manufacturer's instructions. After incubation, the plate was washed three times with PBS-T. The detection antibody solution was made up by combining 60 µl of each detection antibody and adding MSD Diluent 3 to a final volume of 3 ml. Twenty-five µl of this antibody solution was then added to each well before incubating with vigorous shaking for 2 h at room temperature. The plate was washed three times with PBS-T before 150 µl 2X Read Buffer T was added to each well. After the Read Buffer was added the plate was analysed immediately using a Sector Imager 6000 with Discovery Workbench 4.0 software (MSD). Cytokine concentrations were calculated by comparing the samples to a standard curve made from the eight calibrators, before normalising to the total protein measured by BCA assays or the total cell number as measured by HCI on the Opera Phenix and analysis using Columbus software.

For assessment of intracellular cytokine levels, primary macrophages isolated from whole blood samples were seeded at $4x10^6$ cells/dish in 10 cm Primaria

dishes (Corning), with two dishes per donor, and differentiated to macrophages. For each individual donor, one dish was treated with anti-*HTT* siRNA and one with scrambled siRNA as described in section 2.8. These plates were then treated with either 2 µg/ml LPS and 10 ng/ml IFNγ or placed in fresh media only for 24 h. The supernatants were then discarded, and the cells washed once in PBS and harvested in lysis buffer (150 mM NaCl, 20 mM Tris ph7.5, 1 mM EDTA, 1 mM EGTA, 1% triton-X-100, supplemented with Phosphatase inhibitor 1 and Phosphatase inhibitor 2 (Phosphatase Inhibitor Cocktail 3, Phosphatase Inhibitor II, respectively, Sigma Aldrich) as well as Protease inhibitor solution (Product Halt™ Protease Inhibitor Cocktail, EDTA-Free, Pierce Biotechnology) before snap freezing on dry ice and storage at -80 °C until use. Cell lysate samples were thawed immediately before use and assessed for the production of the cytokines IL-6, IL-1β, TNFα, IL-10, and IL-8 using a V-plex Proinflammatory Panel 1 (Human) Kit ELISA by MSD, with the intracellular cytokine samples diluted 1:2.

2.16 Reactive Oxygen Species Assay

Reactive oxygen species (ROS) were assayed using the DCFDA/H2DCFDA assay kit (Abcam), used according to the manufacturer's instructions. Microglial precursors were seeded in CellCarrier-96 well plates (Perkin Elmer) at 25,000 cells/well and cultured for fourteen days as previously described. After this point, the media on the cells was removed and the wells washed once with 1x buffer at 100 µl/well. Negative control wells would remain in 1x buffer for the duration of the experiment. Test and positive control wells were then incubated with 100 µl/well of diluted DCFDA Solution for 45 min at 37 °C protected from light. After this, the wells were changed into 100 µL 1x buffer to assess baseline ROS production, or treated with 110 µM tert-butyl hydrogen peroxide (TBHP) solution diluted in FBS-supplemented 1x buffer (10% FBS) for 4 h. Fluorescence was assessed at 485/535nm (Ex/Em) at specific time points according to the experimental design of each experiment.

2.17 Nitric oxide assays

2.17.1 Griess method

To assess nitrite production in supernatants, first a standard curve was produced. This was done by creating a 100 mM nitrite stock solution from nitrite powder

(Sigma Aldrich) and then adding 0, 0.5, 1, 1.5 and 2 µl respectively, to 2 ml of purified water to create 0, 25, 50, 75 and 100 µM standards. Following thorough vortexing, these standards were then added in triplicate or quadruplicate to a 96-well plate (200 µl/well) along with each microglia-like cell supernatant sample in duplicate or triplicate (200 µl/well), and the plate plan recorded. One hundred microlitres Griess reagent was then added to each well and the plate incubated at room temperature for 15 min protected from light, before reading the plate at 540 nm on an Infinite® 200 PRO microplate reader (Tecan).

2.17.2 Abcam nitric oxide assay kit

To assess both nitrite and nitrate production in lysate and supernatant of samples, the Abcam fluorometric nitric oxide assay kit (Fluorometric) was used according to the manufacturer's instructions. Briefly, standard curves for both nitrite and nitrate were prepared in both assay buffer and cell media using the standards provided by the manufacturer. Supernatant and cell lysate collected in assay buffer, from stimulated and unstimulated cells was collected after the appropriate time period and stored on ice until use. To a 96-well plate, 75 µl of each standard and sample was added in duplicate or triplicate. For the nitrate assay, 5 µl of Nitrate reductase was added to test wells and standards. For nitrite assessment wells and standards, 5 µl of assay buffer was added. All wells were then incubated at room temperature for 3 h. After this point, 5 µl of enhancer was added to each well and incubated at room temperature for 30 min to quench interfering compounds. Then, 5 µl DAN (2,3 diaminonaphthalene) fluorescent probe was added to each well and incubated at room temperature for 10 min. Finally, 5 µl of sodium hydroxide was added to all wells and incubated at room temperature for 10 min before reading on an Infinite® 200 PRO microplate reader (Tecan) 360/450 Ex/Em.

2.18 Statistical analysis

All statistical analysis was conducted using GraphPad Prism 6.07, using the appropriate tests for the type of data being analysed, such as one-way and two-way ANOVAs, with the associated multiple comparisons tests (Dunnett's), as well as Student's t-tests both paired and unpaired as required. All analyses were conducted as recommended by the software, with the necessary multi-

comparison corrections undertaken. Detailed statistical analyses per experiment are summarised in the relevant results sections of Chapters 3, 4 and 5.

All graphs were produced using GraphPad Prism 6.07 and Adobe Illustrator 2019.

3. Chapter 3: Characterisation of human PSC-derived Huntington's disease microglia-like cells

3.1. Background

3.1.1 Existing models of Huntington's disease

A large variety of models of Huntington's disease have been developed in order to study various aspects of the disease. From genetic animal models in species such as mice, rats, *Drosophila*, sheep, pigs and non-human primates (Baxa et al., 2013; Handley et al., 2016; Lewis and Smith, 2016; von Hörsten et al., 2003), to *in vitro* models, including cell lines and primary human cells (Aiken et al., 2004; Wang et al., 2005).

A large portion of basic research into HD has been conducted in rodent models, and such models continue to be a key part of investigating HD. However, there are a number of caveats to using rodent models in HD. For example, typically rodent models contain much longer polyQ repeat lengths than would be found in the average human HD patient (Mangiarini et al., 1996), and the level at which the HTT protein is expressed can also be much higher, see Table 1.1 for details (D.E. Ehrnhoefer et al., 2009). This can lead to much faster progression of disease pathology (Carter et al., 1999; Hickey et al., 2005; Lione et al., 1999; Murphy et al., 2000) which is useful for *in vivo* experiments, and the severe phenotypes rodents develop make for clear read outs when testing therapeutic interventions. However, to date, there has been a very low success rate when translating effective therapies in mouse and other animal models to the clinic. This highlights the need for testing in multiple models, in combination with human cell-based approaches, and ideally, working back from phenotypes found initially in human patient cohorts to better understand the disease and find effective therapeutic targets.

A number of *in vitro* models of HD have also been commonly used. For example, immortalised cell lines with polyQ repeat knock-ins or over-expressing transgenic lines have been produced (Aiken et al., 2004; Wang et al., 2005). However, it is worth noting that the process of immortalising cells can produce artefacts (Grimm, 2004), and as such, results found initially in cell lines must typically be validated extensively in other models.

3.1.2 PSC-derived models of HD

It is on this background that pluripotent stem cells (PSCs) have been developed and their use adopted in labs around the world. The gold standard for PSCs has been embryonic stem cells (ESCs), with the more recent addition of induced pluripotent stem cells (iPSCs) to the field.

iPSCs are particularly useful for producing cell-based models of disease, as somatic cells from patients can be reprogrammed to a pluripotent state, while maintaining their genetic identity. This has been applied in HD, with iPSC lines produced from HD patients and related controls. The benefit of these lines is the theoretically infinite source of patient material that they can produce, with the same polyQ length and expression level as the donor. ESCs are derived from donated blastocysts, either carrying specific disease mutations, or controls that can be edited using genome editing techniques to produce disease models.

In this work, we had access to an allelic series of ESCs generated by the Pouladi group (Ooi et al., 2019), called IsoHD cells, carrying polyQ lengths of 30, 45 and 81 units, respectively. As well as this, a cohort of iPSC lines generated from a family, consisting of one unaffected mother (22Q) and three affected offspring (58, 69, 75Q), referred to as the “HD family lines”, and a number of unrelated control and HD PSC lines were also used. An important weakness to note is that the HTT expression level at the protein level was not quantitatively assessed in the differentiated neurons or microglia-like cells due to limitations of HTT antibodies available and lack of positive and negative controls available. Additionally, the lines were CAG-sized as iPSCs and ESCs, however routine sizing was not conducted in differentiated iPSCs and ESCs, so there is a chance that these lines may have developed increased CAG sizes during the course of experiments. Although based on the data produced by other members in the lab in MSNs, expansion is unlikely to have occurred in any of the lines except the 125Q (unpublished observations), which were used in a limited capacity in this work.

3.1.3 Modelling the innate immune system using PSCs

In terms of the innate immune system, the CNS component has been chronically under studied *in vitro* in humans. This is due to restricted access to the brain. Most studies have been conducted in microglia from animal models of HD or

using indirect assessments in HD patients, either via imaging, *ex vivo* analysis of the peripheral counterparts of microglia, or post mortem analysis of patient brain tissue (Björkqvist et al., 2008; Kwan et al., 2012; Silvestroni et al., 2009). While all of these modalities are useful, they are indirect, or proxy measures, and it would be beneficial to be able to study human microglia directly.

This is where the differentiation of microglia from human iPSCs or ESCs is vital, in order to provide a resource that is extremely limited ordinarily, expressing mHTT at a physiological level and with a range of polyQ lengths that are similar to that seen in patients. Also, if isogenic lines can be used, this reduces the number of different PSC lines that need to be differentiated and tested, and gives greater confidence that results seen are due to the presence of the expanded polyQ in those lines, rather than any other genetic factors. The immune system is highly variable due to its reactive nature, both between individuals but also within the same individual, as a result of environmental and systemic signals, so any method of reducing noise in the system for study *in vitro* is essential.

In order to study the immune system in HD using PSC-derived cell types, it was necessary to review the available protocols and assess which to test further in our lab. Part of the original design of this thesis involved differentiating both the peripheral and CNS-based components of the innate immune system, bone-marrow derived blood macrophages, and tissue resident macrophages in the CNS, microglia, respectively. This would have allowed for comparison of phenotypes between the two counterpart cell types, and the assessment of how applicable the results from the great body of research, conducted historically in primary human blood monocytes and macrophages, was to the CNS.

Several directed differentiation protocols that aimed to recapitulate the steps of development of blood monocytes, from the early embryonic yolk sac, to the bone marrow, to mature blood monocytes had been published close to the inception of this PhD thesis (Van Wilgenburg et al., 2013; Yanagimachi et al., 2013). Of these, Yanagimachi et al., 2013 was chosen for immediate testing on the HD family lines, as it is serum free and does not require feeder cells, thus increasing the consistency and reproducibility of the differentiation procedure.

However, both of these methods, originally published for the production of blood monocytes, underestimated the degree to which the steps of blood monocyte

development overlap with the developmental steps of tissue-resident macrophages, such as microglia, alveolar and kidney macrophages, Kupffer cells, and Langerhans cells. In fact, the only differentiating factor between the two is the particular wave of production from the yolk sac that the initial cells come from (Ginhoux et al., 2013, 2010; Hoeffel et al., 2015). This was realised by Buchreiser et al., 2017, who assessed the dependency of their protocol (Van Wilgenburg et al. 2013) on transcription factors that differentiate the two waves of yolk sac production. This showed that the cells (which were originally claimed to be blood monocytes) were MYB-independent and RUNX1- and SPI1-dependent, which is indicative of a tissue resident macrophage identity. Further evidence of the tissue-resident macrophage identity of these cells has been shown through experiments which recapitulate a neuronal environment to facilitate maturation into microglia, by means of co-culture with cortical cells or exposure to cortical media (Haenseler et al., 2017). Principal component analysis of gene expression data collected in this study showed clustering of the gene expression signature of these cells with that of foetal microglia, distinct from blood monocytes. On this basis, and following comparison with the other available protocols for microglial differentiation at the time, assessed on a number of criteria; cost, time, average yield and requirement of specialist facilities, see Appendix 2 for comparison of protocols (Abud et al., 2017; Muffat et al., 2016; Pandya et al., 2017), the Van Wilgenburg protocol and the Muffat protocol were chosen to be tested for their efficacy of microglia-like cell production from HD PSCs. However, when the Muffat et al., 2016 protocol was first tested in one HD (75Q) and one control line (22Q), there were great technical difficulties with implementing the protocol at the early stages, and so it was dropped from further testing.

Also affected by the revelations regarding tissue resident macrophage development versus blood monocyte development was the Yanagimachi et al., 2013 protocol. Following a year of testing in our lab, for use as PSC-derived monocytes, Douvaras et al., 2017, published an updated version of the Yanagimachi protocol, with an additional growth factor in the “macrophage production” step of the original paper. This new paper referred to the “monocytes” of the Yanagimachi paper as “microglial precursors”, and with the addition of IL-34 to the macrophage production step of the Yanagimachi protocol, it produced

what they refer to as “mature microglia”. While this paper did not assess the dependency of the cells on MYB, RUNX1 and SPI1, they performed extensive gene expression analysis for microglial-specific genes (Butovsky et al., 2013; Haenseler et al., 2017) and found the cells produced were enriched for these markers. Based on this paper, our assessment of Yanagimachi-derived cells was extended to include testing for these microglial markers, and the expression of key microglial genetic markers confirmed. This altered the scope of this work, so the efficacy of these two microglial protocols was assessed and compared before the selection of one for all further testing, rather than assessing one tissue resident macrophage (microglial) protocol and one bone marrow-derived blood monocyte protocol extensively. Any investigations that required blood monocytes were therefore conducted in primary human monocytes isolated from whole blood samples.

3.1.4 Innate immune system dysfunction

Much work already exists investigating the immune system in HD. A large portion of this has been done in mouse models, specifically the R6/2, YAC128 and BACHD models, which are well established to faithfully recapitulate many of the pathological and behavioural phenotypes of HD (Gray et al., 2008; Mangiarini et al., 1996; Slow et al., 2003).

Interestingly, a hyper-reactive phenotype has been consistently found across human and mouse models, with elevated responses to immune stimuli such as LPS or CSE (Björkqvist et al., 2008; Connolly et al., 2016; Trager et al., 2014).

Investigations also uncovered a migration deficit in microglia isolated from both mouse models compared to their WT littermates, when assessed *ex vivo* using a Boyden chamber assay (Kwan et al., 2012). This deficit was additionally found in patient monocytes and macrophages assessed *ex vivo*. As well as this, a more general deficit in motility was shown, with deficits in extension and retraction of processes, as well as actin remodelling.

This work in mouse models is complemented by a number of studies conducted using human HD patients either post mortem or via non-invasive imaging, or using whole blood samples. This research has generally shown upregulated cytokine production at the mRNA level in brain tissue, as well as elevated

cytokines in the periphery in HD samples (Björkqvist et al., 2008; Silvestroni et al., 2009). Post mortem studies have also found marked astrogliosis and microgliosis in multiple brain areas in HD samples, but not in controls (Sapp et al., 2001; Singhrao et al., 1999). Imaging studies have also shown significant increases in activated microglia that correlate with disease severity (Pavese et al., 2006), motor dysfunction, measures of daily living, and perhaps most interestingly, in the case of premanifest HD gene carriers, a correlation with the predicted probability of HD onset in the next 5 years (Politis et al., 2011; Tai et al., 2007). This increased microglial activation was also correlated with elevated plasma levels of pro-inflammatory cytokines in pre-symptomatic gene carriers, who were predicted to be more than 10 years from onset (Politis et al., 2015).

3.1.5 Potential mechanistic basis for the observed dysfunction in the innate immune system

A number of theories exist as to the mechanism underlying the immune dysfunction that is seen in HD. One theory is that aberrant NF-κB pathway activation occurs due to the presence of mHTT (Crotti et al., 2014; Trager et al., 2014).

In addition to this, there is significant evidence suggesting that the presence of mHTT alters ROS production (Wyttenbach et al., 2002), and that ROS have a significant impact on the activation of the NF-κB pathway (Schoonbroodt et al., 2000; Takada et al., 2003). Also, oxidative stress levels affect mHTT aggregation levels (Goswami et al., 2006). In this way, it may be possible that mHTT interacts with the NF-κB pathway directly, and also through affecting ROS production, to cause dysfunction in the immune system.

3.1.6 Exploring the link between innate immune system dysfunction and neurotoxicity

It is possible that mHTT-expressing microglia contribute to the toxic environment of the HD brain through the release of a variety of cytokines and other neurotoxic factors (Nakanishi, 2003). However, it is important to also note the role of non-cell autonomous dysfunction. As previously mentioned, microglia are highly reactive cells, extremely sensitive to their environment, and even non-HD

microglia can become dystrophic through continued exposure to cell debris, aggregates and stress or death signals from neurons. For example, Gibbons et al., 2006, found that treatment with LPS reduced the viability of BV2 microglial cells, but had no effect on neuronal cultures. However, in co-cultures, the addition of LPS resulted in reduced viability of both the microglia and neuronal cell types. In this way, it is clear that even microglia without mHTT expression, when exposed to the appropriate stimulus, can cause neurotoxicity (Gibbons and Dragunow, 2006).

This chapter details the development and characterisation of a human PSC-derived model of HD microglia. In this thesis I have used the updated Van Wilgenburg protocol (as published by Haenseler et al.,) for the bulk of the experiments. Initial work focused on characterising the cells produced by this protocol, and a second protocol by Yanagimachi et al., for microglial-like characteristics. For the purposes of this thesis, differentiated microglial like cells were defined as microglia-like cells if, following 14 days of *in vitro* culturing post-harvest, they met the following criteria: expressed a panel of genes enriched in microglia (*P2RY12, TREM2, TMEM119, IBA1, C1QA, GAS6, GPR34, MERTK* and *PROS1*) at mRNA level, and proteins (TREM2, PU1, IBA1 and TMEM119) as assessed by immunofluorescence, as well as meeting functional criteria, with cells being capable of phagocytosis, cytokine production and ROS production. These criteria are in keeping with the standard measures in other published protocols of microglial differentiation (Abud et al., 2017; Douvaras et al., 2017; Muffat et al., 2016; Pandya et al., 2017).
At this point, it should be clear that the development of an *in vitro* model and characterisation of HD microglia in this context, is a necessary step towards a better understanding of human HD microglia, providing access to a previously under studied cell type in HD.

3.2. Aims

To set up an *in vitro* model of human HD microglia

1. Assess two protocols for the differentiation of microglia-like cells, and select one for in-depth characterisation
2. Assess cells produced using the chosen microglial protocol for any effect of mHTT on microglial function

3.3. Methods

Microglia-like cells were differentiated from PSCs of varying polyQ lengths either according to Yanagimachi et al., 2013 (section 2.5.1) or Van Wilgenburg et al., 2013 with some minor modifications (detailed in section 2.5.2). They were then assessed for microglial identity both at the mRNA level, using RT-qPCR (section 2.9), and the protein level, using high content imaging (HCI) on the Opera Phenix followed by analysis using Columbus software (section 2.10). Control and HD microglia-like cells were then assessed using a battery of functional tests. First, the cytokine expression of HD and control microglia-like cells at the protein level was assessed using MSD cytokine assays (section 2.15). In parallel, the mRNA expression of key pro-inflammatory cytokines was assessed by RT-qPCR (section 2.9). The reactive oxygen species (ROS) production of HD and control microglia-like cells was quantified under baseline and various stimulated conditions (section 2.16). The nitric oxide production was also assessed under baseline and stimulated conditions (section 2.17). The viability of HD and control microglia-like cells was assessed under baseline and stressed conditions using LDH assays (section 2.12.1) and Annexin-V viability assays (section 2.12.3). Finally, the phagocytic activity of both HD and control microglia-like cells was assessed (section 2.13). Statistical analyses were conducted and graphs produced using GraphPad Prism 6.07 and Adobe Illustrator 2019 as described in section 2.19.

3.4. Results

3.4.1. Assessment of two microglial differentiation protocols

Two methods were tested to determine their respective quality, as assessed by the yield of microglial-like cells produced, the expression of key microglial markers, and the purity of cultures produced. A brief investigation into the functional capacity of the microglia produced by both protocols was also undertaken, before one protocol was chosen, and a more in depth characterisation undertaken.

3.4.2. The Yanagimachi et al., 2013 protocol produces microglial-like cells

The first method of microglial differentiation assessed was published in 2013 by Yanagimachi et al.

Cells derived using the Yanagimachi et al., 2013, method were harvested from day 17 onwards, with a harvest every four days, as stipulated by the published protocol. There was a high degree of variability between yields of clones from the same original donor (Figure 3.1). Importantly, these yields were far below what was stated in the published protocol, where each yield produced approximately $1.3x10^6$ cells.

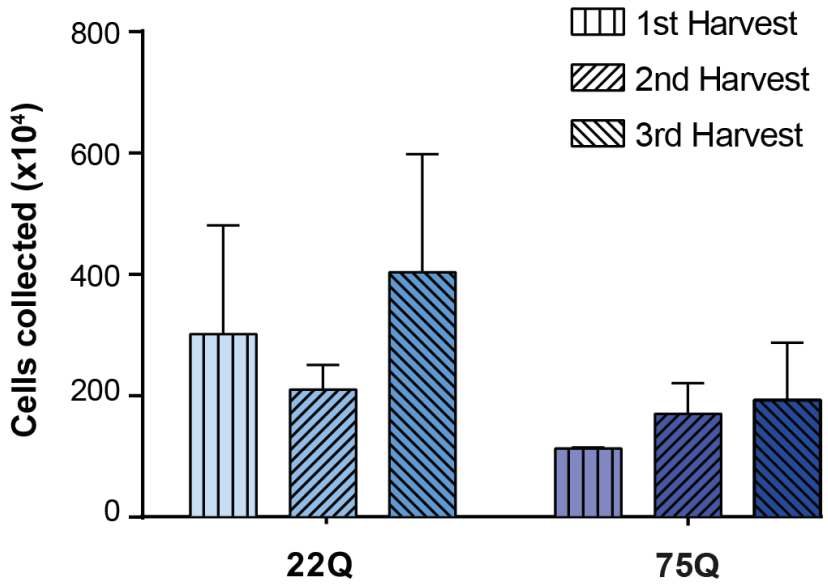

Figure 3.1: Yields from the Yanagimachi protocol were variable from the HD family of iPSC lines and did not meet predictions from the published work. Two lines of the HD family series, differentiated as described in section 2.5.1, carrying 22 and 75Q, were used in this experiment, n= 3 clones per line. Three harvests taken consecutively every four days, revealed variation in the yields both between lines and clones, and suggested lower harvests in the HD line (75Q). These yields are considerably lower than the yields reported in the published protocol. Data shown are the mean ± SD.

Cells differentiated using the Yanagimachi et al., 2013 protocol were also assessed for their expression of a cluster of microglial identity genes that are recognised in the literature as distinctive markers of microglial identity (Butovsky

et al., 2013; Haenseler et al., 2017). *C1QA, GAS6, GPR34, MERTK, P2RY12, PROS1, TMEM119* and *TREM2* were all enriched in the microglial cells derived using the Yanagimachi et al., 2013 protocol relative to primary monocytes, and there was no polyQ-dependent effect (Figure 3.2).

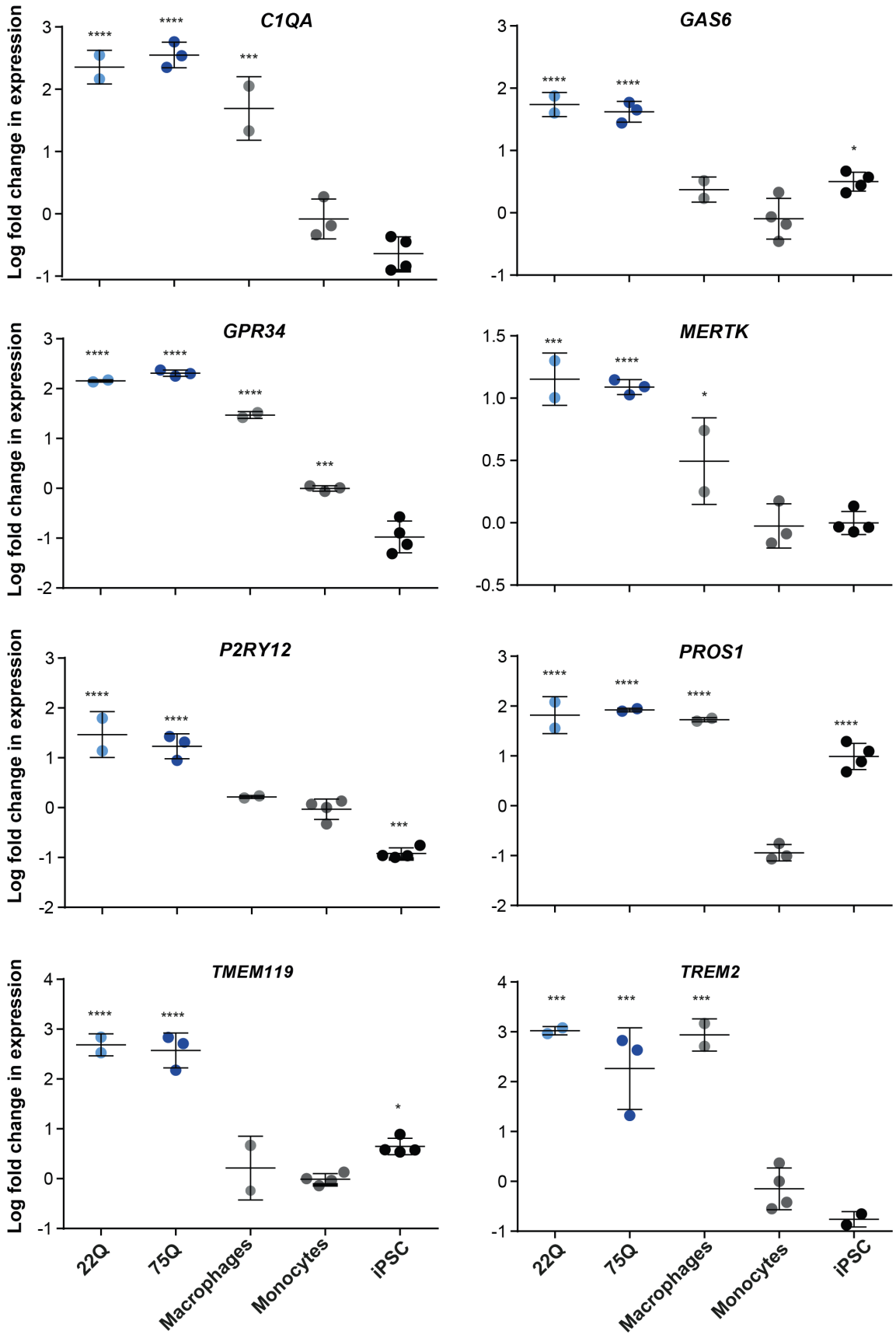

Figure 3.2: qPCR assessment reveals elevated expression of key microglial genes in cells produced by the Yanagimachi et al., 2013, protocol. *C1QA,*

GAS6, GPR34, MERTK, P2RY12, PROS1, TMEM119 and *TREM2* show significantly increased expression in the Yanagimachi differentiated cells relative to primary human monocytes. Data shown are a log transform of the raw data, with all points plotted as a fold change relative to primary monocyte expression which was calculated as the average expression of 4 primary monocyte samples and set as 1. The error bars shown represent the standard deviation (SD). N=2 clones of the 22Q HD family line, n=3 of the 75Q family line, n=2 independent biological samples of primary macrophages for all graphs except *CX3CR1* where n=1, n=4 independent biological samples of primary monocytes for all graphs except *CX3CR1* where n=3, n=4 undifferentiated iPSC lines for all graphs except *TREM2* where n=2. All samples were run in triplicate, and each data point shown is an average of those three values. *P<0.05, **P<0.01, ***P<0.001, ****P<0.0001.

Genes that were not enriched relative to primary monocytes are shown in Figure 3.3. These are genes that would be expected to be highly expressed in monocytes, such as *CD14* and *CD93*, but also include *CX3CR1*, which is known to be expressed by human microglia *in vivo* but is not enriched in the differentiated microglia from this protocol.

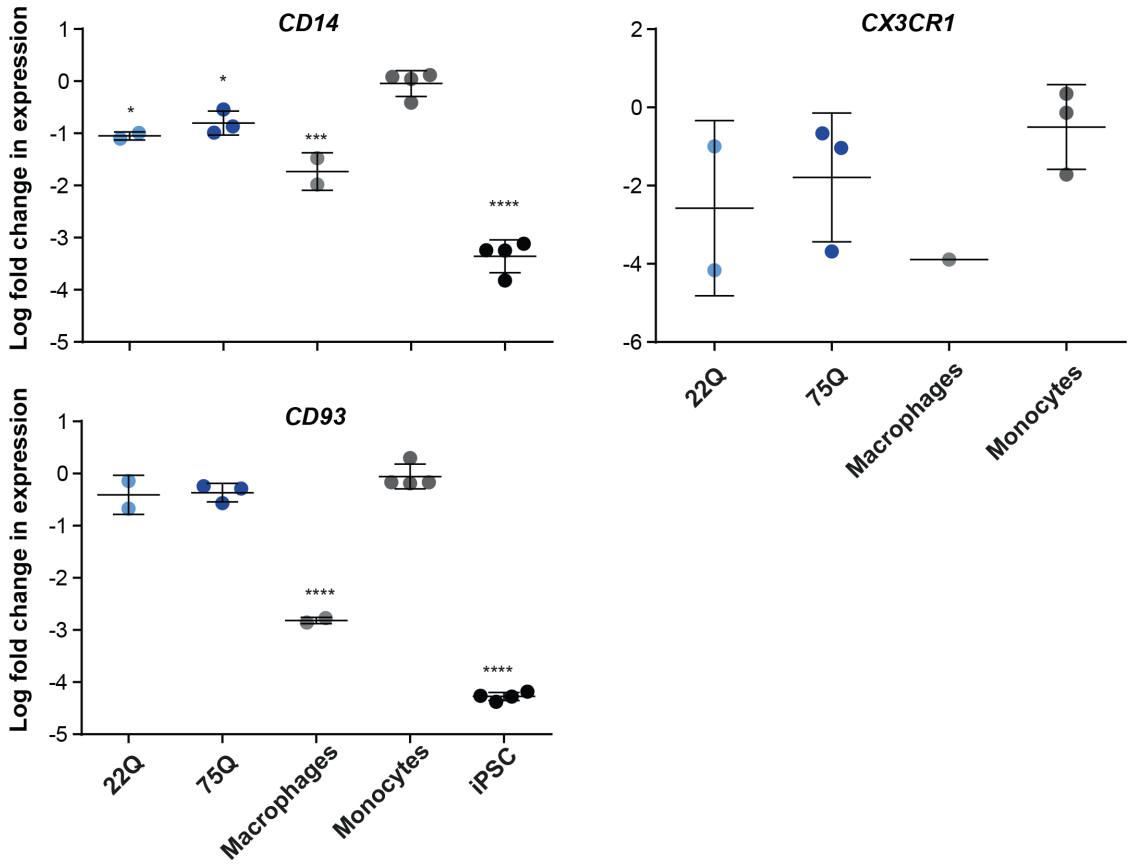

Figure 3.3: qPCR assessment reveals reduced expression of a number of genes in cells produced by the Yanagimachi et al., 2013, protocol relative to primary monocytes. *CD14* expression is significantly reduced in the Yanagimachi cells, relative to primary human monocytes, which express *CD14* strongly. *CD93* is not significantly differently expressed in the Yanagimachi cells relative to the primary human monocytes, but is significantly reduced in the primary macrophage and undifferentiated iPSC samples assessed. *CX3CR1* is not significantly differently expressed between primary human monocytes and the Yanagimachi cells. This marker should be enriched in microglial populations, but does not seem to be expressed *in vitro*. Data shown are a log transform of the raw data, with all points plotted as a fold change relative to primary monocyte

expression which was calculated as the average expression of 4 primary monocyte samples and set as 1. The error bars shown represent the standard deviation (SD). N=2 clones of the 22Q HD family line, n=3 of the 75Q family line, n=2 independent biological samples of primary macrophages for all graphs except *CX3CR1* where n=1, n=4 independent biological samples of primary monocytes for all graphs except *CX3CR1* where n=3, n=4 undifferentiated iPSC lines. All samples were run in triplicate, and each data point shown is an average of those three values. *P<0.05, **P<0.01, ***P<0.001, ****P<0.0001.

To follow up these findings, a brief investigation into the expression of these genes at the protein level was conducted in one clone of the 75Q line, by immunocytochemistry. In this way, expression of CD14 and TREM2 was qualitatively confirmed at the protein level (Figure 3.4).

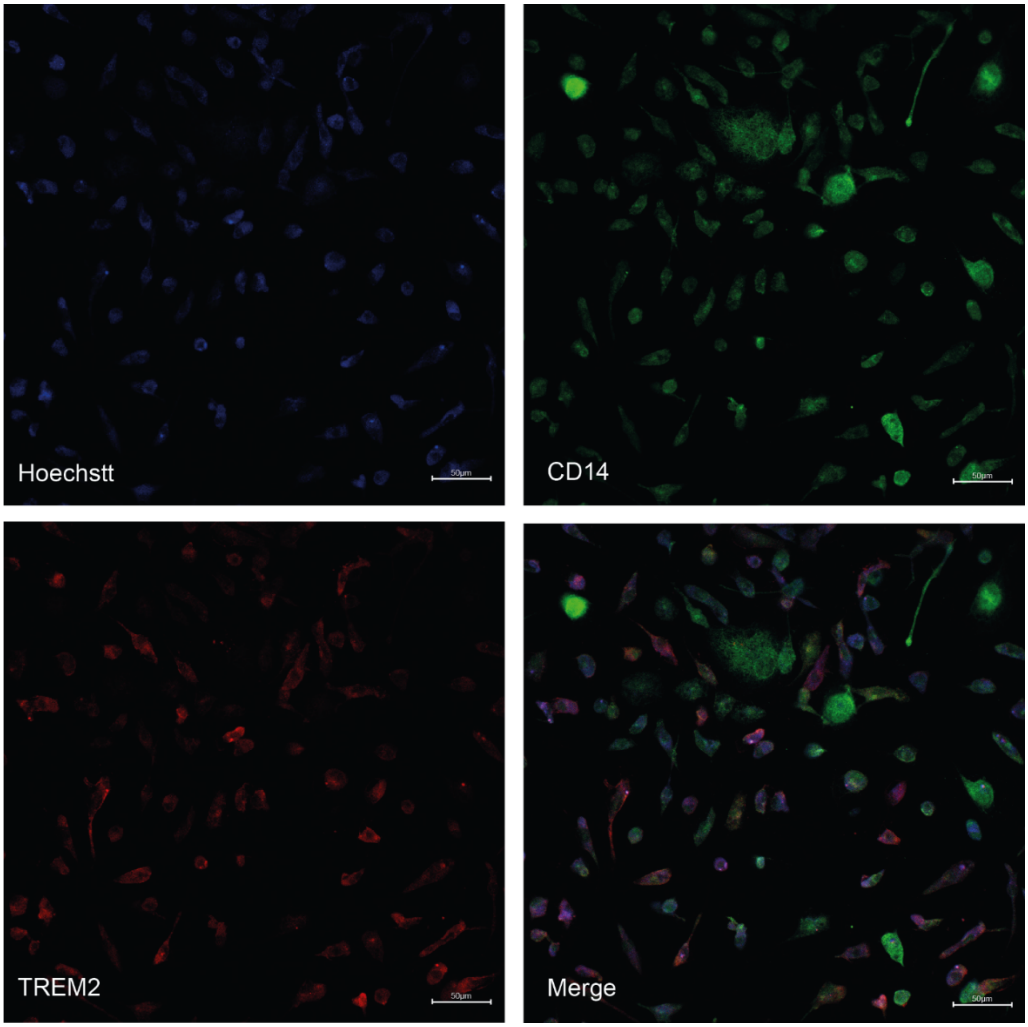

Figure 3.4: qPCR and IF assessment reveal microglial identity of cells produced by the Yanagimachi et al., protocol. Qualitative assessment of expression of CD14 and TREM2 at the protein level in once clone of the 75Q HD family line. N=1 clone. Secondary only controls were conducted as part of the original testing of the antibodies used, however was not repeated in each subsequent experiment. Additionally, this analysis is lacking a positive control, due to the difficulty in obtaining primary human microglia.

3.4.3. Microglia-like cells differentiated using the Yanagimachi et al., 2013 protocol, produced cytokines when stimulated that may be polyQ dependent

Initial functional assessments focused on the capacity of the differentiated cells to produce cytokines, as this is an area known to be dysfunctional in microglia from HD animal models and in innate immune cells from the periphery;

macrophages and monocytes. Three clones from the 22Q control line were differentiated to microglia-like cells, and then treated with LPS and IFNγ, and their cytokine production at baseline and under stimulated conditions assessed using the MSD assay (section 2.15). It was found that these differentiated microglia-like cells could produce a significant increase in cytokine expression in response to stimulation, with IL-6 and IL-8 expression significantly elevated (*P<0.05), as well as IL-1β and TNFα which were even more significantly increased (**P<0.01).

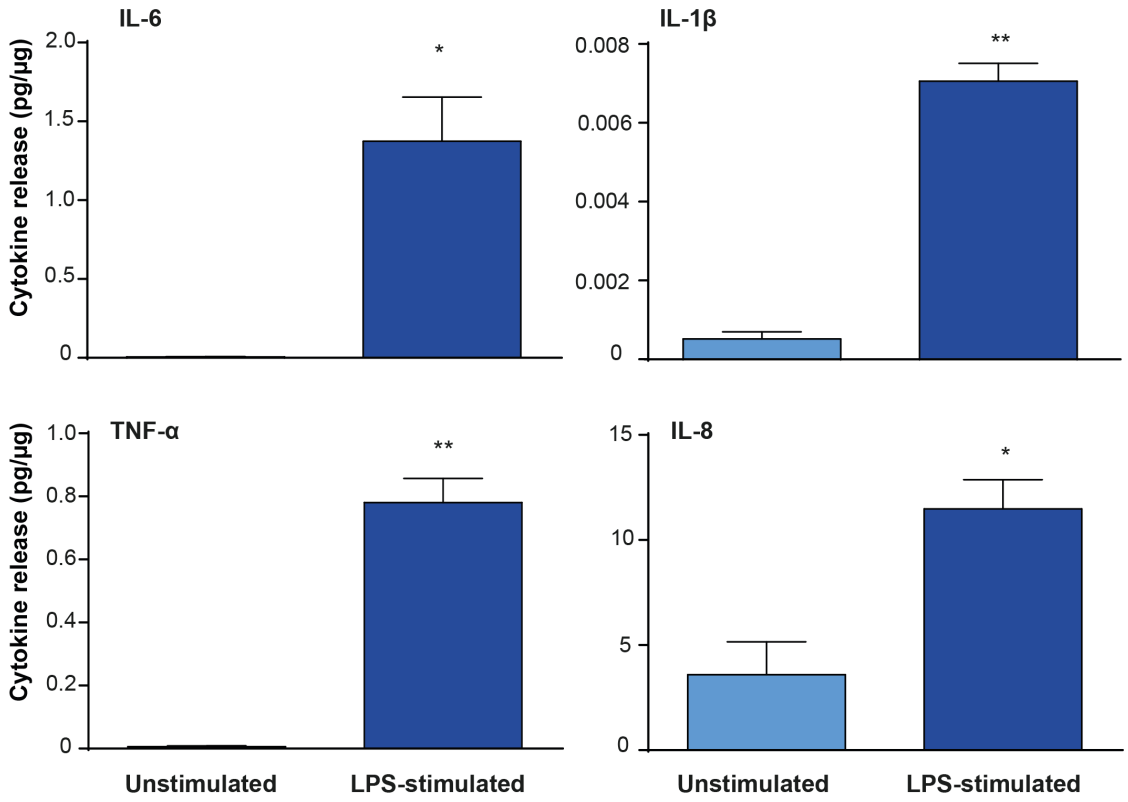

Figure 3.5: iPSC-derived microglia-like cells were responsive in their cytokine production to LPS stimulation. 24 h of stimulation with LPS and IFNγ resulted in increased expression of key pro-inflammatory cytokines IL-6, IL-1β, TNFα and IL-8, in cells differentiated from three clones of a HTT 22Q iPSC line, using Yanagimachi et al., 2013, protocol. Data shown are mean ± SEM. N=3 clones. Each clone's samples were run in triplicate, and the average of those three values taken as the value for that clone. *P<0.05, **P<0.01. Positive and negative controls were provided by the manufacturer for this assessment, and were used to build a standard curve to inform analysis of the test samples results.

Following this assessment, microglial-like cells differentiated from three clones of a HD line (75Q) and three clones of the control line (22Q) from the HD family lines, using the Yanagimachi et al., 2013, protocol were assessed for cytokine release upon stimulation (section 2.15). This experiment suggested higher cytokine release in the HD line (75Q) compared to the control line (22Q) (Figure 3.6). This was not statistically significant, however.

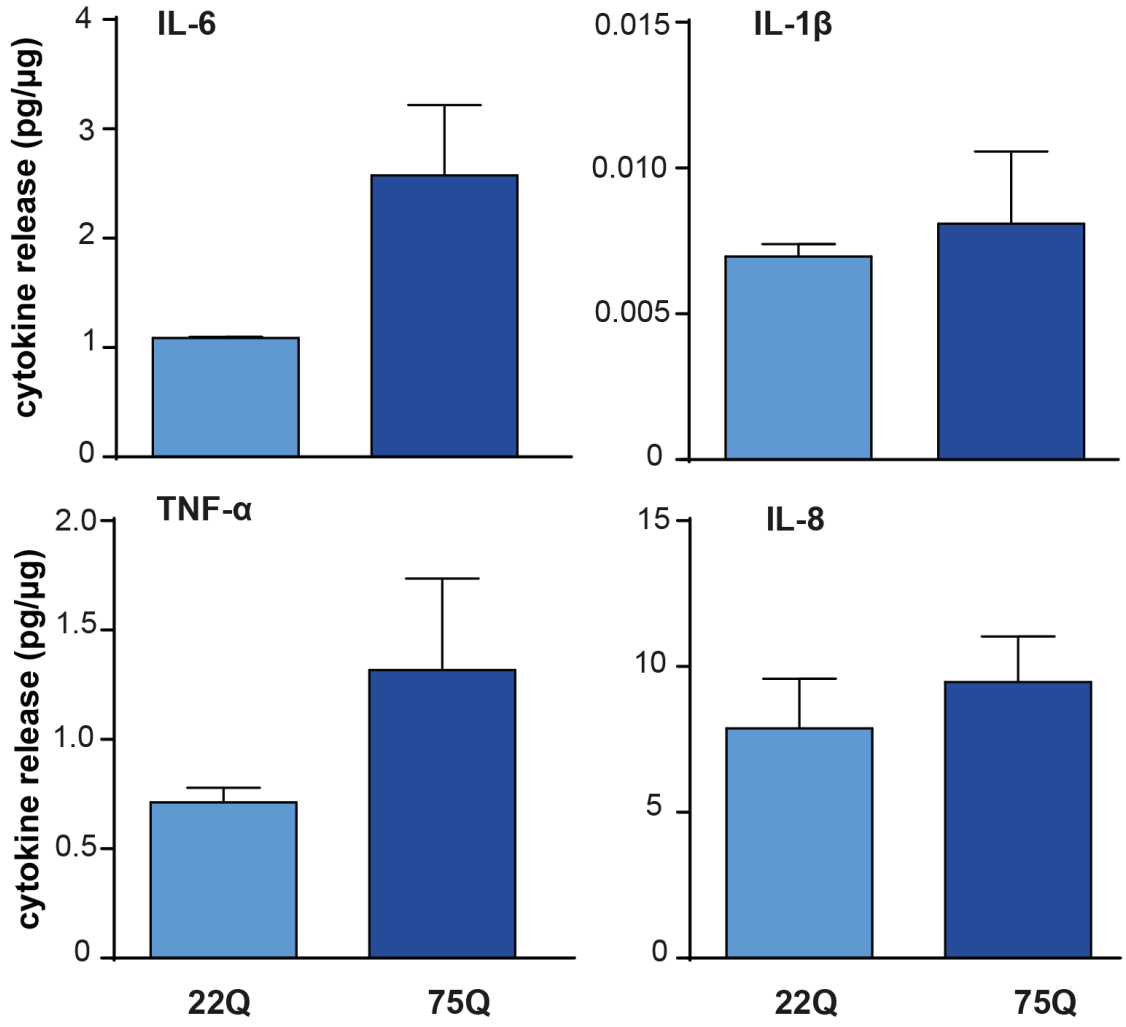

Figure 3.6: iPSC derived microglia-like cells carrying a 75Q expansion may have shown elevated cytokine release compared to control lines. Cells derived using the Yanagimachi et al., 2013, differentiation protocol were stimulated with LPS and IFNγ for 24 h resulting in the release of key pro-inflammatory cytokines IL-6, IL-1β, TNFα and IL-8. There was no significant difference between the 22Q and 75Q lines. Data shown are mean ± SD. N=3 clones per line. Sample from each clone was run in triplicate, and the average

used as the value for that clone. Positive and negative controls were provided by the manufacturer for this assessment, and were used to build a standard curve to inform analysis of the test samples results.

3.4.4. Cells differentiated using the Yanagimachi et al., 2013, protocol show phagocytic activity

Another key feature of microglia function is the ability to phagocytose material. The capacity of cells differentiated to microglia-like cells from both 22Q and 75Q iPSC lines, using the Yanagimachi et al., 2013 protocol was assessed using pHrodo fluorescent beads (section 2.13).

Three clones from each line were differentiated and assessed, and it was found that both lines show phagocytic activity, as they both show internalisation of the pHrodo beads and subsequent fluorescence suggesting the beads were present in the lysosome, with the 22Q line clones appearing to be slightly more phagocytic, (Figure 3.7).

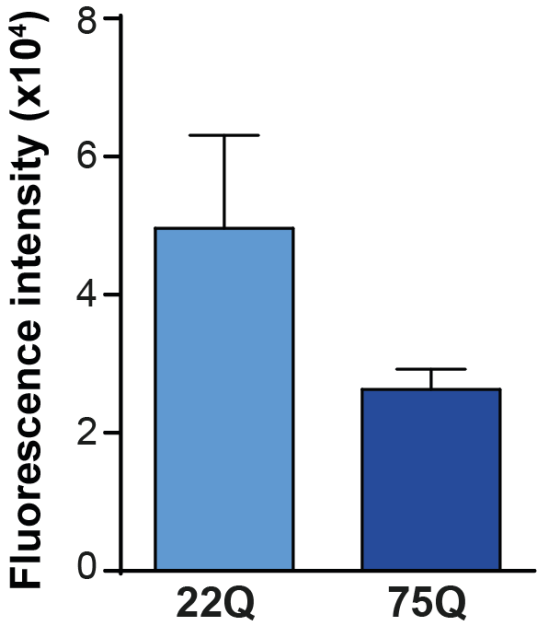

Figure 3.7: iPSC-derived microglia-like cells show phagocytic activity. Cells differentiated using the Yanagimachi et al., 2013, protocol were assessed for

phagocytic activity using the pHrodo bead assay. There was no significant difference in phagocytic activity between the lines tested, p=0.5448. Data shown are mean ± SD. N=3 clones per line, three technical replicates per clone. A negative control of media only wells was included to provide a baseline value, and the fluorescence values subtracted from all test samples.

3.4.5. Microglial-like cells of varying polyQ length, differentiated using the Yanagimachi et al., 2013, protocol, appear to have similar baseline viability

Lastly, cells differentiated from both HD (75Q) and control (22Q) iPSC lines using the Yanagimachi et al., 2013, protocol were assessed for their viability at baseline using an LDH assay, and the 75Q line clones appeared to have higher percentage cell death compared to control line clones, but this was not statistically significant.

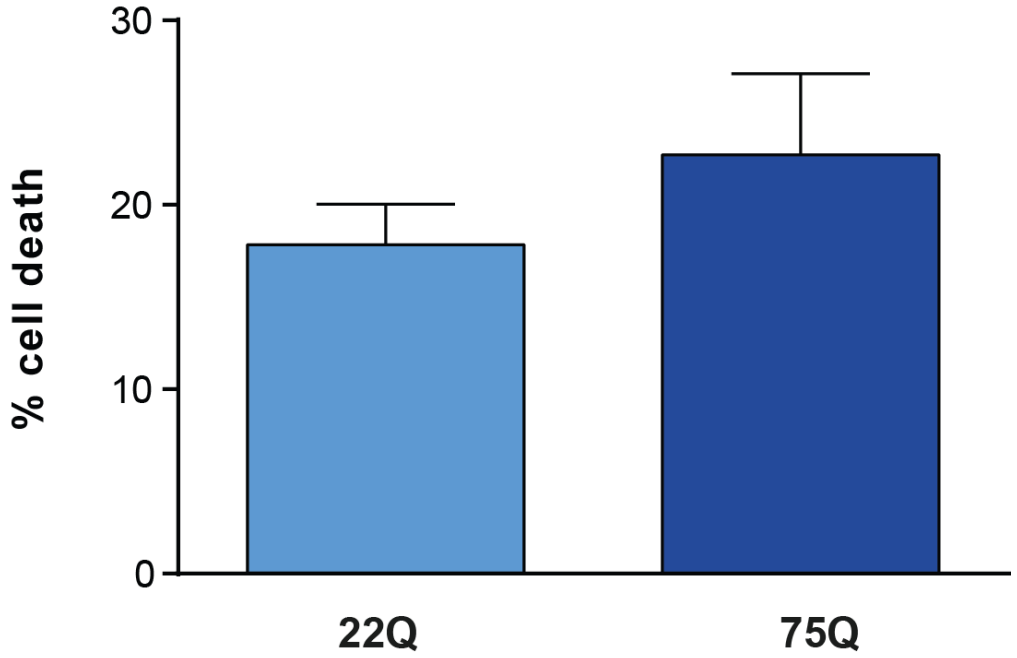

Figure 3.8: Viability of iPSC-derived microglia-like cells appears similar between HD and control Q lengths. Microglia-like cells were assessed for the production of LDH over 9 h. Data shown are the mean ± SD. N=3 clones per line, with three technical replicates per clone, and the average taken from these three and used for that clone. LDH assays include a potent toxin to allow the calculation of 100% cell death in the test wells, this allowed calculation of the percentage cell death in each test well as a proportion of the 100% cell death value.

3.4.6. The Van Wilgenburg et al., 2013 protocol produces microglia-like cells

The second method of differentiating microglia-like cells that was assessed was published by Van Wilgenburg et al., 2013, and an updated version used in Haenseler et al., 2017, that contains a method for differentiating the tissue resident macrophages harvest weekly further into microglia-like cells (Figure 2.2; section 2.5.2).

3.4.7. The Van Wilgenburg et al., 2013 protocol produces a consistently high yield

The first step to assess the robustness of the protocol was to assess a large cohort of lines for their capacity to produce microglia-like cells. To quantify the quality of the cultures produced, the yields of cells at each harvest point were recorded.

This cohort comprised four lines of the HD family series, three lines of the IsoHD isogenic ESC series, as well as additional iPSC and ESC control lines, and one additional HD line, of 125Q.

Embryoid bodies produced microglial precursors at sufficient quantities for a minimum of six harvests to be taken for experiments. There was considerable variation between harvests in the yield for the same cell line, with the first and final yield often being lower. There was also some variation between lines from different backgrounds, with the IsoHD lines producing higher yields, however there was not a polyQ dependent effect on the yield, as within the IsoHD lines, the yields were not significantly different between the control line (30Q) and either of the HD lines (45Q, 81Q). This suggests that Q length does not impact yield significantly, but the cumulated genetic differences between groups of lines may affect yield.

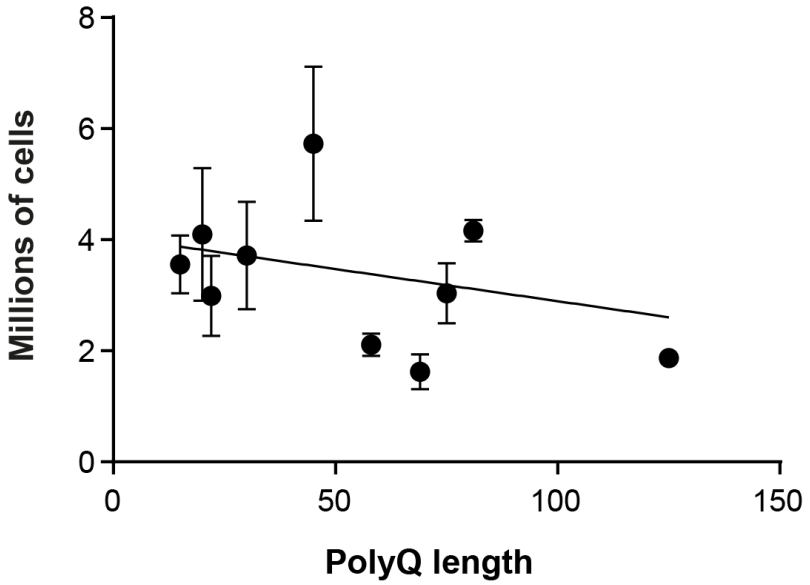

Figure 3.9: A similar spread of variability in yield and overall yield numbers is found across a large cohort of iPSC and ESC lines differentiated to microglia-like cells using the Van Wilgenburg et al., protocol. Lines differentiated using the same protocol show similar variability and total numbers of cells produced per harvest across all polyQ lengths tested. A number of lines show lower production, 58Q, 69Q and 125Q, however these lines were only differentiated once, compared to the other lines differentiated a minimum of twice, which may bias these data. There was no significant correlation between polyQ length and yield, p=0.2179. Data shown are mean, and where N=3 differentiations or clones ± SD. Isogenic lines were differentiated a minimum of three times, and for the HD family lines three clones per line were differentiated, these make up the individual data points used to calculate the mean and SD. Each individual data point was calculated as follows: six harvests were taken from all differentiated clones and lines, and the average yield calculated across those six harvests.

3.4.8. The Van Wilgenburg protocol produces cells that are enriched for a panel of microglial markers as assessed by quantitative PCR

A large panel of microglial-enriched genes were tested across the cohort of PSC lines. In all the lines, key markers of microglial identity including *P2RY12, TREM2, TMEM119, IBA1, C1QA, GAS6, GPR34, MERTK* and *PROS1* were enriched

compared to primary monocytes and undifferentiated iPSCs (Figure 3.10, 3.11). The groups of lines also tended to cluster together, with the IsoHD lines showing similar levels of enrichment, and the HD family lines showing similar levels of enrichment to each other, although all significantly elevated relative to the primary monocytes and undifferentiated iPSCs. Additionally, no overt polyQ effect was shown. The HD family lines also showed lower expression of *CD14* and *CD93*, relative to primary monocytes that typically express these genes strongly (Figure 3.12).

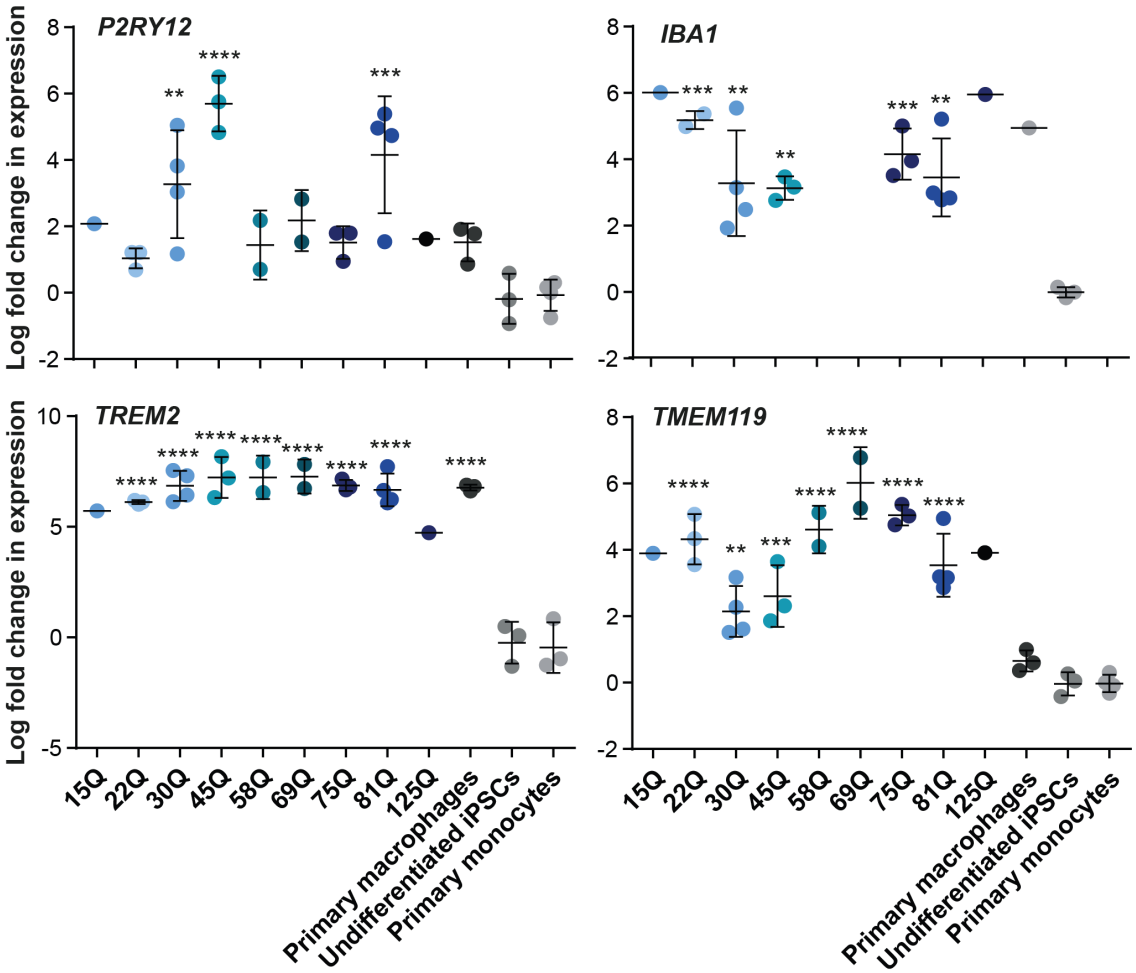

Figure 3.10: qPCR assessment reveals elevated expression of microglial genes in cells produced by the Van Wilgenburg et al., protocol. *P2RY12*, *TMEM119* and *TREM2* show significantly increased expression in Van Wilgenburg differentiated microglia-like cells relative to primary monocytes. *IBA1* shows increased expressed in Van Wilgenburg differentiated microglia relative to undifferentiated iPSCs. Data shown are a log transform of the raw data, with all points plotted as a fold change relative to primary monocyte expression where

the average expression of at least three primary monocytes samples was set as 1. The error bars shown represent the standard deviation (SD). N=1 differentiation of 15Q control iPSC line, n=3 clones of 22Q control iPSC line, n=4 differentiations of control 30Q ESC lines, n=3 differentiations of 45Q ESCs for panel A, n=2 clones of 58Q iPSC lines, n=2 69Q iPSC lines, n=3 clones 75Q iPSC line, n=4 differentiations of 81Q, n=1 125Q iPSC lines, n=3 or 4 independent biological samples of primary monocytes, each sample was run in triplicate and the average of those values used as the value for that sample. Statistical testing was done on any line that had more than one data point. One-way ANOVA, followed by Dunnett's multiple comparison testing for significant change relative to primary monocytes for all genes except *IBA1*, where differentiated microglia-like cells were compared to undifferentiated iPSCs.*P<0.05, **P<0.01, ***P<0.001, ****P<0.0001.

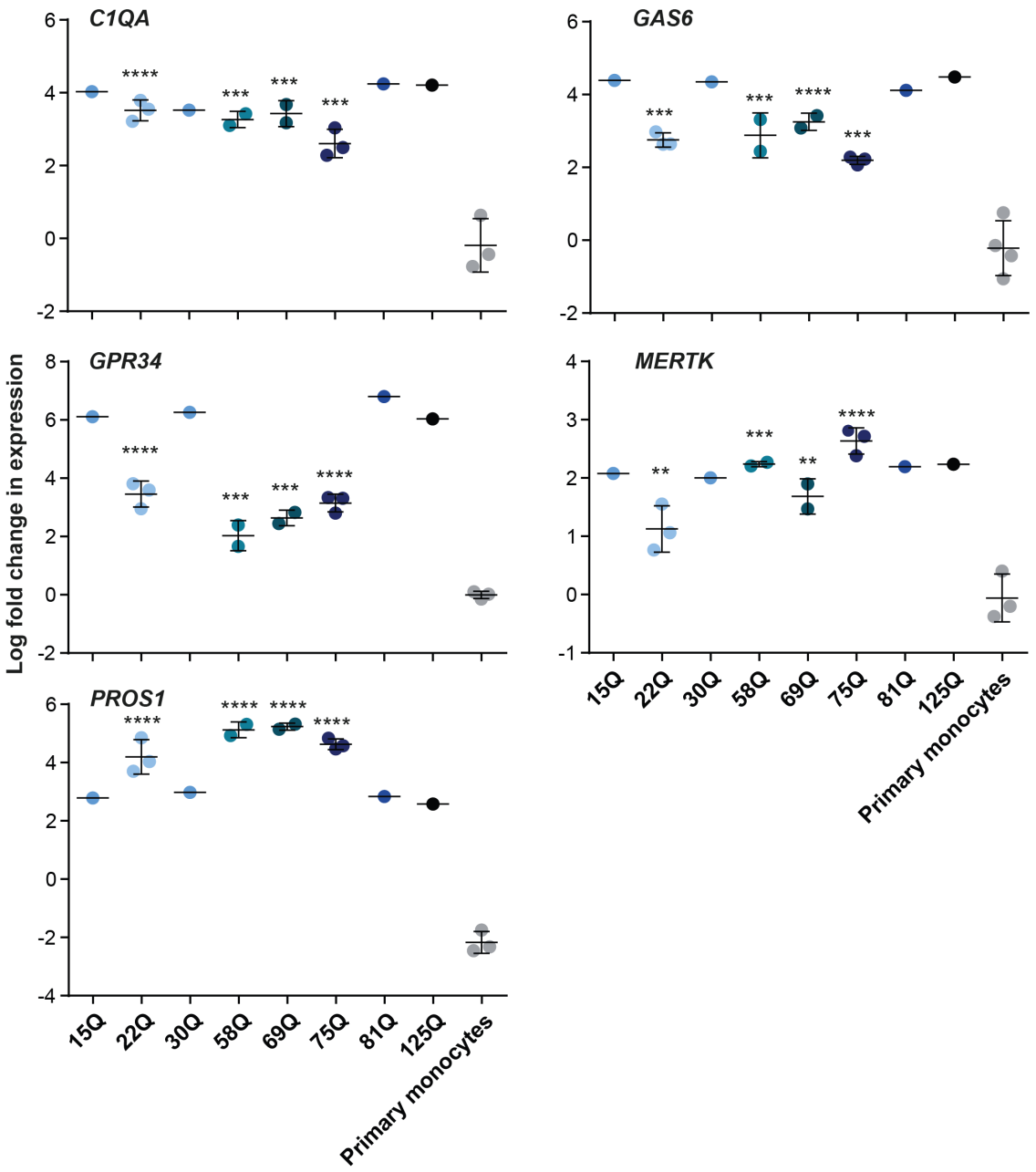

Figure 3.11: qPCR assessment reveals microglia-like identity of cells produced by the Van Wilgenburg et al., protocol. *C1QA*, *GAS6*, *GPR34*, *MERTK*, *PROS1* show increased expression in differentiated microglia-like cells relative to primary monocytes. Data shown are a log transform of the raw data, with all points plotted as a fold change relative to primary monocyte expression where the average expression of at least three primary monocytes samples was set as 1. The error bars shown represent the standard deviation (SD). N=1 differentiation of 15Q control iPSC line, n=3 clones of 22Q control iPSC line, n=1 differentiations of control 30Q ESC lines, n=3 differentiations of 45Q ESCs for panel A, n=2 clones of 58Q iPSC lines, n=2 69Q iPSC lines, n=3 clones 75Q iPSC line, n=1 differentiation of 81Q, n=1 125Q iPSC lines, n=3 or 4 independent

biological samples of primary monocytes. Each sample was run in triplicate, and the average taken and used as the result for that sample. Statistical testing was done on any line that had more than one data point, one-way ANOVA, followed by Dunnett's multiple comparison testing for significant change relative to primary monocytes for all genes.*P<0.05, **P<0.01, ***P<0.001, ****P<0.0001.

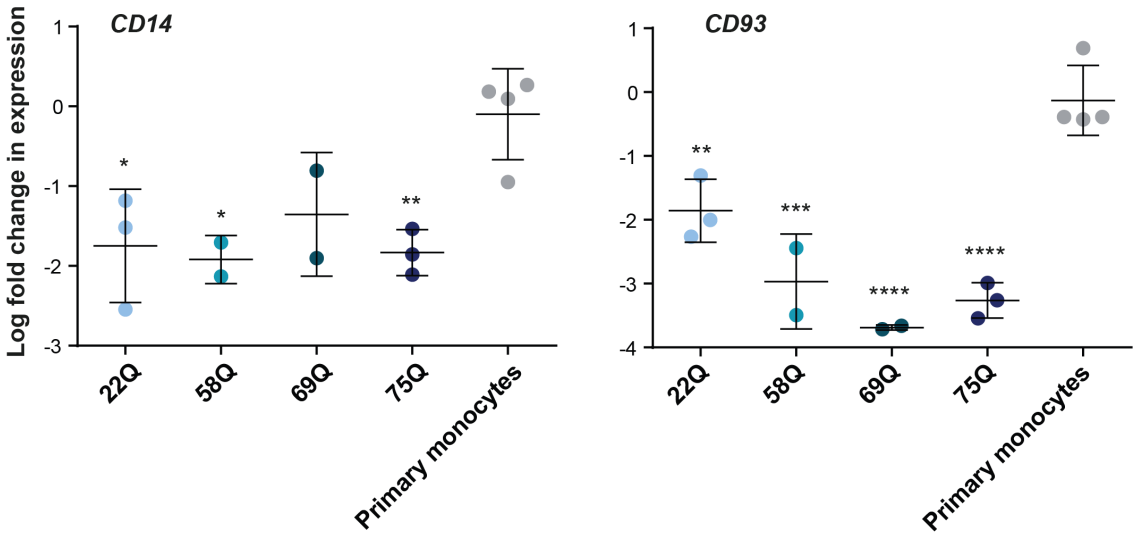

Figure 3.12: qPCR assessment reveals microglia-like identity of cells produced by the Van Wilgenburg et al., protocol. *CD14* and *CD93* expression was reduced relative to primary monocytes. Data shown are a log transform of the raw data, with all points plotted as a fold change relative to primary monocyte expression which was set as 1. The error bars shown represent the standard deviation (SD). N=1 differentiation of 15Q control iPSC line, n=3 clones of 22Q control iPSC line, n=2 clones of 58Q iPSC lines, n=2 69Q iPSC lines, n=3 clones 75Q iPSC line, n=4 independent biological samples of primary monocytes. Each sample was run in triplicate, and the average taken and used as the result for that sample. Statistical testing was done on any line that had more than one data point, One-way ANOVA, followed by Dunnett's multiple comparison testing for significant change relative to primary monocytes for all genes.*P<0.05, **P<0.01, ***P<0.001, ****P<0.0001.

3.4.9. Cells produced using the Van Wilgenburg protocol express key microglial proteins

To follow up this mRNA level assessment of microglial identity, three differentiations of the IsoHD lines were assessed for the expression of key

microglial proteins by high content imaging (section 2.10). This analysis revealed that cells in the cultures expressed TREM2, PU1, IBA1 and TMEM119 (Figure 3.13, A). Additionally, the composition of the cultures was found to be very pure, with close to 100% of viable cells imaged expressing these key markers (Figure 3.14, B).

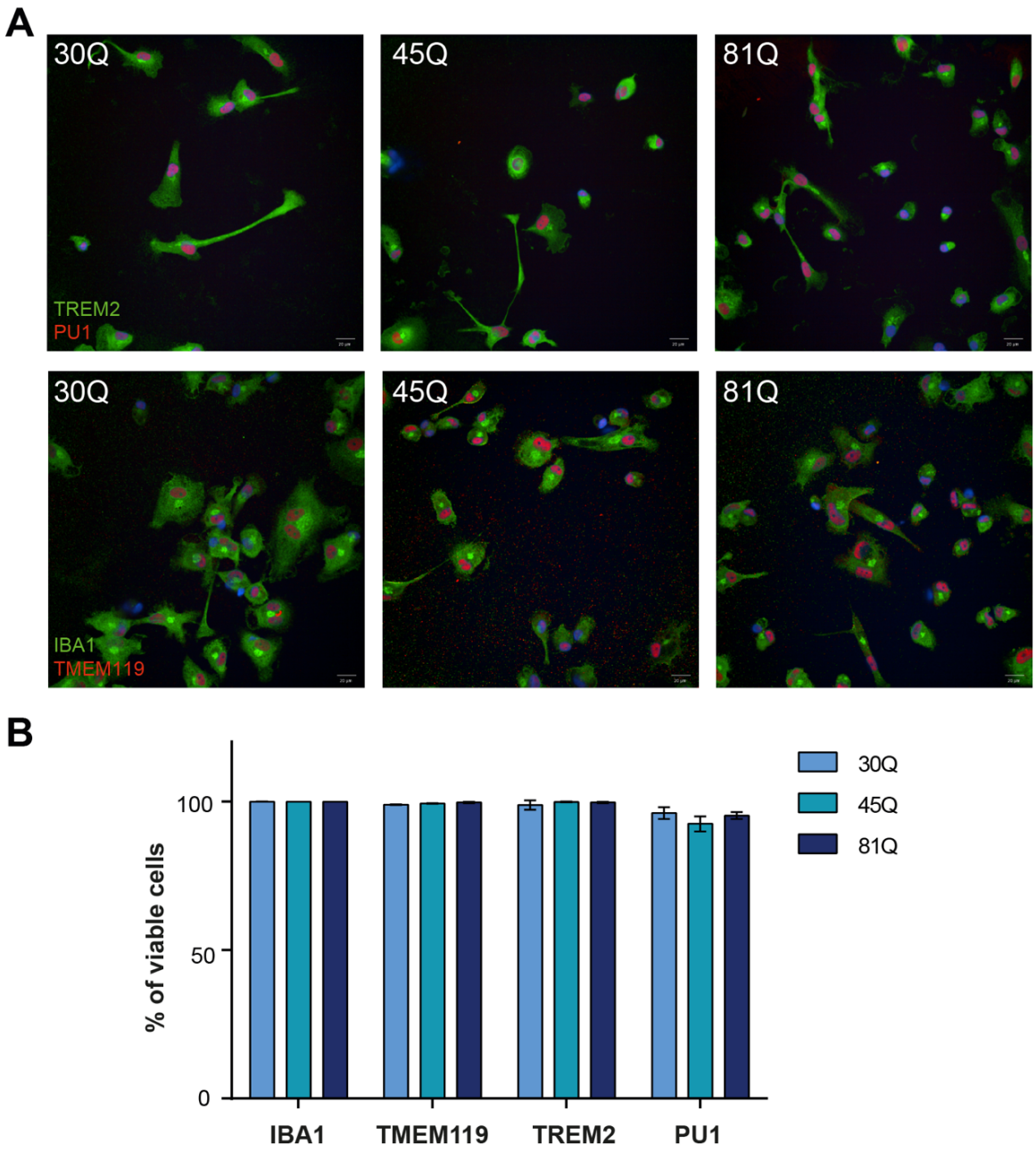

Figure 3.13: IF assessment reveals expression of key microglial genes in cells differentiated using the Van Wilgenburg et al., protocol. **A**) The top row shows example images from 30Q, 45Q and 81Q IsoHD lines differentiated to microglia-like cells and stained for TREM2 (green) and PU1 (red). The second

row shows example images from 30Q, 45Q and 81Q IsoHD lines differentiated to microglia-like cells and stained for IBA1 (green) and TMEM119 (red). **B**) Quantification of microglia-like cell culture composition reveals extremely purity, with close to 100% of viable cells expressing these key markers, as assessed using Columbus software as described (Appendix 1). Data shown are the mean ± SD. N=3 differentiations per line, with a minimum of six technical replicates per line per stain. Initial assessments of all antibodies used involved testing secondary only wells and were shown to have minimal signal; however these were not carried through for all subsequent experiments and therefore are not shown here.

3.4.10. The production of pro-inflammatory cytokines appears to increase with increasing polyQ length

In order to assess the functional impact of mHTT on microglia-like cells, the first experiment tested was the ability of the microglia-like cells to produce and release pro-inflammatory cytokines. This is an area where dysfunction has consistently been found in HD animal model microglia, and in the peripheral counterparts of microglia in humans.

This work focused on the large cohort of lines assessed in previous sections. These were differentiated and stimulated, and the supernatant collected and frozen before assessment using an MSD assay (section 2.15). All experiments contained a paired unstimulated control for each sample, to allow baseline levels to be accounted for. In these experiments, discrepancies in the density of the cells in wells were controlled for by assessing the protein level in each well tested.

The results in Figure 3.14 show a percentage increase from baseline, with the stimulated value divided by the baseline value and multiplied by 100 to give a percentage. This method showed similar patterns of results to the previous method used to assess cytokine production in cells produced by the Yanagimachi et al., 2013 protocol, where all samples could be run within a single plate. This analysis method was used because with the larger number of samples being tested, samples had to be tested across multiple MSD plates, which were not run simultaneously. A significant batch effect was observed between plates and runs as assessed by running duplicate samples across plates (data not shown), and

so to account for this and allow for comparison between samples run on different plates, the analysis method was altered to produce a percentage increase from baseline, rather than an absolute value, with the unstimulated and stimulated samples from each line run on the same plate.

In this way, a general trend towards increased cytokine response in HD lines was found. However, as is clear from Figure 3.14, the 22Q line from the HD family lines showed very high levels of cytokine response, far beyond that of the other control lines tested, and even the HD lines of the same background, highlighting the need to conduct experiments in multiple lines of cells from varying backgrounds.

Furthermore, this result informed the decision to prioritise use of the isogenic ESC series, the IsoHD series, in all future work, to ensure results found were due to the change in polyQ length, or HD status, rather than any other genetic factor.

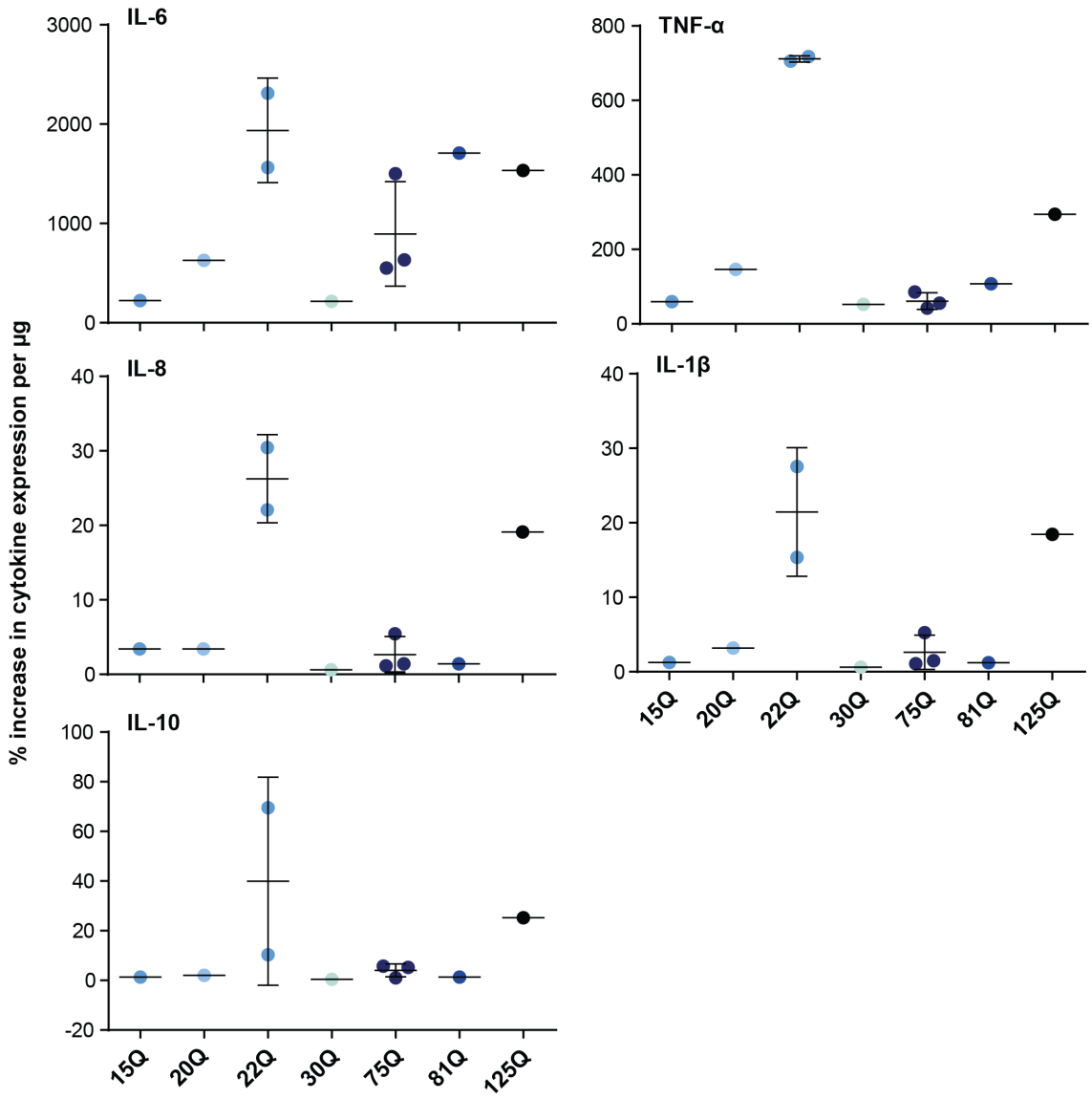

Figure 3.14: The production of key cytokines appears to increase with polyQ length. IL-6, TNFα, IL-8, IL-1β and IL-10 expression levels relative to baseline for each line appear to increase with increasing polyQ length. A notable exception are two clones of the 22Q HD family lines, which show considerably higher expression relative to the other lines of the HD family cohort, and relative to the other control lines assessed. This may be due to specific genetic differences in this line, unrelated to the polyQ length, highlighting the need to replicate results in multiple cohorts and with as many lines as possible. In this case, the correlation between increasing polyQ length and the percentage increase in cytokine expression from baseline is not statistically significant, at least in part due to the 22Q clones high variability, and elevated expression level. N=1 15Q iPSC line, n=1 20Q ESC line, n=2 clones 22Q iPSC line, n=1 differentiation 30Q ESC line, n=3 clones 75Q iPSC line, n=1 differentiation 81Q

ESC line, n=1 125Q iPSC line. Data shown are mean (± SD where applicable). Each sample was run in triplicate, and the average taken as the result for that sample. Positive and negative controls were provided by the manufacturer for this assessment, and were used to build a standard curve to inform analysis of the test samples results.

Further assessment of the pro-inflammatory response to an immune challenge was confined to the IsoHD series of lines in the following assessment. This was done to allow comparisons to be made in an identical genetic background, lowering the noise in the system. This assessment was conducted as described (section 2.15) and found that there was a significant increase in reactivity in the microglia-like cell lines carrying HD mutations, statistically significant in the case of the IL-6 and TNFα response. However, the changes in the levels of IL-8, IL-1β and IL-10 were not statistically significant (Figure 3.15).

It is notable that some variation between the differentiations of each line, conducted in parallel, still exists. This highlights the impact of environmental factors on cytokine production and release, and the inherent variability in the immune response.

Importantly, data shown below are controlled for cell number, as assessed by HCI (section 2.10), rather than using protein concentration, as in Figure 3.14. Additionally, in both figures, the data points shown are a percentage increase from baseline, thus each data point incorporate two separate pieces of information, the baseline and stimulated production of each cytokine per cell. An important control for these experiments would have been to directly assess mHTT expression levels in these microglia-like cell populations at the protein and mRNA level. However, this was not completed as part of these assessments, and so is a weakness of this approach.

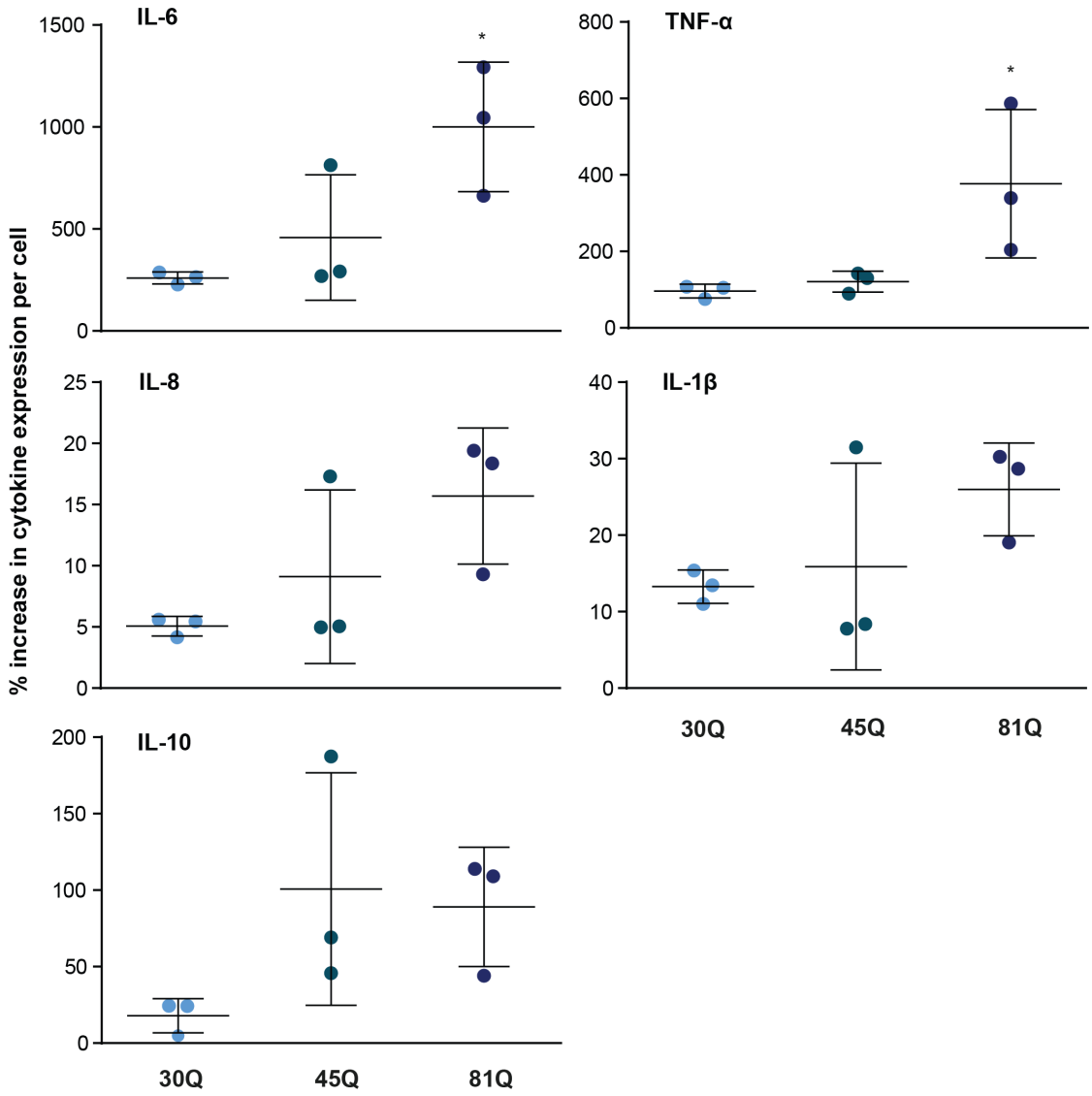

Figure 3.15: The increase from baseline in the production of IL-6 and TNFα is significantly affected by polyQ length. The percentage increase of IL-6 and TNFα are significantly different across the polyQ lengths tested, p=0.0291 and p=0.0422, respectively, tested using one-way ANOVA. IL-8, IL-1β and IL-10 also appear to be increasing with increasing polyQ length, but this is not statistically significant. Data shown are the mean ± SD. N=3 differentiations per line, with three technical replicates per sample. *P<0.05. Positive and negative controls were provided by the manufacturer for this assessment, and were used to build a standard curve to inform analysis of the test samples results.

3.4.11. The expression of key pro-inflammatory cytokines at the mRNA level increases upon stimulation, but shows no HTT polyQ-dependent effect.

To assess the possibility that the increased cytokine release was due to elevated transcription of the corresponding cytokine mRNA, samples were stimulated, and assessed by qPCR for the expression of these key pro-inflammatory cytokines' mRNA, (section 2.9). The results showed no obvious differences between the lines of varying HTT polyQ length.

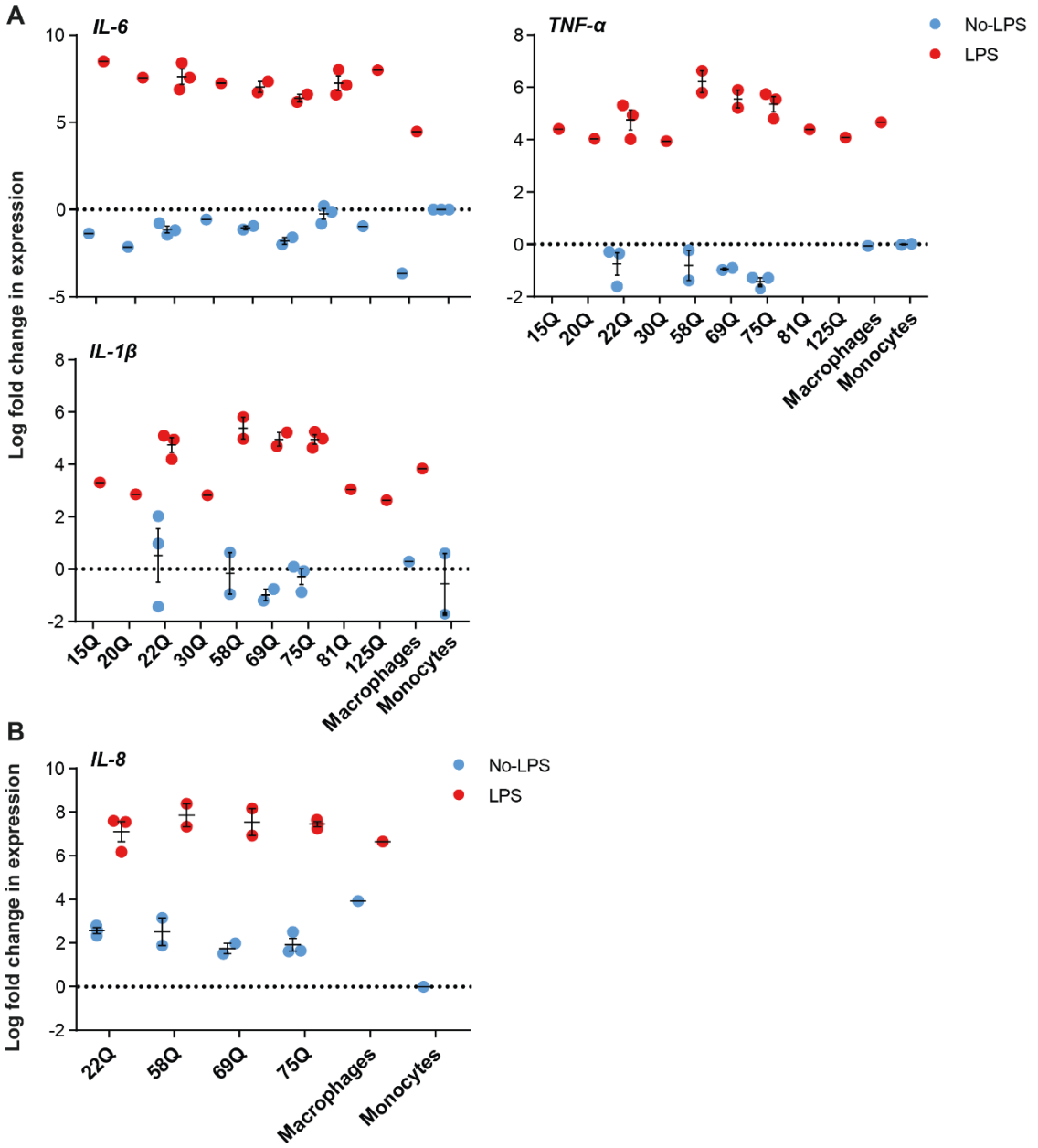

Figure 3.16: Transcripts of key pro-inflammatory cytokines increases following stimulation, but is not significantly different across varying polyQ lengths. **A**) *IL-6*, *TNF*α, and *IL-1*β mRNA expression was assessed in microglia-like cells differentiated from a large cohort of PSC lines, as well as primary macrophages and monocytes, using qPCR and revealed no clear differences in baseline of stimulated expression of mRNA across the polyQ lengths tested. **B**) *IL-8* mRNA expression at baseline and following 4 h stimulation was also assessed, in the HD family lines and primary human monocytes and macrophages, and again not significant. N=1 15Q iPSC line, n=1 20Q ESC line, n=3 clones 22Q iPSC line, n=1 differentiation 30Q ESC line, n=2 clones 58Q

iPSC line, n=2 clones 69Q iPSC line, n=3 clones 75Q iPSC lines, n=1 differentiation 81Q ESC line, n=1 125Q iPSC line, n=1 primary macrophage line, n=2 primary monocyte lines, except for IL-8 where n=1. Each sample was run in triplicate, and the average taken as the result for that sample. Baseline or unstimulated samples were not available for a number of lines of PSC derived microglia-like cells, and LPS-simulated data was not available for the primary monocyte samples. Data shown are the mean (± SEM, where applicable). mRNA expression for each gene tested was controlled back to expression of two housekeeping genes *GAPDH* and *ACTB*

3.4.12. Microglia-like cells cells show elevated production of Reactive Oxygen Species (ROS) in a polyQ dependent manner

Microglia-like cells were then tested for the production of ROS, which has been shown to be induced by the presence of mHTT in other models, and can cause oxidative stress and damage in cells. In this experiment, microglia-like cells differentiated from the cohort of PSC lines were assessed for their production of ROS after four hours under baseline conditions and upon stimulation with a ROS production-inducing toxin, TBHP (section 2.16). Analysis revealed a polyQ-dependency in ROS production upon stimulation with TBHP (Figure 3.17).

To follow, three lines of the IsoHD series (30Q, 45Q and 81Q) were differentiated three times in parallel, and ROS activity assessed under baseline conditions, or with TBHP treatment or stimulated with LPS and IFNγ, and readings taken at a series of earlier time points, as well as at four hours. This allows for comparison of the production of each IsoHD line in greater detail, to include assessment of earlier waves of ROS production. This assessment of production over time revealed significantly higher ROS production across four hours under baseline conditions, with the 45Q and 81Q lines significantly different to the 30Q control line, across three differentiations. When treated with TBHP and LPS, this difference appeared to remain, but was no longer significant (Figure 3.18).

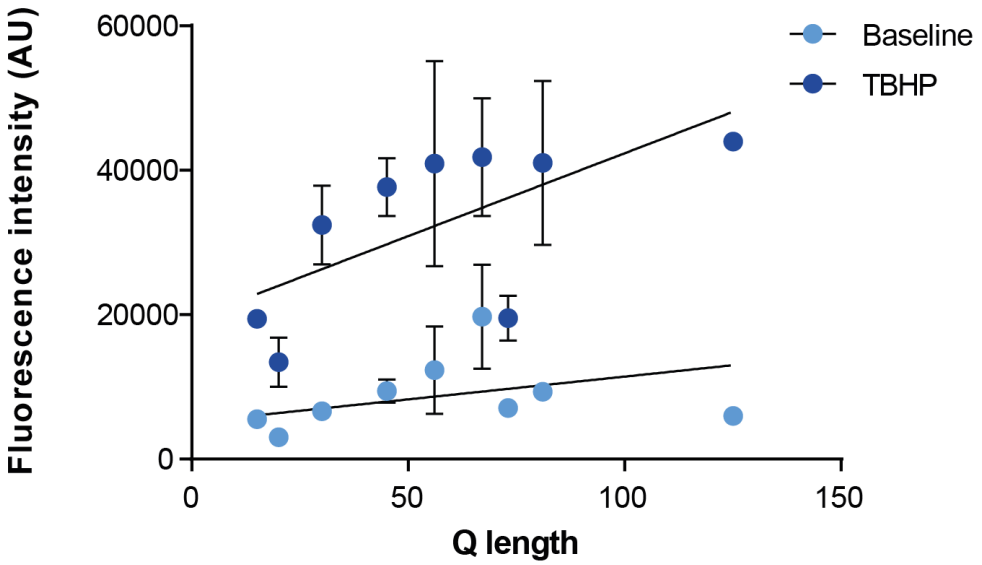

Figure 3.17: Production of ROS appears to increase in a polyQ-dependent manner in a cohort of PSC-derived microglia-like cells. Microglia-like cells

differentiated using the Van Wilgenburg protocol were assessed for ROS production using DCFDA/H2DCFDA – Cellular ROS Detection Assay Kit (Abcam), both untreated to give a baseline measure, and when treated with ROS-inducing toxin, TBHP for 4 h. At baseline, after 4 h, linear regression analysis found that the slope of DCFDA staining against polyQ length was not significantly non-zero. Following 4 h TBHP treatment, linear regression analysis found that the slope of DCFDA staining against Q length was significantly non-zero, $p=0.0040$. Data shown are the mean ± SD, where multiple differentiations (IsoHD lines) or clones (HD family lines) were assessed. N=1 differentiation 15Q iPSC, n=3 clones 22Q iPSC with an average calculated for each clone from a minimum of three experiments, n=4 differentiations 30Q ESC, n=3 differentiations 45Q ESC, n=2 clones 58Q iPSC with an average calculated for each clone from a minimum of three experiments, n=2 clones 69Q iPSC, with an average calculated for each clone from a minimum of three experiments, n=3 clones 75Q iPSC with an average calculated for each clone from a minimum of three experiments, n= 4 differentiations 81Q ESC, n=1 differentiation 125Q iPSC. For each sample six technical replicates were included, and the average taken as the result for that sample. Negative controls of unstained cells from each sample in baseline buffer and treated with TBHP were included in all ROS experiments, and the value for each line taken as a baseline for that line and subtracted from the value of the experimental wells for that line. In this way, the negative control data was included in the data shown here, and has not been plotted separately.

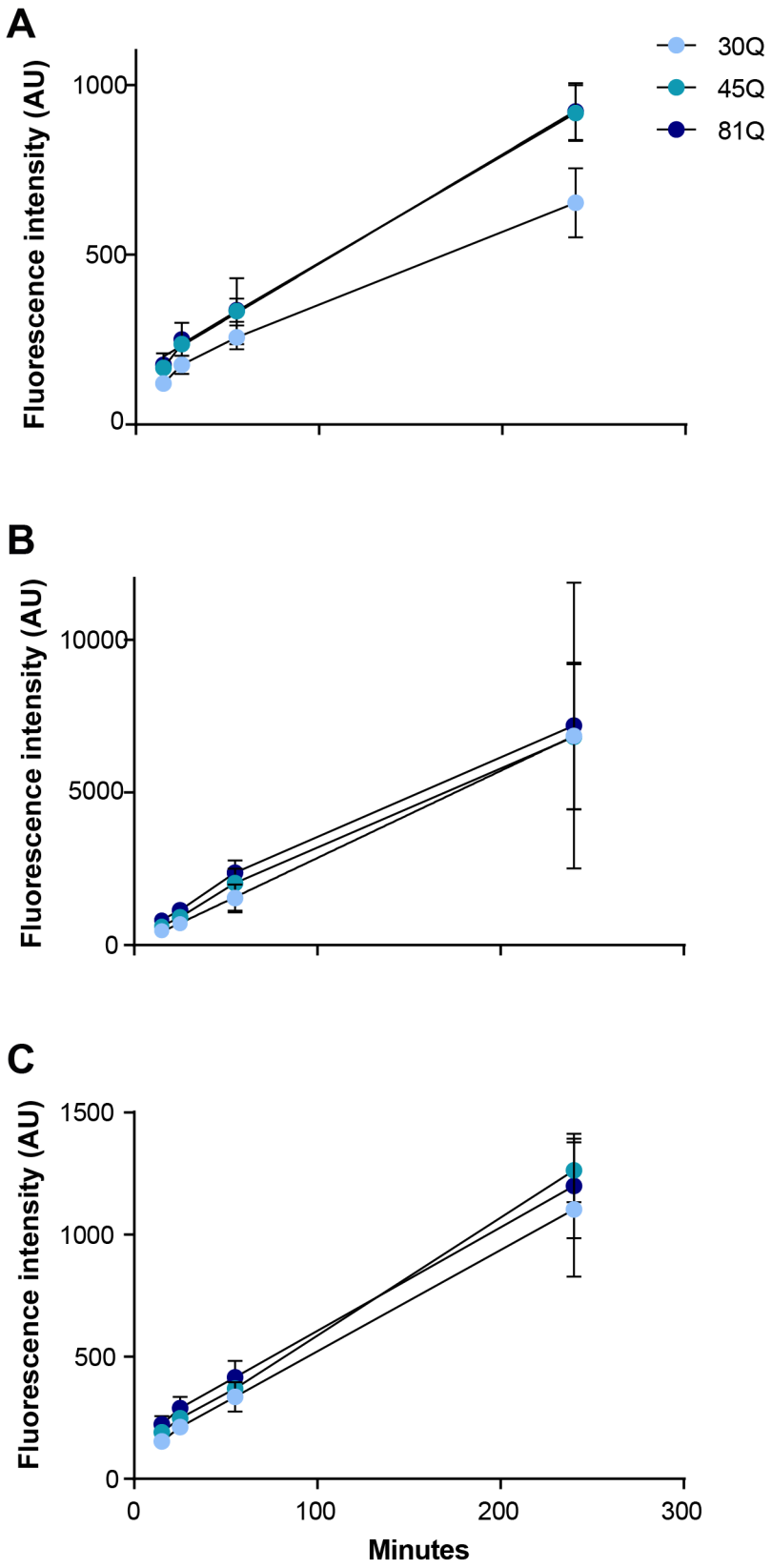

Figure 3.18: Significant differences in ROS production exist over 4h in the untreated condition in IsoHD microglia-like cells of varying Q lengths. A) Readings taken at 15, 25, 55 and 240 min from 30Q, 45Q and 81Q microglia-like cells in baseline buffer, reveal a significant difference in the slope in the 45Q and

81Q lines compared to the 30Q line, p=0.000. **B**) Parallel wells were treated with TBHP, however the difference between the lines was no longer significant. This may be partially driven by the high variation in readings at 4 h between the three differentiations of each line, p=0.982 **C**) Parallel wells were treated with LPS and IFNγ and the changes in ROS production in the 45Q and 81Q were not statistically significant, p=0.399. N=3 differentiations per line, with six technical replicates per test condition in each line in each differentiation. Data shown are the mean ± SD. Negative controls of unstained cells from each sample in baseline buffer and treated with TBHP were included in all ROS experiments, and the value for each line taken as a baseline for that line and subtracted from the value of the experimental wells for that line. In this way, the negative control data was included in the data shown here, and has not been plotted separately.

3.4.13. Production of Nitric Oxide species is similar across an isogenic series carrying varying polyQ lengths

Following the assessment of ROS production, the next logical step was to assess Nitric Oxide (NO) production in the microglia-like cell cultures, as the balance between nitrosative and oxidative stress is key to determining whether NO and ROS production result in cellular damage, with low levels of both ROS and NO species used for intracellular signalling. Crucially, the production of NO has been shown to be altered in the HD brain in models of HD. This was achieved through the use of two methods to assess NO production, first looking at intracellular production using a fluorometric method, and then looking at released levels of NO species in the supernatant (section 2.17).

The production of NO species, specifically nitrate and nitrite, under baseline conditions and following stimulation was assessed after 24 h using a fluorometric method (section 2.17.2). Under these conditions, it was found that intracellular levels of both nitrate and nitrite were not significantly different between the control polyQ length cells (30Q) and the HD lines (45Q and 81Q), and these HD lines were also not significantly different from each other. This suggests that there is no significant difference in NO species production with increasing polyQ length. Interestingly, treatment with LPS and IFNγ did not appear to induce elevated NO species production, as might be expected, with the stimulated cells actually showing slightly lower levels of nitrate. The supernatants from these treatment groups was also assessed, but levels of nitrate and nitrite were undetectable using this particular method.

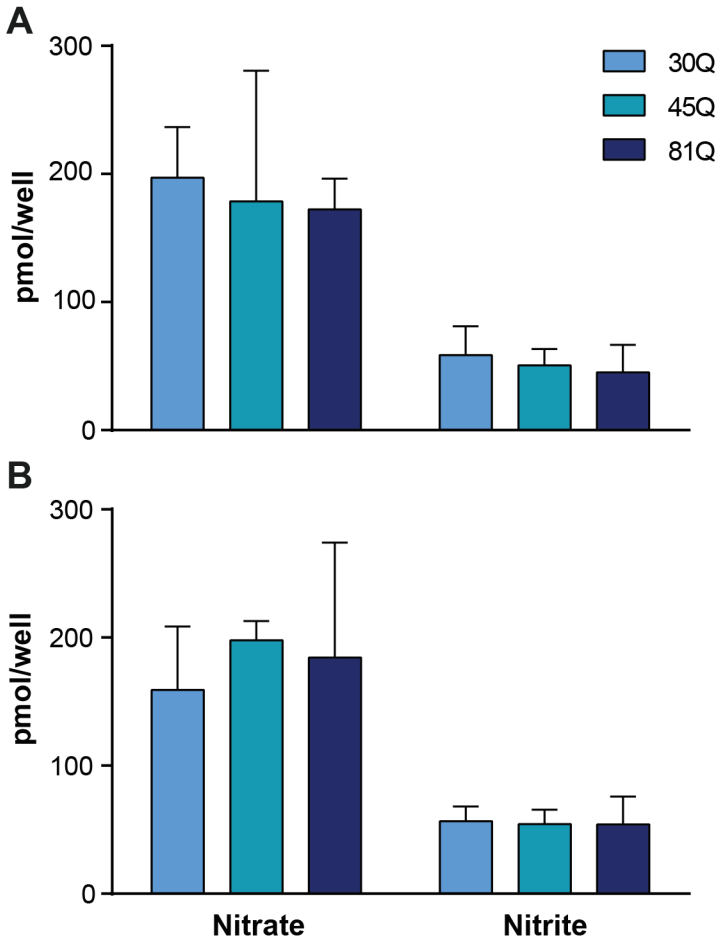

Figure 3.19: The production of nitrate and nitrite in microglia-like cells is not significantly affected by polyQ length. **A**) Under baseline conditions, after 24 h there is no significant production between lines of varying polyQ length in either nitrate or nitrite levels intracellularly. **B**) When stimulated with LPS and IFNγ for 24h, there is also no significant difference between lines carrying varying polyQ lengths. Interestingly it appears this stimulation does not appear to have increased nitrate or nitrite production intracellularly, as might be expected based on the literature. Data shown are the mean ± SD. N=3 differentiations per line, with three technical replicates per sample tested. The manufacturer of this test kit provides nitrate and nitrite standards which were used to create a standard curve for each, allowing quantification of the levels in the experimental samples. In this way, positive control data was incorporated in these data shown above.

The production of nitrite in the supernatant of microglia-like cells was then assessed using the Griess method of nitrate detection as described in (section 2.17.1). This method allowed detection in the supernatant that was not possible using the previous method. At 24 h and 48 h, there was not a significant difference

between the control (30Q) and HD members of the isogenic series (45Q, 81Q). Additionally, as seen previously, there did not appear to be an elevated production of nitrite following LPS and IFNγ treatment at either the 24 h or 48 h time points.

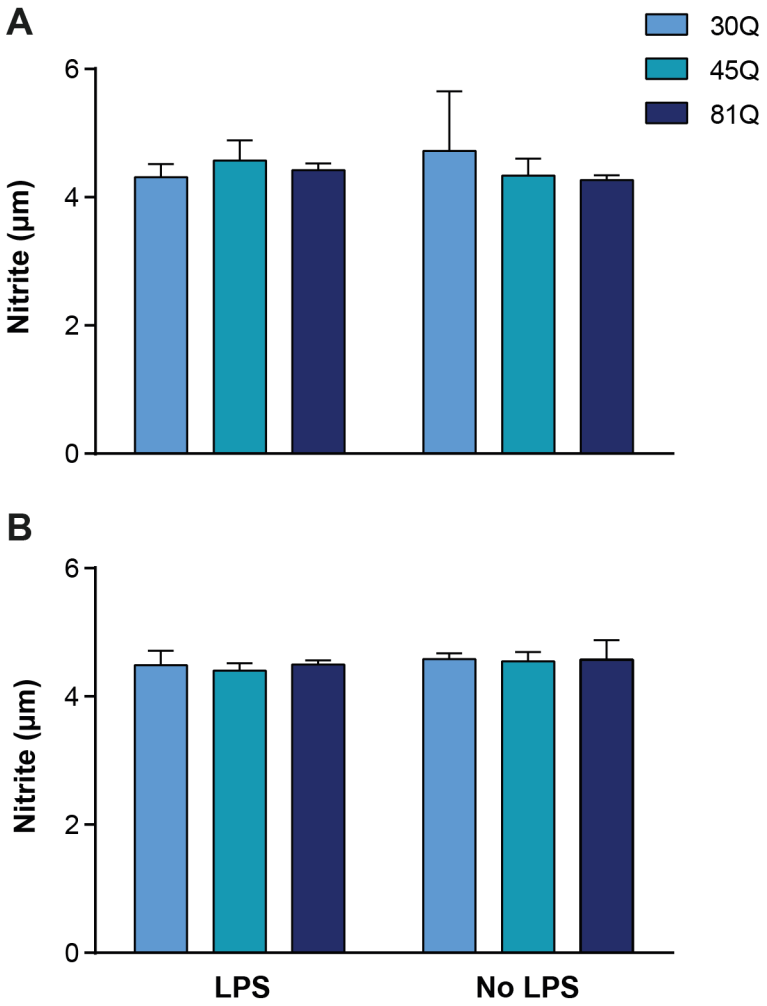

Figure 3.20: Nitrite production at 24 h and 48 h under stimulated and baseline conditions is similar across three polyQ lengths. A) Following 24 h of incubation, microglia-like cells treated with LPS and IFNγ, or untreated, show similar levels of nitrite released into the supernatant across 30Q, 45Q and 81Q carrying lines, with no significant impact of treatment type or polyQ length. **B**) Parallel wells were incubated for 48 h and a similar pattern seen, with no significant impact of treatment group or polyQ length on nitrite release into the supernatant. Data shown are the mean ± SD. N=3 differentiations per line, with three technical replicates per sample. Nitrite standards were generated and used to create a standard curve, allowing quantification of the levels in the

experimental samples. In this way, positive control data was incorporated in these data shown above.

3.4.14. PSC-derived microglia-like cells show decreased viability at baseline

It was then important to assess the impact of mHTT on the viability of microglia-like cells at baseline and under stressed conditions. In the HD brain, the environment becomes increasingly toxic, and it may be the case that mHTT-carrying microglia-like cells not only contribute to the production of a toxic environment through the production of pro-inflammatory cytokines and ROS species, but that they themselves are more sensitive to this toxic environment, and become less viable, releasing apoptotic and cell damage signals into the brain milieu, feeding the cycle of hyper-reactive microglia-like cells, and damage to the CNS tissues.

Assessment of viability at baseline, 9 h following a media change, using an LDH assay, revealed that there was an increase in percentage cell death with increasing polyQ length, with ~25% increase in cell death in the 125Q compared to the 15Q line. Analysis using linear regression revealed this slope to be significantly non-zero, $p=0.0268$.

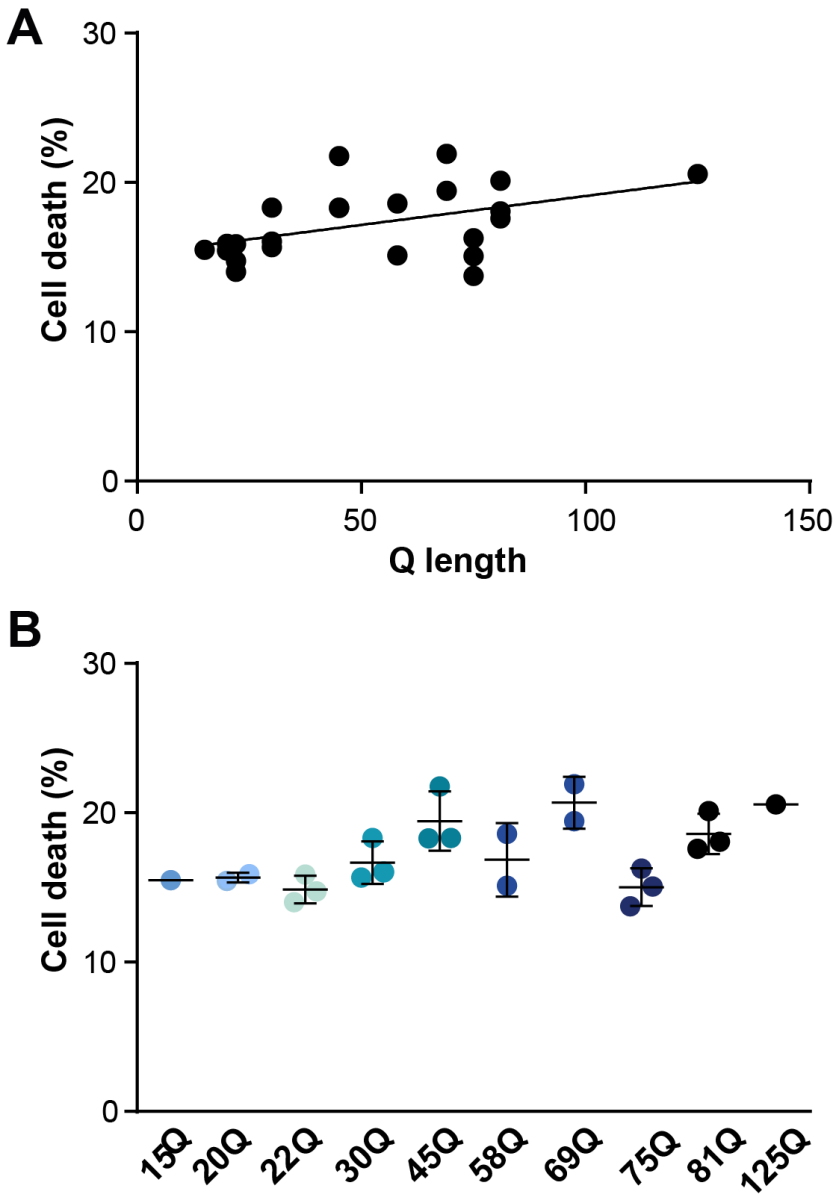

Figure 3.21: PSC-derived microglia-like cells show reduced viability at baseline in a polyQ-dependent manner. A) Linear regression analysis of the relationship between polyQ length and percentage cell death shows the slope is significantly non-zero, p=0.0268. **B**) The percentage of cell death found following 9 h in fresh media across a large cohort of PSC and ESC lines. N=1 differentiation 15Q iPSC, n=3 clones 22Q iPSC with an average calculated for each clone from a minimum of three experiments, n=4 differentiations 30Q ESC, n=3 differentiations 45Q ESC, n=2 clones 58Q iPSC with an average calculated for each clone from a minimum of three experiments, n=2 clones 69Q iPSC, with an average calculated for each clone from a minimum of three experiments, n=3 clones 75Q iPSC with an average calculated for each clone from a minimum of three experiments, n=4 differentiations 81Q ESC, n=1 differentiation 125Q iPSC.

All samples were run in triplicate and the average taken as the value for that sample. Data shown in panel A are all individual data points, as well as the line calculated through linear regression analysis. Data shown in panel B are all individual data points as well as the mean of each line ± SD where applicable. LDH assays include a potent toxin to allow the calculation of 100% cell death in the test wells, this allowed calculation of the percentage cell death in each test well as a proportion of the 100% cell death value.

3.4.15. PSC-derived microglia-like cells show decreased viability following exposure to an autophagy inhibitor

The first stressor to be assessed for its impact on microglia-like cell viability was the autophagy inhibitor, Bafilomycin A1. Microglia-like cells differentiated from the HD family lines iPSCs, the IsoHD series as well as additional control lines (20Q ESC, and 15Q iPSC) and an additional HD line (125Q iPSC), were treated with 20ng of Bafilomycin A1 for 9 h, and the levels of cell death assessed using an LDH assay (section 2.12.1). This assay revealed a polyQ-dependent increase in cell death that was statistically significant (Figure 3.22). This assay was internally controlled through production of a 100% cell death reading for each well.

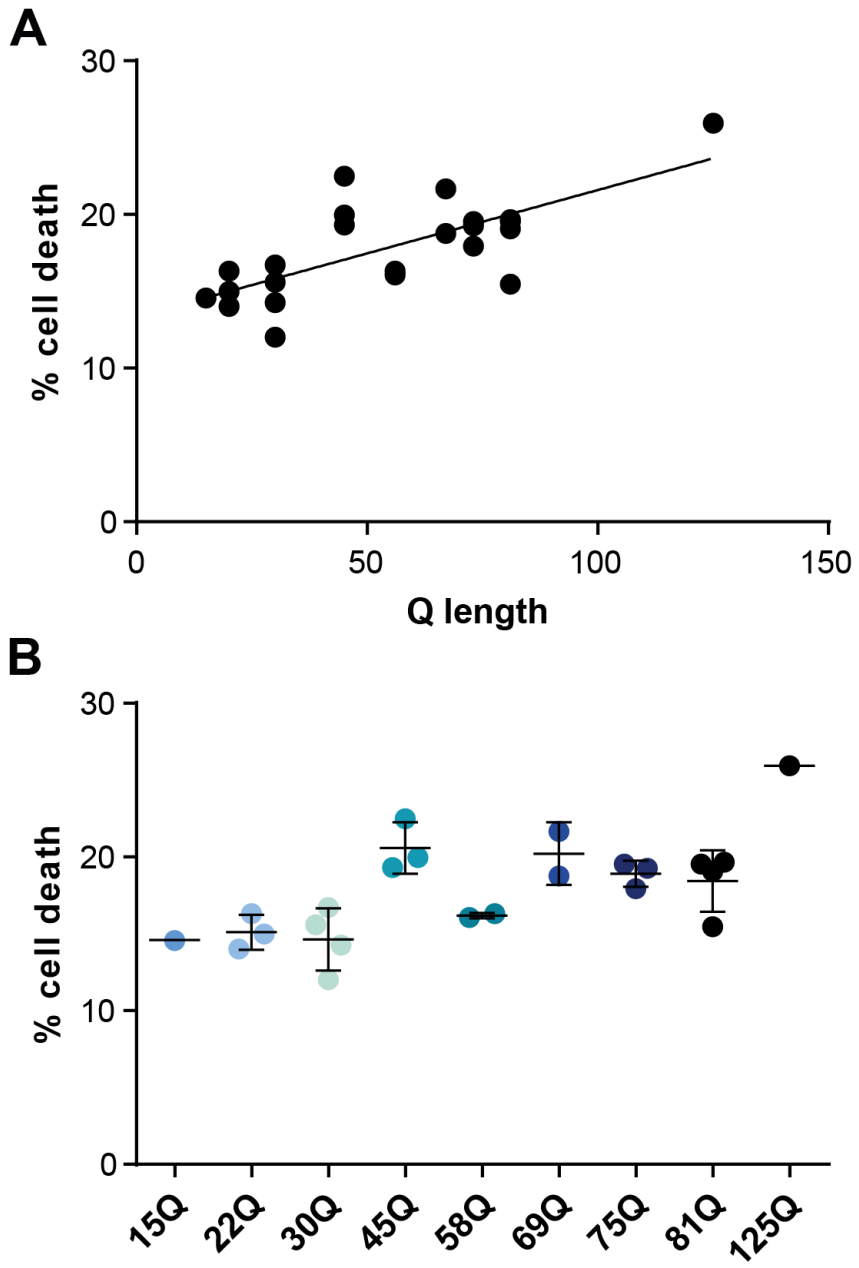

Figure 3.22: PSC-derived microglia-like cells show increasing sensitivity to Bafilomycin A1 exposure in a polyQ-dependent manner. A) Linear regression analysis of the relationship between polyQ length and percentage cell death shows the slope is significantly non-zero, p=0.0001. **B**) The percentage of cell death found following 9 h of Bafilomycin A1 treatment across a large cohort of PSC and ESC lines, relative to the 100% cell death reading for each well of each condition. N=1 differentiation 15Q iPSC, n=3 clones 22Q iPSC with an average calculated for each clone from a minimum of three experiments, n=4 differentiations 30Q ESC, n=3 differentiations 45Q ESC, n=2 clones 58Q iPSC

with an average calculated for each clone from a minimum three experiments,, n=2 clones 69Q iPSC, with an average calculated for each clone from a minimum of three experiments, n=3 clones 75Q iPSC with an average calculated for each clone from a minimum of three experiments, n= 4 differentiations 81Q ESC, n=1 differentiation 125Q iPSC. Each sample was tested in triplicate and the average used as the result for that sample. Data shown in panel A are all individual data points, as well as the line calculated through linear regression analysis. Data shown in panel B are all individual data points as well as the mean of each line ± SD, where applicable. LDH assays include a potent toxin to allow the calculation of 100% cell death in the test wells, this allowed calculation of the percentage cell death in each test well as a proportion of the 100% cell death value.

3.4.16. PSC-derived microglia-like cells show decreased viability in the presence of an inducer of oxidative stress, hydrogen peroxide

The next toxin to be assessed for its impact on microglia-like cells viability was the oxidative stress inducer, hydrogen peroxide. Microglia-like cells differentiated from the HD family lines iPSCs, the IsoHD series as well as additional control lines (20Q ESC, and 15Q iPSC) and an additional HD line (125Q iPSC), were treated with 12.5mM of Hydrogen Peroxide for 1 h, and the levels of cell death assessed using an LDH assay (section 2.12.1). This assay revealed a polyQ-dependent increase in cell death that was statistically significant (Figure 3.23). This assay was internally controlled through production of a 100% cell death reading for each well.

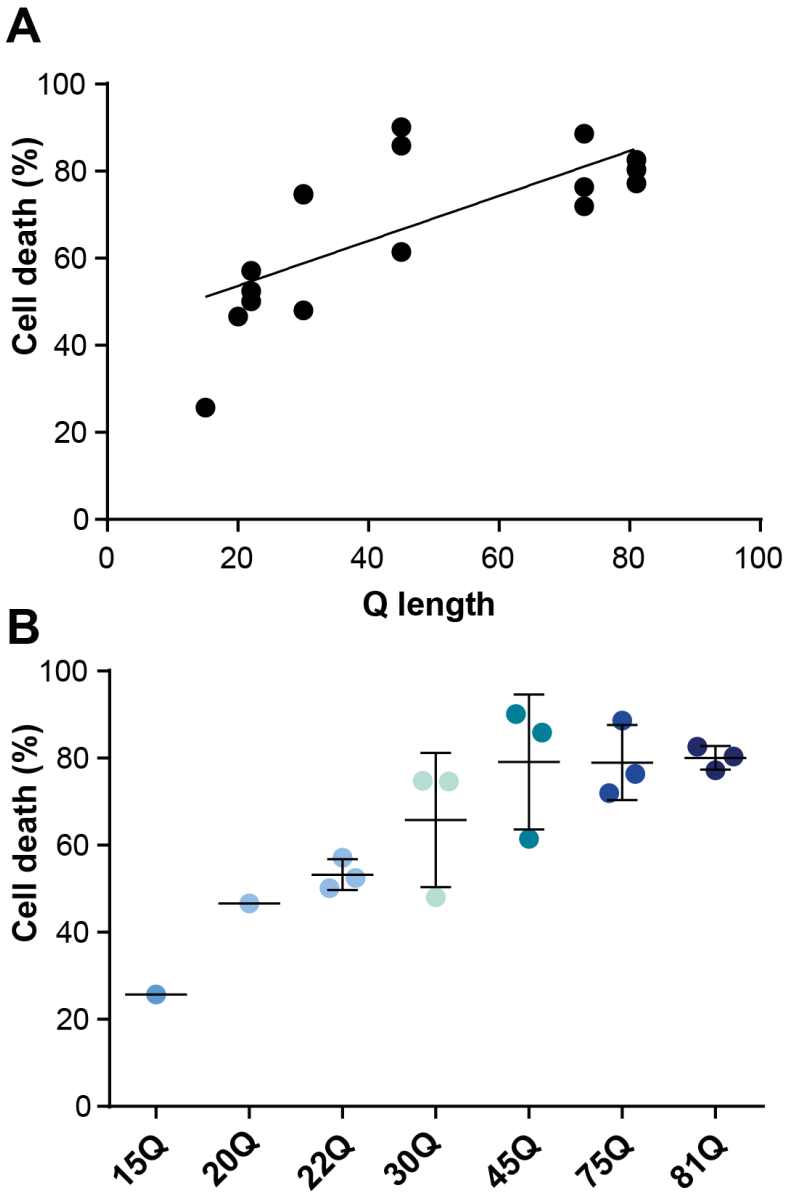

Figure 3.23: PSC-derived microglia-like cells show increasing sensitivity to Hydrogen Peroxide exposure in a polyQ-dependent manner. A) Linear regression analysis of the relationship between polyQ length and percentage cell death shows the slope is significantly non-zero, p=0.0013. **B**) The percentage of cell death found following 1 h of Hydrogen Peroxide treatment across a large cohort of PSC and ESC lines, relative to the 100% cell death value calculated for each well of each condition. N=1 differentiation 15Q iPSC, n=1 differentiation 20Q ESC, n=3 clones 22Q iPSC, n=3 differentiations 30Q ESC, n=3 differentiations 45Q ESC, n=3 clones 75Q iPSC, n=3 differentiations 81Q ESC. Each sample was tested in triplicate and the average used as the result for that sample. Data shown in panel A are all individual data points, as well as the line calculated

through linear regression analysis. Data shown in panel B are all individual data points as well as the mean of each line, ± SD where applicable. LDH assays include a potent toxin to allow the calculation of 100% cell death in the test wells, this allowed calculation of the percentage cell death in each test well as a proportion of the 100% cell death value.

3.4.17. PSC-derived microglia-like cells show a polyQ dependent increase in apoptosis in the presence of stressors

To follow this blunt assessment of microglia-like cell viability in response to various stressors using the LDH assay, a more sensitive assessment of the induction of apoptotic activity using these stressors was conducted. Differentiated microglia-like cells from the IsoHD isogenic series containing control (30Q) or HD (45Q and 81Q) polyQ lengths were treated with two toxins and the level of apoptosis assessed using a Promega assay kit (section 2.12.3).

Treatment with 40ng of Bafilomycin A1 over 24 h revealed elevated levels of apoptosis in both the 45Q and 81Q lines, that was statistically significant as assessed by linear regression analysis (Figure 3.24, A).

Treatment with Hydrogen Peroxide (8mM) for 24 h also showed elevated levels of apoptosis in the HD microglia-like cells (45Q and 81Q) over the treatment period compared to the control microglia-like cells (30Q). This was statistically significant as assessed by linear regression analysis (Figure 3.24, B).

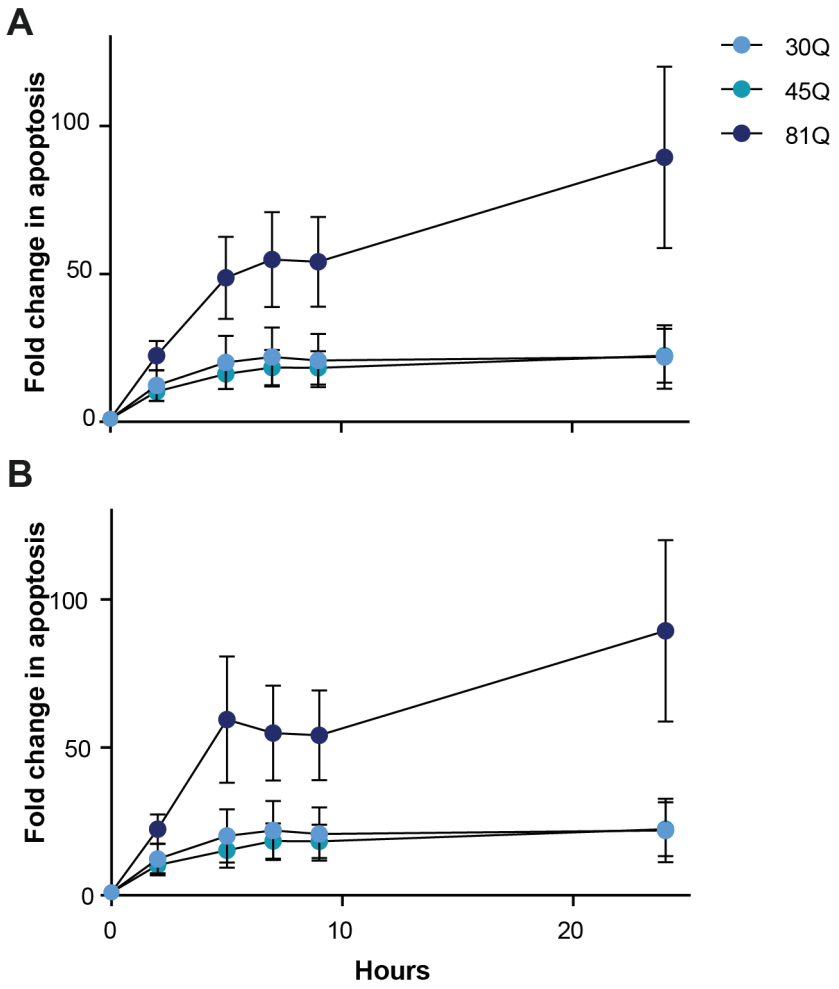

Figure 3.24: Exposure to toxins results in higher levels of apoptosis in a HTT polyQ-dependent manner. A) Data plotted from periodic readings over a 24 h treatment with Bafilomycin A1, show an increase in apoptotic activity over time. Linear regression analysis found that the slope of the 45Q and 81Q microglia-like cells was significantly non-zero, p=0.0299 and p=0.0013 respectively. The slope of the 30Q line was not significantly non-zero, p=0.1645. **B**) Data plotted from periodic readings over a 24 h treatment with Hydrogen Peroxide, show an increase in apoptotic activity over time. Linear regression analysis found that the slope of the 45Q and 81Q microglia-like cells was significantly non-zero, p=0.0298 and p=0.0034 respectively. The slope of the 30Q line was not significantly non-zero, p=0.1645. Data shown are the mean ± SD. N=3 differentiations per line, with three technical replicates per sample. Negative control well of cells untreated by toxins, and cell-free wells were included and the values used to establish baseline values for each line, which were subtracted from experimental values to give the results shown above.

3.4.18. PSC-derived microglia-like cells show phagocytic activity that is unaffected by polyQ length

Finally, the last area of microglial functionality assessed was phagocytic activity. A number of studies have previously found phagocytic activity to be elevated in microglia from the R6/2 mouse model of HD and in peripheral macrophages from HD patients.

Levels of phagocytic activity were assessed. Microglia-like cells carrying a range of polyQ lengths differentiated from two lines from the HD family lines (22Q, 75Q) as well as a control and HD line from the IsoHD series (30Q and 81Q, respectively) and additional controls (20Q ESC, 15Q iPSC) and an additional HD line (125Q iPSC), were assessed for phagocytic activity using pHrodo *Zymosan A* beads (section 2.13). Data shown is from one differentiation of each line, with two clones of 20Q HD family line and three clones of the 75Q HD family line. This analysis revealed no significant difference in phagocytic activity across the polyQ lengths tested and the different cohorts of lines tested. The phagocytic activity was controlled for the protein concentration in each sample, to account for any small discrepancies in total cell number.

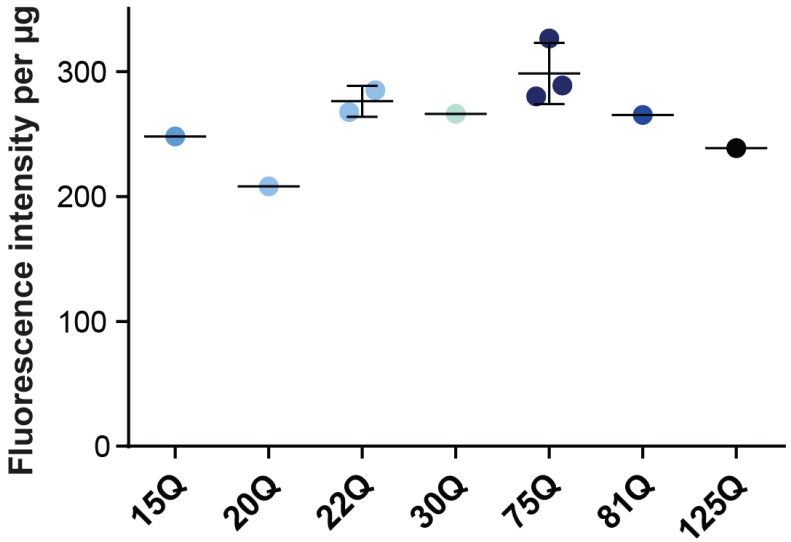

Figure 3.25: PSC-derived microglia-like cells show phagocytic activity which is not affected by polyQ length. Microglia-like cells of varying polyQ length show similar phagocytic activity as measured by pHrodo *Zymosan A* beads. N=1 differentiation of 15Q iPSC, n=1 differentiation of 20Q ESC, n=2 clones of 22Q iPSC, n=1 differentiation of 30Q ESC, n=3 clones of 75Q iPSC, n=1 clone of 81Q ESC, n=1 clone of 125Q iPSC. Data shown are the mean (±

SD where applicable). Six technical replicates per sample tested were run. Negative control wells of cells without phagocytic beads and cell-free wells with beads were also run, and the values used to establish a baseline for each line tested, and that baseline value subtracted from the experimental value found to give the data shown above.

The same cohort of lines was differentiated, and the microglia-like cells assessed for phagocytic activity using pHrodo *E.coli* beads (section 2.13). This analysis showed a similar pattern to the previous experiment, with no significant differences between HD lines and controls.

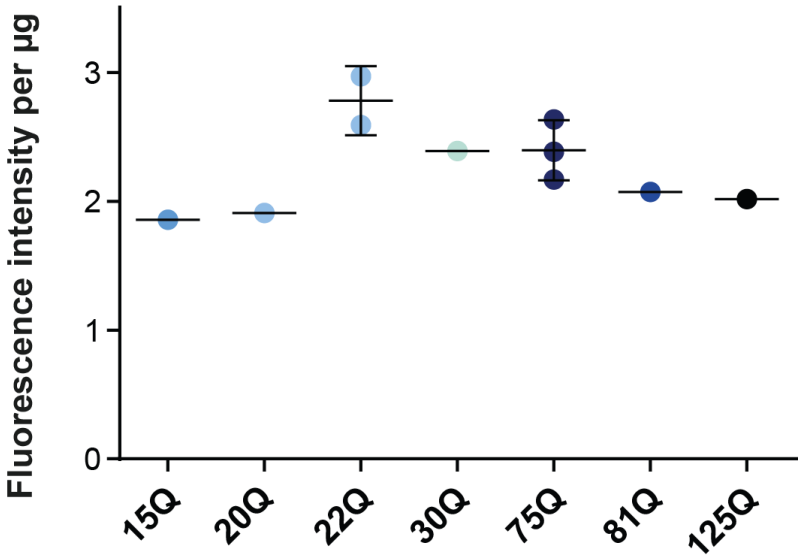

Figure 3.26: PSC-derived microglia-like cells show phagocytic activity which is unaffected by polyQ length. Microglia-like cells of varying polyQ length show similar phagocytic activity as measured by pHrodo *E.coli* beads. N=1 differentiation of 15Q iPSC, n=1 differentiation of 20Q ESC, n=2 clones of 22Q iPSC, n=1 differentiation of 30Q ESC, n=3 clones of 75Q iPSC, n=1 clone of 81Q ESC, n=1 clone of 125Q iPSC. Data shown are the mean (± SD where SD can be calculated). Six technical replicates per sample tested were run. Negative control wells of cells without phagocytic beads and cell-free wells with beads were also run, and the values used to establish a baseline for each line tested, and that baseline value subtracted from the experimental value found to give the data shown above.

3.5. Discussion

Two microglial differentiation protocols were initially assessed for their ability to produce microglia-like cells, as assessed by their expression of key microglial genes (*P2RY12, TREM2, TMEM119, IBA1, C1QA, GAS6, GPR34, MERTK* and *PROS1*) at mRNA level, and proteins (TREM2, PU1, IBA1 and TMEM119) as assessed by immunofluorescence, as well as meeting functional criteria, with cells being capable of phagocytosis, cytokine production and ROS production. These criteria are in keeping with the standard measures in other published protocols of microglial differentiation (Abud et al., 2017; Douvaras et al., 2017; Muffat et al., 2016; Pandya et al., 2017). One was then selected for use in an in-depth investigation into the effect of mHTT on microglia-like cell functionality. The first protocol tested was that published by Yanagimachi et al. 2013, which was initially tested under the remit of finding a high quality blood monocyte differentiation protocol, but following revelations in the field, was re-classified as a microglia-like or tissue resident macrophage differentiation protocol (Douvaras et al., 2017). Here, the yield of cells from this protocol was low relative to that achieved by the protocol's authors. Nevertheless, assessment using qPCR found that the harvested cells were enriched for a panel of key microglial genes, with subsequent experiments confirming the expression of two key genes at the protein level. The cells displayed phagocytic activity and their viability was consistent at baseline. Unfortunately, the low yield of this protocol, the limited time period over which harvesting could take place and the cost of supplying growth factors for the protocol meant that it was not an ideal choice for further use. The protocol also presented some technical difficulties, with the initial seeding density determining its later success. The challenging nature of this was highlighted by difficulties that other members of the lab had in adopting the protocol. If this method had actually produced blood monocytes, it is likely that its use would have continued, providing a peripheral counterpart to the microglia-like cells produced by other protocols being tested. However, given that the cells produced were actually microglia-like in identity, this protocol's limitations meant that it was dropped from use in this project.

The second protocol to be tested was that designed by Van Wilgenburg et al. 2013, which was also originally published as a blood monocyte differentiation

protocol, but was corrected prior to testing beginning in this project (Buchrieser et al., 2017). The initial assessment of this protocol found that the total yields were considerably higher than that achieved with the Yanagimachi et al., 2013 protocol, and the method less technically challenging. Therefore, given that assessments by qPCR confirmed the microglia-like identity of these cells and that cells could be harvested for at least six weeks after the initial harvest, if not longer, and in their publication the authors had shown the cells produced also showed key aspects of microglia functionality; phagocytic capacity and cytokine release, it was decided use this method. These aspects of function were particularly of interest for experiments assessing the effects of mHTT expression on microglial function, as previous research had shown microglia from HD rodent models to be hyper-reactive in their cytokine production, and the peripheral counterparts of microglia, macrophages, had been reported to have differential phagocytic activity compared to controls (Connolly et al., 2016; Kwan et al., 2012).

To test this, a large cohort of HD and control PSC lines were differentiated by this method to test for any impact of mHTT, containing a range of polyQ lengths, on the differentiation process. Thorough assessment found that while there were some differences between groups of lines, i.e. the HD family iPSC and IsoHD ESC series, there was no significant HTT polyQ effect in the enrichment of key microglia genes or total yield. The microglial identity of the cells produced from every line was confirmed through the assessment of key microglial gene expression. The IsoHD series was also assessed for culture composition, finding that that the purity of these cultures was extremely high, with close to 100% of viable cells expressing the key microglial markers tested for and no clear HTT polyQ length-dependent differences in the differentiation of PSCs to microglia-like cells.

With this confirmed, the next step was to look at the function of the cells produced, to assess whether these differentiated cells show the capacity of human microglia for cytokine production, ROS and NO production and phagocytosis. An additional layer of interest was to assess the capacity of HD versus control microglia-like cells, to ascertain whether human HD cells show dysfunction as has been seen in rodent microglia. The first area of function assessed was the inflammatory response. In order to assess the inflammatory capacity of HD versus control

microglia-like cells, the production of key pro-inflammatory cytokines in response to an immune challenge was assessed.

This was done using LPS and IFNγ treatment for 24 h for assessments at the protein level with each stimulated sample matched to an untreated control sample from the same cell population. Gene expression levels of these cytokines was also assessed, after 4 h of stimulation.

It is important to note that LPS is a commonly used stimulant of immune cells, and it was used in this thesis to allow comparison to the existing body of work in rodent models and in peripheral immune cells. However, it should be noted that it is not the ideal stimulant, and a more physiologically relevant stimulant such as MMP9 would have been interesting to use.

Interestingly, mRNA levels of *IL-6*, *TNFα*, *IL-1β* and *IL-8*, while significantly elevated upon stimulation, did not show any HTT polyQ-dependent changes. This is different to what has been found in human post mortem studies, where elevated mRNA expression of pro-inflammatory cytokines has been found in a number of brain areas (Björkqvist et al., 2008; Silvestroni et al., 2009). However, primary mouse YAC128 cultures show the same pattern as found here, with no differences at the mRNA level, despite changes at the protein level (Connolly et al., 2016). This may be due to a lack of sensitivity in the qPCR method to detect smaller changes in expression level, which result in meaningful differences in protein levels produced, or perhaps the protein expression levels are modulated in a different way, downstream of the transcription of mRNA. It may also be the case that the mRNA differences found in human post mortem studies do not originate from the microglia in these brain areas.

As for the cytokine response at the protein level, there was a general trend towards an increased response compared to baseline, in the HD lines. However, the control line from the HD family series showed an increased response compared to the other control lines tested, and even the other lines from the HD family series, with expanded HTT polyQ-lengths. This was the case even when controlled for cell number using the proxy of protein concentration. This suggested that this particular facet of the immune response in microglia-like cells carrying HTT 22Q from the HD family series was altered, perhaps through the presence of different genetic factors in that line relative to the related remaining

HD family lines. The impact of these other genetic factors, and possibly epigenetic differences caused by biases during the reprogramming process to produce iPSCs, was very evident, leading to the decision to confine future work to the isogenic, IsoHD lines, where any results found could be attributed to solely to HTT polyQ-length.

Three parallel differentiations for each IsoHD line were conducted, so that any differences introduced as a result of being a temporally separate differentiation, likely due to slightly altered application of the protocol by the user each time, could be controlled for.

These parallel differentiated microglia-like cells were assessed, and their cytokine profiles showed some variability, even when cell number per well was controlled for directly through the use of HCI, and the implementation of synchronised or parallel differentiations. Results shown were controlled for baseline levels of cytokine production, as became necessary due to samples being compared from different MSD plates, run across a number of days. It is important to note that the graphs shown are in fact conveying two distinct, if related, pieces of information at once - both the baseline cytokine level and the stimulated cytokine level. This became necessary in order to control for batch effects between different plates and the general variability in total immune responses that are found. In this way, it was found that HD microglia-like cells showed larger reaction to LPS and IFNγ treatment than control lines, with the largest polyQ length (81Q) showing the greatest response. The level of variability encountered may suggest a weakness in this model for assessing this function, however it should be noted that *in vivo* the human immune system is also highly variable, so any model will have a certain element of this variability if it is to recapitulate the human immune system.

In mouse models, such as the YAC128 and R6/2 models, microglia isolated *ex vivo* show elevated levels of cytokines released, and these results were controlled for protein level, but not baseline levels of production (Björkqvist et al., 2008; Connolly et al., 2016). The effect size may be larger in these mouse models due to the larger polyQ length, as in the results shown in this chapter, with the highest polyQ lengths tested, 125Q and 81Q, showing the largest response compared to baseline. It may also be the case that the microglia-like cells

differentiated in this thesis are more foetal in their identity and function, and as such the aging of cultures may result in greater effect sizes. There is evidence that microglia become increasingly primed for activation during ageing through upregulation of MHCII proteins and TLRs (Norden and Godbout, 2013).

It is beneficial to establish this difference in inflammatory responsiveness in the HD lines *in vitro* in this model, as it has been seen before in primary mouse cultures *ex vivo*, but it has not been shown directly in human microglia. It is also meaningful that this phenotype is found *in vitro*, outside the influence of other cell types as would be the case in the brain. This suggests a cell autonomous effect of the HD mutation, albeit at a lower effect size than previously found with rodent models.

In the CNS in HD, microglia are unlikely to be reacting to immune challenges such as bacterial infections often, more likely is that microglia would be activated by damage or stress signals from degenerating neurons. Additionally, the presence of other cell types modulates microglia responses, for example Haenseler et al., 2017 showed that differentiated microglia were less pro-inflammatory when co-cultured with cortical neurons. In that particular study, the cortical neurons were healthy however, so it would be interesting to assess the cytokine profile of microglia in the presence of unhealthy neurons, to see if this dampening down of pro-inflammatory cytokine production in a neuronal environment remains in the presence of damage signals, as would be present in a HD brain. Given the level of damage in the HD brain at symptom onset, one imagines that the microglial response would be pro-inflammatory, however this remains to be tested directly.

As such, it would be interesting to co-culture HD and control microglia-like cells with both HD and control neurons of various sub types, and assess the responsiveness of microglia-like cells when stimulated under co-culture conditions. This would allow assessment the impact of mHTT on microglia-like cell responsiveness in a neuronal environment. It would also be possible to investigate the impact of mHTT-containing microglia-like cells on the health and signalling of neurons in such a paradigm and how that in turn the neuronal population would impact the microglia-like cells co-cultured with them.

Additionally, it would be of interest to age both the MSN cultures and the microglia-like cell cultures and assess their interactions under these more senescent conditions, which might be closer to the environment where we begin to see dysfunction in adult onset patients.

Thinking more broadly, this model could be used to assess microglia-like cells differentiated from iPSCs or ESCs generated from patients of many neurodegenerative diseases. Of particular interest would be Alzheimer's disease, where genetic studies have heavily implicated microglia and inflammation in the disease (Jones et al., 2010). Of course, as AD is not a monogenic disease (beyond the familial forms of the disease), this would require assessing a much larger numbers of lines, to try and capture an AD-specific effect.

Another area that was assessed, and where a consistent HD and HTT polyQ-dependent effect was found in this work, was ROS production. ROS production is required for normal redox signalling, but large increases in production, and imbalances between ROS and reactive nitrogen species (RNS) production, are associated with oxidative stress and damage to the cell.

Comparing across a large cohort of PSC lines differentiated to microglia-like cells when treated with TBHP, an inducer of oxidative stress, a significant correlation between increased ROS production and increasing HTT polyQ-length was found. These data are largely in keeping with that found in animal models of HD, where the R6/1 model shows elevated ROS production before the onset of symptoms, with lipid peroxidation appearing later. This suggests that there is an elevated ROS production phenotype in the HD brain, that begins to cause significant damage to the tissue with age, as anti-oxidant mechanisms become less able to counteract the higher production (Kovtun et al., 2007; Pérez-Severiano et al., 2004, 2000). It may be that microglia contribute in part to HD pathogenesis in this way.

More generally, there is significant evidence of mitochondrial dysfunction in HD, not just in microglia, with elevated ROS production driven by mHTT expression and correlated with increasing polyQ sizes (Hands et al., 2011) and an accumulation of oxidative damage found post mortem in HD patients (Browne et al., 1997). Mitochondria are not just a producer of ROS, they are also a target of ROS-mediated damage, and oxidative damage has been shown to accumulate

in mitochondrial DNA in a murine model of HD and in patient fibroblasts (Wang et al., 2013). It would be of interest to assess the possible mitochondrial dysfunction in the microglia-like cells produced by this protocol, and investigate the presence of oxidative damage in the mitochondrial DNA.

To follow up these initial experiments, earlier time points were assessed using only the IsoHD lines. Interestingly, in this experimental paradigm, there were statistically significantly higher levels of ROS production in the HD lines under baseline conditions. This result was not with TBHP or LPS and IFNγ exposure so the effect must be assumed not to be real in this set up, as the changes were not statistically significant. Notably, there appeared to be quite high variability between the differentiations of each line in the TBHP-treated condition. This may be due to differences between the differentiations in terms of sensitivity to TBHP, or due to slight differences in seeding density, resulting in increased noise in the data. Additionally, it may be worth extending the period of assessment of ROS production in response to LPS and IFNγ to 24 h, as this is generally the time point at which cytokine production has peaked. This was not possible in this work, as the manufacturer of the DCFDA kit used could not guarantee the stability of the DCFDA stain beyond the time points tested. It may be possible to pre-treat with LPS, before spiking the cultures with DCFDA stain for the last 4 h and assess ROS production, but this would require optimisation to preserve the viability of the cell culture, given that the readings must be done in either phenol-red-free media or buffer.

Crucially, this assessment did not isolate which ROS specifically were altered, instead taking a broad look at ROS generally. In the future, it would be useful to isolate which specific species are driving the increases seen here, and where they are produced in the cell, from the mitochondria or if it is NAPDH oxidase-derived. The detail of the timescale over which these increases occur would also be interesting to look at with a more sensitive assessment method. It would also be interesting to assess a more physiologically relevant stressor, such as MMP3 or MMP9, to see if these resulted in increased ROS production. The stimulant used in these works, TBHP is a very strong stimulant, and while useful for an initial assessment in a maxed-out system, it may not reflect the sort of stressors that microglia would naturally experience. As such, the results shown using TBHP

should be considered preliminary, and may not reflect the response of microglia to endogenous stressors. Finally, an extension of this work would be to assess the expression levels and activity of anti-oxidising agents in HD and control microglia-like cells, to assess whether the elevated levels seen relate to a deficit in anti-oxidant activity.

These results fit with evidence from other research in this area, which suggests that elevated levels of lipid peroxidation, DNA strand breaks, cytoplasmic lipofuscin, and the accumulation of oxidative markers in DNA, caused by oxidative stress, occur in the HD brain (Stack et al., 2008), and that levels of the antioxidants, SOD and ascorbate, are reduced in the brains of transgenic mouse models of HD. In addition to this, *in vitro* studies have found decreased levels of anti-oxidant proteins in culture, and interventions upregulating these antioxidants attenuate mHTT-induced toxicity of neurons (Lee et al., 2011; Pitts et al., 2012; Rebec et al., 2002; Santamaría et al., 2001). A large number of antioxidant therapeutics have been assessed for use in HD, and while some preclinical studies were very promising, evidence of efficacy in clinical trials has been mixed thus far (Gil-Mohapel et al., 2014). In fact, all major trials for antioxidants in HD have been negative to date (Hersch et al., 2017, 2006; Peyser et al., 1995; Ranen et al., 1996).

A related area that was assessed was NO production. The balance between nitrosative and oxidative stress is key to determining whether NO and ROS production result in cellular damage, with low levels of both ROS and NO species used for intracellular signalling.

Two methods for assessing NO levels were used; the first using a DAN fluorescent probe, and the production of nitrate and nitrite standard curves, combined with paired lysate samples with and without nitrate conversion, allowing for the assessment of both nitrate and nitrite levels in the cell lysate. Unfortunately, the assay was not sensitive enough to pick up either NO product in the supernatant and there was no significant difference in either nitrate or nitrite production in the lysate across the three IsoHD lines tested, either under baseline conditions or following LPS and IFNγ stimulation.

Crucially, it appears that the stimulation treatment was ineffective, with nitrate and nitrite production on a par, if not lower than the unstimulated samples. This

could be due to limitations of the method, perhaps there was a lack of sensitivity in the measurements, or as the NO product levels was close to the lower limit of detection, it may be that there was too much noise in the data to see an effect.

This was followed by an assessment of NO production using the Griess method. This was conducted only in the supernatant from stimulated or unstimulated microglia-like cells at 24 and 48 h. Again, there was no difference across the three IsoHD lines tested and no significant induction of NO production in response to stimulation. The Griess method involves the production of nitrite standards, so in this way there was a positive and negative control included, and the lack of NO production seen in the samples must be assumed to be an issue with the samples rather than the assessment method. However, it has been previously found that human microglia produce much lower amounts of NO, and must be more harshly stimulated to do so, than rodent microglia (Smith and Dragunow, 2014). As such, a more sensitive testing method may find there is NO production, just at very low levels. Corresponding RNA samples were collected for each supernatant sample, converted to cDNA and assessed for iNOS expression by qPCR, however two different sets of primers were unable to pick up any iNOS gene expression. This may be due to issues with the primers, as there was also no positive control for this assessment, although the design of the primers was from published papers (Guo et al., 2003; Lara-Marquez et al., 2002; McAdam et al., 2012; Skorokhod et al., 2007). Alternatively, it may have been the case that there simply was insufficient iNOS expression for it to be picked up by qPCR, or that a low amount in the starting cell lysate was quickly degraded prior to the production of the cDNA. To follow up this work, it would be important to successfully assess iNOS production.

In summary, both methods to assess NO production suggest that no differences exist due to the presence of mHTT. The results also suggest that in this model LPS and IFNγ stimulation are insufficient to induce higher NO production. This may be alleviated by pre-treatment with IFNγ before LPS stimulation, rather than simultaneous exposure as was done here. Additionally, the use of more physiologically relevant NO inducers such as MMP3 or MMP9 may be of interest.

Finally, it may be the case that altered NO production occurs only in an aged microglial culture, which was not assessed in this work. This may be in keeping

with what has been found in the assessment of NO activity in the R6/1 mouse model of HD, where significant differences from controls only appear at 19 weeks, with 11 week old animals unchanged from controls (Pérez-Severiano et al., 2002). Another study which looked specifically at nNOS, found that there were reduced neuronal levels in the R6/1 mouse model at later stages of the disease, which correlated with disease phenotypes such as body weight and clasping. However, administration of an iNOS inhibitor appeared to have no effect on behavioural symptom progression. Interestingly, mice lacking nNOS showed accelerated disease progression, whereas mice with one copy of the nNOS gene showed delayed onset of symptoms compared to mice carrying both copies of the gene. This suggest a complex phenotype surrounding nNOS and iNOS expression in HD (Deckel et al., 2002). A similar study looked at iNOS and nitrotyrosine levels in the R6/2 model of HD, and found elevated levels of both compared to controls (Tabrizi et al., 2000). This was combined with assessments of mitochondrial function, which revealed significant reductions in both aconitase and mitochondrial complex IV activities in the striatum, as well as a decrease in complex IV activity in the cerebral cortex.

In conclusion, it appears that in this *in vitro* model of HD, microglia-like cells do not show elevated levels of NO production, and although assessment at the mRNA level was not possible, the protein level of nitrate was assessed using two different techniques and confirmed to be unchanged. These results may be unexpected given the changes in ROS production found in this model; however, it is clear that changes in NO production are complex in HD.

An important area of microglial cell function to assess in HD lines compared to controls was the ability to respond to cellular stressors and toxins. The bulk of this work was done using the LDH assay. Using this method, it was found that at baseline in the absence of any additional stressors, there was a minor but significant difference in viability across the lines tested. With this established, the viability of HD and control microglia-like cell cultures was assessed in the presence of two stressors, either Bafilomycin A1, an autophagy inhibitor, or Hydrogen Peroxide, which causes oxidative stress. These stressors were chosen as autophagy is known to be impaired with age, as well as in HD specifically, and

hydrogen peroxide treatment results in oxidative damage, which as has been previously mentioned, is known to occur in HD (Browne et al., 1999).

In the presence of these toxins, a clearer relationship between HTT polyQ-length and viability emerged, with the longer Q lengths being less viable, with greater cell death. Some variability was found between the differentiations, although this cannot be due to differences in composition, as the cultures produced were shown to consistently be of very high purity of microglia-like cells across multiple differentiations. Additionally, small variations in cell numbers in the tested wells were controlled for using a 100% cell death measurement for each well. It is therefore likely that the small differences between differentiations were due to slight variation in how the cells were treated up until the point of the assay, and the execution of the assay itself; user-error induced variability. Nonetheless, the effect found was significant, and was found consistently across the IsoHD ESC lines, the HD iPSC family lines and additional control and HD lines. This suggests an increasing inability to cope with stress in the cell in the presence of increasing HTT polyQ lengths, and is significant if one considers the toxic environment of the HD brain, particularly as neurons begin to degenerate and damage signals and debris. However, studies of HD patients have shown an accumulation of microglia (Khoshnan et al., 2017b; Tai et al., 2007). As such, it would be useful to devise an *in vivo* version of these experiments to test if this effect is real and physiologically relevant.

Finally, the phagocytic ability of HD and control microglia-like cells was assessed in a cohort of iPSC and ESC-derived microglia-like cells, carrying a variety of polyQ sizes.

This assessment found that all lines show phagocytic activity indicating that they show this functional capacity of microglia, However, there was no significant difference across varying polyQ sizes.

This is at odds with what has been found in primary R6/2 mouse microglia and in primary patient macrophages, where increased levels were found (Träger et al., 2015). This may be due to the foetal nature of the microglia-like cells tested here, compared to those tested in the R6/2 and compared to the patient macrophages, as microglia from young mice have been shown to be more phagocytically active than aged microglia (Bliederhaeuser et al., 2016; Floden and Combs, 2011; Njie

et al., 2012). In this way, it could be that the HD and control microglia-like cells show similar high levels of phagocytosis, at this early developmental stage, and that differences appear related to the aging process. Interestingly, a study in rhesus monkeys showed the opposite effect, with increased phagocytic activity exhibited by microglia with increasing age. This was postulated to be due to increased myelin damage in certain brain areas and was assessed using stereology, as opposed to *ex vivo* culturing, which may impact the results (Shobin et al., 2017).

It is also important to reiterate that microglia are heavily influenced by their environment. For example, research has found that RNA sequencing of microglia immediately upon isolation from a human donor, versus *ex vivo* cultured microglia from the same donor, show a significantly altered RNA expression signature. Specifically, culturing harvested microglia *ex vivo* results in the downregulation of specific microglial signatures (for example, CX3CR1), and when comparing between two individuals, *ex vivo* culturing makes microglia from two donors more similar to each other (Gosselin et al., 2017). This suggests that microglia may lose some of their environment-specific gene expression signature, and therefore phenotype, rapidly in culture. These findings have relevance for this work also, suggesting that studying microglia-like cells in very pure cultures, as is described in this chapter, without the guiding signals of other cell types, may result in a loss of disease phenotypes that might be found in HD microglia *in vivo*. For these reasons, the characterisation of HD microglia-like cells in isolation in the chapter, is followed by co-culture type assessments in the subsequent chapter.

As touched upon in this introduction, another caveat to this work is that there is evidence for different types of microglia in the human CNS, with region-specific identities and functional capacities. This may be due in part to innate differences in the cells in those areas, but also the impact of the environmental signals in each area, resulting in epigenetic changes, which is no doubt a large contributing factor. This *in vitro* model represents microglia-like cells in the absence of these environmental cues, and so these results may not be applicable to microglia in all parts of the human CNS.

Finally, it should be noted that one cannot rule out that the differences seen in cytokine and ROS production, and viability, may in part be due to differences in

differentiation capacity of HD vs control iPSCs and ESCs. While all lines were assessed for their expression of key microglial genes and proteins, and these were satisfactorily expressed, it may be the case that the HD or control lines were more or less differentiated than each other, which may have been revealed in the testing of functional capacities. This is challenging to untangle, and further research using this model could consider testing for a broader range of markers of adult microglia, or try to isolate the impact of mHTT expression but using a model with conditional expression that could be induced following the differentiation period.

3.6. Summary

Both methods used produced cells that express key microglial genes at the mRNA and protein level, and showed the necessary functionalities of the resident immune cells of the CNS; with phagocytic capacity, cytokine production in response to stimuli and ROS production. Given the larger yields available using the Van Wilgenburg protocol, however, it was chosen to take forward for an in depth characterisation of the impact of mHTT of increasing polyQ-length on microglial function.

In comparing HD and control microglia-like cells, it was found that the presence of mHTT has an impact on the viability of microglia-like cell cultures, results in increased ROS production, and results in increased pro-inflammatory responses to immune challenges, with a statistically significant, or non-significant trend towards polyQ dependency in the strength of the effect in all modalities tested. Unchanged by the presence of mHTT in the cells was their phagocytic ability, and nitric oxide production, in the specific conditions tested here.

Going forward, it will be necessary to assess the interaction of microglia-like cells with other cell types, as this is far more physiologically relevant. The subsequent chapter begins the process of assessing the impact of cell-cell interactions.

4 Chapter 4: PSC-derived microglia and medium spiny neurons- Co-cultures

4.1 Background

Studies of microglia in culture have yielded significant understanding of many aspects of their function, including of course how they are affected by mHTT and what they might contribute to HD pathology. However, they do not exist in isolation in the brain. Instead, they function in the context of astrocytes, endothelial cells, vascular components and other CNS cell types. At rest, microglia consistently survey their environment and are capable of responding to not only foreign antigens, but also damage or stress signals from the cells around them (Davalos et al., 2005; Nimmerjahn et al., 2005; Wake et al., 2009). As such, studies of cultured primary human microglia *ex vivo* have shown that they quickly lose some key gene expression patterns, and differences between donors that are present when tested immediately after isolation were lost after *in vitro* culturing. This suggests the CNS environment is important, at least in part, for the maintenance of an individual's microglial phenotypes, and is likely essential in the induction and maintenance of certain disease phenotypes (Gosselin et al., 2017). Alternatively, the CNS environment may result in a dampening down of phenotypes seen in microglia cultured *in vitro*. For example, Haenseler et al., 2017, found that microglia in co-culture with neurons were less inflammatory, and produced elevated VEGF and other factors required for remodelling the extracellular space, as well as elevated IL-10, an anti-inflammatory cytokine. This points to altered microglial function according to their environmental context.

In HD, it has been shown that dopaminergic neurons expressing a mutant HTT exon 1 fragment produce elevated IL-34 in response to increasing aggregation levels. IL-34 is a neuronal interleukin that causes proliferation of microglia. Exposure to DNA damage-inducing toxins or NMDA resulted in similar IL-34 production, suggesting this is a more generalised response to cell stress, and may partially explain the expanded numbers of microglia seen in the HD brain (Khoshnan et al., 2017). Again, this highlights how the cellular environment in which microglia find themselves can determine how they function.

Here, I sought to study the function of HD microglia-like cells in the context of an environment provided by disease-associated neurons. HD is characterised by a pattern of neurodegeneration in which the striatum is heavily affected and its medium spiny neurons (MSNs) are preferentially lost. This striatal degeneration is thought to underlie the motor and cognitive phenotypes seen in the disease (Rikani et al., 2014). For this reason, neuronal cultures enriched for MSNs were chosen for this next stage of assessment, investigating the impact of such cultures on microglial health, and vice versa.

Several microglia-neuron co-culture paradigms exist already, outside of the context of HD. Most originate from rodent models, which have been used to study the impact of microglia on cerebellar cortex neurons (Adams et al., 2015), cortical neurons (Gresa-Arribas et al., 2012) and hippocampal neurons (Park et al., 2001). In addition, a number of co-culture models using human PSC-derived microglia and neurons have been described. For example, Haenseler et al., 2017, found that co-culturing microglia with cortical neurons or merely culturing them in isolation in neuronal-type media, resulted in microglia adopting similar gene expression profiles in both conditions, specific to a neuronal environment.

Most recently, researchers have started to define protocols to culture microglia in 3D with neurons. For example, Schwartz et al., 2015, developed a 3D culture with neurons, microglia, endothelial cells and mesynchymal cells, all differentiated from ESCs, on PEG hydrogel. Brownjohn et al., 2018, took this one step further and added microglia to cerebral organoids, and found that microglia integrated into such organoids and survived without supplementation of colony-stimulating factors in the media. These 3D culture protocols, using either PEG hydrogel or organoids, are in their infancy and have not yet been fully characterised (Brownjohn et al., 2018; Schwartz et al., 2015).

Here, therefore, it was decided to begin characterising the impact of a neuronal environment on microglial health and function in the context of HD by means of using conditioned media. This approach allows easier maintenance of consistent levels of the individual culture components than may be achieved using cerebral organoids or mixed cultures, as well as allowing the assessment of microglia-like cell and neuronal responses without complicated isolation procedures. It also allows the direction of influence to be determined, separating cause and effect

for the influence of one cell type on another. Finally, it specifically addresses whether any such effects are caused by the secretion of factors into the extracellular space. Conversely, there are a number of clear caveats to this approach. Firstly, the unidirectional nature of this approach cannot fully reflect signalling between these cell types that would be continuous and bidirectional *in vivo*. Secondly, there are undoubtedly effects exerted by microglia that require physical contact with neurons, which are lost in this paradigm.

That being said, this conditioned media approach is a simple system by which the impact of secreted factors of both microglia and neurons on each other can be assessed. It also provides a strong basis on which to inform future shared-media paradigms or physical co-culture to follow up findings.

4.2 Aims

1. To assess the effects of HD neurons on microglia-like cell health and function.
2. To assess effects of HD microglia-like cells on striatal MSN health.

4.3 Methods

Microglia-like cells were differentiated using the Van Wilgenburg et al., 2013 protocol (section 2.5.2); striatal MSNs were differentiated using the Arber et al., 2015 protocol (section 2.6). PSC-derived microglia-like cells expressing HTT with 30, 45 or 81Q repeats were treated with media from MSN cultures of the same genotypes with and without heat-stress. In parallel, the microglia-like cells were treated with CSF from HD patients and controls as described in section 2.7.

Microglia-like cells were assessed for viability by LDH assay (section 2.12.1) for ROS production (section 2.16), and activation using Caspase 3 immunofluorescence on a high content imaging platform (section 2.10).

PSC-derived MSNs were treated with conditioned media from microglia-like cells, as described in section 2.9.3. They were assessed for markers of MSN health and culture composition by high content immunofluorescence for H2AX, Caspase 3, DARP32, CTIP2, Nestin and Hoechst (sections 2.10). Statistical analyses were conducted as described in section 2.18.

4.4 Results

4.4.1 Investigating the effects of HD MSN-conditioned media on microglia-like cells

4.4.1.1 HTT polyQ expansion and heat-induced cellular stress combine to cause striatal MSNs-to release factors that induce loss of microglial viability

PSC-derived microglia-like cells differentiated from lines expressing 30, 45 and 81Q HTT were treated with conditioned media from MSN cultures differentiated from the same starting ESCs. These lines were not re-sized during the experimental process, so it is possible that expansions in CAG size occurred, although based on observations of these lines by other members of the lab, is unlikely (unpublished observations). The MSNs had been either heat shock-treated or not. Following five days of conditioned media treatment of the microglia-like cell populations, the media was harvested and an LDH assay was performed. This showed that LDH release was significantly higher in the microglia-like cells treated with heat shock-treated HTT 81Q MSN-conditioned media, compared to all the baseline media treatments regardless of the microglia-like cell's HTT status (Figure 4.1, A). Microglia-like cell populations treated with heat shock-treated HTT 30Q MSN media released higher levels of LDH than those treated with baseline HTT 30Q MSN media. This suggests a more generalised heat-shock effect, which is then exacerbated by the presence of the expanded polyQ. Indeed, statistical analysis showed a significant general effect of heat shock treatment, with a significant decrease in the viability of microglia-like cells treated with heat shock treated MSN media, compared to baseline MSN media. $p=0.0085$, paired two-tailed t-test.

There was also a significant difference between the HTT 30Q and 81Q microglia-like cell lines across all media conditions (Figure 4.1, B).

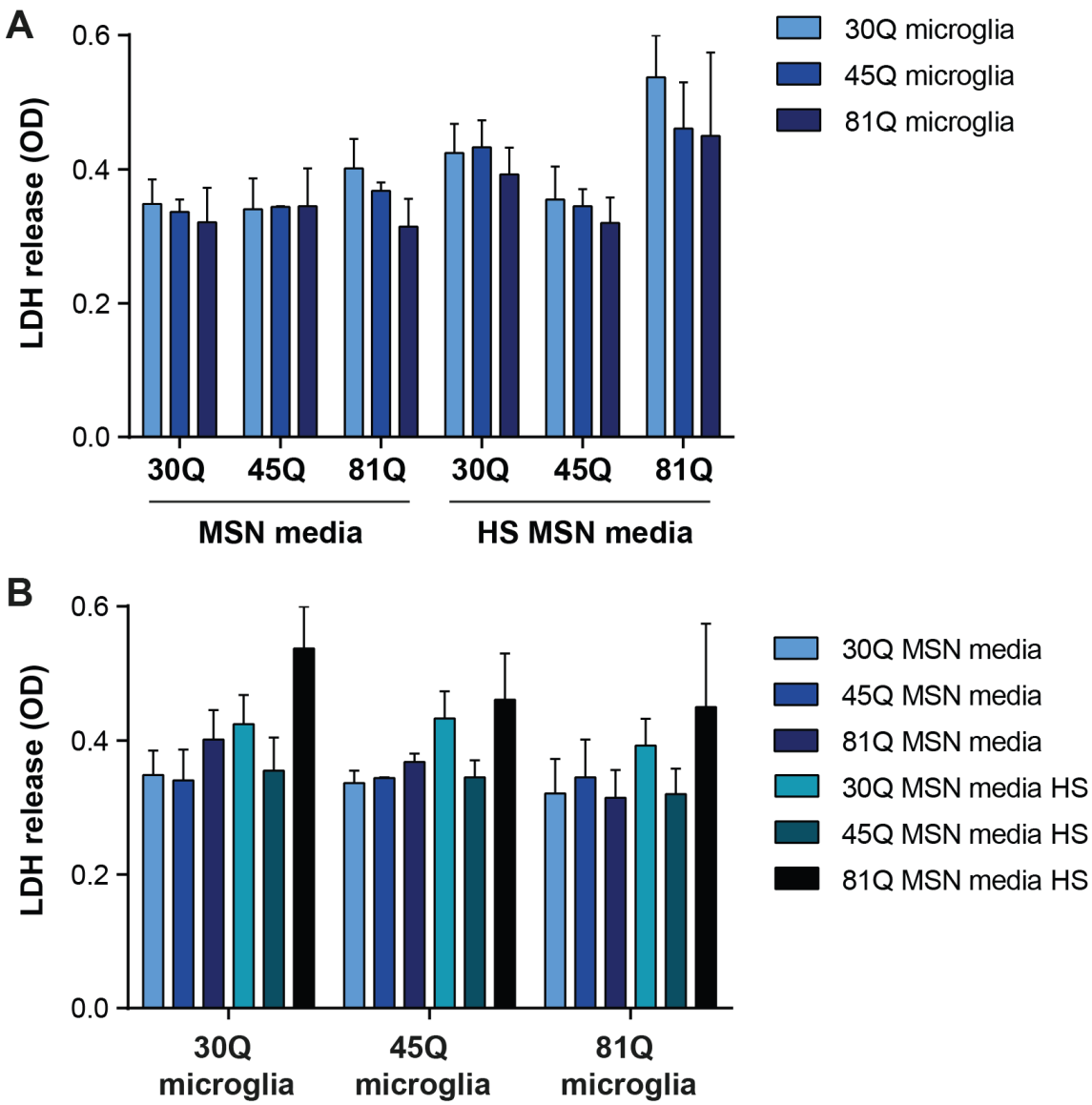

Figure 4.1: Microglia-like cells showed elevated LDH release when treated with heat shocked 81Q MSN-conditioned media. A) Microglia-like cells differentiated from ESCs expressing HTT 30, 45 or 81Q were treated with conditioned MSN media from MSNs differentiated from the same cohort, either at baseline or following a heat-shock treatment. This revealed elevated LDH release in all microglia-like cells treated with heat shock treated 81Q MSN media, regardless of HTT polyQ length. **B**) Arranging the same data according to HTT polyQ length of the microglia-like cells treated revealed a significant difference in LDH release by microglial genotype between the 30Q and 81Q microglia-like cells. N= 3 differentiations of each microglia-like cell line, with three technical replicates per stain per line. Parallel wells of microglia-like cells in unconditioned MSN media and unconditioned microglia were intended for use as controls, but these cells became infected and could not be used. Future experiments should

include these key controls. LDH assays include a potent toxin to allow the calculation of 100% cell death in the test wells as an internal control, this allowed calculation of the percentage cell death in each test well as a proportion of the 100% cell death value.

Table 4.1 Summary of statistical differences in Figure 4.1

Two-way ANOVA				
Source of Variation	% of total variation	P value	Significant?	Summary
Interaction	4.772	P = 0.8712	No	ns
Conditioned media treatment	55.35	P < 0.0001	Yes	****
Microglial HD status	6.239	P = 0.0468	Yes	*
Tukey's multiple comparisons test				
Conditions compared	Mean Diff.	95% CI of diff.	Significant?	Summary
30Q MSN media vs. 30Q HS MSN media	-0.08134	-0.1539 to -0.008761	Yes	*
30Q MSN media vs.81Q HS MSN media	-0.1475	-0.2201 to -0.07492	Yes	****
45Q MSN media vs. 30Q HS MSN media	-0.07366	-0.1462 to -0.001081	Yes	*
45Q MSN media vs. 81Q HS MSN media	-0.1398	-0.2124 to -0.06724	Yes	****
81Q MSN media vs. 81Q HS MSN media	-0.1215	-0.1941 to -0.04891	Yes	***
30Q HS MSN media vs. 45Q HS MSN media	0.07672	0.004136 to 0.1493	Yes	*
45Q HS MSN media vs. 81Q HS MSN media	-0.1429	-0.2155 to -0.07029	Yes	****
30Q microglia vs. 81Q microglia	0.04401	0.002315 to 0.08571	Yes	*

4.4.1.2 HTT polyQ expansion caused striatal MSNs to release factors that induce microglial activation

To further investigate the health of microglia-like cell cultures in a neuronal type environment, microglia-like cells expressing HTT with 30, 45 and 81Q were differentiated and treated with MSN-conditioned media, as above. Following five days of treatment, the cells were fixed and stained for Caspase 3, a marker of microglial activation, as well as IBA1, a marker of microglial identity.

This showed that microglia treated with HTT 81Q MSN media showed increased levels of Caspase 3 staining, across all the microglial HTT polyQ lengths tested (Figure 4.2, A). Plotting by microglia-like cell polyQ length showed no significant differences (Figure 4.2, B).

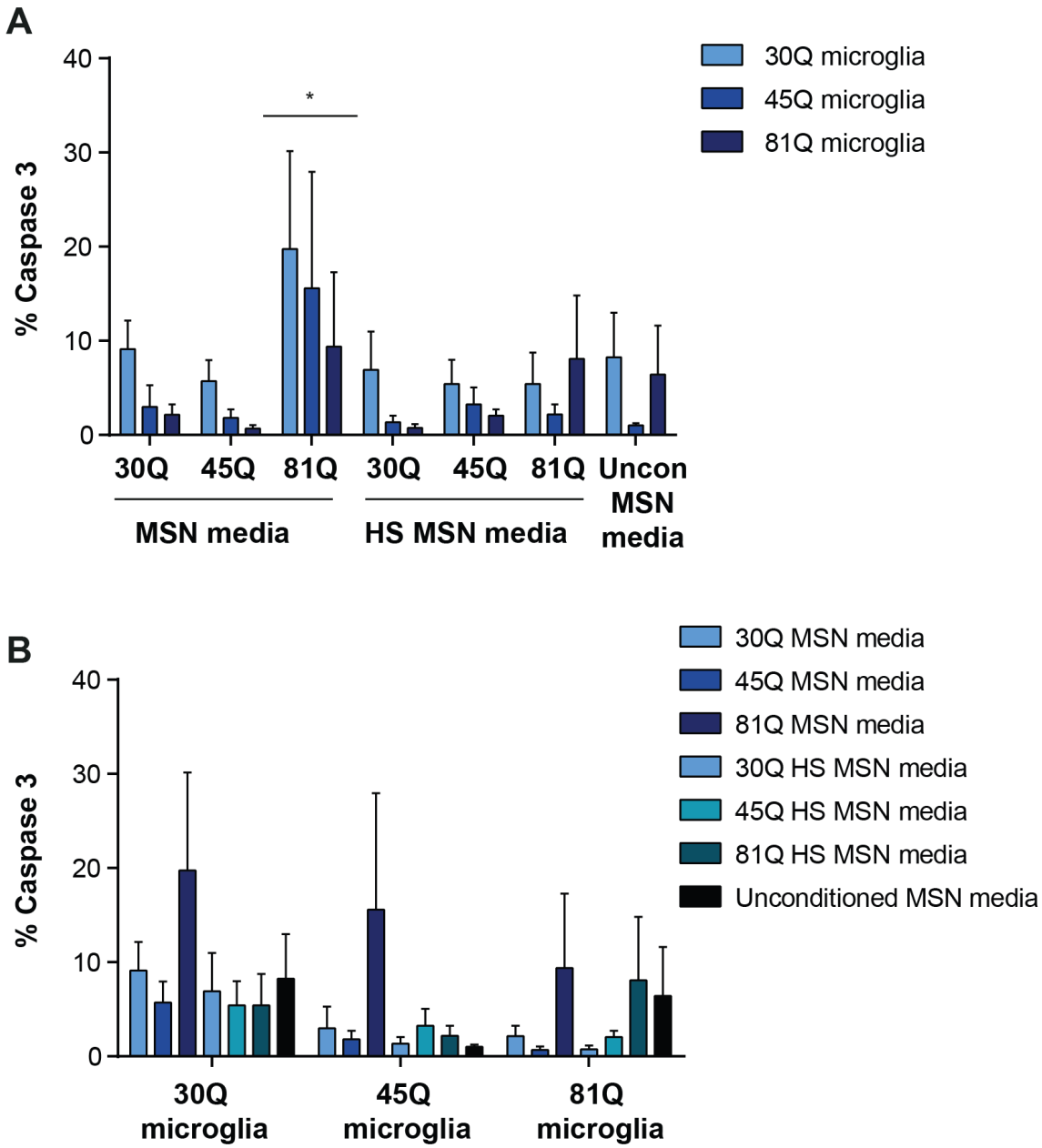

Figure 4.2: Microglia-like cells showed elevated Caspase 3 when treated with 81Q MSN-conditioned media. A) Microglia-like cells differentiated from ESCs expressing HTT 30, 45 or 81Q were treated with conditioned media from MSNs differentiated from the same cohort, either at baseline or following a heat-shock treatment. This revealed elevated Caspase 3 staining in microglia of all HTT polyQ lengths when treated with HTT 81Q MSN. **B**) The same data was then plotted according to the HTT polyQ length of the microglia-like cells tested showed no significant differences. N= 3 differentiations of each microglia-like cell line with a minimum of 6 technical replicates per stain per line, with 20 fields of view per replicate. *P<0.05. Parallel wells of microglia-like cells in unconditioned

MSN media and unconditioned microglia were intended for use as controls, but these cells became infected and could not be used. Future experiments should include these key controls.

4.4.2 Investigating the effects of HD patient CSF on microglia-like cells

The previous experiments using MSN-conditioned media were extended to investigate whether CSF from HD patients and controls might have a similar effect on microglia-like cells. CSF was chosen as a sort of proxy for a "neuronal environment," and following numerous publications showing differences between HD and control CSF in stimulants such as markers of neuronal damage (Lauren M Byrne et al., 2018b; Lauren M. Byrne et al., 2018), it was thought that these differences might cause differences in microglia responses.

Microglia-like cells differentiated from control (HTT 30Q) and HD (HTT 81Q) ESCs, were treated with CSF from controls or manifest HD patients, and assessed for Caspase 3 staining and LDH release to ascertain the state of the microglia-like cell cultures. As well as this, their ROS activity was assessed in order to investigate whether exposure to disease CSF would provide the stimulus required for elevated ROS production by hyper-reactive HD microglia-like cells, as are described in Chapter 3. Details of the CSF samples used can be found in Appendix 5.

4.4.2.1 HD CSF did not elevate microglial activation, but HD microglia have a diminished response to human CSF irrespective of whether it is HD or not

Control or HD PSC-derived microglia-like cells were treated with control or HD CSF, and immunostained for Caspase 3, as described (section 2.10). In this paradigm, it was found that treatment with HD CSF resulted in elevated Caspase 3 staining in the HTT 30Q microglia-like cells compared to the HTT 81Q microglia-like cells treated with the same CSF samples or control samples (Figure 4.3). This suggests that HD CSF has a similar effect on control microglia-like cells to MSN conditioned media, causing microglia activation.

Interestingly, this elevated Caspase staining was not replicated in the 81Q microglia-like cells, which showed low levels of Caspase 3 staining in both CSF treatment groups, that was not significantly different. This suggests that the HD

microglia-like cells are less activated by the CSF than the control microglia-like cells generally. However staining levels overall were very low, and variable, as such it may be that these results are not physiologically relevant. This experiment should be repeated to assess the validity of these findings.

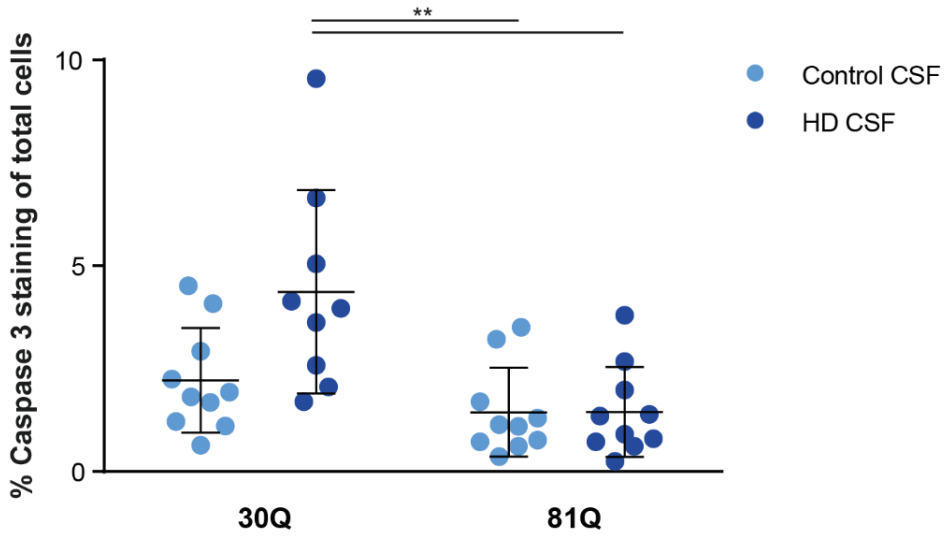

Figure 4.3: Microglia-like cells did not show elevated Caspase 3 when treated with HD patient CSF. Microglia-like cells differentiated from 30Q and 81Q ESCs were treated with CSF from HD patients (42-47Q) or controls (>35Q) for 24 h, then fixed and immunostained for Caspase 3. This revealed elevated Caspase 3 levels in HTT 30Q microglia-like cells treated with HD CSF compared to HTT 81Q microglia-like cells. HTT 30Q microglia-like cells treated with control CSF, and 81Q microglia-like cells treated with either control or HD CSF were not significantly different from each other. Data shown are mean ± SD. N=10 biologically independent CSF samples for both HD and control CSF samples, with six technical replicates per line, with 20 fields of view per replicate. **P<0.01. Parallel wells of cells in microglia media were not included as negative controls in this assessment as significant previous work had established the standard caspase 3 levels in untreated microglia-like cells. However this may be considered a weakness of this assessment.

4.4.2.2 HD CSF did not diminish microglia-like cell viability

Control or HD microglia-like cells were treated with control or HD CSF, and their LDH release assessed (section 2.12.1). This revealed no significant difference in viability between control or HD microglia-like cells, or between those treated with control or HD CSF (Figure 4.4).

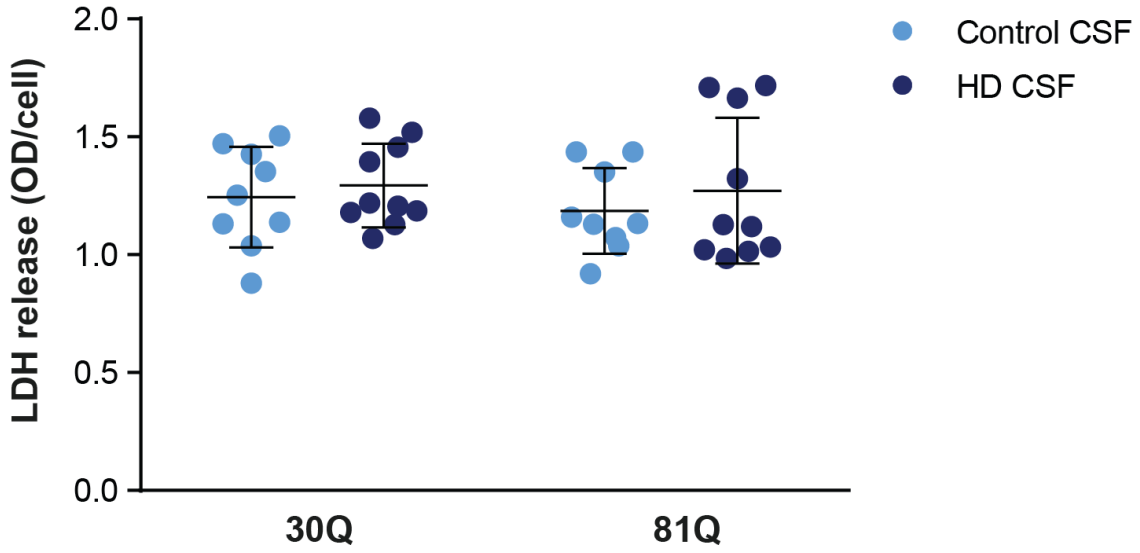

Figure 4.4: HD and control microglia-like cells treated with CSF from HD patients and controls show similar levels of LDH release. Microglia-like cells treated with HD or control CSF were assessed for LDH release following 24 h exposure. This revealed no significant differences between control (30Q), or HD (81Q), microglia-like cells, and no significant differences between control and HD CSF treated cells. Data shown are mean ± SD. N=10 biologically independent CSF samples for both HD and control CSF samples, with three technical replicates per sample. Parallel wells of cells in microglia media were not included as negative controls in this assessment as significant previous work had established the standard LDH release levels in untreated microglia-like cells. However this may be considered a weakness of this assessment. However, LDH assays include a potent toxin to allow the calculation of 100% cell death in the test wells as an internal control; this allowed calculation of the percentage cell death in each test well as a proportion of the 100% cell death value.

4.4.2.3 HD CSF did not elevate microglial ROS production

To assess the impact of CSF on microglia-like cell function, HD and control microglia-like cells were treated with HD or control CSF to assess whether ROS production would be affected (section 2.16). This showed no significant different in ROS production between microglia-like cells expressing either HTT 30Q or 81Q when treated with HD or control CSF (Figure 4.5, A). There was not a statistically significant difference between the control and HD microglia-like cells in their ROS response either (Figure 4.5, B). Assessment in baseline buffer showed no significant difference in ROS production in the 81Q microglia-like cells

(Figure 4.5, C). However, treatment with a ROS inducing agent, TBHP, revealed a marginal but statistically significant increase in ROS production in the 81Q microglia-like cells (Figure 4.5, D), in keeping with the data described in Chapter 3.

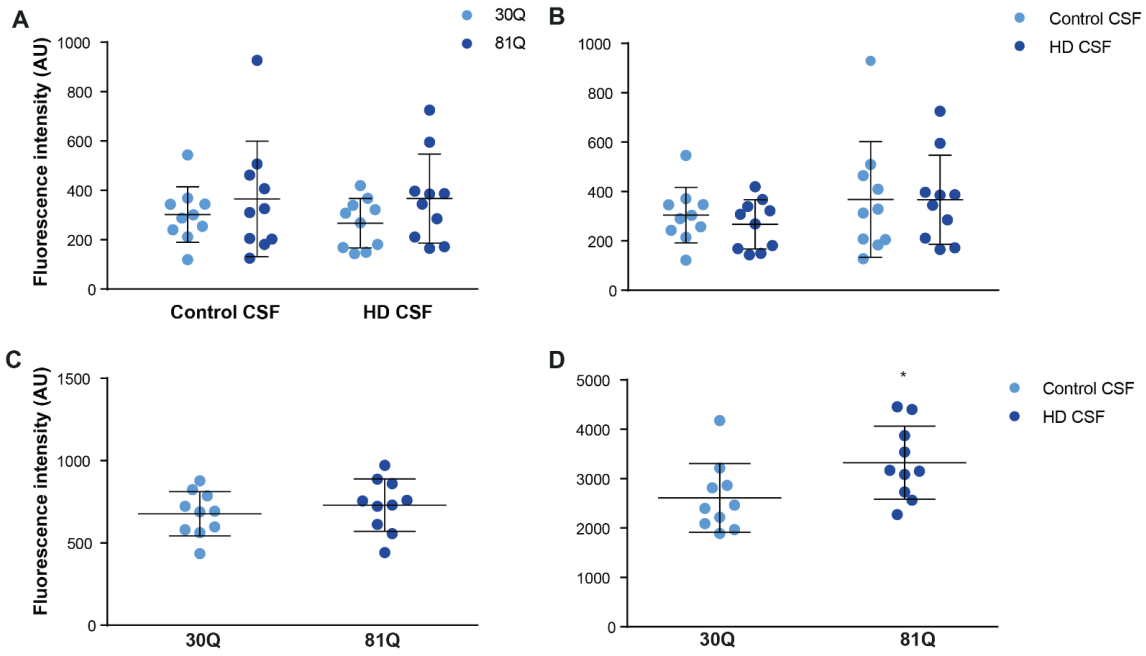

Figure 4.5: HD and control microglia-like cells treated with CSF from HD patients and controls show similar ROS production. A) Treatment with both control and HD CSF resulted in ROS production in HTT 30Q and 81Q microglia-like cells. **B**) The same data arranged according to polyQ length of the microglia-like cells revealed no significant difference between the 30Q and 81Q microglia, although the 81Q in both CSF conditions had a greater range of values, and was slightly higher. **C**) Control measures conducted in baseline assay buffer show no significant differences between 30Q and 81Q wells used for each repeat. **D**) Control measures conducted using a known stimulant of ROS, TBHP, and revealed elevated ROS production in the 81Q microglia-like cells. Data shown are mean ± SD. N=10 biologically independent CSF samples for both HD and control CSF samples, with two technical replicates per condition. *P<0.05. Negative controls of unstained cells from each sample in baseline buffer and treated with TBHP were included in all ROS experiments, and the value for each line taken as a baseline for that line and subtracted from the value of the experimental wells for that line. In this way, the negative control data was included in the data shown here, and has not been plotted separately.

4.4.3 Investigating the effects of HD microglia-like cell-conditioned media on neurons

4.4.3.1 Differentiation of ESCs to striatal MSNs was unaffected by HTT polyQ length

Differentiation of ESC cultures resulted in the production of neuronal cultures enriched with DARP32, CTIP2, βIII-tubulin positive cell populations, as shown using high content immunofluorescence imaging. The overall health of the cultures at baseline was assessed by Caspase 3 staining, which remained low. Additionally, the levels of Nestin positive neural stem cells remained consistent. Across three differentiations, the composition of the cultures was relatively consistent, and across the three HTT polyQ lengths tested, there were no significant differences, (Figure 4.6).

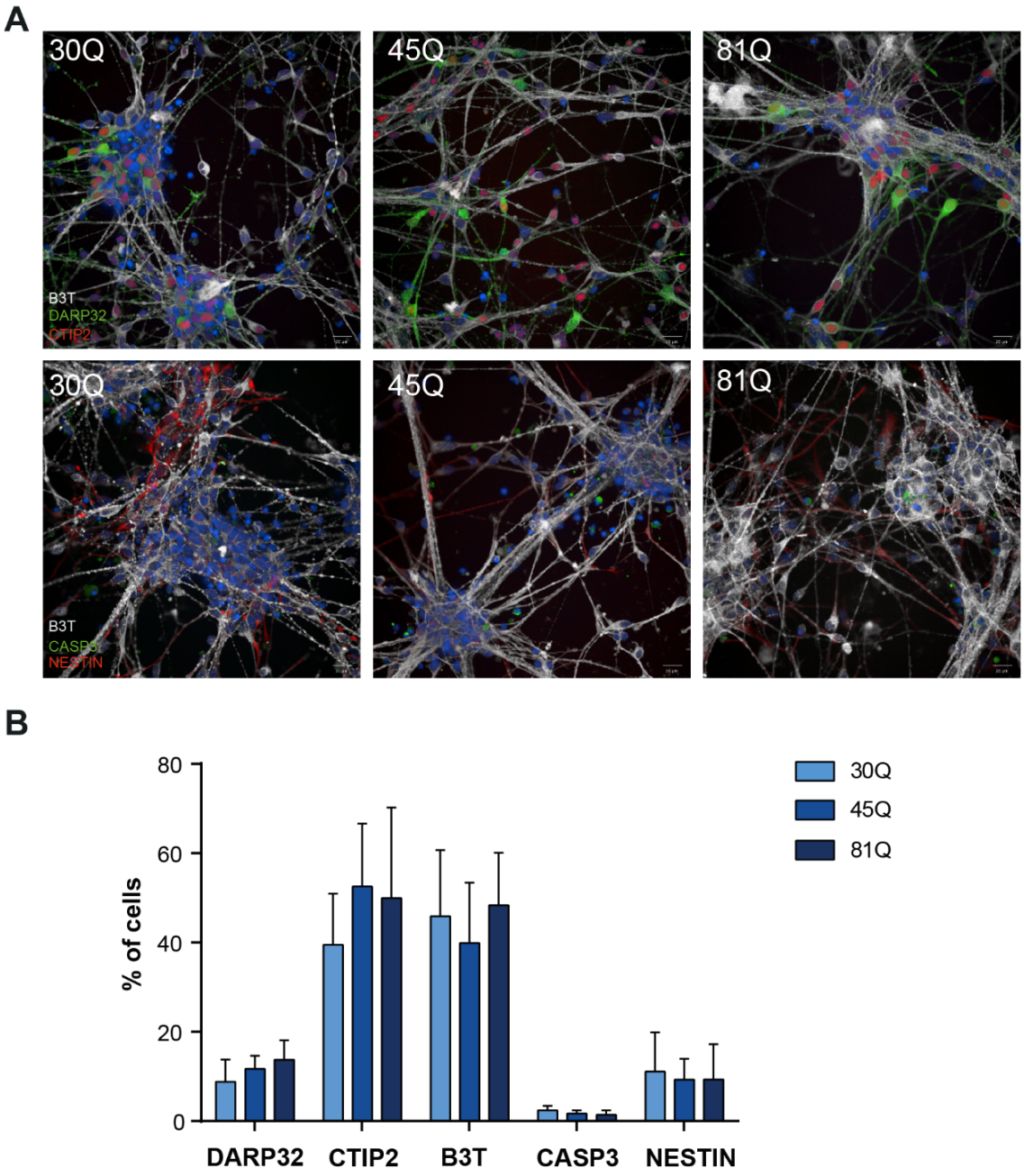

Figure 4.6: PSC-derived MSN cultures of different HTT polyQ-lengths did not differ in their overall composition. A) Example images of MSN cultures differentiated from HTT 30Q, 45Q and 81Q ESCs. First row, βIII-tubulin shown in white, DARP32 shown in green, CTIP2 shown in red. Second row βIII-tubulin shown in white, Caspase 3 shown in green, Nestin shown in red. **B**) Quantification of MSN culture composition across three differentiations for each ESC line. There were no significant differences between the three lines differentiated for each of the markers assessed. N= 3 differentiations of each line, with six technical replicate wells, containing 20 fields of view were assessed for each condition for each stain. Data shown are mean ± SD. Initial testing for the antibodies used

included secondary only staining and showed minimal signal. However, later experiments did not include these controls, hence they are not shown here. This may be considered a weakness of this assessment.

4.4.3.2 HD microglia-like cell-conditioned media did not affect MSN H2AX expression

In order to assess the impact of microglia-like cell-conditioned media on MSN health, a number of markers of reduced health or damage were assessed following a conditioned media treatment paradigm. The findings of the previous chapter, that HD microglia-like cells express higher levels of ROS and cytokines when stimulated, suggested that these higher levels of toxins in HD microglia-conditioned media might affect MSN health. The first marker of MSN health assessed was H2AX, a marker of double strand DNA breaks, which is particularly interesting in the context of HD, where the polyQ expansion is linked with impaired DNA damage repair, and mutations in DNA damage repair pathways are linked with altered age at onset (Massey and Jones, 2018). Somatic instability was not assessed in this experimental paradigm, however, which can impact the level of H2AX staining, which is a weakness of this assessment. The conditioned media treatment plan was as follows.

MSNs differentiated from HTT 30, 45 and 81Q ESCs were treated with microglia-like cell-conditioned media from microglia-like cells differentiated from the same lines, with and without treatment with LPS and IFNγ. Unconditioned microglia and MSN media were used as controls, either un-supplemented or with LPS and IFNγ added.

Upon treatment with microglia-like cell-conditioned media from either HTT 30, 45 or 81Q microglia, or with control unconditioned microglia or MSN media, there was no significant difference in H2AX staining in any of the MSN populations according to media treatment group, (Figure 4.7, A, C). However, a significant difference between the HTT 30Q and the 45 and 81Q MSNs was revealed, with the HTT 30Q MSNs showing a significantly higher percentage of nuclei with greater than ten spots across all the media treatments tested (Figure 4.7, B). Interestingly, in the stimulated conditioned media cohort, this difference become more prominent (Figure 4.7, D).

An alternative analysis of the H2AX staining was also undertaken, with a threshold of greater than four H2AX spots per nucleus, revealing much the same pattern (Figure 4.8).

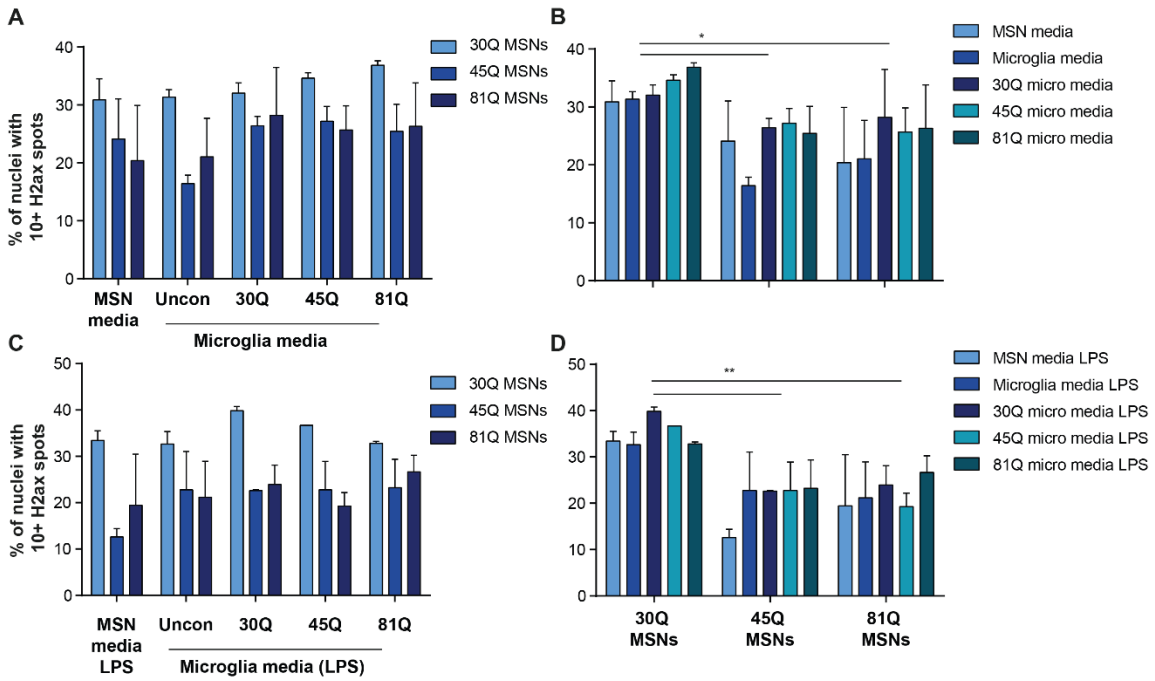

Figure 4.7: HD and control MSN cultures show significant differences in numbers of cells with 10+ H2AX spots regardless of media treatment. PSC-derived MSNs were treated for five days with conditioned media from microglia-like cells expressing various HTT polyQ lengths either at baseline (**A**, **B**) or following stimulation with LPS and IFNγ for 24 h (**C**, **D**). These MSNs were then fixed and stained for H2AX, a marker of DNA damage. Shown here are the percentage of nuclei in each condition that contain greater than 10 H2AX spots, first presented according to the media treatment received, and second split by the HTT polyQ length of the MSN cultures tested. This revealed a significant difference between the control (30Q) and HD (45Q and 81Q) MSNs, with the HTT 30Q MSNs showing the highest percentage of nuclei with greater than 10 H2AX spots (**B**). There was no significant effect of which media treatment was received (**A**, **C**), although the difference between MSNs of differing polyQ lengths became more significant in the stimulated samples (**D**). N= 2 differentiations of each ESC line to MSNs, with a minimum of 6 wells, containing 20 fields of view assessed for each condition. Data shown are the mean ± SEM. *P<0.05, **P<0.01, analysed using Two-way ANOVA, followed by Tukey's multiple comparisons tests. Initial testing for the antibodies used included secondary only staining and showed minimal signal. However, later experiments did not include these controls, hence they are not shown here. This may be considered a weakness of this assessment.

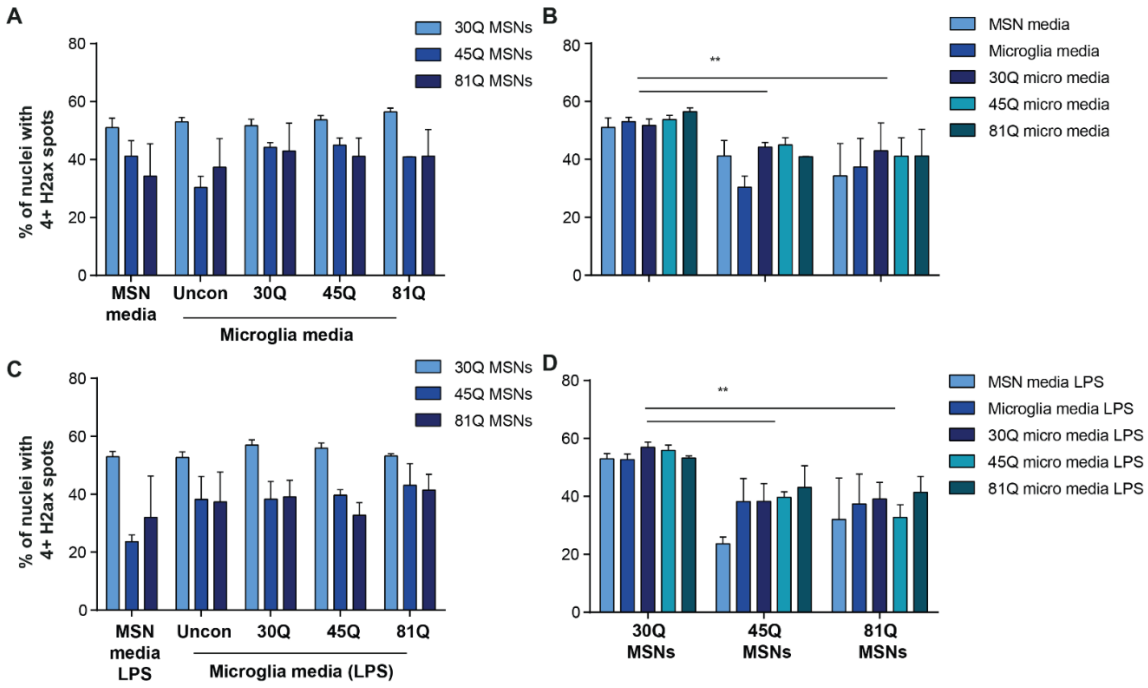

Figure 4.8: HD and control MSN cultures show significant differences in numbers of cells with 4+ H2AX spots regardless of media treatment. Mature MSNs were treated for 5 days with conditioned media from microglia-like cells of varying Q lengths either at baseline (**A**, **B**) or following stimulation with LPS and IFNγ for 24 h (**C**, **D**). These MSNs were then fixed and stained for H2AX, a marker of DNA damage. Shown here are the percentage of nuclei in each condition that contain greater than 4 H2AX spots, either presented according to the media treatment received (**A**, **C**), or by the HTT polyQ length of the MSN cultures tested (**B**, **D**). This revealed a significant difference between the control (30Q) and HD (45Q and 81Q) MSNs, with the 30Q MSNs showing the highest percentage of nuclei with greater than 4 H2AX spots (**B**, **D**). There was no significant effect of which media treatment was received (**A**, **C**). N= 2 differentiations of each ESC line to MSNs, with a minimum of 6 wells, containing 20 fields of view assessed for each condition. Data shown are the mean ± SEM. **P<0.01, analysed using Two-way ANOVA, followed by Tukey's multiple comparisons tests. Initial testing for the antibodies used included secondary only staining and showed minimal signal. However, later experiments did not include these controls, hence they are not shown here. This may be considered a weakness of this assessment.

4.4.3.3 HD microglia-like cell-conditioned media did not affect MSN Caspase 3 expression

Microglia-like cell-conditioned media treated MSNs were also assessed for Caspase 3 expression, a marker of apoptosis in neurons. The conditioned media treatment plan was conducted in the manner described (section 2.7.3).

Upon treatment with microglia-like cell-conditioned media from either HTT 30, 45 or 81Q microglia-like cells, or with control unconditioned microglia or MSN media, there were no significant differences in Caspase 3 staining in any of the MSN populations according to media treatment group (Figure 4.9, A, C). There was also no significant difference between the HTT 30Q MSNs and the 45 and 81Q MSNs across the baseline media treatments tested (Figure 4.9, B). Interestingly, following treatment with the stimulated conditioned media cohort, a significant difference between the HTT 30Q and the HTT 45Q and 81Q MSNs emerged (Figure 4.9, D).

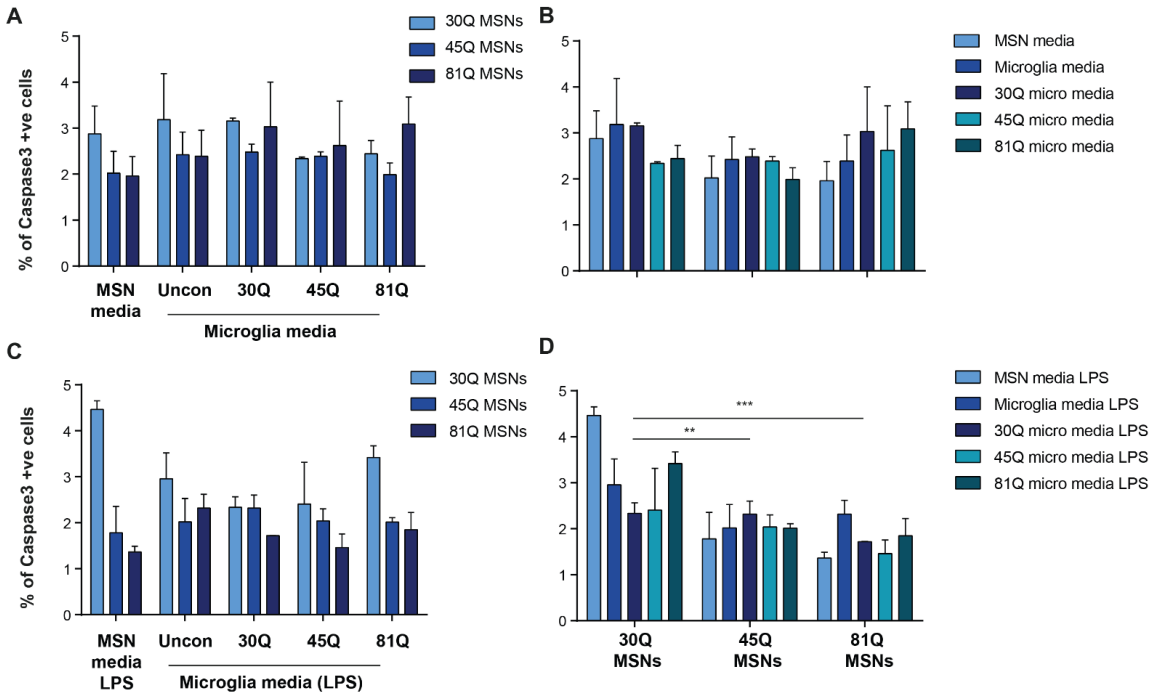

Figure 4.9: HD and control MSN cultures show significant differences in Caspase 3 staining under stimulated conditions. Mature MSNs were treated for 5 days with conditioned media from microglia-like cells of varying Q lengths either at baseline (**A**, **B**) or following stimulation with LPS and IFNγ for 24 h (**C**, **D**). These MSNs were then fixed and stained for Caspase 3, a marker of apoptosis. Shown here are the percentage of Caspase 3 positive cells in each

condition either presented according to the media treatment received (**A**, **C**), or by the HTT polyQ length of the MSN cultures tested (**B**, **D**). This revealed a significant difference between the control (30Q) and HD (45Q and 81Q) MSNs, with the 30Q MSNs showing the highest percentage of Caspase 3 positive cells in LPS-stimulated media (**D**). There was no significant effect of which media treatment was received (**A**, **C**). N= 2 differentiations of each ESC line to MSNs, with a minimum of 6 wells, containing 20 fields of view assessed for each condition. Data shown are the mean ± SEM. **P<0.01, ***P<0.001 analysed using Two-way ANOVA, followed by Tukey's multiple comparisons tests. Initial testing for the antibodies used included secondary only staining and showed minimal signal. However, later experiments did not include these controls, hence they are not shown here. This may be considered a weakness of this assessment.

4.4.3.4 HD microglia-like cell-conditioned media did not affect MSN culture composition

In combination with the above measure of MSN culture health and damage, a combination of markers were used to assess the overall culture composition, to see if any cell type was lost due to exposure to microglia-like cell conditioned media.

The markers assessed were: DARP32, a marker of MSN identity; βIII-tubulin, a marker of neuronal identity; CTIP2, expressed in early MSNs; and Nestin, a marker of neural stem cells.

There were no statistically significant differences in any of these markers across any of the MSN populations or media treatments, (Figures 4.10-4.13), suggesting unchanged culture composition in the HD cultures compared to controls, and a lack of effect on composition by any media condition.

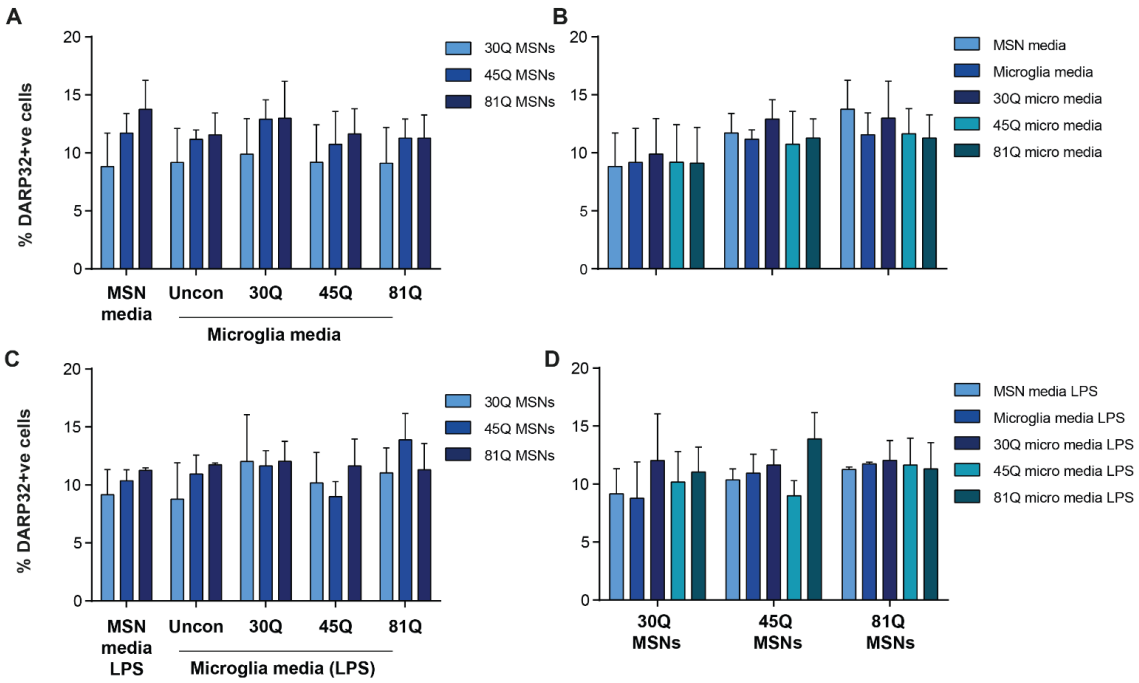

Figure 4.10: HD and control MSNs show no significant differences in DARP32 staining, regardless of media treatment or Q length. Mature MSNs were treated for 5 days with conditioned media from microglia-like cells of varying Q lengths either at baseline (**A**, **B**) or following stimulation with LPS and IFNγ for 24 h (**C**, **D**). These MSNs were then fixed and stained for DARP32, a marker of mature MSNs. Shown here are the percentage of DARP32 positive cells in each condition either presented according to the media treatment received (**A**, **C**), or by the HTT polyQ length of the MSN cultures tested (**B**, **D**). This revealed no significant difference between the different media treatments, and no significant differences between the different Q length MSN cultures. N= 2 differentiations of each ESC line to MSNs, with a minimum of 6 wells, containing 20 fields of view assessed for each condition. Data shown are the mean ± SEM. Initial testing for the antibodies used included secondary only staining and showed minimal signal. However, later experiments did not include these controls, hence they are not shown here. This may be considered a weakness of this assessment.

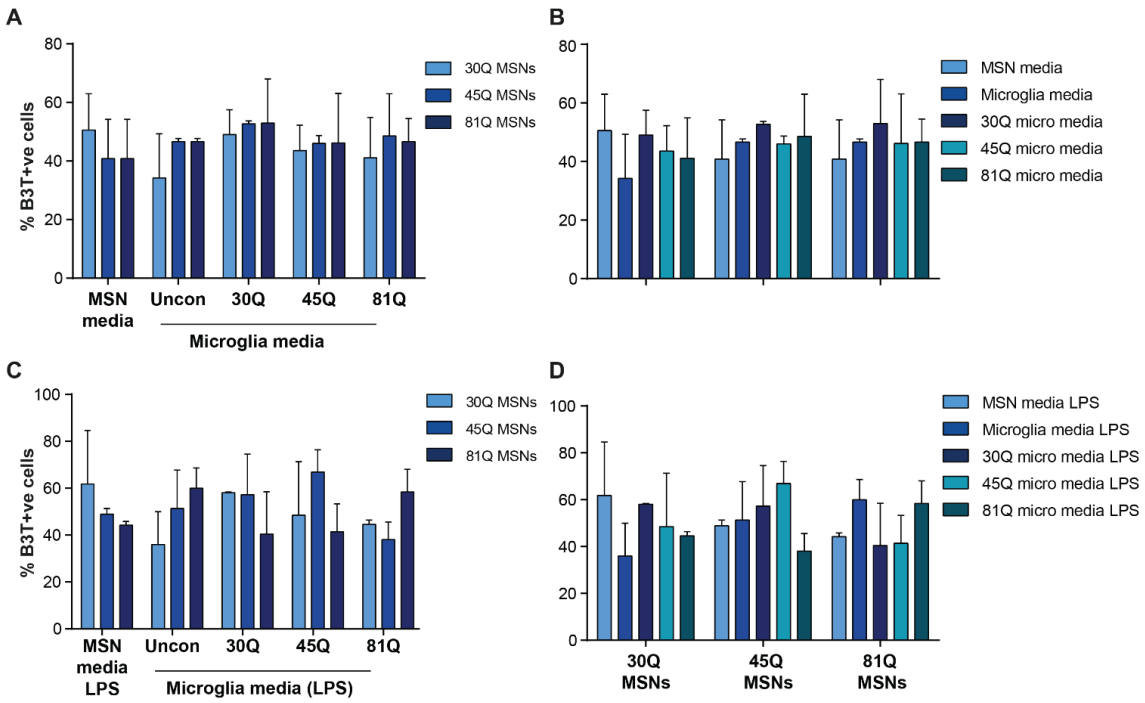

Figure 4.11: HD and control MSNs show no significant differences in βIII-tubulin staining, regardless of media treatment or Q length. Mature MSNs were treated for 5 days with conditioned media from microglia-like cells of varying Q lengths either at baseline (**A**, **B**) or following stimulation with LPS and IFNγ for 24 h (**C**, **D**). These MSNs were then fixed and stained for βIII-tubulin, a microtubule protein in neurons, used as a marker of neuronal identity. Shown here are the percentage of βIII-tubulin positive cells in each condition either presented according to the media treatment received (**A**, **C**), or by the HTT polyQ length of the MSN cultures tested (**B**, **D**). This revealed no significant difference between the different media treatments, and no significant differences between the different Q length MSN cultures. N= 2 differentiations of each ESC line to MSNs, with a minimum of 6 wells, containing 20 fields of view assessed for each condition .Data shown are the mean ± SEM. Initial testing for the antibodies used included secondary only staining and showed minimal signal. However, later experiments did not include these controls, hence they are not shown here. This may be considered a weakness of this assessment.

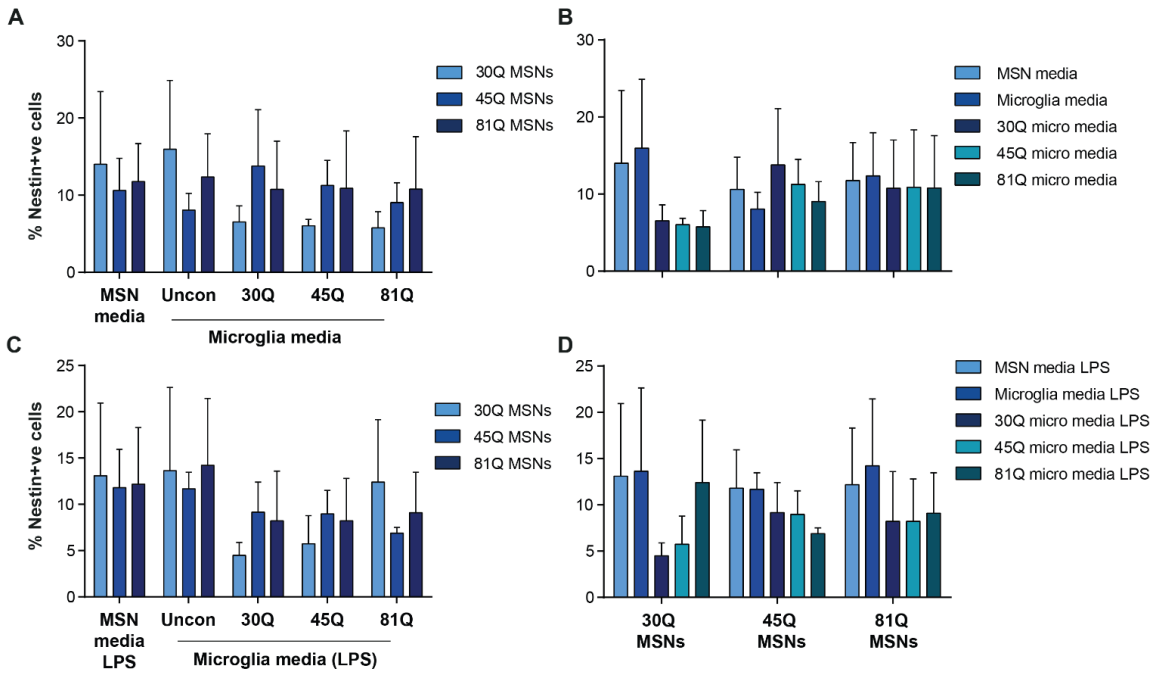

Figure 4.12: HD and control MSNs show no significant differences in Nestin staining, regardless of media treatment or Q length. Mature MSNs were treated for 5 days with conditioned media from microglia-like cells of varying Q lengths either at baseline (**A**, **B**) or following stimulation with LPS and IFNγ for 24 h (**C**, **D**). These MSNs were then fixed and stained for Nestin, a marker of neural stem cells. Shown here are the percentage of Nestin positive cells in each condition either presented according to the media treatment received (**A**, **C**), or by the HTT polyQ length of the MSN cultures tested (**B**, **D**). This revealed no significant difference between the different media treatments, and no significant differences between the different Q length MSN cultures. N= 2 differentiations of each ESC line to MSNs, with a minimum of 6 wells, containing 20 fields of view assessed for each condition. Data shown are the mean ± SEM. Initial testing for the antibodies used included secondary only staining and showed minimal signal. However, later experiments did not include these controls, hence they are not shown here. This may be considered a weakness of this assessment.

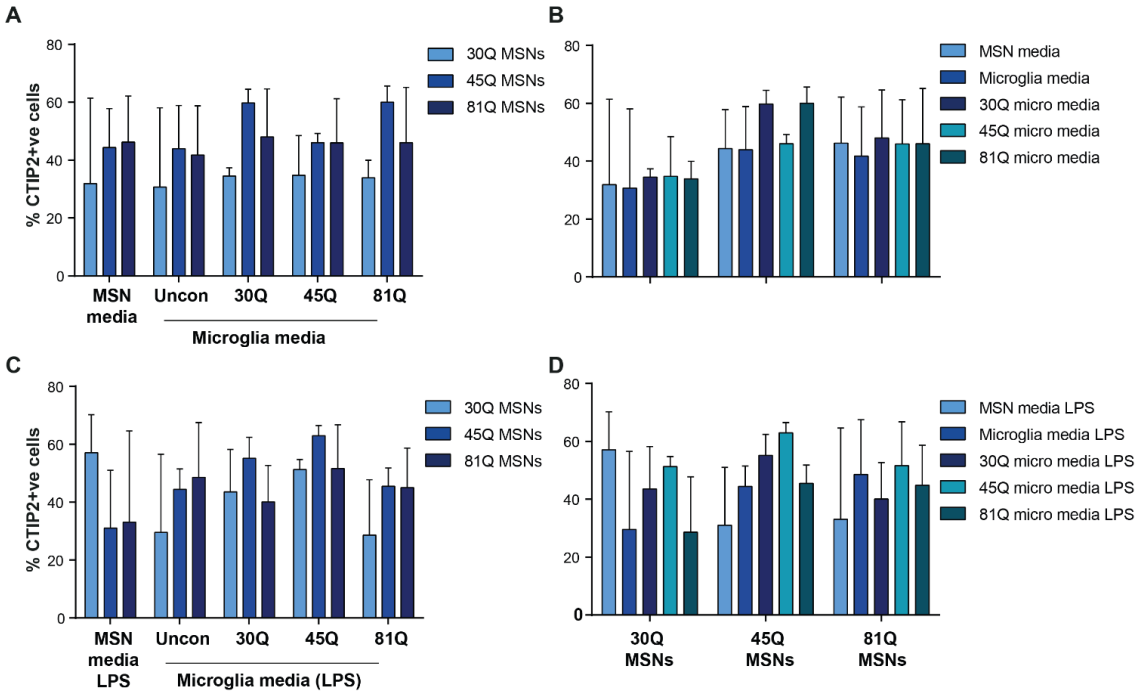

Figure 4.13: HD and control MSNs show no significant differences in CTIP2 staining, regardless of media treatment or Q length. Mature MSNs were treated for 5 days with conditioned media from microglia-like cells of varying Q lengths either at baseline (**A**, **B**) or following stimulation with LPS and IFNγ for 24 h (**C**, **D**). These MSNs were then fixed and stained for CTIP2, expressed in early MSNs and layer 5 cortical neurons. Shown here are the percentage of CTIP2 positive cells in each condition either presented according to the media treatment received (**A**, **C**), or by the HTT polyQ length of the MSN cultures tested (**B**, **D**). This revealed no significant difference between the different media treatments, and no significant differences between the different Q length MSN cultures. N= 2 differentiations of each ESC line to MSNs, with a minimum of 6 wells, containing 20 fields of view assessed for each condition. Data shown are the mean ± SEM. Initial testing for the antibodies used included secondary only staining and showed minimal signal. However, later experiments did not include these controls, hence they are not shown here. This may be considered a weakness of this assessment.

4.2 Discussion

This research had the dual aims of looking at the impact of an HD neuronal environment on microglia-like cell health and function, as well as the impact of HD microglia-like cells on potentially vulnerable striatal MSNs. In order to achieve this, conditioned-media experiments were conducted, and showed that MSN conditioned media from heat-shocked 30Q and 81Q MSNs caused elevated LDH release in both control and HD microglia-like cells. Additionally, increased Caspase 3 staining was seen in the microglia-like cells following exposure to 81Q MSN-conditioned media, however due to the low levels of Caspase 3 staining overall and the variability in the system, this result may not be real, and should be repeated. Conditioned media from microglia-like cells of HD and control polyQ lengths showed no impact on MSN culture composition or health as assessed by IF. However, this assessment did reveal reduced H2AX staining in the HD lines compared to the control line, in all media conditions tested.

The first aim, of investigating the impact of a neuronal environment on microglia-like cell health and function, was assessed initially using a conditioned media paradigm, taking conditioned media from MSN cultures of both HD and control HTT polyQ lengths to treat HD and control microglia-like cells.

This showed elevated LDH release from microglia-like cells, irrespective of HTT polyQ-length, when treated with MSN conditioned media from 81Q MSNs following a heat shock treatment. This suggested the presence of additional toxic substrates, or simply higher levels of certain toxic substrates in the heat shock treated 81Q MSN media, compared to all other conditions tested. This is interesting because heat shock treatment was required to reveal this HTT 81Q specific toxicity. This suggests that at baseline, there may be sufficient compensation mechanisms in place intracellularly to prevent the production and release of toxic substrates into the supernatant. This is relevant for HD patients, as it suggests that cells can cope with an expanded CAG to an extent, but in the presence of additional stressors, these coping mechanisms can be overwhelmed. While in HD patients the additional stressor is very unlikely to be heat shock, it may occur to a lesser extent due to endogenous stressors. It is also notable that the microglia-like cell populations assessed here showed the same pattern of

results in response to the heat shock-treated HTT 81Q MSN media, suggesting that the control and HD microglia-like cells have similar vulnerability in this case.

Additionally, there was a significant increase in LDH release in all microglia-like cell populations treated with heat shock treated HTT 30Q MSN media, compared to baseline HTT 30Q MSN media, and this elevated response was not significantly different to what was found in the microglia-like cells in heat shock treated HTT 81Q MSN media. This suggests a generalised increase in toxicity of MSN media following heat shock treatment, even in control HTT polyQ lengths. Interestingly, only heat shock treated 45Q MSN media did not result in significantly elevated LDH release compared to baseline. Given that the majority of adult onset HD patients carry polyQ expansions closer to 45Q in length, this is significant for translating these results to patients. However, in this case, it may be due to experimental variability in the HTT 45Q MSN cultures, where the absolute number of neurons in the HTT 45Q MSN cultures was lower compared to the 30 and 81Q MSN cultures, although the percentage of viable cells and the overall composition was comparable, resulting in reduced concentrations of toxins. This is an unfortunate complication of minor differences in seeding densities at key passages. It may also be the case that there was a lack of toxicity caused by the 45Q MSNs simply due to the fact that the 45Q MSNs cultured in vitro didn't surpass the pathological threshold of CAG expansion due to a lack of somatic instability, unlike what has been shown to occur in patient *in vivo* (Gonitel et al., 2008; Massey and Jones, 2018).

In parallel to this LDH measure of cell viability, cells were stained for Caspase 3 following MSN media exposure. Caspase 3 staining in microglia relates to their activation and does not precede cell death, as is seen in other cell types such as neurons (Burguillos et al., 2011). Indeed, a number of publications have shown that Caspase 3 signalling in the immune system appears to be necessary for normal function, such as proliferation of T cells, and activation the NF-κB pathway for an effective immune response following stimulation (Burguillos et al., 2011; Kennedy et al., 1999). In this conditioned media paradigm, HTT 81Q MSN media resulted in significantly elevated Caspase 3 staining in all microglia-like cell populations tested. This suggests media from MSNs expressing HTT with an especially long polyQ length causes elevated microglia-like cell activation, which

would contribute towards pro-inflammatory cytokine production. Again, there is an absence of this phenotype in the HTT 45Q MSN media treated cells, which may be due to the lower numbers of cells in the HTT 45Q MSN cultures. The overall level of Caspase 3 staining remained very low, however, and as such, these experiments should be repeated at a larger scale to provide confidence that the effect shown is real. It may be the case that this small change in Caspase 3 levels is real in this *in vitro* set up, but with such a small effect size is unlikely to be physiologically relevant *in vivo*, where the system might cope well with this small change.

A better measure might have been to test for microglial proliferation in response to MSN media exporsure as neuronal production of IL-34 caused by mHTT accumulation has previously been shown to cause proliferation of microglia (Khoshnan et al., 2017b). As such, IL-34 may be a candidate substrate to assess in the HD MSN media. However, to date, mHTT accumulation has not been shown in these MSN cultures in our lab (unpublished observations). It may be the case that soluble mHTT also causes sufficient stress to the neuronal cells to stimulate IL-34 production. It would be interesting, therefore, to investigate whether there IL-34 is elevated in the HD MSN media, and whether there is any proliferation of the microglia-like cell cultures following HD MSN media exposure.

There are a number of caveats with the experimental set-up that should be noted. Specifically, the time frame of the experiment may be too contracted to fully reveal the impact of MSN-conditioned media on microglia-like cell health and activation. Also, as previously mentioned, there is variability in the differentiation protocol for MSNs that creates noise in the data.

Additionally, the areas of microglia-like cell health and function which could be assessed in this set-up were limited by practicalities such as the prohibitive cost of growth factors associated with the differentiation protocol resulting in a limited number of differentiations, as well as the cost of multiplex ELISA plates (MSD). Therefore, a more significant effect may have been missed. For example, it would be interesting to assess the impact of these various media treatments on the inflammatory response of the cells, specifically the cytokine profile and the activity in the NF-κB pathway. As well as this, it may be the case that MSN-conditioned media primes the microglia-like cells for altered responses or patterns of activity,

but these would only be revealed following the application of an additional stressors. Additionally, it would be interesting to conduct an RNAseq at baseline and following MSN media exposure to take a broader look at the impact of the conditioned media treatments. For example, in this experiment there was no impact on IBA1 expression at the protein level, but it may be the case that other markers of microglial identity or function were changed.

To follow up the work using conditioned media from neuronal cultures, CSF from HD patients and controls was obtained. Microglia-like cells of various HTT polyQ lengths were then treated with this CSF from controls or HD patients to assess its impact on microglia-like cell health and function. This revealed elevated Caspase 3 staining in HTT 30Q microglia-like cells when treated with HD CSF, suggesting higher levels of microglia-like cell activation. Interestingly, 81Q microglia-like cells treated with the same patient CSF did not show elevated Caspase 3 staining. This may be due to the presence of some noise in the system and the relatively low levels of Caspase 3 staining overall, suggesting these findings may not be physiologically relevant.

Next, the impact of CSF treatment on microglia-like cell function was assessed, specifically on their ability to produce ROS. This revealed no significant difference in the CSF-treated microglia-like cells, either between the HTT 30Q and 81Q microglia-like cells, or between HD and control CSF treated, populations. Interestingly, the absolute values of ROS production from microglia in CSF appeared lowered than microglia-like cells incubated in baseline buffer, suggesting that substrates in the CSF may prevent ROS production to some extent. Treatment with TBHP revealed a significant difference between the 30Q and 81Q microglia in ROS production, which is a replication of results reported in the previous chapter.

LDH release was also assessed following 24 h of CSF treatment. This revealed no significant differences in LDH release by HTT 30Q and 81Q microglia in either HD patient or control CSF. This suggests that while it has been shown that HD CSF contains increased levels of stimulants such as Trem2, neurofilament and tau (Lauren M Byrne et al., 2018b; Lauren M. Byrne et al., 2018), and in other neurodegenerative diseases such as PD and ALS, CSF from patients has been toxic (Ding et al., 2015; Hao et al., 1995; Schiess et al., 2010) there is no

significant effect of HD CSF on viability of microglia-like cells as assessed by LDH release, and this result is unchanged with control CSF. Interestingly, the HTT 30Q and 81Q microglia-like cells show the same level of vulnerability in this context. Previous work in this thesis found a significant difference in vulnerability in the presence of an autophagy inhibitor, Bafilomycin A1 and a ROS-inducing toxin, Hydrogen Peroxide. This experimental set up, by comparison, reveals no significant difference. It may be the case that the level of toxicity is generally lower in CSF than that induced by the specific toxins tested previously. Additionally, this experiment ran over 24 h, where the half-life of LDH is only 9 h, and previous work was done under this time frame or less.

There are a number of caveats for this experimental paradigm. Specifically, this experiment was conducted under the premise that CSF is a proxy for the CNS environment. This is partially true, but circulating CSF reflects the average environment across the whole brain. This is significant, as regional differences in the levels of certain toxins and damage signals may be diluted out by the rest of the CNS environment. Not only that, while HD CSF has been shown to have some differential levels of key proteins that might activate microglia, such as neurofilament light and tau (markers of neurodegeneration), this was shown at a population level and it might be the case at the level of the individual level. As such, it would be of great value to take parallel samples of the CSF samples used and assess them individually for level of mHTT aggregates, neurofilament light, tau, Trem2 and any others previously shown to be elevated at a population level in HD (Lauren M Byrne et al., 2018a, 2018b; Rodrigues et al., 2016), and in this way correlate the effects on the microglia-like cells with the level of these key factors in the CSF.

Additionally, these experiments were conducted over 24 h, as an early assessment of the impact of CSF on microglia-like cells. This was in part due to the scarcity of CSF as a resource, and as such multiple media changes could not form part of the experimental plan. However, future studies should extend CSF treatment over a longer time period, as studies using ALS and PD patient CSF have only seen changes in microglia function and morphology after at least 4 days exposure, with the longest experimental exposure of 28 days revealing the greatest changes in the microglia exposed to ALS CSF (Ding et al., 2015; Schiess

et al., 2010). Future studies should also extend the assessment to include assessments of proliferation and structured morphological assessments.

The second aim of this research was to assess the impact of HD microglia-like cells on MSN health. In the previous chapter, the results pointed to altered microglia-like cell function in the HD context, with a hyper-reactive phenotype seen in their cytokine profile following stimulation, elevated ROS production both at baseline and in the presence of an oxidative stressor, and reduced viability in response to stress. On this basis, it was hypothesised that conditioned media from HD microglia-like cells under baseline and stimulated conditions may contain substrates that could impact MSN health, such as ROS and inflammatory cytokines, or others. This would be of particular interest if the phenotypes of HD microglia-like cells impacted the selective vulnerability of MSNs seen in HD generally.

The results from treating MSNs with microglia-like conditioned cell media showed no significant patterns of differences caused by the different media treatments. However, the experimental set up did reveal differences between MSN cultures of different HTT polyQ lengths that were most significant in the LPS-treated media conditions.

The first area assessed was H2AX staining, quantified by the percentage of nuclei with greater than ten spots, as well as the percentage of nuclei with greater than four spots. This method found the percentage to be lowered in both the HTT 45Q and 81Q MSN cultures compared to the control 30Q MSN cultures. The difference between the control and HD MSN cultures became more significant under LPS-stimulated conditions, suggesting that this inflammatory environment may exacerbate the difference between the control and HD cultures.

This reduction in H2AX staining is in keeping with what is known in the field. For example, HD fibroblasts have been shown to carry abnormally reduced numbers of recognised double strand breaks (DSBs), as assessed by H2AX and 53BP1 staining, following irradiation treatment. This study also found a significant number of unrepaired DSBs 24 h after irradiation in HD fibroblasts compared to controls (Ferlazzo et al., 2014). This suggests that in HD, the machinery for identifying DSBs may be impaired.

This is possibly due to a loss of function of the mHTT, as HTT has a known role as a sensor for DNA damage (Anne et al., 2007), and has been shown to act as a scaffold for proteins of the DNA damage response pathway following oxidative stress, which has been found to be impaired in the presence of mHTT (Maiuri et al., 2016). HTT has also been shown to act as a sensor of ROS production (DiGiovanni et al., 2016). In this way, it appears that this reduction of H2AX staining is a real HD phenotype in these MSN cultures. The increased significance of the reduction of staining in the LPS-treated media groups suggests that there is some impact of inflammation on the level of DNA damage that occurs, or perhaps the ability of HD MSN cultures to respond to that damage.

The next area assessed was Caspase 3 staining, which was found to be significantly lowered in both the 45 and 81Q MSN cultures in the LPS treated media conditions only. This suggests a reduced incidence of apoptotic cells in the HD MSN cultures compared to controls. This is not in keeping with previously published works, which generally have found mHTT-expressing lines show elevated levels of Caspase 3/7 (Chae et al., 2012), although such studies have not been conducted in cultures of human MSNs. For example, elevated Caspase 3/7 activity was found at baseline in iPSCs and in response to stressors, such as growth factor withdrawal at the neural stem cell stage of neuronal differentiation (Chae et al., 2012; Zhang et al., 2010). Crucially, on-going research in this lab has found that HD and control PSC-derived MSNs do not show clear differences in Caspase 3 staining in baseline media (Unpublished observations, Dr. Ralph Andre). This suggests that the LPS stimulated conditioned media plays some part in revealing this difference. However, it is important to note that the absolute percentages remain very low in all MSN cultures, with the highest value still under 5% of total cells, so while the differences are statistically significant, they may not be meaningful in a physiological setting.

The other proteins assessed by HCI were related to the composition of the MSN cultures; DARP32, CTIP2, βIII-tubulin and Nestin. While there was variability, there was no significant difference in any of the markers, either due to the media treatments employed or due to polyQ lengths of the MSN cultures.

Unfortunately, the impact of the microglia-like cell-conditioned media from cultures of varying HTT polyQ length did not reach significance in this

experimental set up in any of the stains measured. This may be due to the time frame of the experiment, where microglia-like cell-conditioned media was introduced at day zero, and the experiment terminated at day five. It may be the case that a longer period of exposure is required to reveal differential effects between the HD microglia-like cell-conditioned media and controls. Additionally, it may simply be the case that while HD microglia-like cells produce elevated levels of certain inflammatory factors and toxins compared to control microglia-like cells, these may be present in the media at concentrations too low to affect MSN health and function. It might also be the case that the impact of microglial substrates on MSN health is indirect, requiring astrocytes and other glial populations to amplify the effects, upon activation by microglia. For example, it has been recently shown in mice that activated microglia cause a shift in astrocyte populations to a so-called A1 phenotype, where astrocytes lose the ability to promote neuronal survival, outgrowth, synaptogenesis and phagocytosis, and instead induce death of neurons and oligodendrocytes (Liddelow et al., 2017). It would be interesting, therefore, to assess the impact of HD microglia-like cells on control and HD astrocytes, and eventually assess these cell types all together in a mixed neuronal-microglia-like cell-astrocyte co-culture.

Another caveat of this work is that the MSN-enriched cultures assessed are mixed neuronal cultures, with low percentages of actual MSNs. In this way, the differences seen between HD and control neuronal cultures cannot be attributed to differences in the MSN population alone, but rather relate to an effect in neurons more generally. For example, it is known that MSNs are not the only vulnerable neuronal population in HD. Specifically, cortical projection neurons which project to, and provide trophic support to the striatum are found to be lost in HD, and the specific cortical regions that are lost dictate the symptoms patients present with, highlighting the critical importance of those populations (Mehrabi et al., 2016). Finally, another element of the CNS environment that hasn't been assessed here are the oligodendrocytes, and the impact of HD microglia-like cells on oligodendrocyte health and function. It has been previously shown that elevated levels of TNFα released by stimulated microglia are toxic to developing oligodendrocytes, when in the presence of astrocytes (J. Li et al., 2008), and in HD major white matter abnormalities have been documented even in premanifest gene carriers, as well as manifest patients (Phillips et al., 2016). With this in mind,

future work investigating the impact of HD microglia on oligodendrocyte populations, as well as cortical neurons would be of great interest.

4.3 Summary

Microglia-like cells show altered phenotypes of increased LDH release and Caspase 3 staining following exposure to MSN-conditioned media, particularly following heat shock treatment. Specifically, microglia-like cells treated with heat shock treated 81Q MSN conditioned media show elevated levels of LDH release, suggesting decreased microglial viability. Caspase 3 staining is also elevated in microglia-like cells when treated with 81Q MSN media, suggesting elevated microglia-like cell activation.

Microglia-like cells show mild phenotypic changes when treated with CSF from HD patients or controls, with elevated Caspase 3 staining in 30Q microglia-like cells when treated with HD patient CSF.

MSN cultures exposed to microglia-like cell-conditioned media, however, did not show differences in composition, or caspase 3 staining. This experimental paradigm did, however, reveal significant differences between HD and control MSN cultures in DNA damage response and apoptosis. Intriguingly, this appeared to be more significant in the LPS-treated media conditions, but there was no significant impact of each different media condition. This may be due to contracted time frame of the experiment, or due to microglial conditioned media being too dilute. Further experiments should be conducted over a longer time period, and conditioned media harvested from larger numbers of microglia in lower volumes of media.

Additionally, it may be that bidirectional signalling is necessary to reveal greater microglia-like cell toxicity on MSNs, for example we and others have shown that MSNs can alter microglial population (Khoshnan et al., 2017), this may in turn result in increased activation and proliferation of microglia-like cells, increased production of toxic substrates and thus impact MSN health more significantly .

5 Chapter 5: Wild-type HTT function in human macrophages

5.1 Background

The role of wild-type HTT (wtHTT) at a molecular and physiological level has not been fully elucidated, both within the context of HD and more generally. There are a number of areas, however, where it seems clear HTT has a role, and these are discussed below. The structure of wtHTT was reviewed in chapter 1 and so here I will focus on its known biological functions.

WtHTT has been shown to have a number of functions at the molecular level. Firstly, wtHTT appears to have a role in trafficking between the ER, the Golgi and extracellular space (Strehlow et al., 2007). It has also been shown to have a role in transport via endocytic and secretory pathways, with wtHTT required for secretory vesicle fusion at the membrane (Brandstaetter et al., 2014; Velier et al., 1998). It has also been shown that wtHTT plays a role in receptor mediated endocytosis via HIP1 and HIP14 (Rao et al., 2002; Singaraja et al., 2002; Waelter et al., 2001). As well as this, a body of work has shown that wtHTT interacts with dynein and dynactin, leading to the suggestion of models where wtHTT plays a global role in vesicle and organelle transport in the cell (Caviston et al., 2007; Caviston and Holzbaur, 2009). Similarly, wtHTT has been implicated in the correct positioning of both endosomes and lysosomes in the cell, with depletion in a cell line of either wtHTT or dynein resulting in dispersed endosomes and lysosomes. Interestingly, intracellular trafficking in these cells was only slightly impaired (Caviston et al., 2011).

A large body of work suggests that wtHTT interacts with RAB GTPase proteins, which regulate vesicle formation, actin- and tubulin-dependent vesicle movement, and membrane fusion (Stenmark and Olkkonen, 2001). WtHTT is believed to activate RAB11 as well as play a role in trafficking RAB11 vesicles (X. Li et al., 2008; McClory et al., 2014; Power et al., 2012). Other RABs have also been shown to be affected by a reduction in wtHTT including RAB2, RAB3, RAB7, and RAB8 and RAB19 vesicles (White et al., 2015). These interactions

with RABs may be a mechanism through which wtHTT can have a large impact on cellular vesicle trafficking.

As well as this, a number of studies have implicated wtHTT in the process of selective macroautophagy. Specifically, wtHTT has been shown to interact with p62, and a number of autophagy related proteins, suggesting a “scaffold” function of wtHTT in the autophagy process. Interestingly, in HD, a deficit in autophagy appears to be present, which may be related to a reduced ability of the mHTT form of the protein to perform this scaffold function (Ochaba et al., 2014; Rui et al., 2015; Wong and Holzbaur, 2014).

wtHTT is also known to be involved in the process of intracellular protein trafficking. Firstly, it has been shown to be involved in bidirectional transport of vesicles in neurons, in both the dendrites and axons (Colin et al., 2008; Engelender et al., 1997; Gauthier et al., 2004; Gunawardena et al., 2003; Li et al., 2002; McGuire et al., 2006; Strehlow et al., 2007; Twelvetrees et al., 2010; Waterman-Storer et al., 2002). In terms of retrograde transport, this has been found to occur either via direct interaction with the dynein motor complex or via an interaction with HAP1 (HTT associated protein 1) and the p150Glued subunit of dynactin (Block-Galarza et al., 1997; Engelender et al., 1997; S.-H. Li et al., 2018; Li et al., 1995). WtHTT is also involved in anterograde transport, with HAP1 interacting with a subunit of the kinesin anterograde motor complex, kinesin light chain-1 (McGuire et al., 2006). Interestingly, wtHTT appears to be involved in the switch between anterograde and retrograde transport, as phosphorylation of wtHTT at S421 results in preferential recruitment of kinesin-1 heavy chain to microtubules, vesicles and organelles for anterograde transport. De-phosphorylation results in release of the kinesin-1 motor and the remaining motor complex containing wtHTT then favours retrograde transport (Colin et al., 2008).

WtHTT has also been shown to have a role in transcription and chromatin modification. Specifically, wtHTT has been found to interact with REST/NRSF to modulate the transcription of NRSF-controlled neuronal genes, including BDNF (Zuccato et al., 2001). WtHTT has also been shown to interact with CBP (CREB binding protein), which itself regulates acetylation and deacetylation of histones, controlling access to genes for transcription, as well as p53 which is also involved in transcription regulation (Steffan et al., 2000). Additionally, wtHTT has been

shown to regulate the transcription of a number of nuclear receptors (Futter et al., 2009). Investigations in mouse embryonic fibroblasts have also shown that loss of wtHTT expression results in altered gene expression associated with several areas of cell function, including lipid metabolism, cell division, protein degradation, development and the extracellular matrix composition (Zhang et al., 2008), although it is not clear at what level wtHTT-lowering causes these gene expression changes.

As well as this, wtHTT appears to interact with mRNA post-transcriptionally, to alter protein expression. This has been shown with wtHTT interacting with its own mRNA (Culver et al., 2016). Additionally, reduced expression of wtHTT results in reduced transport of mRNAs in the cell, and in rats it has been found that wtHTT co-localises with *BDNF, ACTB*, *DHC* and *KIF5A* mRNA (Culver et al., 2012; Ma et al., 2011).

Fundamentally, the HEAT repeats of the wtHTT protein are also found in transcription factors and proteins associated with the chromosome, such as condesin- and cohesion-associated proteins. It is possible, therefore, that these HEAT repeats might function as flexible scaffolds binding specific substrates in a manner similar to that found with transcription factors (Neuwald and Hirano, 2000).

WtHTT also has a clear role in development, as knock out is lethal prior to CNS development in the embryo (Duyao et al., 1995; Nasir et al., 1995). However, this phenotype is rescued by extra embryonic tissue expression of wtHTT, as far as E12.5 (Dragatsis et al., 1998). Interestingly, lowered expression of Hdh (the mouse homologue of wtHTT) results in perinatal lethality and aberrant brain development. However, normal levels of expression of the mutant version of the gene alleviate these phenotypes, suggesting that mHTT retains these key developmental functions (White et al., 1997). *In vitro*, researchers were able to differentiate null Hdh embryonic stem cells to neurons for up to 20 days in culture with no overt differences. However, this may be due to a lack of strong phenotypes in this particular experimental set up (Metzler et al., 1999). In perinatal animals, conditional knock out of wtHTT results in premature death, due to acute pancreatitis (Wang et al., 2016).

Looking at wtHTT's role in embryonic development in more detail, it has been found to be important for proper neurogenesis. Specifically, wtHTT has been found to associate with centrosomes of neural progenitors as they undergo cell division. WtHTT interacts with p150(Glued) subunit of dynactin, dynein, and the large nuclear mitotic apparatus NuMA protein at the centrosome in this context, and in this way regulates the mitotic spindle orientation. WtHTT lowering or ablation has been shown to cause misorientation and the altered cell fate of cortical progenitors of the ventricular zone (Godin et al., 2010; Godin and Humbert, 2011). In the developing cortex of mice, it has been shown that wtHTT is enriched in the projection neurons. Depleting wtHTT in these cells has shown that wtHTT is necessary for the multipolar-bipolar transition of these projection neurons and for the maintenance of their bipolar shape during radial migration. wtHTT appears to mediate these effects *in vivo* through the regulation of RAB11-dependent N-Cadherin trafficking, which as mentioned before is a known interacting partner of wtHTT, an interaction that is disrupted in HD (Barnat et al., 2017).

WtHTT has also been found to play a role in ciliogenesis, which is crucial in normal development, in the CNS as well as the periphery. Specifically, it has been shown to regulate the formation of cilia by interacting with pericentriolar material 1 protein (PCM1) via HAP1. In mouse cells, a reduction in wtHTT results in impaired retrograde trafficking of PCM1, and a resultant reduction in primary cilia. *In vivo*, this results in alteration of the cilia layer and hydrocephalus, a condition where CSF accumulates in the brain (Keryer et al., 2011). Research in the model organism, *Xenopus*, has confirmed this finding, with knockdown of wtHTT resulting in a reduced number of cilia, altered lengths of cilia in the epidermal cells, as well as altered polarity and function of cilia, resulting in whole body paralysis (Haremaki et al., 2015).

WtHTT has also been shown to have a role in excitatory synapse development in the cortex and striatum. Indeed, in the absence of wtHTT accelerated synapse formation is found in these regions, compared to controls. This elevated synapse formation is then gradually lost over time in the cortex, accompanied by reactive gliosis without cell loss. The presence of mHTT had a similar effect to wtHTT loss, suggesting that this function of wtHTT is lost in the mutant form of the protein

(McKinstry et al., 2014). In addition to this, in the mature brain, wtHTT has been implicated in the formation and maintenance of the post synaptic density (PSD). Firstly, wtHTT has been shown to interact with PSD95, an essential scaffolding protein for the organisation of the PSD (Parsons et al., 2014). As well as this, HAP1 has been found to regulate the expression of TrkA and the related neurite outgrowth (Rong et al., 2006). WtHTT is also found to interact with TrkB, regulating retrograde transport following BDNF signalling (Liot et al., 2013). Lastly, wtHTT appears to interact with BDNF trafficking, an essential neurotrophic factor essential for the growth, differentiation and maintenance of neurons. As described previously, wtHTT has a role in trafficking via HAP1 and p150Glued, a subunit of dynactin, and in this way wtHTT aids in trafficking of BDNF in the CNS and therefore has a role in neuronal survival (Gauthier et al., 2004).

WtHTT has also been shown to have a role in the cell stress response, generally serving as a protective factor against toxicity. There are a number of ways wtHTT functions to bolster the cell stress response. Firstly, wtHTT acts as an anti-apoptotic protein, by preventing Caspase 3 activity and inhibiting procaspase 9 processing (Rigamonti et al., 2001, 2000). WtHTT has also been shown to modulate the interaction between HIP1 and HIPPI, which can form a pro-apoptotic heterodimer that recruits Caspase 8 (Cheng et al., 2003; Gervais et al., 2002). In addition to this, wtHTT appears to act as a sensor for both ROS production, and DNA damage (Anne et al., 2007; DiGiovanni et al., 2016). Additionally, wtHTT has been shown to aid in a fast stress response that is impaired in HD (Nath et al., 2015). WtHTT has also been shown to play a role in the Heat Shock Response (HSR) pathway, which is impaired in HD, possibly via altered chromatin architecture (Chafekar and Duennwald, 2012; Labbadia et al., 2011; Wyttenbach et al., 2002). In this way, it is clear that wtHTT functions in a number of different cell stress response pathways, and as such, its loss can impact cell viability under stressed conditions, resulting in less viable cell populations in the wtHTT-lowered condition.

In the adult system, brain-specific conditional knock out of wtHTT causes neurodegeneration, motor phenotypes and early mortality, although not to the extent seen in HD, suggesting a toxic gain of function of the mHTT as the primary driver of disease (Dragatsis et al., 2000). Nonetheless, the presence of wtHTT in

the HD system appears to be protective. For example, wtHTT knockout mice exhibit increased apoptosis (Zeitlin et al., 1995). Conversely, overexpression of wtHTT in HD mice leads to a reduction in striatal cell loss (Leavitt et al., 2006, 2001; Rigamonti et al., 2000).

WtHTT is protective during traumatic events in the CNS. For example, in a model of ischaemia, mice expressing higher levels of wtHTT show a reduction in lesion size of 17%, compared to their littermates. Additionally, wtHTT levels were found to be reduced in mouse models of traumatic brain injury and spinal cord injury, which was blocked by administration of a broad caspase inhibitor, suggesting this depletion is due to wtHTT's role as a caspase substrate (Zhang et al., 2003).

Interestingly, research in amoeba has shown that those lacking the homologue for wtHTT have deficits in cell shape, cell fate, cell-cell adhesion, the formation of multicellular structures and a deficit in sensitivity (Myre et al., 2011).

WtHTT also appears to have a protective effect in models of HD, in keeping with what is found during traumatic events in the CNS generally. Specifically, the loss of wtHTT can contribute to the HD phenotype in animal and cell models of the disease. For example, research has shown worsened motor phenotypes, survival rates and cell vulnerability in the absence of wtHTT in a number of models of HD (Van Raamsdonk et al., 2005; Zhang et al., 2003; Zuccato et al., 2003, 2001).

Interestingly, HD patients homozygous for mHTT, and therefore lacking wtHTT entirely, do not appear to have a more severe progression or age at onset (Cubo et al., 2019). However, homozygous patients are very rare, and as such if there are differences with a small effect size, this may not be clear in this patient group. In HD mice, overexpression of wtHTT resulted in reduced striatal loss, but not all measures are improved, pointing again to the toxic gain of function of the mutant form as the disease driver (Leavitt et al., 2006, 2001; Rigamonti et al., 2000). Additionally, as previously mentioned, lowered wtHTT results in increased apoptosis. This is the case generally, but applies in HD also, where all patients are at least heterozygous, and as such have significantly lowered wtHTT levels.

The DNA damage response has recently been implicated in disease onset and progression in HD, with gene variants impacting DNA damage repair pathways being implicated (Flower et al., 2019; Goold et al., 2019; J.-M. Lee et al., 2015;

Long et al., 2018). WtHTT has been shown to be a sensor for DNA damage and this function may be altered in HD (Anne et al., 2007).

The innate immune system has been shown to be dysfunctional in HD. As part of investigations into this disease phenotype, Träger et al., 2014 found that siRNA-mediated HTT-lowering resulted in reduced cytokine release in control individual's blood monocytes and macrophages. As well as this, Beçanovic et al., 2015, found that an NF-κB binding site in the *HTT* promoter resulted in lowered expression of the cis allele, and if it was present in the promoter upstream of wtHTT, HTT levels were lowered, and the age at onset reduced. The NF-κB pathway is a key stimulant response pathway in the immune system, and as such, the presence of a feedback loop whereby NF-κB can lower wtHTT levels suggests a key role of wtHTT in the immune response.

Based on these observations; the large number of roles wtHTT plays at both a molecular and physiological level, particularly via interactions with the cytoskeleton and trafficking, it seems plausible that an, as yet, undescribed novel function for wtHTT exists in the function of macrophages. The present work aims to investigate this further, by first confirming the results found by Träger et al., 2014, before performing a battery of assays to assess the overall function of human myeloid cells when wtHTT expression levels are reduced.

Further investigation into the role of wtHTT is particularly relevant to the HD community at this time, as a large number of HTT-lowering treatments are in pre-clinical and clinical testing, some of which are not allele-specific and will result in lowering both mHTT and wtHTT (Kaemmerer and Grondin, 2019). Thus far, HTT-lowering in adults in non-human primates, and now in humans via ASO treatment, appears to be safe and well-tolerated (Tabrizi et al., 2019). However, possible implications for the immune system might be relevant when individuals receive long-term treatment and/or if treatments such as small molecules are delivered systemically where effects in the periphery are possible too.

5.1 Aims

To investigate the role of wild-type HTT (wtHTT) in the function of macrophages of the innate immune system.

5.2 Methods

Primary human monocytes were isolated from whole blood samples (section 2.2), differentiated to macrophages (section 2.3) and treated with β-1,3-D-glucan-encapsulated siRNA particles (GeRPs) containing anti-HTT siRNA or scrambled siRNA (section 2.8). Anti-HTT and SCR-treated primary human macrophages were assessed for HTT knockdown using RT-qPCR (section 2.9). With efficient and prolonged HTT-lowering confirmed, macrophages were then assessed for functional differences between the HTT-lowered and controlled groups. Cytokine profiles in the supernatant and intracellularly were quantified using MSD cytokine assays (section 2.15) at baseline and following stimulation. In parallel, expression of pro-inflammatory cytokines at the mRNA level was assessed using RT-qPCR (section 2.9). This was followed by an assessment of NF-κB pathway activity using imaging flow cytometry (section 2.11). Phagocytic activity was also assessed in the HTT-lowered and control macrophages, using pHrodo bead assays (section 2.13). Finally, viability was assessed using both LDH and ATP assays (section 2.12).

5.3 Results

5.3.1 Wild-type HTT was efficiently lowered in primary human macrophages

HTT-lowering was achieved by treatment with siRNA-containing GeRPs, as described in section 2.8. To confirm *HTT* knockdown, parallel wells for each sample were seeded and treated with GeRPs carrying scrambled siRNA (control) or anti-HTT siRNA, which were then harvested. RT-qPCR showed that cells treated with anti-HTT siRNA GeRPs contained significantly lowered *HTT* levels (Figure 5.1).

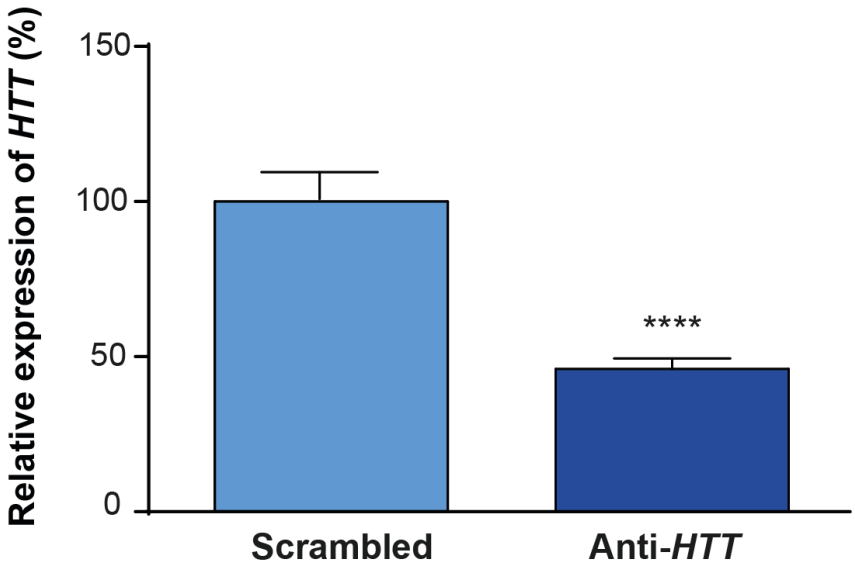

Figure 5.1: Treatment of human primary macrophages with anti–HTT siRNA resulted in a significant lowering of *HTT* mRNA expression. Data shown are mean *HTT* expression levels in macrophages treated with anti-HTT siRNA GeRPs ± SEM, relative to expression levels in macrophages treated with scrambled siRNA GeRPs. N=23, three technical replicates per sample, paired two-tailed Student's t-test, ****$p<0.0001$. Values were normalised to *ACTB* and *GAPDH* housekeeping genes results for each sample, also run in triplicate.

5.3.2 HTT-lowering was stable over a prolonged period of time

To ensure *HTT* levels remained lowered throughout the time course of the experiments described, the lowering effects of anti-*HTT* GeRPs over time were investigated. Samples were collected at 48, 72 and 96 h post-treatment and *HTT* levels assessed by RT-qPCR. *HTT* levels remained significantly reduced from 48 h onwards, and there was no significant difference in *HTT*-lowering between time points (Figure 5.2). All experiments were consequently conducted between 72 and 96 h post GeRP treatment.

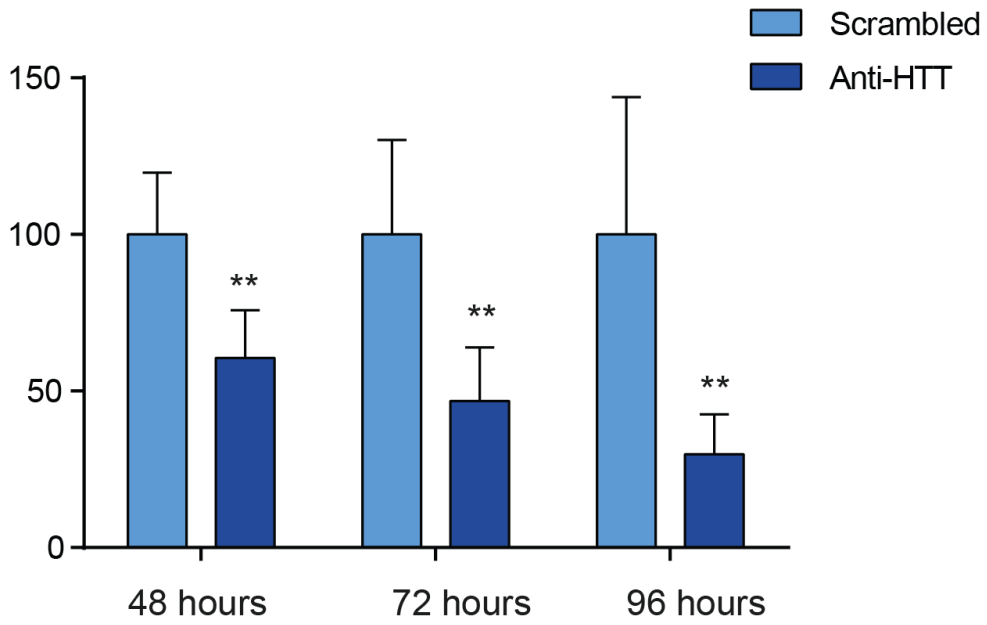

Figure 5.2: HTT knockdown in human primary macrophages using GeRP-mediated anti-*HTT* siRNA remained stable over time. *HTT* levels remained significantly lowered from 48 h, with no significant difference between time points. All experiments were conducted 72-96 h post-GeRP treatment. Data shown are mean *HTT* expression levels in macrophages treated with anti-HTT siRNA carrying GeRPs ± SEM, relative to expression levels in macrophages treated with scrambled siRNA carrying GeRPs. N=5, three technical replicates per sample, paired two-tailed t-test, **P<0.01. Values were normalised to *ACTB* and *GAPDH* housekeeping genes results for each sample.

5.3.3 Cytokine production and release by activated primary human macrophages was reduced upon HTT-lowering

The effects of HTT-lowering on cytokine expression by primary human macrophages was assessed. After HTT-lowering using GeRPs, macrophages were stimulated with LPS and IFNγ for 24 h (section 2.15). Controls for each sample included parallel unstimulated wells and scrambled siRNA GeRP-treated wells. This provided data for basal cytokine production, as well as normal cytokine production in response to stimuli in the presence of normal HTT expression. This allowed for comparison within an individual biological replicate, controlling for the high levels of variability in both baseline and peak cytokine production levels between individual samples. The supernatant from each experimental condition for each sample was then collected and assessed for the levels of a panel of six cytokines by multiplex ELISA. Of the six cytokines assessed, four pro-

inflammatory cytokines, IL-6, IL-8, TNFα and IL-1B were found to be significantly reduced following HTT-lowering (Figure 5.3).

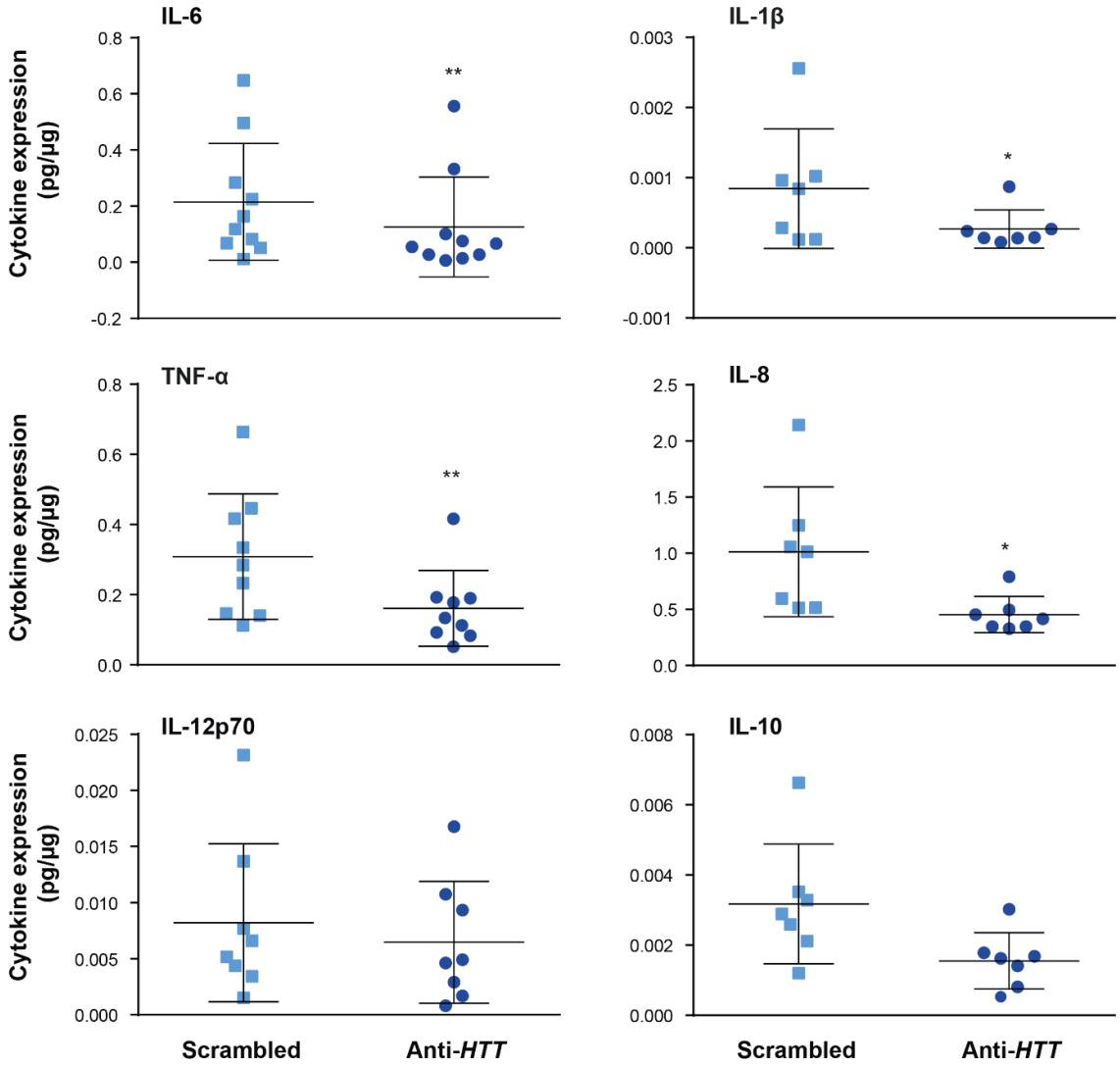

Figure 5.3: HTT-lowering decreased pro-inflammatory cytokine production by primary human macrophages. Regulators of the innate immune system, such as IL-6, IL-8, TNFα and IL-1β, were significantly decreased following lowering of HTT levels in primary human macrophages. The pro-inflammatory cytokine, IL-12p70, and anti-inflammatory cytokine, IL-10, were not statistically significantly changed. Data show are mean concentrations per µg protein ± SEM, n=7-10 individual biological repeats, three technical replicates per sample, paired two-tailed Student's t-test, *P<0.05; **P<0.01. Positive and negative controls were provided by the manufacturer for this assessment, and were used to build a standard curve to inform analysis of the test samples results.

5.3.4 Cytokine gene transcription in activated primary human macrophages was reduced upon HTT-lowering

Following the confirmation of the results published by Trager et al., 2014, showing reduced cytokine release following HTT-lowering, it was decided to try and assess the underlying cause of the altered cytokine release. The first step of this investigation was to assess whether the pro-inflammatory cytokines that showed reduced release in a HTT-lowered setting, were also reduced at the mRNA level. In this way, it would be possible to test whether HTT-lowering interacted with cytokine expression at the level of transcription or above. Primary macrophages treated with anti-HTT or scrambled siRNA containing- GeRPs were stimulated with LPS and IFNγ for 4 h. The cell lysate from each sample was harvested and assessed by RT-qPCR for the expression of the following key cytokine genes; *IL-6*, *IL-8*, *TNFα* and *IL-1β* (section 2.9).

Of the four cytokines assessed in this way, *IL-6*, *TNFα* and *IL-1β* showed significant reductions compared to the scrambled siRNA-treated cells (Figure 5.4).

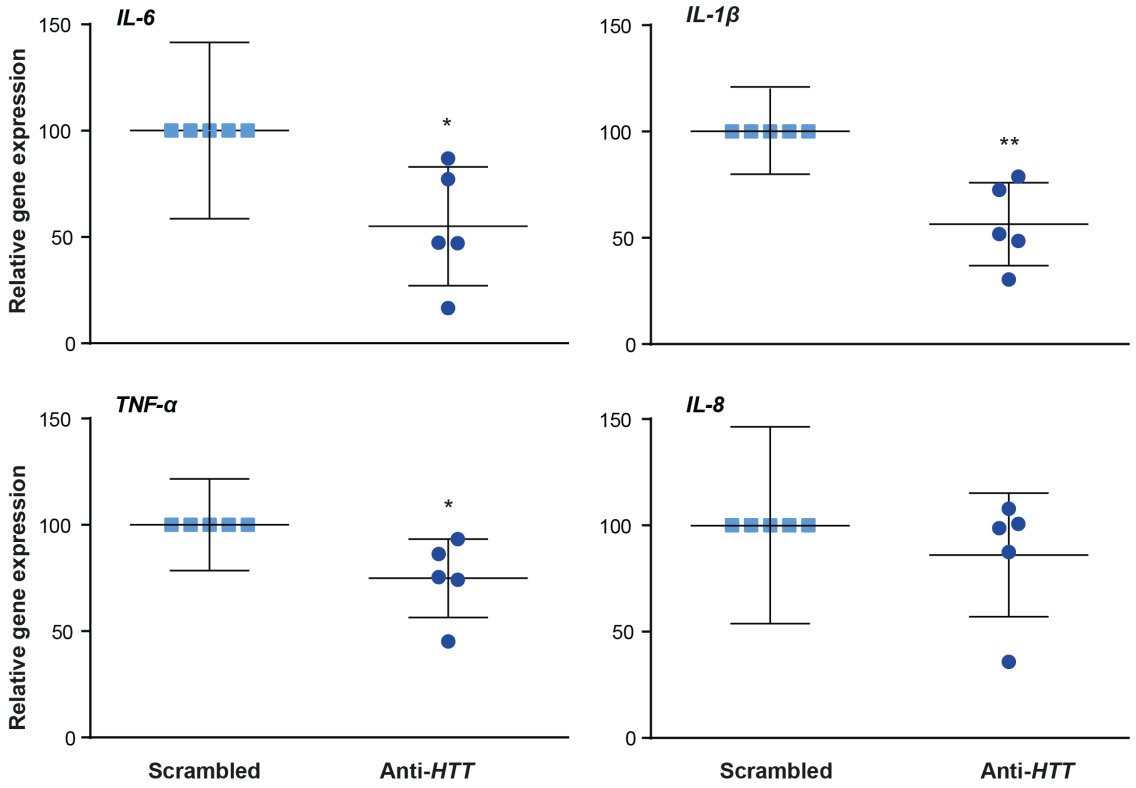

Figure 5.4: Knockdown of HTT decreased pro-inflammatory cytokine gene expression in human macrophages. Regulators of the innate immune system such as *IL-6*, *IL-8*, *TNFα* and *IL-1β*, were significantly decreased at the mRNA

level following lowering of HTT levels in primary human macrophages. Data show are the mean percentage expression relative to the paired scrambled treated sample ± SD, n= 5 individual biological repeats, three technical replicates per sample, paired two-tailed t-test, *P< 0.05; **P< 0.01.

5.3.5 Intracellular cytokine levels in activated primary human macrophages were not altered by HTT-lowering

Following the confirmation of reduced pro-inflammatory cytokine expression at the mRNA level following HTT-lowering, it was decided to assess the possibility that the reduced cytokine release seen following HTT-lowering might also be due to a reduction in transport and release. HTT has a well-established role in trafficking and secretion, so it was plausible that HTT-lowering might reduce cytokine release in this way also. In order to assess the effects of HTT-lowering on intracellular cytokine levels, the following experimental program was used. After HTT-lowering using GeRPs, macrophages were stimulated with LPS and IFNγ for 24 h. The cell lysate from each experimental condition for each sample was collected and assessed for the levels of a panel of five cytokines by MSD cytokine assay (section 2.15). This method revealed no significant differences in intracellular cytokine levels at 24 h (Figure 5.5), the time point at which there are significantly reduced levels of released pro-inflammatory cytokine in the supernatant in the HTT-lowered condition.

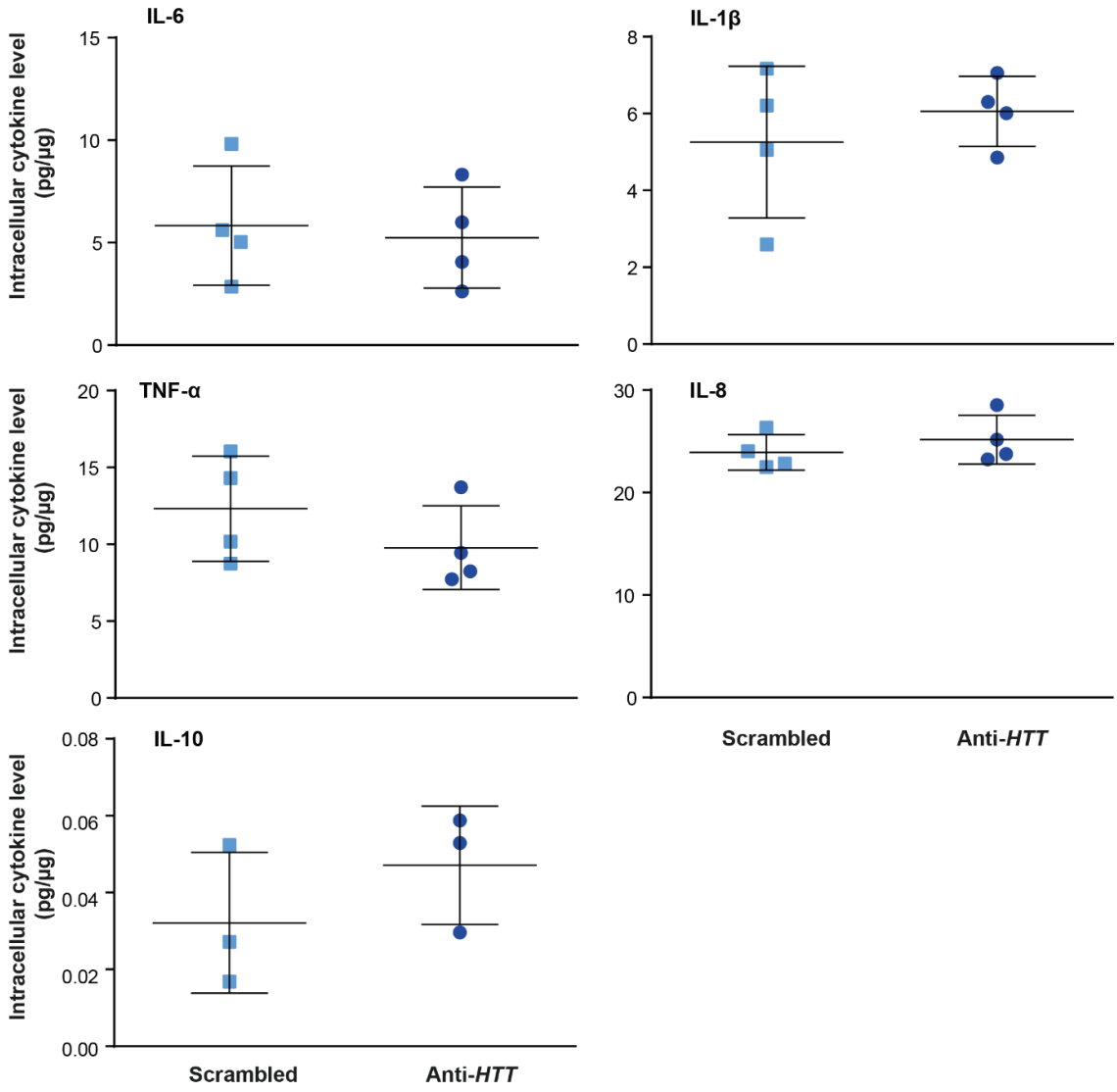

Figure 5.5: Knockdown of HTT resulted in unchanged intracellular levels of pro-inflammatory in human macrophages at 24 h. Regulators of the innate immune system such as IL-6, IL-8, TNFα, and IL-1β and IL-10 were not significantly decreased intracellularly following lowering of HTT levels in primary human macrophages. Data shown are mean concentrations per µg protein ± SD, n= 4 individual biological repeats for all cytokine except IL-10 where n=3, all samples were run in triplicate. Paired two-tailed t-tests were conducted. IL-6, p=0.4036, IL-1β, p=0.4279, TNFα, p=0.0654, IL-8, p=0.4982, IL-10=0.2396. Positive and negative controls were provided by the manufacturer for this assessment, and were used to build a standard curve to inform analysis of the test samples results. A method for blocking cytokine release was tested as a positive control (monensin), however it was ineffective.

5.3.6 HTT-lowering does not affect RELA (p65) translocation in primary human macrophages

Previous work by Träger et al., 2014, found that an increase in cytokine expression in HD patient monocytes cultured *ex vivo* was partially explained by an interaction of mHTT with the NF-κB pathway, with elevated levels of RELA translocation to the nucleus following LPS stimulation, that remained translocated for longer in HD samples than controls.

In order to assess if the changes seen upon HTT-lowering were also related to this pathway, a similar experiment was conducted. Primary human macrophages from control individuals were treated with GeRPs containing anti-HTT or scrambled siRNA as described in section 2.8. These samples were then treated with LPS for 45 min, the time point at which translocation had peak in control and HD samples in previous studies (Trager et al., 2014), and the level of RELA translocation assessed using imaging flow cytometry (ImageStreamX) as described in section 2.11. This revealed no differences between *HTT*-lowered and SCR-treated samples for each individual biological replicate, and there were no group differences (Figure 5.6).

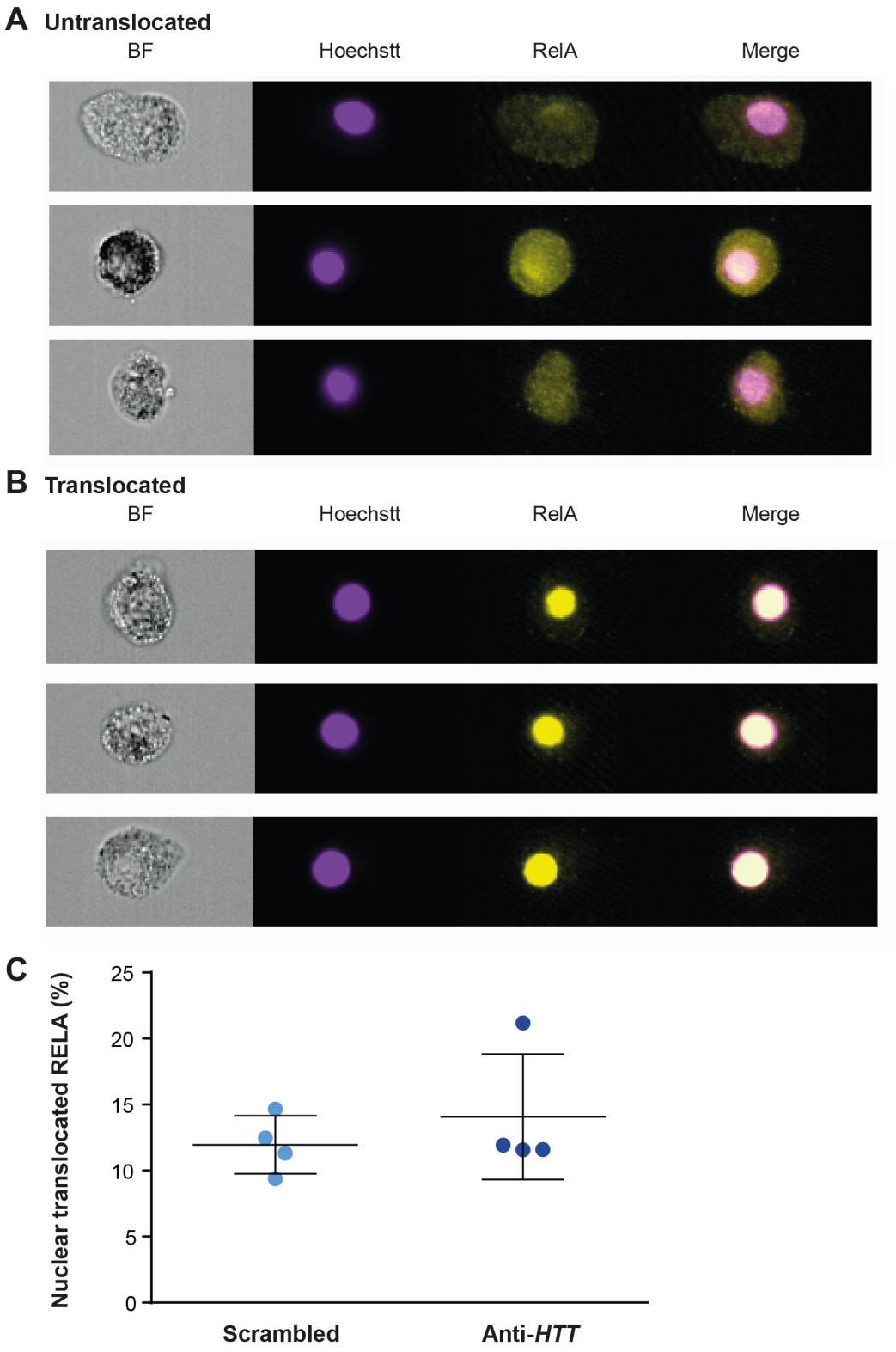

Figure 5.6: Knockdown of HTT resulted in no significant difference in translocation of the NF-κB transcription factor RELA to the nucleus. Primary human macrophages treated with LPS for 45 min and assessed for translocation of RELA (p65) using imaging flow cytometry, see **A**) for example images of un-translocated RELA, where the yellow RELA stain is found in the cytoplasm, and

B) for example images of cells with RELA translocated to the nucleus, with overlapping yellow RELA staining and purple Hoechstt staining. **C**) There was no significant difference in the percentage of total cells showing RELA translocation into the nucleus, n=4 individual biological samples, a minimum of 5000 cells imaged. Data shown as percentage of translocated cells of total ± SD, paired two-tailed t-test, p=0.2866.

5.3.7 HTT-lowering increased phagocytic activity in primary human macrophages

Another key area of macrophage function in the immune system is phagocytosis, with macrophages known to phagocytose foreign material and cell debris (Geissmann et al., 2010). In order to investigate if phagocytic activity was affected by HTT-lowering, the following experimental plan was undertaken. Each biological replicate was seeded at 100,000 cells/well and placed in serum free media overnight to stimulate phagocytosis. To assess levels of phagocytosis, *Zymosan A* or *E.coli* pHrodo™ beads were added. Assessment of phagocytic activity in this way suggests there is a significant increase in phagocytic activity in HTT-lowered macrophages compared to control macrophages (Figure 5.7).

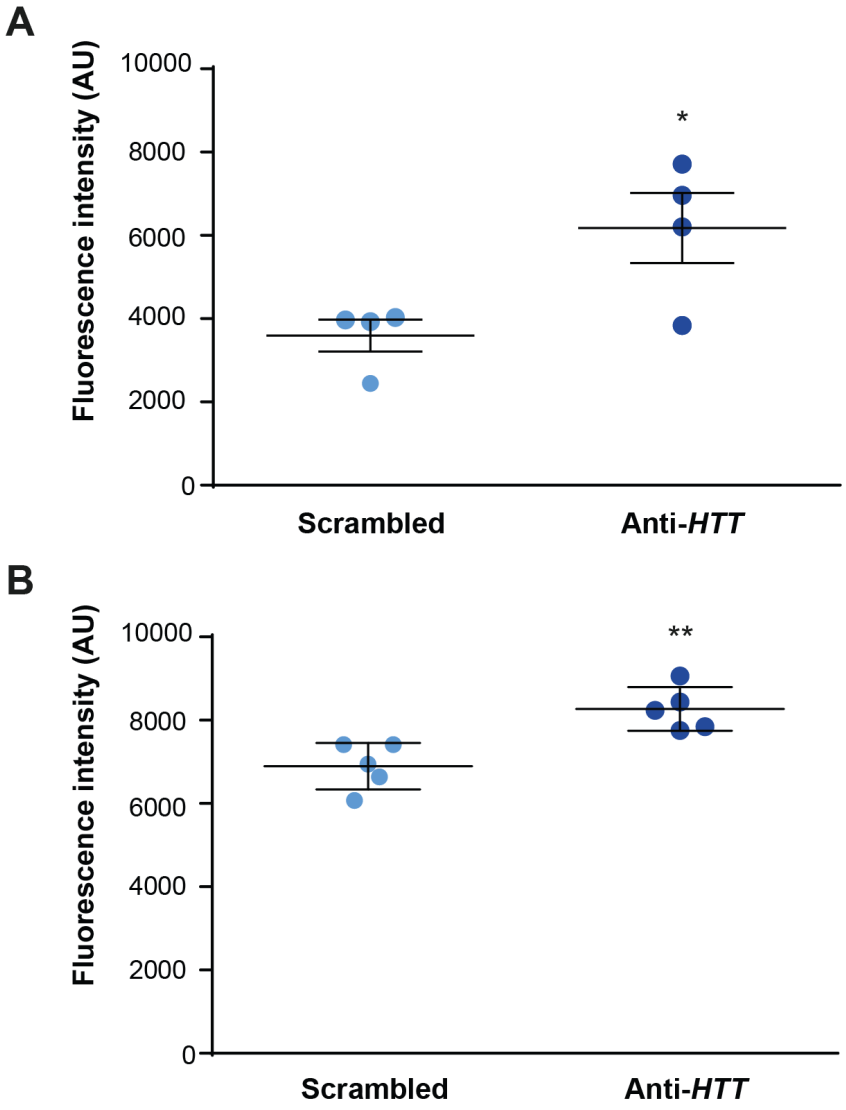

Figure 5.7: Knockdown of HTT resulted elevated phagocytic activity in human macrophages. Phagocytic activity as assessed using **A**) *Zymosan A* pHrodo beads) and **B**) *E.coli* pHrodo beads was significantly increased in primary human macrophages treated with anti-*HTT* siRNA compared to those from the same donors treated with scrambled siRNA. Data mean ± SD, n=4 individual biological repeats for *Zymosan A* n=5 individual biological repeats for *E.coli*, paired two-tailed Student's t-test, *Zymosan A*, p=0.0153, *E.coli*, p=0.0040. Six technical replicates were included for each sample, and the average taken as the result for that sample. Negative control wells of cells without phagocytic beads and cell-free wells with beads were also run, and the values used to establish a baseline for each line tested, and that baseline value subtracted from the experimental value found to give the data shown above.

5.3.8 HTT-lowering in primary human macrophages resulted in a reduction in their viability in the presence of an autophagy inhibitor

Finally, given the wealth of literature which suggests protective effects of HTT in a HD context and more generally, viability under HTT-lowered conditions were assessed. Initially, baseline viability was investigated, which HTT-lowering did not appear to alter (Figure 5.8, A). However, following introduction of a cell stressor, the autophagy inhibitor bafilomycin A1, a significant difference between the control and HTT-lowered groups emerged (Figure 5.8, B). Assessment using a potentially more sensitive assay, testing intracellular ATP levels, suggested reduced viability in the HTT-lowered group, but this was not statistically significant (Figure 5.8, C). This may be due to the experimental set up for the ATP assay, which lacks a method for controlling for variations in cell number, which are internally controlled for in the LDH assay using maximum LDH release values.

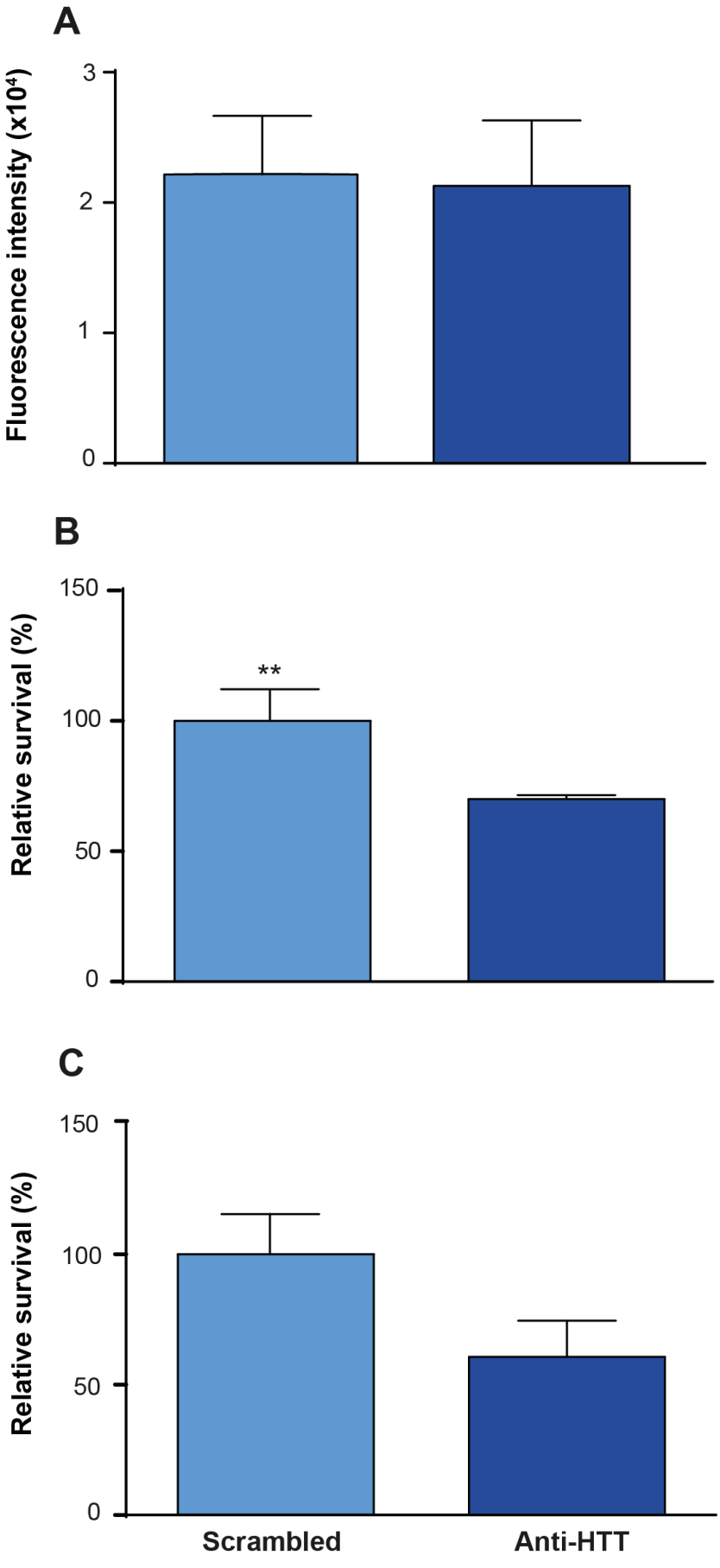
A
Fluorescence intensity (x10⁴)
3
2
1
0
B
Relative survival (%)
150
100
50
0
**
C
Relative survival (%)
150
100
50
0
Scrambled
Anti-HTT

Figure 5.8: In the presence of an inhibitor of autophagy, Bafilomycin A1, HTT-lowering resulted in a significant reduction in human macrophage survival. A) HTT-lowering does not appear to affect basal viability. Data shown are mean fluorescence intensity ± SEM. N= 6. **B**) Survival of macrophages, assessed by experimental LDH release relative to maximum LDH release per well, is reduced upon HTT-lowering. Data shown are mean ± SEM, with the scrambled condition set to 100%, N= 3, paired two-tailed t-test, **P< 0.01. **C**). Assessment of macrophage survival following Bafilomycin A1 treatment using an ATP release assay shows a reduction in survival relative to the control group. This reduction was not statistically significant. Data shown are mean ± SEM, with the scrambled condition set to 100%, N= 3, with three technical replicates per sample. LDH assays include a potent toxin to allow the calculation of 100% cell death in the test wells, this allowed calculation of the percentage cell death in each test well as a proportion of the 100% cell death value.

5.4 Discussion

In this research, primary human macrophages from healthy individuals were assessed using a battery of functional assessments, looking at cytokine production at the protein level in the supernatant and intracellularly and at the mRNA level, phagocytosis and viability, under baseline and stimulated conditions following siRNA treatment against HTT or SCR siRNA. RELA translocation was also assessed following stimulation, to test the interaction of wtHTT with the NF-κB pathway. In this way, it was possible to assess the impact of wtHTT-lowering on primary human macrophages *ex vivo*.

The first assessments focused on the efficiency and longevity of wtHTT-lowering, and found that GeRP-delivered anti-HTT siRNA significantly and consistently reduced *HTT* levels by over 50%, as assessed by RT-qPCR. Prior work in the lab has shown this correlates with a 50% reduction in HTT protein levels (Miller et al., 2017). However, knockdown at the protein level was not directly assessed in this work, which is a definite weakness of this assessment and should be assessed in future experiments.

The next assessment focused on following up the published work by Träger et al., 2014, which showed dampened pro-inflammatory cytokine expression in response to an immune challenge under HTT-lowered conditions. The cytokine

profiles of paired samples from control donors treated with either SCR siRNA or anti-HTT siRNA, and then treated with LPS and IFNγ or not, were assessed. In this way, it was found that the levels of proinflammatory cytokines released into the supernatant following 24 h of stimulation were significantly reduced in the HTT-lowered samples, compared to the SCR-treated samples. This is clear evidence for a novel role for HTT in macrophage cytokine expression. There may be a number of mechanisms through which HTT interacts with cytokine expression and secretion. Given the documented roles of HTT in trafficking and secretion (Brandstaetter et al., 2014; Strehlow et al., 2007; Velier et al., 1998), it is plausible that HTT-lowering impairs that function, and so less proinflammatory cytokines are trafficked and released as a result.

It may also be the case the HTT lowering causes reduced cytokine expression by interacting with the process further upstream. For example, there is ample evidence showing HTT has the capacity to affect transcription, either through interacting with transcription factors (Zuccato et al., 2001), or through interactions with chromatin modifying proteins (Steffan et al., 2000). In this way, it is possible that HTT alters cytokine expression at the transcriptional level.

There was no apparent difference in the unstimulated samples. This may be due to the very low levels of cytokines secreted under baseline conditions, resulting in a poor signal to noise ratio in the MSD system, masking possible effects. Alternatively, it may be that there is no difference in cytokine release at baseline, and that lowered levels of HTT only begin to exert an effect on cytokine expression following stimulation and the cascade of intracellular signalling associated with it.

These results were followed up with an investigation into the mRNA expression levels of each of the significantly reduced pro-inflammatory cytokines, to assess whether the changes in supernatant levels seen were related to a difference in gene expression. This revealed that HTT-lowering resulted in a significant reduction of gene expression of the pro-inflammatory cytokines assessed, but no significant changes in the housekeeping genes. The unstimulated samples showed no differences between SCR and anti-HTT treated groups. This suggests that HTT-lowering alters the response of macrophages to an immune challenge at least at the level of gene expression. As previously mentioned, HTT has been

shown to have a role in transcription. Specifically, it has been shown in neurons that HTT interacts with the transcription factor REST/NRSF to sequester it away from binding NRSE-containing genes. This interaction is reduced with mHTT, and results in reduced expression of these neuronal genes, including BDNF (Zuccato et al., 2001). Therefore, it may be the case that in healthy controls HTT interacts with a transcription factor that affects the transcription of these proinflammatory cytokines. One candidate for such a transcription factor is NF-κB, which HTT is known to bind to (Träger et al., 2014), and plays a role in cytokine expression (Liu et al., 2017).

It has also been shown that HTT interacts with CBP, which controls access to genes for transcription through regulating acetylation and deacetylation of histones (Steffan et al., 2000). It may be the case in the immune system that this interaction allows access to pro-inflammatory genes, which is lost when HTT is lowered and there is reduced interaction with CBP. However, this finding does not preclude the possibility that HTT-lowering alters cytokine expression via interactions further downstream of transcription also, and that the lowered expression is a result of a combination of mechanisms.

In order to investigate the pathway through which HTT-lowering could result in reduced expression of proinflammatory cytokines, at the mRNA and protein level, the activity of the NF-κB pathway was assessed, which has long been implicated in inflammatory responses, and is known to be altered in HD.

Specifically, the translocation of RELA into the nucleus following stimulation was assessed. In HD, it has been previously established that an elevated percentage of cells showed RELA translocation following LPS stimulation and that this translocation event persists over a longer period (Träger et al., 2014). This was proposed to be the pathway through which elevated cytokine responses in HD were caused. As such, it was decided to investigate whether HTT-lowering altered the activity in this pathway, and specifically the translocation of RELA in response to an immune stimulus. It was hypothesised that the percentage of cells with translocated RELA would be lowered in the HTT-lowered populations, and that this reduced activation signal could explain the reduced proinflammatory mRNA and protein expression found under these conditions. However, this investigation revealed no significant differences between the HTT-lowered and

control populations for each individual, and no group differences. This suggests that the mechanism through which HTT participates in the expression of cytokines may be distinct to the pathological gain of function activation of the NF-κB pathway that occurs in HD via mutant HTT expression.

The lowered HTT levels may also affect interactions further downstream than this, perhaps reducing translation of these mRNA transcripts into protein. As previously mentioned, given the role of HTT in trafficking and secretion, it is possible that a reduction in HTT may contribute to reduced supernatant levels via reduced trafficking and release of each cytokine.

This possibility was assessed next, with intracellular levels of each cytokine assessed under stimulated conditions, following anti-HTT siRNA treatment. This found no significant differences in intracellular cytokine levels at 24 h.

This time point was chosen to mirror the supernatant assessments that were conducted. However, this may be a limitation of this experiment, as it is possible that differences may occur at an earlier timepoint following stimulation. Additionally, a clear positive control sample would be useful, to allow for assessment of the experimental set up itself, however this was not possible in this work. As well as this, a great body of work implicates HTT in trafficking and secretion, and while this method was unable to identify changes, a more sensitive technique to assess each element, both trafficking, and secretion, would be important to test, in order to fully rule out a cytokine trafficking deficit.

Given the results as they are, however, it seems that the underlying cause of reduced supernatant levels of proinflammatory cytokines in the HTT-lowered group are lowered mRNA levels of these cytokines.

Following on from this work, the phagocytic ability of primary human macrophages was assessed. Phagocytic activity is a key element of macrophage function in the immune response, and as such it was important to investigate if this element was changed also. Macrophages treated with SCR or Anti-HTT siRNAs were assessed for phagocytic activity following a period of starvation using pHrodo beads. In this way, phagocytosis was assessed.

Interestingly, cells with lowered levels of HTT showed elevated phagocytosis as assessed by both *Zymosan A* and *E.coli* pHrodo beads. This suggests that a

function of HTT is to regulate phagocytosis. In HD, phagocytosis levels are found to be elevated in primary macrophages (Kwan et al., 2012). These results suggests that this HD phenotype may be in part caused by lowered levels of wtHTT. This effect may orchestrated through an interaction with actin, and the cytoskeleton more generally, which wtHTT is known to interact with. For example, existing research has found that wtHTT has a role in nuclear actin reorganisation that is impaired upon HTT-lowering (Munsie et al., 2011).

Typically, potent phagocytic ability is associated with so-called "M2" macrophages, or anti-inflammatory macrophages (Shapouri-Moghaddam et al., 2018; Tarique et al., 2015), which exhibit phagocytic activity but do not produce pro-inflammatory cytokines. In this way, the phenotypes observed upon wtHTT-lowering are similar to known phenotypes of M2 macrophages. However M2 macrophages retain their secretory capacity, secreting high levels of the anti-inflammatory cytokine IL-10; the secretion of which was reduced following wtHTT-lowering in this study.

Another possibility is that wtHTT-lowering results in altered interactions with the extra cellular matrix (ECM) as it has been previously shown that macrophages show upregulated phagocytosis following interaction with ECM proteins (Kirkham et al., 2004), however this is less likely.

WtHTT-lowering in primary macrophages appears to reduce their viability under stressed conditions. In the absence of a stress, there is no discernible difference between wtHTT-lowered and control macrophages, this suggests that under baseline conditions, in healthy individuals wtHTT-lowering could be well tolerated. Following treatment with Bafilomycin A1, an autophagy inhibitor however, assessment by LDH assay revealed a significant difference in survival between the wtHTT-lowered and control macrophages. A parallel experiment was conducted, where Bafilomycin A1 treatment was extended to 20 h, and viability assessed by a more sensitive assay of ATP. A reduction in viability of the wtHTT-lowered group did not reach statistical significance. This may be due to small variations in cell number, which cannot be controlled for within the ATP assay, introducing an added degree of variability in the data.

This reduced ability to cope with cellular stressors under wtHTT-lowered conditions fits with wtHTT's known roles in the cell stress response. Specifically,

wtHTT has been shown to be anti-apoptotic, preventing Caspase 3 activity as well as recruitment of Caspase 8 (Cheng et al., 2003; Gervais et al., 2002; Rigamonti et al., 2001, 2000).

WtHTT has also been found to play a role in the HSR pathway, via interactions with chromatin architecture (Chafekar and Duennwald, 2012; Labbadia et al., 2011; Wyttenbach et al., 2002).

In a HD context, the presence of mHTT acts a significant stressor, and has been specifically shown to affect autophagy (Martin et al., 2015).

Interestingly, it has been previously shown that overexpression of wtHTT leads to a reduction in striatal cell loss in a mouse model of HD (Leavitt et al., 2006; Rigamonti et al., 2000). In addition to this, a number of HD phenotypes were found to be worsened in the absence of the wtHTT protein (Leavitt et al., 2006; Zhang et al., 2003; Zuccato et al., 2003, 2001). In this way, the impact of wtHTT-lowering on viability under stressed conditions may be mediated through one or a number of these known interactions with stress response pathways.

This investigation has established a novel role of wtHTT as a regulator of macrophage function. Specifically, we have uncovered evidence for a role of wtHTT in pro-inflammatory cytokine expression, phagocytosis and viability. This is particularly interesting in the context of HD, but it is also relevant to the immune system more generally, where wtHTT could be a novel target for immune suppression in inflammatory disorders.

In light of these results, it would be useful to assess gene expression in my wtHTT-lowered condition more generally, with a follow up RNA sequencing investigation. This would be a significant endeavour, but would allow the identification of altered pathways in the HTT-lowered condition, and guide the next round of mechanistic investigations.

Additionally, it would be informative to run a parallel set of experiments in control microglia, in wtHTT-lowered conditions. In this way, it would be possible to assess the impact of wtHTT-lowering on the immune system in the CNS, which is where a number of wtHTT-lowering therapeutics are focused.

It would also be useful to assess whether this role is recapitulated *in vivo* using a rodent model, to test whether there are any compensatory effects of the

immune system as a whole when wtHTT is lowered, and if the impact of wtHTT-lowering is as significant.

In the context of HD, these results shed some light on the immune dysfunction found in the disease. For example, in HD elevated levels of pro-inflammatory cytokines are found in the periphery up to 16 years before symptom onset, with primary monocytes and macrophages the source (Björkqvist et al., 2008; Träger et al., 2014). This hyper-reactive phenotype is caused by a gain of function for the mHTT, rather than a 50% reduction in wtHTT levels, which heterozygous HD gene carriers would have. We have shown here that this level of wtHTT reduction would result in reduced pro-inflammatory cytokine production, and therefore does not contribute to elevated plasma levels found in pre-symptomatic HD gene carriers.

RNAseq of patient monocytes has shown elevated expression of inflammatory genes, such as *IL-6*, prior to any stimulation (Miller et al., 2016), whereas wtHTT-lowering resulted in reduced expression of pro-inflammatory cytokines under stimulated conditions. On a similar note, activity in the NF-κB pathway was found to be upregulated in HD (Träger et al., 2014), but was unchanged upon wtHTT-lowering, under the experimental conditions described. Collectively, these results point to a gain of function of mHTT rather than a loss of wtHTT function in HD, resulting in elevated cytokine expression mediated at least in part through the NF-κB pathway, and priming of pro-inflammatory pathways at rest.

In terms of phagocytosis, in HD we see elevated activity. This is mirrored by the phenotype observed in this research upon wtHTT-lowering. This suggests that the disease phenotype is at least in part caused by a loss of function of mHTT.

Finally, upon wtHTT-lowering the capacity of primary macrophages to cope with a cellular stressor, such as Bafilomycin A1, was reduced, although the underlying cause for this reduced resistance to stress was not assessed. In HD, it has been found that mHTT causes defective actin remodelling during stress, caused by a loss of function in the mutant protein (Munsie et al., 2011). In this way wtHTT-lowering could similarly reduce the cell's capacity for actin remodelling during stress and result in reduced viability.

It is also of note that the effects observed here upon wtHTT-lowering in primary human macrophages, are likely to be replicated in primary human microglia. In this way, the impact of non-allele-specific HTT-lowering is highly relevant in the context of HD and HTT-lowering trials targeting the CNS, for the treatment of HD.

There are a number of therapies that target only the mHTT allele are in testing for use in HD, leveraging the fact that a single nucleotide polymorphism in the target mRNA compared to the complementary siRNA can significantly alter the siRNA's activity (Bilsen et al., 2008; Carroll et al., 2011; Zhang et al., 2009). However, there are a number of caveats to this approach. Firstly, it would be essential to be able to efficiently identify which allele specific SNPs were on, to ensure only the mHTT allele was targeted. This can be achieved through SNP linkage by circularization (Liu et al., 2008), however this is a challenging method and scaling up to treat patients clinically would require significant optimisation.

Secondly, there is not one single SNP associated with the mHTT allele. A number of studies have investigated the number of SNPs and corresponding siRNAs that would be required to treat the majority of the HD population in the EU and USA. The first of these found that a repertoire of seven allele specific siRNAs could treat 85.6% of patients in Europe shown to be treatable by at least one siRNA (Lombardi et al., 2009). A similar study found that five siRNAs targeting just three SNPs could provide therapy for 75% of the US and EU HD populations (Pfister et al., 2009). It is likely that these allele-specific therapies will move forward in development, but it may be the case that this is slowed by the task of testing multiple siRNAs in clinical trials, which at present would require a separate trial for each siRNA.

Given the challenges of allele-specific HTT-lowering, development and assessment of siRNAs and anti-sense oligonucleotides (ASOs) that are not mHTT specific, has progressed significantly, with the most advanced, IONIS-HTTRx, now moving to Phase 3 clinical trials. The rationale for these non-allele-specific therapeutics is that the benefits of lowering mHTT will outweigh the negatives of HTT lowering. Additionally, significant pre-clinical work has established that HTT-lowering is well tolerated in non-human primates over several months (Grondin et al., 2012; McBride et al., 2011; Stiles et al., 2012). Additionally, in oncology chemotherapeutic agents have been used to treat

cancers which have devastating effects on the immune system, far beyond what was shown in this thesis, and are still used. Therefore, a potential impact on the immune system does not preclude the extensive use of HTT-lowering therapeutics, but the immune system should be monitored for reduced reactivity as part of routine care.

The delivery of these HTT-lowering drugs is focused on delivery to the CNS in HD, for obvious reasons. As such, the impact on the peripheral immune system may be minimal. However, the innate immune cells of the CNS, microglia, are likely to be affected. This would likely result in reduced pro-inflammatory cytokine production, both due to reduced mHTT load and reduced HTT load, and in the context of the CNS, this is most likely to have a net beneficial effect. The impact on viability may have a similar net effect, with a reduction in mHTT being protective, while a reduction in HTT would result in a corresponding reduction in viability under stressed conditions. Crucially, this effect of reduced viability in wtHTT-lowered conditions is only found under stressed conditions, so it is possible that reducing the presence of the toxic mHTT, and therefore reducing the stress on the cell, would mean the protective effects of wtHTT would be less required. This loss of protection would become more meaningful with increasing age of the patients, as systems become less capable of dealing with stress, and so should be monitored in long term trials.

It would also be possible to focus on increasing wtHTT levels in the future, as this has been shown to have beneficial effects in YAC128 mice, although it would be required to be in combination with mHTT-lowering therapeutics to fully alleviate HD phenotypes (Van Raamsdonk et al., 2006).

Future HTT-lowering therapeutics that are administered systemically to the periphery should monitor the immune system output in patients, particularly in the cases of infections etc., to ensure sufficient preservation of innate immune system function in the wtHTT-lowered condition.

Collectively, these data point to novel roles for HTT in human monocyte-derived macrophages, including in pro-inflammatory cytokine expression, phagocytosis and maintaining viability in the presence of a stressor.

5.5 Summary

In summary, wtHTT regulates the expression of pro-inflammatory cytokines and the genes encoding them following an immune challenge. A follow-up assessment of intracellular levels of these cytokines was unable to identify any changes in the wtHTT-lowered condition.

As well as this, in the wtHTT-lowered condition, viability in the presence of a stressor was lowered, and phagocytosis as assessed by *Zymosan A* and *E.coli* pHrodo beads was increased.

Finally, investigations into the intracellular signalling pathway that underlie these phenotypes showed that the NF-κB pathway was unchanged in the wtHTT-lowered condition. Future work should focus on investigating other possible mechanisms through which wtHTT-lowering causes the phenotypes described.

6 Chapter 6: Discussion & future works

This thesis demonstrates the dysfunction of CNS cells of the innate immune system in HD, and begins to investigate the impact of this dysfunction on other cell types of the CNS. This thesis also highlights a novel role for wtHTT in the peripheral innate immune system, which is likely to be applicable to the CNS immune system and is of key interest in the context of HTT-lowering trials.

6.1 A novel HD microglia model

The first aim of this thesis was to investigate the CNS component of the innate immune system, microglia, in HD. To do this, a novel human PSC-derived microglia-like cell model of HD was established. Microglia-like cells were differentiated from iPSC and ESC cohorts carrying control and HD-causing HTT polyQ lengths, using a modified version of the Van Wilgenburg et al., 2013, protocol, as described by Haenseler et al., 2017. Once expression of key microglia genes and proteins by these cells, and the purity of the cultures produced was confirmed, they were subject to a battery of functional tests, to investigate the possible differences in function between HD and control microglia-like cells. This found that HD microglia-like cells show elevated pro-inflammatory cytokine responses to an immune challenge, as well as elevated ROS production at baseline and under stimulation. A general defect in viability was also shown, with a small but significant increase in cell death with increasing HTT polyQ length under baseline conditions that became more prominent in the presence of additional cellular stressors. Unchanged by the presence of mHTT were both the phagocytic ability and the nitric oxide production of the differentiated microglia.

Previous work conducted in primary human peripheral monocytes and macrophages found that HD patients' cells *ex vivo* are hyper-reactive (Björkqvist et al., 2008), with elevated cytokine production that is reduced upon HTT-lowering (Trager et al., 2014). This phenotype was mirrored in rodent models of HD, where microglia displayed elevated cytokine production (Connolly et al., 2016; Kwan et al., 2012). Additionally, evidence of microgliosis has been found in human brain samples post mortem, and imaging studies have suggested that microglial accumulation and proliferation may be early disease events in HD, and

correlate with the elevated levels of cytokines found in the periphery (Pavese et al., 2006; Politis et al., 2011, 2015; Sapp et al., 2001; Singhrao et al., 1999; Tai et al., 2007).

The work presented herein confirmed that a similar elevated cytokine response exists in PSC-derived HD microglia-like cells, but the effect size was smaller than that seen in primary human cells or in rodent models. This may be a limitation of the experimental set up, but it does suggest that while this phenotype is present, it is less prominent in this PSC-derived microglia model. This may also be due to the relative immaturity of the microglia-like cells, which display a transcriptomic signature closer to foetal human microglia than adult microglia. As such, it may be the case that should these cells be aged considerably, a greater effect could be found.

There was a clear HD-related effect on ROS production that was replicated across both iPSC and ESC cohorts, under baseline and stimulated conditions, which is in keeping with previous work on the effect of mHTT expression in cell lines (Wyttenbach et al., 2002) and suggests this is part of a HD phenotype in the immune system. It would be interesting to follow up this result with an *in vivo* investigation in microglia from a HD rodent model, or in primary human macrophages. One might have expected elevated NO species production or phagocytosis following LPS stimulation in this model which was not found, and there was no HD effect in either function. In this way, this model does not recapitulate all aspects of HD pathology.

In the future, there are a number of areas that would be of significant interest to investigate using this model. Firstly, it would be interesting to assess the impact of immune system stimulants that might be more (patho)physiologically relevant than LPS, such as MMP3 and MMP9. MMP3 and MMP9 have been shown to be elevated in HD CSF, and HD rodent microglia have been found to be hyper-reactive in response to MMP3 (Connolly et al., 2016). Another avenue for stimulation would be to prime the microglia with IFNγ, or a low dose of LPS, ahead of high dose LPS stimulation, rather than simultaneous addition of IFNγ and LPS, as was done in this thesis. These priming methods do not activate the cells in the classical sense, but prepare them for later stimulation through transcriptional changes, resulting in larger responses to future stimulation (Da Silva et al., 2015).

This would allow examination of the effects of priming, and whether those pathways affected, are altered in HD. Another area of interest would be to assess the migratory capacity of the HD microglia-like cells in this model, as this has been assessed previously in primary HD macrophages and HD rodent microglia (Kwan et al., 2012). This was initially attempted in the characterisation of this HD microglia-like cell model, but the Boyden chamber assay preferred by previous work was found to be unreliable, with a lack of reproducibility between experiments.

Beyond these observational assessments, it would be of interest to assess the underlying mechanism through which mHTT has these effects on microglial function. Specifically, it would be interesting to conduct RNAseq on HD and control microglia under baseline and stimulated conditions. Those data could be assessed using the gene set enrichment analysis (GSEA) method to isolate areas of enriched differential expression among functional gene sets corresponding to biological pathways (Subramanian et al., 2005). This could be accompanied by upstream regulator analysis to identify any upstream regulators of the transcriptional changes seen in the data set. A candidate pathway is the NF-κB pathway, which has been shown to be altered in HD in a number of different models (Crotti et al., 2014; Trager et al., 2014). This could be assessed in follow up studies as described here, through assessment of RELA translocation. Additionally, a series of directed experiments on the NF-κB pathway could be done, using inhibitors or targeted knock out of specific intermediates in the pathway to identify how mHTT may be interacting with the pathway.

This novel model allows *in vitro* assessment of human HD microglia-like cells, at a large scale, for the first time. The benefits of using this human PSC-derived model are numerous. In theory, PSCs can provide a limitless supply of starting material, allowing continued production of a large number of microglia-like cells, as and when they are needed for experiments. Compare this to primary human HD microglia, which generally can only be collected post-mortem and in small numbers, significantly compromising the range of experiments that can be conducted into microglial function in HD. As well as this, the expression level and HTT polyQ lengths tested are similar those found in human disease, both juvenile

and adult onset, rather than the very large expansions and elevated expression levels which can be found in rodent models. Additionally, the rodent immune system, while similar in many ways to the human immune system, has some crucial differences, such that investigations in human models are much needed (Smith and Dragunow, 2014). This work showcases the benefit, and indeed requirement of, using isogenic series over a related series of HD lines, to assess HD in particular, given the variability of results in some experiments using the HD family lines. It has been previously shown that results using non-isogenic lines may be confounded by other genetic variables (Germain and Testa, 2017), and as such, large numbers of lines should be used to determine if an effect is real. Isogenic lines allow for the more confident conclusion that results found are due to the HTT polyQ length alone, although ideally at least two isogenic series would be used, rather than one as is used in this thesis. However, a large study has recently shown that when two iPSC lines were differentiated to neurons in multiple labs, the greatest source of variability found was attributed to which host lab the cells were differentiated in (Volpato et al., 2018). This is important to consider and control for if this model is to be used more widely.

There are some broader caveats to the use of this model. Firstly, the assessment of these microglia-like cells in isolation, in very pure cultures, as described in Chapter 3, is not truly representative of microglia in the brain. *In vivo*, microglia are highly reactive cells, consistently surveying their environment, and interacting with neighbouring cells (Nimmerjahn et al., 2005). In this way, it is necessary to assess the impact of other cell types on microglial function in HD. Future studies in HD should focus on co-culture paradigms, using isogenic PSC lines, with sufficient replication to account for variability between differentiations. Nevertheless, this microglial-like cell monoculture model will remain useful for testing for intrinsic effects of mHTT in microglia, as the purity of the cultures makes for simpler experimental design and read-outs.

6.2 The influence of HD microglia-like cells and MSNs on each other

In order to assess the impact of microglia-like cells on neuronal cultures, and vice versa, a series of conditioned media experimental paradigms were established. To begin, the impact of a control or HD neuronal environment on control or HD

microglia was assessed. Firstly, using conditioned media from untreated and heat-shock treated human PSC-derived MSN cultures, following by an assessment using control and HD CSF as a proxy for a neuronal environment. In this way, it was found that MSN conditioned media collected from heat-shock treated cultures was significantly more toxic for microglia-like cells than baseline MSN conditioned media. This was most apparent in the heat shock treated HTT 81Q MSN conditioned media, where it seemed that the expanded HTT polyQ length, combined with heat treatment, resulted in the most toxic effects on microglia of all genotypes. Future work could involve an unbiased assessment of these MSN-conditioned media to identify active compounds that could contribute to changes in microglial viability. There are a number of candidates specific to HD, based on previous studies. For example MMP3 and MMP9 have both been shown to be elevated in HD patient CSF, and are capable of activating microglia (Connolly et al., 2016). IL-34 release from HD neurons has also been shown to be elevated compared to controls (Khoshnan et al., 2017), which would encourage proliferation of microglia. Microglia also express a wide variety of receptors for neurotransmitters, which alter microglial activation in a variety of ways, although generally resulting in dampening down of inflammatory responses (Biber et al., 2007; Pocock et al., 2016). However, there are a few notable exceptions. Glutamate, for example, has been shown to increase TNF release from microglia (Noda et al., 2000; Taylor and Feng, 1991), and serotonin has been shown to result in elevated IL-6 release (Mahé et al., 2005). MSNs do not produce either glutamate or serotonin themselves, however the striatum does receive glutamatergic inputs from the cortex (Paraskevopoulou et al., 2019). It is also worth noting that the MSN cultures that media was collected from were mixed cultures with approximately 15% MSNs, with the remainder other neuronal cell types, so may be better referred to as neuronal cultures enriched for MSNs, but were referred to as MSN cultures for brevity in this thesis. It may be that the effects seen are not due to MSNs particularly, but rather the general neuronal environment. It might also be the case that microglia become activated in the presence of HTT aggregates in the HD brain, as is the case in AD and PD (Bertram et al., 2008; Butovsky et al., 2005; Guerreiro et al., 2012; Hollingworth et al., 2011; Jonsson et al., 2013; Lambert et al., 2013, 2009; Naj et al., 2011; Zhang et al., 2005) although there has been very little direct evidence of this

occurring in HD (Kraft et al., 2012). In this work there has been no consistent evidence of HTT aggregate formation in HD neuronal cultures, so this is unlikely to be causing microglial activation in this context. However, future studies should look to investigate whether soluble HTT is present in these cultures.

This work was followed by an assessment of the impact of HD CSF on microglial health and function, as a proxy for a neuronal environment, in the context of actual patient samples. Interestingly, there was no significant difference in viability or ROS production between HTT 30Q and 81Q microglia in the presence of either control or HD CSF. There was however, a significant difference in ROS production between HTT 30Q and 81Q microglia when treated with TBHP, an oxidative stress inducer. This suggests that a difference in ROS production between control and HD lines does exist, but that CSF insufficiently induces ROS production to reveal this. The only significant difference that was found following CSF treatment was in Caspase 3 staining, which was found to be highest in HTT 30Q microglia treated with HD CSF, compared to 81Q microglia in either HD or control CSF treatment groups. This suggests reduced microglial activation in the 81Q microglia, which is surprising. However, given the percentages of activated microglia remain low in all conditions, this difference may not be physiologically relevant.

The lack of differences seen between samples treated with control or HD CSF may be due to the fact that the CSF used in this study was collected from the spinal cord, and as such contains substrates from all areas of the brain, mixed together. In this way, regional differences in particular toxins, growth factors and cellular debris may be diluted out. For example, in HD brains one might expect to find higher concentrations of toxic substrates around the striatum, than in a less affected region, such as the cerebellum. However, that being said, it was previously shown that a number of possible activating signals are significantly elevated in CSF samples from HD patients collected in this way, such as MMP3 and MMP9, as well as neurofilament light, a marker of axonal damage (Lauren M Byrne et al., 2018b; Connolly et al., 2016). In future experiments it would be prudent to assess the levels of these molecules in the CSF samples to be used, and correlate the results in the microglial-like cells back to these levels. In these experiments however, it is likely that the time frame was insufficient to cause

changes in the microglial populations, rather than a lack of significant levels of toxins and activating substrates or significant differences in levels between control and HD CSF samples.

It would also be interesting to look at the baseline and stimulated cytokine profile of microglia-like cells following treatment with MSN-conditioned media, or CSF, to assess whether a neuronal environment has a dampening effect on pro-inflammatory cytokine expression, as has been previously reported (Haenseler et al., 2017), and if this effect is maintained in HD neuronal environments. In this way, it would possible to assess the contribution of microglia to the cytotoxic environment of the brain in HD, in a physiologically relevant context.

To complete this work, the effect of HD microglia-like cell-conditioned media on PSC-derived MSN-enriched cultures was assessed. This was done by treating MSN-enriched cultures of varying HTT polyQ lengths with conditioned media from PSC-derived microglia of varying HTT polyQ lengths, collected under baseline conditions and following immune stimulation to induce cytokine release. This investigation revealed no significant differences caused by the different conditioned media treatments used. This lack of effect may be due to the limited time course of the experiments. Alternatively, it may be that substrates in the conditioned media that might impact MSN health were present at concentrations too low to cause an effect. Given the impact of MSN conditioned-media on microglia-like cell cultures seen in this work, it is also plausible that microglia in the CNS require activating signals from neurons to become toxic to surrounding cells. It may also be the case that microglia require the presence of additional cell types, such as astrocytes, to amplify their effects and cause neuronal toxicity.

This work did reveal, however, a significant effect of MSN genotype, particularly on the prevalence of H2AX staining, a marker of double strand DNA breaks, which was found to be reduced in the HD PSC-derived MSN cultures relative to the control line. This is in keeping with previous studies in HD fibroblasts , which also showed a significant increase in unrepaired DSBs 24 h after irradiation treatment (Ferlazzo et al., 2014). This is interesting in the context of HD, where genetic variation in DNA repair genes have been shown to significantly affect age at onset (Hensman Moss et al., 2017) and it has been suggested that the HTT

polyQ expansion itself exacerbates DNA repair defects (Massey and Jones, 2018).

Future work should focus on interrogating which neuronal subtypes show reduced H2AX staining, and whether prolonged exposure to HD microglia-like cell-conditioned media affects H2AX staining and DNA damage levels more generally, looking at single strand breaks and levels of PARylation (PolyADP-ribosylation). Additionally, it would be of interest to look at whether microglia-conditioned media influences BDNF release, which is known to be reduced in HD (Gauthier et al., 2004), or IL-34 release, a stimulant of microglial proliferation that is known to be released at elevated levels when neurons are under stress (Khoshnan et al., 2017).

Longer term, it would be of interest to improve this model of microglial and neuronal interactions in HD. For example, conducting shared-media, or direct-contact experiments with microglia and MSNs from control and HD backgrounds. This would be particularly physiologically relevant, as it would allow for bidirectional signalling, and the greater effects of any released substrates through closer proximity between the cell types. This has been achieved in other diseases using rodent models (Adams et al., 2015; Gresa-Arribas et al., 2012; Park et al., 2001) and PSC-derived cells (Haenseler et al., 2017), but has not yet been applied to HD. Such models would be more physiologically relevant, but it would be more difficult to tease out cause and effect in that context. For example, the read-outs of cellular health would be more complicated, with supernatant-based assays less useful and immunofluorescence required to establish cellular identity in each measurement.

The impact of other glial cells, such as astrocytes, would also be interesting to explore but would require the establishment of a robust astrocyte and/or oligodendrocyte differentiation protocols in an HD context and appropriate methods to isolate the contributions of each cell type to phenotypes found. A number of protocols exist for the co-culture of neurons with astrocytes, but are exclusively in rodent models (Park et al., 2001; Roqué and Costa, 2017; Wei et al., 2019).

Another avenue to explore would be the emerging possibility of three-dimensional cultures, using scaffolds or organoids (Brownjohn et al., 2018; Krencik et al.,

2017; Schwartz et al., 2015), to bring together multiple cell types, which could be used, once more established, to confirm results found in the present more tractable two-dimensional culture system. Three-dimensional cultures are more physiologically relevant, however, as the system is more complex, naturally there is increased variability between experiments. As well as this, it would be difficult to assess cause and effect between different cell types, and observations would be confined to imaging and whole systems level molecular analyses. Therefore, the conditioned media co-culture paradigms described here could be used for initial assessments of pharmacological interventions targeting mHTT, the innate immune system and mechanisms of DNA damage, ahead of follow up studies in direct co-culture systems and then *in vivo*.

In this way, these iPSC and ESC-derived models may begin to be used to answer the key question of whether the immune system is important in HD pathogenesis, which has not been achieved in this thesis.

6.3 A novel function of wild type HTT in the innate immune system

The second aim of this thesis was to assess the role of wtHTT in the human peripheral innate immune system. This was achieved through the use of control primary human monocytes, isolated from whole blood samples, and differentiated into macrophages *ex vivo*. These macrophages were treated with anti-HTT siRNA to lower HTT levels or SCR siRNA as a control. Once *HTT*-lowering had been established, these macrophages were assessed using a battery of functional tests to establish which aspects of macrophage function wtHTT might have a role in. Initial work confirmed results seen by Trager et al., 2014, with cytokine release following stimulation reduced in the wtHTT-lowered condition. This was followed by an investigation into the source of the reduced cytokines, first looking at the mRNA level and finding a similar level of reduction there, and secondly looking at intracellular levels of cytokines at 24 h, to see if a deficit in trafficking and release was also a partial cause. While the experimental set up in this work failed to find a deficit in release, a more focused assessment on members of the intracellular trafficking machinery and secretory vesicles would clarify wtHTT's role in that regard. Finally, to assess a possible mechanism through with wtHTT-lowering exerted these effects on mRNA transcription and

cytokine release, the activity of the NF-κB pathway under wtHTT-lowered conditions was assessed. Interestingly, it was found to be unchanged. This is particularly surprising given the altered NF-κB pathway activity seen in HD, and the established interaction between HTT and IKKγ and IKKαβ (Trager et al., 2014). However, it may be the case that wtHTT's function in cytokine expression is partially via other pathways than those aberrantly activated by mHTT.

This work is particularly interesting in the context of HTT-lowering trials for the treatment of HD. Currently, the most advanced clinical trials for HTT-lowering are of non-allele-specific lowering methods, so that wtHTT is lowered along with mHTT. The theory behind this is that the benefits of lowering the toxic mHTT species levels outweigh the negatives of lowering wtHTT. Current literature would support this theory, as numerous animal models have shown no adverse effects due to wtHTT-lowering, though some have lowered levels less than 50% (Boudreau et al., 2009; Grondin et al., 2012; McBride et al., 2011).

It is clear from my work, that wtHTT-lowering might affect the function of innate immune cells, for example lowering cytokine production and release. However, given the elevated cytokine levels in the presence of mHTT in HD, a reduction in cytokine expression is most likely to be beneficial to patients and is unlikely to drop to levels below what is found in non-HD individuals. Indeed, 7 months of HTT-lowering in HD patients has not resulted in any adverse immune reactions to date (Tabrizi et al., 2019). In the future, methods to artificially increase wtHTT levels in these patients could be investigated to mitigate any possible negative effects of reduced wtHTT, should that be deemed necessary.

Allele-specific HTT-lowering is also being investigated pre-clinically, but a number of technical difficulties will need to be overcome to scale up treatment to the clinic. For example, a method known as SNP linkage by circularization (W. Liu et al., 2008), can be used to effectively identify which allele specific SNPs are on, to ensure that the disease allele is selectively lowered. However, this method is very technically challenging and labour intensive, and as such would require optimisation for use at a clinical scale. Additionally, there is not a single SNP associated with the mHTT allele that can be targeted in all patients. In fact, a number of studies have investigated the number of SNPs and corresponding siRNAs that would be required to treat the majority of the HD population in the

EU and USA and found that a repertoire of five to seven allele specific siRNAs could treat 75-85.6% of patients in the US and Europe, respectively (Lombardi et al., 2009; Pfister et al., 2009). In this way, changes to the drug approval landscape might be required to allow testing of multiple siRNAs, targeting different SNPs, at once, to make the endeavour financially viable for pharmaceutical companies.

More generally, beyond HD, it seems that wtHTT has a previously undescribed role in cytokine production by monocytes and macrophages, whereby the relative level of wtHTT expression correlates with the levels cytokine expression in these cells. This fits with what has been found in control subjects as part of HD-focused studies, where wtHTT-lowering results in reduced cytokine expression (Träger et al., 2014). From the literature it appears that HTT's many interactions with components of the intracellular trafficking pathways may underlie this effect, as cytokine release relies on a number of different mechanisms of trafficking and release (Lacy and Stow, 2011). As well as this, this thesis has shown that wtHTT-lowering also reduces expression of cytokines at the mRNA level, suggesting a role of wtHTT in the induction of cytokine transcription, perhaps through interactions with important transcription factors.

It would be of interest to study in the population generally whether levels of wtHTT expression in PBMCs correlate to the levels of cytokine expression in those cells. In both measures, previous studies have found huge variability between control individuals and even within an individual when multiple samples are taken (Weiss et al., 2012). Interestingly, HD patients show increasing accumulation of mHTT in their immune cells as the disease progresses, and an increase in pro-inflammatory cytokines is also found with increasing disease stage (Björkqvist et al., 2008; Weiss et al., 2012). This may not be directly correlated, and in fact in HD, it may be that separate disease processes result in the elevated levels of inflammatory cytokines. However, it would be interesting to look at this correlation directly, and in healthy individuals, to assess if there is a general link between wtHTT expression levels and inflammatory cytokine production. If a link is established, causation can be investigated and the possibility of targeting wtHTT for the treatment of immune disorders can be assessed.

In theory, wtHTT-lowering could be a potential method of immunosuppression in diseases such as rheumatoid arthritis. This would be an attractive prospect, as long term use of current treatments are associated effects such as increased risk of infection, malignant cancers, cardiovascular disease and bone marrow suppression resulting in osteoporosis (Hsu and Katelaris, 2009). ASO-mediated wtHTT-lowering for example, is unlikely to have as large an effect as corticosteroids, given that only the innate immune system has been shown to be affected thus far and therefore may be a good alternative.

Future works should focus on uncovering which pathways are affected by wtHTT-lowering. This might be achieved by conducting a thorough RNAseq investigation, looking at baseline and under stimulated conditions in wtHTT-lowered macrophages to identify altered pathways. Altered pathways could be identified using bioinformatic tools such as pathway analyses. RNAseq candidates could then be confirmed with follow up assessments at the protein level, for example, using co-precipitation to assess protein-protein interactions or chromatin immunoprecipitation to assess DNA-protein interactions. Several candidate signalling pathways exist based on what is known of the intracellular signalling pathways following immune stimulation. For example, p38-MAPK or ERK pathways are known to be important for immune cell activation.

Longer term, it would be interesting to conduct *in vivo* experiments in rodent models, where the expression of wtHTT in the immune system could be easily manipulated. For example, via conditional knockout of wtHTT in the immune system specifically to varying degrees, followed by immune stimulation. The cytokine expression levels in the plasma and CSF could then be assessed, coupled with *ex vivo* assessment of myeloid cells, to assess the impact of wtHTT-lowering in this context, and see if there is a replication of the results found in this thesis.

6.4 The innate immune system as a modifier of HD

Taken together, the evidence from this thesis suggests that while the innate immune system is dysfunctional in HD in certain aspects, in the co-culture model presented here this was insufficient to effect neuronal health. While there are caveats to the experimental set up in the model, these results in isolation suggest that the innate immune system is unlikely to be a major modifier of HD onset and

progression. This fits with what has been seen in clinical trials, with the failure of immune system focussed therapeutics for HD, such as minocycline and laquinomod (Cudkowicz, 2010; Kieburtz et al., 2018). However, this may be part of a more generalised failure to translate therapeutics that are effective in HD animal models to the clinic.

As well as this, a recent GWAS failed to highlight any genetic modifiers in HD that relate to the immune system, where similar studies in AD identified a plethora of immune system related genes (Jones et al., 2010; Lambert et al., 2010; Liu et al., 2018). Instead, genes related to DNA repair pathways were highlighted (Hensman Moss et al., 2017; J. M. Lee et al., 2015; Lee et al., 2019). Related to this, it may be the case that chronic inflammation impacts the levels of DNA damage seen in HD, through elevated levels oxidative stress. This is plausible given the results seen in H2AX staining in LPS-stimulated media in this work.

Despite the previous failures of immune focused therapeutics, there remain several promising immune system targets that have been shown to be effective in rodent models. For example, CB2 cannabinoid receptors are expressed in microglia and their peripheral counterparts and their activation is anti-inflammatory. A CB2 agonist caused suppression of motor deficits and CNS inflammation in transgenic mice, whilst extending their life span (Bouchard et al., 2012). A pilot trial has also been completed in HD patients using Sativex, a botanical extract with an equimolecular combination of delta-9-tetrahydrocannabinol and cannabidiol, which was found to be tolerated and safe, but not effective against disease phenotypes at the dose given (López-Sendón Moreno et al., 2016). Future studies will look at increased dosage and extended treatment periods, in an attempt to match the results seen in HD mice (Valdeolivas et al., 2017). Additionally, manipulating the KMO pathway of tryptophan degradation in peripheral immune cells results in extended lifespan of HD mice, with prevention of synaptic loss and a reduction in microglial activation (Zwilling et al., 2011). More recent studies have also highlighted the neuroprotective effects of KMO pathway inhibitors in HD *Drosophila* (Zhang et al., 2019).

Finally, it could be the case that while the chronic elevation of cytokine levels in patient plasma may not affect disease onset or progression, it may still impact

patients' quality of life. For example, there is extensive evidence supporting the emergence of sickness behaviour in individuals with elevated cytokine levels (Dantzer et al., 2008). It may be the case that some of the symptoms that HD patients present with, such as depression and irritability, are linked to this underlying immune phenotype. Therefore, it remains of interest to assess the impact of immunosuppression on phenotypes related to sickness behaviour, with the possibility of having a profound impact on patients' quality of life.

Appendices

Appendix 1

Table A1.1 Perkin Elmer Columbus software parameters used for the unbiased analysis of each immunofluorescence imaging metric in the study.

Cell feature	Columbus building block	Specifics	Method	Output name
Nuclei	Find Nuclei	Channel: HOECHST 33342 Region: None	Method: M Diameter: 15 µm Splitting coefficient: 0.4 Common threshold: 0.1	Population: Nuclei
	Calculate Intensity Properties	Channel: HOECHST 33342 Population: Nuclei Region: Nucleus	Method: Standard, mean	Properties: Intensity nuclear HOECHST 33342
	Calculate Morphology Properties	Population: Nuclei Region: Nucleus	Method: Standard, area, roundness	Properties: Nucleus morphology
	Select Population	Population: Nuclei	Method: Filter by property Nucleus area [µm²]: >= 40 Intensity nucleus HOECHST 33342 mean: <= 18512 Nucleus area [µm²]: <= 200 Boolean operations:	Population: Viable nuclei

			F1 and F2 and F3	
Caspase 3 +ve neurons	Find Cytoplasm	Channel: Alexa 488 Nuclei: Nuclei	Method: B Common threshold: 0.45 Individual threshold: 0.15	
	Calculate Intensity Properties	Channel: Alexa 488 Population: Nuclei Region: Cytoplasm	Method: Standard, mean	Properties: Caspase 3 cytoplasmic intensity in all cells
	Select Population	Population: Nuclei	Method: Filter by property Intensity cytoplasmic caspase 3 in all cells, mean: >= 1000	Population: Cells with cytoplasmic caspase 3 over a threshold
Caspase 3 +ve microglia	Find Cytoplasm	Channel: Alexa 488 Nuclei: Nuclei	Method: B Common threshold: 0.45 Individual threshold: 0.15	
	Calculate Intensity Properties	Channel: Alexa 568 Population: Nuclei Region: Cytoplasm	Method: Standard, mean	Properties: Caspase 3 cytoplasmic intensity in all cells

	Select Population	Population: Nuclei	Method: Filter by Property Caspase 3 cytoplasmic intensity in all cells Mean: >= 335	Population: Cells with Caspase 3 over a threshold
Nestin+ cells	Find Cells	Channel: Alexa 568 ROI: Viable nuclei ROI Region : Cell	Method: B Common threshold: 0.4 Area: > 70 µm² Split factor: 7 Individual threshold: 0.5 Contrast: > 0.3	Population: Nestin+ cells
	Find Cytoplasm	Channel: Alexa 568 Nuclei: Viable nuclei	Method: B Common threshold: 0.45 Individual threshold: 0.15	
	Calculate Intensity Properties	Channel: Alexa 568 Population: Viable nuclei Region: Cytoplasm	Method: Standard, mean	Properties: Intensity cytoplasm Alexa 568
	Select Population	Population : Viable nuclei	Method: Filter by Property Intensity cytoplasm Alexa 568, mean: >= 1500	Population: Viable nuclei with cytoplasmic Nestin over a threshold

BIII-tubulin+	Find Cytoplasm	Channel: Alexa 647 Nuclei: Viable nuclei	Method: B Common threshold: 0.45 Individual threshold: 0.15	
	Calculate Intensity Properties	Channel: Alexa 647 Population: Viable nuclei Region: Cytoplasm	Method: Standard, mean	Properties: Intensity cytoplasm Alexa 647
	Select Population	Population: Viable nuclei	Method: Filter by Property Intensity cytoplasm Alexa 647, mean: >= 1200	Population: Viable nuclei with cytoplasmic B3tubulin over a threshold
CTIP2+	Calculate Intensity Properties	Channel: Alexa 568 Population: Viable nuclei Region: Nucleus	Method: Standard, mean	Properties : Intensity nucleus Alexa 568
	Select Population	Population: Viable nuclei	Method: Filter by property Intensity nucleus Alexa 568 mean: >= 500	Population: CTIP+ cells
DARPP-32+ neurons	Find Cells	Channel: Alexa 488 Region: None	Method: B Common threshold: 0.4 Area: > 70 µm² Split Factor: 7 Individual threshold: 0.5	Population: DARPP32+ cells (Find Cells)

			Contrast: > 0.3	
	Calculate Intensity Properties	Channel: Alexa 488 Population: DARPP32+ cells (Find Cells) Region: Cell	Method: Standard, mean	Properties: Intensity of DARPP32+ cells
	Find Image Region	Channel: Alexa 488 Region: None	Method : Common threshold Threshold: 0.5 Area: > 10 µm²	Population: DARPP32+ area Region: DARPP32+ total staining
	Calculate Morphology Properties	Population: DARPP32+ area Region: DARPP32+ total staining	Method: Standard, area, roundness	Properties: DARPP32+ total staining
	Calculate Intensity Properties	Channel: Alexa 488 Population: DARPP32+ area Region: DARPP32+ total staining	Method: Standard, sum	Properties: Intensity DARPP32+ total staining
	Find Cytoplasm	Channel: Alexa 488 Nuclei: Viable nuclei	Method: B Common threshold: 0.45 Individual threshold: 0.15	
	Calculate Intensity Properties	Channel: Alexa 488 Population: Viable nuclei Region: Cell (2)	Method: Standard, mean	Properties: Intensity Cell Alexa 488
	Select Population	Population: Viable nuclei	Method: Filter by Property	Population: Viable nuclei with cytoplasmic

			Intensity Cell Alexa 488 Mean: >= 1200	DARPP32+ over a threshold
H2AX+ spots	Find Spots	Channel: Alexa 488 Region: Viable nuclei	Method: C Radius: < 5px Contrast: > 0.1 Uncorrected Spot to Region Intensity: > 1 Distance: > 3px Spot Peak Radius: 0 px Calculate Spot Properties	Population: H2AX+ spots in viable nuclei
	Select Population	Population: Viable nuclei	Method: Filter by property Number of spots: > 4	Population: Viable nuclei with >4 H2AX+ spots
	Select Population	Population: Viable nuclei	Method: Filter by property Number of Spots: > 10	Population: Viable nuclei with >10 H2AX+ spots
Tmem119+ ve cells	Calculate Intensity Properties	Channel: Alexa 568 Population: Viable nuclei Region: Nucleus	Method: Standard, mean	Properties: Intensity Nucleus Alexa 568
	Select Population	Population: Viable nuclei	Method: Filter by property Intensity Nucleus Alexa 568 Mean: >= 380	Population: Tmem119+ve viable cells (nuclear stain)
	Find Cytoplasm	Channel: Alexa 488 Nuclei: Viable Nuclei	Method: B Common Threshold: 0.45	

IBA1+ve cells			Individual Threshold: 0.15	
	Calculate Intensity Properties	Channel: Alexa 488 Population: Viable Nuclei Region: Cytoplasm	Method: Standard, mean	Properties: Intensity Cytoplasm Alexa 488
	Select Population	Population: Viable Nuclei	Method: Filter by Property Intensity Cytoplasmic Alexa 488 Mean: >= 300	Population: Viable nuclei with cytoplasmic IBA1 over a threshold
PU1+ cells	Calculate Intensity Properties	Channel: Alexa 568 Population: Viable Nuclei Region: Nucleus	Method: Standard, mean	Properties: Intensity Nucleus Alexa 568
	Select Population	Population: Viable Nuclei	Method: Filter by Property Intensity Nucleus Alexa 568 Mean: >= 380	Population: PU1+ viable nuclei
Trem2+ cells	Find Cytoplasm	Channel: Alexa 488 Nuclei: Viable nuclei	Method: B Common Threshold: 0.45 Individual Threshold: 0.15	
	Calculate Intensity Properties	Channel: Alexa 488, Population: Viable Nuclei Region: Cytoplasm	Method: Standard, mean	Properties: Intensity Cytoplasm Alexa 488
	Select Population	Population: Viable Nuclei	Method: Filter by Property	Population: Viable nuclei with cytoplasmic

			Intensity Cytoplasm Alexa 488 Mean: >= 200	Trem2+ over a threshold

Appendix 2

Table A2.1 Comparison of available Microglia Protocols in 2017

Protocol	Pandya	Muffat	Abud (Blurton-Jones)	Van Wilgenburg (Haensler)	Douvaras (new Yanagimachi)
Yield	2-3 per starting iPSC	0.5-4 per starting iPSC	30-40 per starting iPSC	10-43 per starting iPSC, and can continue for 1 year	2.24 per starting iPSC
Cost	Low o2 incubator prohibitively expensive to purchase, rest of protocol average cost	/	Low o2 incubator prohibitive, FACS sorting additional cost (main campus) Extensive growth factor list- increased cost	Growth factor list average cost	High cost of extensive growth factor list, as well as FACS sorting additional cost (main campus)
Time until harvest	29 days	2 months	39 days	21 days, to one month	45 days
Co-culture tested?	Cd39 sorted Monoculture post astro-coculture step	Briefly-transwells exposing pMGLs to neuron/astrocyte media, plus adding GFP-pMGLs to 3D neuron/astrocyte culture in transwell	With rat hippocampal neurons, and 3D ipsc brain organoids (astrocytes, oligos, neurons)	With iPSC cortical neurons-adopt a very different phenotype In corning 96, 6 well and ibidi 8 well slide (cschas)-macs sort **cd11b** beads	No
	Stemdiff	Neuro-Glial	TeSR-E8	mTeSR then X-	mTeSR Custom

Media	APEL mediu m, IMDM	Differenti ation media - formula disclose d -B27, N2, lactic acid (85% syrup stock) 200uL Sodium Pyruvate (100mM stock) 10mL glutamax (100x stock) 10mL Biotin 3.5ug lipidated BSA (Albuma x I) 2g Ascorbic Acid 2.5mg Pen/Stre p 10mL NaCl 5M 10mL Neuroba sal	1. IMDM (50%), F12 (50%), insulin (0.02 mg/ ml), holo-transferrin (0.011 mg /ml), sodium selenite (13.4 µg/ ml), ethanola mine (4 µg/ml) (can use ITSG-X, 2% v/v, Thermo Fisher Scientific) , L-ascorbic acid 2-Phosphat e magnesiu m (64 µg/ml; Sigma), monothio glycerol (400 µM), PVA (10 µg/ml; Sigma), Glutamax (1X), chemicall y-defined lipid concentra te (1X), non-essential amino acids (NEAA; 1X), Penicillin/ Streptom ycin (P/S; 1% V/V).	VIVO15 with 2 mM glutamax , 100 U/mL penicillin and 100 µg/mL streptom ycin, and 0.055 mM β-mercapto ethanol. ADMEM/ F12+ N2 supp +IL-34 and GM-CSF for co-pmg	medium (STEMCELL Technologies) 1.Containing 80 ng/mL BMP4. 2.25 ng/mL bFGF, 100 ng/mL SCF and 80 ng/mL VEGF in StemPro-34 SFM (with 2 mM GutaMAX, Life Technologies) 3. 50 ng/mL SCF, 50 ng/mL IL-3, 5 ng/mL thro mbopoietin, 50 ng/mL macrophage CSF (M-CSF) and 50 ng/m L Flt3l, and from day 14 with 50 ng/mL M-CSF, 50 ng/mL Flt3l, and 25 ng/mL GM-CSF. 4. Microglial Medium (RPMI-1640 [Life Technologies] with 2 mM GlutaMAX-I, 10 ng/mL GM-CSF, and 100 ng/mL IL-34)

			Use 0.22 µm filter. 2. Phenol-free DMEM/F12 (1:1), insulin (0.02 mg/ml), holo-transferrin (0.011 mg/ml), sodium selenite (13.4 µg/ml) (can use ITS-G, 2%v/v, Thermo Fisher Scientific), B27 (2% v/v), N2 (0.5%, v/v), monothioglycerol (200 µM), Glutamax (1X), NEAA (1X), and additional insulin (5 µg/ml; Sigma) and filtered through a 0.22 µm filter.		
Growth factors	VEGF, BMP4, SCF, Activin A, Flt3L, IL3, IL6, G-CSF, GM-CSF	IL-34, M-CSF (CSF1)	FGF2, BMP4, Activin A, LiCl, VEGF, TPO, SCF, IL3, IL6 to make iHPCS (5% and then 20% o2) then facs sort and use MCSF, IL34, TGFB1, insulin, cd200,	BMP4, SCF, VEGF, M-CSF, IL-3 Rock-inhibitor	BMP4, bFGF, SCF, VEGFA, IL-3, TPO, M-CSF, FLT-3, GM-CSF, IL-34

			cx3cl1 to make microglia		
Reproducible?	2 lines (iPSC)	20 lines (iPSC and ES)	10 lines (iPSC)	28 lines (ES and iPSC)	16 iPSC lines
O2 changes?	5% o2 for first 15 days	/	5% o2 then 20% o2 for iHPC differentiation	/	/
Key microglial gene expression?	P2RY12, GPR34, MERTK, C1QA, PROS1, GAS6	Gene level: TMEM119, MERTK, PROS1, C1QA, LAIR1, GPR34, P2RY12, TGFB1, ENTPD1, TGFBR1, SELPLG, CST3, TXNIP, OLFML3, SERINC3, CTSD, ITM2B, CD164, RGS10, ITGB5 Protein level: tmem119, iba1, p2ry12, cd45	P2RY12, GPR34, C1Q, CABLES1, BHLHE41, TREM2, ITAM PROS1, APOE, SLCO2B1, SLC7A8, PPARD, CRYBB1, RUNX1, PU.1, and CSF1R	C1QA, GAS6, GPR34, PROS1, MERTK, P2RY12, TMEM119, TREM2, CD11B, CD14, CD45, CD11C, CD33, HLA-DR	Gene: C1QA, GAS6, GPR34, MERTK, P2RY12, PROS1. Protein: IBA1, CD11c, TMEM119, and P2RY12.
ROS production?	Yes	/	/	/	/
Migration/motility/chemotaxis?	/	Yes	Yes	Yes	Yes
Cytokine production?	Yes (LPS)	Yes (LPS)	Yes (LPS)	Yes (LPS, and LPS, IFNy)	Yes (LPS)
Phagocytosis?	Yes	Yes	Yes	Yes	Yes
NO production?	/	/	/	/	/
Morphological characteristics?	/	Yes	Yes	Yes	/

Appendix 3

Table A3.1 Primary antibodies used in IF

Antibody	**Species**	**Dilution**	**Catalogue Number**	**Supplier**
IBA1 (isoforms 1 and 3)	Goat	1:500	NB100-1028	Novus Biologicals
PU1	Rabbit	1:100	#2266	Cell Signalling Technology
TREM2	Goat IgG	1:50	AF1828	R&D Systems
TMEM119	Rabbit	1:200	HPA052650	Atlas
CTIP2	Rat	1:300	Ab18465	Abcam
Caspase 3	Rabbit	1:400	#9664	Cell Signalling Technology
Darp32	Rabbit	1:200	sc11365	Santa Cruz
Tuj1/B3 Tubulin	Chicken	1:500	Ab18207	Abcam
Nestin	Mouse	1:600	MAB5326-10C2	Millipore
Gamma H2AX (phosphoS139)	Rabbit	1:200	Ab11174	Abcam

Table A3.2 Secondary antibodies used in IF

Antibody	**Supplier**
Goat anti rat 488	Life Technologies
Goat anti rabbit 488	Life Technologies
Goat anti mouse 568	Life Technologies
Goat anti chicken 647	Life Technologies
Donkey anti goat 488	Life Technologies
Donkey anti rabbit 568	Life Technologies

Appendix 4

Media compositions

Table A4.1 Composition of RPMI 1640, no glutamine Catalogue Number(s) 31870025, 31870074

Components	Molecular Weight	Concentration (mg/L)	mM
Amino Acids			
Glycine	75.0	10.0	0.13333334
L-Arginine	174.0	200.0	1.1494253
L-Asparagine	132.0	50.0	0.37878788
L-Aspartic acid	133.0	20.0	0.15037593
L-Cystine	240.0	50.0	0.20833333
L-Glutamic Acid	147.0	20.0	0.13605443
L-Histidine	155.0	15.0	0.09677419
L-Hydroxyproline	131.0	20.0	0.15267175
L-Isoleucine	131.0	50.0	0.3816794
L-Leucine	131.0	50.0	0.3816794
L-Lysine hydrochloride	146.0	40.0	0.2739726
L-Methionine	149.0	15.0	0.10067114
L-Phenylalanine	165.0	15.0	0.09090909
L-Proline	115.0	20.0	0.17391305
L-Serine	105.0	30.0	0.2857143
L-Threonine	119.0	20.0	0.16806723
L-Tryptophan	204.0	5.0	0.024509804
L-Tyrosine	181.0	20.0	0.110497236
L-Valine	117.0	20.0	0.17094018
Vitamins			
Biotin	244.0	0.2	8.1967213E-4
Choline chloride	140.0	3.0	0.021428572
D-Calcium pantothenate	477.0	0.25	5.24109E-4
Folic Acid	441.0	1.0	0.0022675737

Niacinamide	122.0	1.0	0.008196721
Para-Aminobenzoic Acid	137.0	1.0	0.00729927
Pyridoxine hydrochloride	206.0	1.0	0.004854369
Riboflavin	376.0	0.2	5.319149E-4
Thiamine hydrochloride	337.0	1.0	0.002967359
Vitamin B12	1355.0	0.005	3.690037E-6
i-Inositol	180.0	35.0	0.19444445
Inorganic Salts			
Calcium nitrate (Ca(NO3)2 4H2O)	236.0	100.0	0.42372882
Magnesium Sulfate (MgSO4-7H2O)	246.0	100.0	0.40650406
Potassium Chloride (KCl)	75.0	400.0	5.3333335
Sodium Bicarbonate (NaHCO3)	84.0	2000.0	23.809525
Sodium Chloride (NaCl)	58.0	6000.0	103.44827
Sodium Phosphate dibasic (Na2HPO4) anhydrous	142.0	800.0	5.633803
Other Components			
D-Glucose (Dextrose)	180.0	2000.0	11.111111
Glutathione (reduced)	307.0	1.0	0.0032573289
Phenol Red	376.4	5.0	0.013283741

Table A4.2 Composition of DMEM/F-12, no glutamine, no HEPES. Catalogue Number(s) 21331020

Components	**Molecular Weight**	**Concentration (mg/L)**	**mM**
Amino Acids			
Glycine	75.0	18.75	0.25
L-Alanine	89.0	4.45	0.049999997
L-Arginine hydrochloride	211.0	147.5	0.69905216
L-Asparagine-H2O	150.0	7.5	0.05
L-Aspartic acid	133.0	6.65	0.05
L-Cysteine hydrochloride-H2O	176.0	17.56	0.09977272
L-Cystine 2HCl	313.0	31.29	0.09996805
L-Glutamic Acid	147.0	7.35	0.05
L-Histidine hydrochloride-H2O	210.0	31.48	0.14990476
L-Isoleucine	131.0	54.47	0.41580153
L-Leucine	131.0	59.05	0.45076334
L-Lysine hydrochloride	183.0	91.25	0.4986339
L-Methionine	149.0	17.24	0.11570469
L-Phenylalanine	165.0	35.48	0.2150303
L-Proline	115.0	17.25	0.15
L-Serine	105.0	26.25	0.25
L-Threonine	119.0	53.45	0.44915968
L-Tryptophan	204.0	9.02	0.04421569
L-Tyrosine disodium salt dihydrate	261.0	55.79	0.21375479
L-Valine	117.0	25.85	0.22094017
Vitamins			
Biotin	244.0	0.0035	1.4344263E-5
Choline chloride	140.0	8.98	0.06414285
D-Calcium pantothenate	477.0	2.24	0.0046960167
Folic Acid	441.0	2.65	0.0060090707

Niacinamide	122.0	2.02	0.016557377
Pyridoxine hydrochloride	206.0	2.0	0.009708738
Riboflavin	376.0	0.219	5.824468E-4
Thiamine hydrochloride	337.0	2.17	0.0064391694
Vitamin B12	1355.0	0.68	5.0184503E-4
i-Inositol	180.0	12.6	0.07
Inorganic Salts			
Calcium Chloride (CaCl2) (anhyd.)	111.0	116.6	1.0504504
Cupric sulfate (CuSO4-5H2O)	250.0	0.0013	5.2E-6
Ferric Nitrate (Fe(NO3)3"9H2O)	404.0	0.05	1.2376238E-4
Ferric sulfate (FeSO4-7H2O)	278.0	0.417	0.0015
Magnesium Chloride (anhydrous)	95.0	28.64	0.30147368
Magnesium Sulfate (MgSO4) (anhyd.)	120.0	48.84	0.407
Potassium Chloride (KCl)	75.0	311.8	4.1573334
Sodium Bicarbonate (NaHCO3)	84.0	1200.0	14.285714
Sodium Chloride (NaCl)	58.0	6995.5	120.61207
Sodium Phosphate dibasic (Na2HPO4) anhydrous	142.0	71.02	0.50014085
Sodium Phosphate monobasic (NaH2PO4-H2O)	138.0	62.5	0.45289856
Zinc sulfate (ZnSO4-7H2O)	288.0	0.432	0.0015
Other Components			
D-Glucose (Dextrose)	180.0	3151.0	17.505556
Hypoxanthine Na	159.0	2.39	0.015031448
Linoleic Acid	280.0	0.042	1.4999999E-4
Lipoic Acid	206.0	0.105	5.097087E-4

Phenol Red	376.4	8.1	0.021519661
Putrescine 2HCl	161.0	0.081	5.031056E-4
Sodium Pyruvate	110.0	55.0	0.5
Thymidine	242.0	0.365	0.0015082645

Table A4.3 Composition of NEUROBASAL™ Medium (1X) liquid. Catalogue Number(s) 21103049

Components	**Molecular Weight**	**Concentration (mg/L)**	**mM**
Amino Acids			
Glycine	75.0	30.0	0.4
L-Alanine	89.0	2.0	0.02247191
L-Arginine hydrochloride	211.0	84.0	0.39810428
L-Asparagine-H2O	150.0	0.83	0.0055333334
L-Cysteine	121.0	31.5	0.2603306
L-Histidine hydrochloride-H2O	210.0	42.0	0.2
L-Isoleucine	131.0	105.0	0.8015267
L-Leucine	131.0	105.0	0.8015267
L-Lysine hydrochloride	183.0	146.0	0.7978142
L-Methionine	149.0	30.0	0.20134228
L-Phenylalanine	165.0	66.0	0.4
L-Proline	115.0	7.76	0.06747826
L-Serine	105.0	42.0	0.4
L-Threonine	119.0	95.0	0.79831934
L-Tryptophan	204.0	16.0	0.078431375
L-Tyrosine	181.0	72.0	0.39779004
L-Valine	117.0	94.0	0.8034188
Vitamins			
Choline chloride	140.0	4.0	0.028571429
D-Calcium pantothenate	477.0	4.0	0.008385744
Folic Acid	441.0	4.0	0.009070295
Niacinamide	122.0	4.0	0.032786883
Pyridoxal hydrochloride	204.0	4.0	0.019607844
Riboflavin	376.0	0.4	0.0010638298
Thiamine hydrochloride	337.0	4.0	0.011869436
Vitamin B12	1355.0	0.0068	5.0184503E-6

i-Inositol	180.0	7.2	0.04
Inorganic Salts			
Calcium Chloride (CaCl2) (anhyd.)	111.0	200.0	1.8018018
Ferric Nitrate (Fe(NO3)3"9H2O)	404.0	0.1	2.4752476E-4
Magnesium Chloride (anhydrous)	95.0	77.3	0.8136842
Potassium Chloride (KCl)	75.0	400.0	5.3333335
Sodium Bicarbonate (NaHCO3)	84.0	2200.0	26.190475
Sodium Chloride (NaCl)	58.0	3000.0	51.724136
Sodium Phosphate monobasic (NaH2PO4-H2O)	138.0	125.0	0.9057971
Zinc sulfate (ZnSO4-7H2O)	288.0	0.194	6.736111E-4
Other Components			
D-Glucose (Dextrose)	180.0	4500.0	25.0
HEPES	238.0	2600.0	10.92437
Phenol Red	376.4	8.1	0.021519661
Sodium Pyruvate	110.0	25.0	0.22727273

Composition proprietary and therefore not available:

Media:

Essential 8

StemPro 34

Supplements:

N2

B27

Appendix 5

Table A5.1 Details of CSF samples used

CSF experiment				
Subject Group	N	Age (mean +/- SD)	CAG (mean +/- SD)	Sex
Control	10	54.777 +/- 12.85466	n/a	3 female, 7 male
HD	10	56.4840522 +/- 5.541302	42.7 +/- 1.888562	5 female, 5 male

References

Aarum, J., Sandberg, K., Haeberlein, S.L.B., Persson, M.A.A., 2003. Migration and differentiation of neural precursor cells can be directed by microglia. Proc. Natl. Acad. Sci. U. S. A. 100, 15983–15988. https://doi.org/10.1073/pnas.2237050100

Abud, E.M., Ramirez, R.N., Martinez, E.S., Healy, L.M., Nguyen, C.H.H., Newman, S.A., Yeromin, A. V., Scarfone, V.M., Marsh, S.E., Fimbres, C., Caraway, C.A., Fote, G.M., Madany, A.M., Agrawal, A., Kayed, R., Gylys, K.H., Cahalan, M.D., Cummings, B.J., Antel, J.P., Mortazavi, A., Carson, M.J., Poon, W.W., Blurton-Jones, M., 2017. iPSC-Derived Human Microglia-like Cells to Study Neurological Diseases. Neuron 94, 278-293.e9. https://doi.org/10.1016/j.neuron.2017.03.042

Adams, A.C., Kyle, M., Beaman-Hall, C.M., Monaco, E.A., Cullen, M., Vallano, M. Lou, 2015. Microglia in Glia–Neuron Co-cultures Exhibit Robust Phagocytic Activity Without Concomitant Inflammation or Cytotoxicity. Cell. Mol. Neurobiol. 35, 961–975. https://doi.org/10.1007/s10571-015-0191-9

Aiken, C.T., Tobin, A.J., Schweitzer, E.S., 2004. A cell-based screen for drugs to treat Huntington's disease. Neurobiol. Dis. 16, 546–555. https://doi.org/10.1016/J.NBD.2004.04.001

Alberts B, Johnson A, Lewis J, et al., 2002. Molecular Biology of the Cell, 4th ed, Garland Science. New York.

An, M.C., O'Brien, R.N., Zhang, N., Patra, B.N., De La Cruz, M., Ray, A., Ellerby, L.M., 2014. Polyglutamine Disease Modeling: Epitope Based Screen for Homologous Recombination using CRISPR/Cas9 System. PLoS Curr. 6, 1–19. https://doi.org/10.1371/currents.hd.0242d2e7ad72225efa72f6964589369a

Anne, S.L., Saudou, F., Humbert, S., 2007. Phosphorylation of Huntingtin by Cyclin-Dependent Kinase 5 Is Induced by DNA Damage and Regulates Wild-Type and Mutant Huntingtin Toxicity in Neurons. J. Neurosci. 27, 7318–7328. https://doi.org/10.1523/jneurosci.1831-07.2007

Arber, C., Precious, S. V, Cambray, S., Risner-Janiczek, J.R., Kelly, C., Noakes, Z., Fjodorova, M., Heuer, A., Ungless, M.A., Rodríguez, T.A., Rosser, A.E., Dunnett, S.B., Li, M., 2015. Activin A directs striatal projection neuron differentiation of human pluripotent stem cells. Development 142, 1375–86. https://doi.org/10.1242/dev.117093

Arrasate, M., Mitra, S., Schweitzer, E.S., Segal, M.R., Finkbeiner, S., 2004. Inclusion body formation reduces levels of mutant huntingtin and the risk of neuronal death. Nature 431, 805–10. https://doi.org/10.1038/nature02998

Auffray, C., Sieweke, M.H., Geissmann, F., 2009. Blood monocytes: development, heterogeneity, and relationship with dendritic cells. Annu. Rev. Immunol. 27, 669–92. https://doi.org/10.1146/annurev.immunol.021908.132557

Aung, H.T., Schroder, K., Himes, S.R., Brion, K., van Zuylen, W., Trieu, A., Suzuki, H., Hayashizaki, Y., Hume, D.A., Sweet, M.J., Ravasi, T., 2006. LPS regulates proinflammatory gene expression in macrophages by altering histone deacetylase expression. FASEB J. 20, 1315–1327. https://doi.org/10.1096/fj.05-5360com

Bain, C.C., Bravo-Blas, A., Scott, C.L., Gomez Perdiguero, E., Geissmann, F.,

Henri, S., Malissen, B., Osborne, L.C., Artis, D., Mowat, A.M., 2014. Constant replenishment from circulating monocytes maintains the macrophage pool in the intestine of adult mice. Nat. Immunol. 15, 929–37. https://doi.org/10.1038/ni.2967

Bar-Nur, O., Russ, H.A., Efrat, S., Benvenisty, N., 2011. Epigenetic Memory and Preferential Lineage-Specific Differentiation in Induced Pluripotent Stem Cells Derived from Human Pancreatic Islet Beta Cells. Cell Stem Cell 9, 17–23. https://doi.org/10.1016/j.stem.2011.06.007

Barnat, M., Le Friec, J., Benstaali, C., Humbert, S., 2017. Huntingtin-Mediated Multipolar-Bipolar Transition of Newborn Cortical Neurons Is Critical for Their Postnatal Neuronal Morphology. Neuron 93, 99–114. https://doi.org/10.1016/j.neuron.2016.11.035

Bates, G., 2003. Huntingtin aggregation and toxicity in Huntington's disease. Lancet. https://doi.org/10.1016/S0140-6736(03)13304-1

Bates, G.P., Dorsey, R., Gusella, J.F., Hayden, M.R., Kay, C., Leavitt, B.R., Nance, M., Ross, C. a., Scahill, R.I., Wetzel, R., Wild, E.J., Tabrizi, S.J., 2015. Huntington disease. Nat. Rev. Dis. Prim. 15005. https://doi.org/10.1038/nrdp.2015.5

Baxa, M., Hruska-Plochan, M., Juhas, S., Vodicka, P., Pavlok, A., Juhasova, J., Miyanohara, A., Nejime, T., Klima, J., Macakova, M., Marsala, S., Weiss, A., Kubickova, S., Musilova, P., Vrtel, R., Sontag, E.M., Thompson, L.M., Schier, J., Hansikova, H., Howland, D.S., Cattaneo, E., DiFiglia, M., Marsala, M., Motlik, J., 2013. A transgenic minipig model of Huntington's Disease. J. Huntingtons. Dis. 2, 47–68. https://doi.org/10.3233/JHD-130001

Becher, M.W., Kotzuk, J.A., Sharp, A.H., Davies, S.W., Bates, G.P., Price, D.L., Ross, C.A., 1998. Intranuclear Neuronal Inclusions in Huntington's Disease and Dentatorubral and Pallidoluysian Atrophy: Correlation between the Density of Inclusions andIT15CAG Triplet Repeat Length. Neurobiol. Dis. 4, 387–397. https://doi.org/10.1006/nbdi.1998.0168

Benarroch, E.E., 2013. Microglia: Multiple roles in surveillance, circuit shaping, and response to injury. Neurology. https://doi.org/10.1212/WNL.0b013e3182a4a577

Benn, C.L., Sun, T., Sadri-Vakili, G., McFarland, K.N., DiRocco, D.P., Yohrling, G.J., Clark, T.W., Bouzou, B., Cha, J.-H.J., 2008. Huntingtin modulates transcription, occupies gene promoters in vivo, and binds directly to DNA in a polyglutamine-dependent manner. J. Neurosci. 28, 10720–33. https://doi.org/10.1523/JNEUROSCI.2126-08.2008

Bertram, L., Lange, C., Mullin, K., Parkinson, M., Hsiao, M., Hogan, M.F., Schjeide, B.M.M., Hooli, B., DiVito, J., Ionita, I., Jiang, H., Laird, N., Moscarillo, T., Ohlsen, K.L., Elliott, K., Wang, X., Hu-Lince, D., Ryder, M., Murphy, A., Wagner, S.L., Blacker, D., Becker, K.D., Tanzi, R.E., 2008. Genome-wide Association Analysis Reveals Putative Alzheimer's Disease Susceptibility Loci in Addition to APOE. Am. J. Hum. Genet. 83, 623–632. https://doi.org/10.1016/j.ajhg.2008.10.008

Biber, K., Neumann, H., Inoue, K., Boddeke, H.W.G.M., 2007. Neuronal "On" and "Off" signals control microglia. Trends Neurosci. https://doi.org/10.1016/j.tins.2007.08.007

Bilsen, P.H.J. van, Jaspers, L., Lombardi, M.S., Odekerken, J.C.E., Burright, E.N., Kaemmerer, W.F., 2008. Identification and Allele-Specific Silencing of the Mutant Huntingtin Allele in Huntington's Disease Patient-Derived Fibroblasts. Hum. Gene Ther. 19, 710–718.

https://doi.org/10.1089/hum.2007.116
Björkqvist, M., Wild, E.J., Thiele, J., Silvestroni, A., Andre, R., Lahiri, N., Raibon, E., Lee, R. V., Benn, C.L., Soulet, D., Magnusson, A., Woodman, B., Landles, C., Pouladi, M.A., Hayden, M.R., Khalili-Shirazi, A., Lowdell, M.W., Brundin, P., Bates, G.P., Leavitt, B.R., Möller, T., Tabrizi, S.J., 2008. A novel pathogenic pathway of immune activation detectable before clinical onset in Huntington's disease. 205. https://doi.org/10.1084/jem.20080178
Bliederhaeuser, C., Grozdanov, V., Speidel, A., Zondler, L., Ruf, W.P., Bayer, H., Kiechle, M., Feiler, M.S., Freischmidt, A., Brenner, D., Witting, A., Hengerer, B., Fändrich, M., Ludolph, A.C., Weishaupt, J.H., Gillardon, F., Danzer, K.M., 2016. Age-dependent defects of alpha-synuclein oligomer uptake in microglia and monocytes. Acta Neuropathol. 131, 379–391. https://doi.org/10.1007/s00401-015-1504-2
Block-Galarza, J., Chase, K.O., Sapp, E., Vaughn, K.T., Vallee, R.B., DiFiglia, M., Aronin, N., 1997. Fast transport and retrograde movement of huntingtin and HAP 1 in axons. Neuroreport 8, 2247–51.
Bonelli, R., Bonelli, C., Obermayer-Pietsch, B., Hofmann Karl, P., 2007. Osteoporosis in Huntington's disease due to neuroleptic medication? Olanzapine for Huntington's disease: An open label study. Neurodegener. Dis. 4, 304.
Bouchard, J., Truong, J., Bouchard, K., Dunkelberger, D., Desrayaud, S., Moussaoui, S., Tabrizi, S.J., Stella, N., Muchowski, P.J., 2012. Cannabinoid receptor 2 signaling in peripheral immune cells modulates disease onset and severity in mouse models of Huntington's disease. J. Neurosci. 32, 18259–68. https://doi.org/10.1523/JNEUROSCI.4008-12.2012
Boudreau, R.L., McBride, J.L., Martins, I., Shen, S., Xing, Y., Carter, B.J., Davidson, B.L., 2009. Nonallele-specific silencing of mutant and wild-type huntingtin demonstrates therapeutic efficacy in Huntington's disease mice. Mol. Ther. https://doi.org/10.1038/mt.2009.17
Bradford, J., Shin, J.-Y., Roberts, M., Wang, C.-E., Li, X.-J., Li, S., 2009. Expression of mutant huntingtin in mouse brain astrocytes causes age-dependent neurological symptoms. Proc. Natl. Acad. Sci. 106, 22480–22485. https://doi.org/10.1073/pnas.0911503106
Brandstaetter, H., Kruppa, A.J., Buss, F., 2014. Huntingtin is required for ER-to-Golgi transport and for secretory vesicle fusion at the plasma membrane. Dis. Model. Mech. 7, 1335–1340. https://doi.org/10.1242/dmm.017368
Browne, S.E., 2008. Mitochondria and Huntington's disease pathogenesis: Insight from genetic and chemical models, in: Annals of the New York Academy of Sciences. pp. 358–382. https://doi.org/10.1196/annals.1427.018
Browne, S.E., Bowling, A.C., MacGarvey, U., Baik, M.J., Berger, S.C., Muqit, M.M.K., Bird, E.D., Beal, M.F., 1997. Oxidative damage and metabolic dysfunction in huntington's disease: Selective vulnerability of the basal ganglia. Ann. Neurol. 41, 646–653. https://doi.org/10.1002/ana.410410514
Browne, S.E., Ferrante, R.J., Beal, M.F., 2010. Oxidative Stress in Huntington's Disease. Brain Pathol. 9, 147–163. https://doi.org/10.1111/j.1750-3639.1999.tb00216.x
Browne, S.E., Ferrante, R.J., Beal, M.F., 1999. Oxidative stress in Huntington's disease. Brain Pathol. 9, 147–63.
Brownjohn, P.W., Smith, J., Solanki, R., Lohmann, E., Houlden, H., Hardy, J.,

Dietmann, S., Livesey, F.J., 2018. Functional Studies of Missense TREM2 Mutations in Human Stem Cell-Derived Microglia. Stem Cell Reports 10, 1294–1307. https://doi.org/10.1016/J.STEMCR.2018.03.003
Brubaker, S.W., Bonham, K.S., Zanoni, I., Kagan, J.C., 2015. Innate Immune Pattern Recognition: A Cell Biological Perspective. Annu. Rev. Immunol. 33, 257–290. https://doi.org/10.1146/annurev-immunol-032414-112240
Buchrieser, J., James, W., Moore, M.D., 2017. Human Induced Pluripotent Stem Cell-Derived Macrophages Share Ontogeny with MYB-Independent Tissue-Resident Macrophages. Stem Cell Reports 8, 334–345. https://doi.org/10.1016/j.stemcr.2016.12.020
Burguillos, M.A., Deierborg, T., Kavanagh, E., Persson, A., Hajji, N., Garcia-Quintanilla, A., Cano, J., Brundin, P., Englund, E., Venero, J.L., Joseph, B., 2011. Caspase signalling controls microglia activation and neurotoxicity. Nature 472, 319–324. https://doi.org/10.1038/nature09788
Butovsky, O., Jedrychowski, M.P., Moore, C.S., Cialic, R., Lanser, A.J., Gabriely, G., Koeglsperger, T., Dake, B., Wu, P.M., Doykan, C.E., Fanek, Z., Liu, L., Chen, Z., Rothstein, J.D., Ransohoff, R.M., Gygi, S.P., Antel, J.P., Weiner, H.L., 2014. Identification of a unique TGF-β-dependent molecular and functional signature in microglia. Nat. Neurosci. 17, 131–43. https://doi.org/10.1038/nn.3599
Butovsky, O., Jedrychowski, M.P., Moore, C.S., Cialic, R., Lanser, A.J., Gabriely, G., Koeglsperger, T., Dake, B., Wu, P.M., Doykan, C.E., Fanek, Z., Liu, L., Chen, Z., Rothstein, J.D., Ransohoff, R.M., Gygi, S.P., Antel, J.P., Weiner, H.L., 2013. Identification of a unique TGF-β–dependent molecular and functional signature in microglia. Nat. Neurosci. 17, 131–143. https://doi.org/10.1038/nn.3599
Butovsky, O., Talpalar, A.E., Ben-Yaakov, K., Schwartz, M., 2005. Activation of microglia by aggregated β-amyloid or lipopolysaccharide impairs MHC-II expression and renders them cytotoxic whereas IFN-γ and IL-4 render them protective. Mol. Cell. Neurosci. 29, 381–393. https://doi.org/10.1016/j.mcn.2005.03.005
Butovsky, O., Ziv, Y., Schwartz, A., Landa, G., Talpalar, A.E., Pluchino, S., Martino, G., Schwartz, M., 2006. Microglia activated by IL-4 or IFN-γ differentially induce neurogenesis and oligodendrogenesis from adult stem/progenitor cells. Mol. Cell. Neurosci. 31, 149–160. https://doi.org/10.1016/j.mcn.2005.10.006
Byrne, Lauren M., Rodrigues, F.B., Johnson, E.B., De Vita, E., Blennow, K., Scahill, R., Zetterberg, H., Heslegrave, A., Wild, E.J., 2018. Cerebrospinal fluid neurogranin and TREM2 in Huntington's disease. Sci. Rep. 8, 4260. https://doi.org/10.1038/s41598-018-21788-x
Byrne, Lauren M, Rodrigues, F.B., Johnson, E.B., De Vita, E., Blennow, K., Scahill, R., Zetterberg, H., Heslegrave, A., Wild, E.J., 2018a. Cerebrospinal fluid neurogranin and TREM2 in Huntington's disease. Sci. Rep. 8, 4260. https://doi.org/10.1038/s41598-018-21788-x
Byrne, Lauren M, Rodrigues, F.B., Johnson, E.B., Wijeratne, P.A., De Vita, E., Alexander, D.C., Palermo, G., Czech, C., Schobel, S., Scahill, R.I., Heslegrave, A., Zetterberg, H., Wild, E.J., 2018b. Evaluation of mutant huntingtin and neurofilament proteins as potential markers in Huntington's disease. Sci. Transl. Med. 10, eaat7108. https://doi.org/10.1126/scitranslmed.aat7108
Calderon, B., Carrero, J.A., Ferris, S.T., Sojka, D.K., Moore, L., Epelman, S.,

Murphy, K.M., Yokoyama, W.M., Randolph, G.J., Unanue, E.R., 2015. The pancreas anatomy conditions the origin and properties of resident macrophages. J. Exp. Med. 212, 1497–1512. https://doi.org/10.1084/jem.20150496
Carpenter, A.F., Carpenter, P.W., Markesbery, W.R., 1993. Morphometric analysis of microglia in alzheimer's disease. J. Neuropathol. Exp. Neurol. 52, 601–608. https://doi.org/10.1097/00005072-199311000-00007
Carrasco, E., Werner, P., 2002. Selective destruction of dopaminergic neurons by low concentrations of 6-OHDA and MPP+: protection by acetylsalicylic acid (aspirin). Parkinsonism Relat. Disord. 8, 407–411. https://doi.org/10.1016/S1353-8020(02)00022-6
Carroll, J.B., Warby, S.C., Southwell, A.L., Doty, C.N., Greenlee, S., Skotte, N., Hung, G., Bennett, C.F., Freier, S.M., Hayden, M.R., 2011. Potent and selective antisense oligonucleotides targeting single-nucleotide polymorphisms in the huntington disease gene / allele-specific silencing of mutant huntingtin. Mol. Ther. 19, 2178–2185. https://doi.org/10.1038/mt.2011.201
Carter, R.J., Lione, L.A., Humby, T., Mangiarini, L., Mahal, A., Bates, G.P., Dunnett, S.B., Morton, A.J., 1999. Characterization of Progressive Motor Deficits in Mice Transgenic for the Human Huntington's Disease Mutation. J. Neurosci. 19, 3248–3257. https://doi.org/10.1523/JNEUROSCI.19-08-03248.1999
Cattaneo, E., Zuccato, C., Tartari, M., 2005. Normal huntingtin function: An alternative approach to Huntington's disease, Nature Reviews Neuroscience. Nature Publishing Group. https://doi.org/10.1038/nrn1806
Caviston, J.P., Holzbaur, E.L.F., 2009. Huntingtin as an essential integrator of intracellular vesicular trafficking. Trends Cell Biol. 19, 147–155. https://doi.org/10.1016/j.tcb.2009.01.005
Caviston, J.P., Ross, J.L., Antony, S.M., Tokito, M., Holzbaur, E.L.F., 2007. Huntingtin facilitates dynein/dynactin-mediated vesicle transport. Proc. Natl. Acad. Sci. U. S. A. 104, 10045–50. https://doi.org/10.1073/pnas.0610628104
Caviston, J.P., Zajac, A.L., Tokito, M., Holzbaur, E.L.F., 2011. Huntingtin coordinates the dynein-mediated dynamic positioning of endosomes and lysosomes. Mol. Biol. Cell 22, 478–492. https://doi.org/10.1091/mbc.e10-03-0233
Chae, J.-I., Kim, D.-W., Lee, N., Jeon, Y.-J., Jeon, I., Kwon, J., Kim, J., Soh, Y., Lee, D.-S., Seo, K.S., Choi, N.-J., Park, B.C., Kang, S.H., Ryu, J., Oh, S.-H., Shin, D.A., Lee, D.R., Do, J.T., Park, I.-H., Daley, G.Q., Song, J., 2012. Quantitative proteomic analysis of induced pluripotent stem cells derived from a human Huntington's disease patient. Biochem. J. 446, 359–71. https://doi.org/10.1042/BJ20111495
Chafekar, S.M., Duennwald, M.L., 2012. Impaired Heat Shock Response in Cells Expressing Full-Length Polyglutamine-Expanded Huntingtin. PLoS One 7. https://doi.org/10.1371/JOURNAL.PONE.0037929
Chakrabarty, P., Li, A., Ceballos-Diaz, C., Eddy, J.A., Funk, C.C., Moore, B., DiNunno, N., Rosario, A.M., Cruz, P.E., Verbeeck, C., Sacino, A., Nix, S., Janus, C., Price, N.D., Das, P., Golde, T.E., 2015. IL-10 alters immunoproteostasis in APP mice, increasing plaque burden and worsening cognitive behavior. Neuron 85, 519–33. https://doi.org/10.1016/j.neuron.2014.11.020

Chang, K.-H., Lee-Chen, G.-J., Huang, C.-C., Lin, J.-L., Chen, Y.-J., Wei, P.-C., Lo, Y.-S., Yao, C.-F., Kuo, M.-W., Chen, C.-M., 2019. Modeling Alzheimer's Disease by Induced Pluripotent Stem Cells Carrying APP D678H Mutation. Mol. Neurobiol. 56, 3972–3983. https://doi.org/10.1007/s12035-018-1336-x

Chen, C.-M., Wu, Y.-R., Cheng, M.-L., Liu, J.-L., Lee, Y.-M., Lee, P.-W., Soong, B.-W., Chiu, D.T.-Y., 2007. Increased oxidative damage and mitochondrial abnormalities in the peripheral blood of Huntington's disease patients. Biochem. Biophys. Res. Commun. 359, 335–340. https://doi.org/10.1016/J.BBRC.2007.05.093

Chen, H., Jacobs, E., Schwarzschild, M.A., McCullough, M.L., Calle, E.E., Thun, M.J., Ascherio, A., 2005. Nonsteroidal antiinflammatory drug use and the risk for Parkinson's disease. Ann. Neurol. 58, 963–967. https://doi.org/10.1002/ana.20682

Chen, H., Zhang, S.M., Hernán, M.A., Schwarzschild, M.A., Willett, W.C., Colditz, G.A., Speizer, F.E., Ascherio, A., 2003. Nonsteroidal Anti-inflammatory Drugs and the Risk of Parkinson Disease. Arch. Neurol. 60, 1059. https://doi.org/10.1001/archneur.60.8.1059

Chen, M., Ona, V.O., Li, M., Ferrante, R.J., Fink, K.B., Zhu, S., Bian, J., Guo, L., Farrell, L.A., Hersch, S.M., Hobbs, W., Vonsattel, J.-P., Cha, J.-H.J., Friedlander, R.M., 2000. Minocycline inhibits caspase-1 and caspase-3 expression and delays mortality in a transgenic mouse model of Huntington disease. Nat. Med. 6, 797–801. https://doi.org/10.1038/77528

Chen, S., Berthelier, V., Yang, W., Wetzel, R., 2001. Polyglutamine aggregation behavior in vitro supports a recruitment mechanism of cytotoxicity. J. Mol. Biol. 311, 173–182. https://doi.org/10.1006/jmbi.2001.4850

Cheng, C.-M., Huang, S., Chang, Y.-F., Chung, W.-Y., Yuo, C.-Y., 2003. The viral death protein Apoptin interacts with Hippi, the protein interactor of Huntingtin-interacting protein 1. Biochem. Biophys. Res. Commun. 305, 359–64. https://doi.org/10.1016/s0006-291x(03)00764-2

Choi, J., Ifuku, M., Noda, M., Guilarte, T.R., 2011. Translocator protein (18 kDa)/peripheral benzodiazepine receptor specific ligands induce microglia functions consistent with an activated state. Glia 59, 219–230. https://doi.org/10.1002/glia.21091

Choi, Y.J., Kim, S.I., Lee, J.W., Kwon, Y.S., Lee, H.J., Kim, S.S., Chun, W., 2012. Suppression of aggregate formation of mutant huntingtin potentiates CREB-binding protein sequestration and apoptotic cell death. Mol. Cell. Neurosci. 49, 127–137. https://doi.org/10.1016/j.mcn.2011.11.003

Colin, E., Zala, D., Liot, G., Rangone, H., Borrell-Pagès, M., Li, X.J., Saudou, F., Humbert, S., 2008. Huntingtin phosphorylation acts as a molecular switch for anterograde/retrograde transport in neurons. EMBO J. 27, 2124–2134. https://doi.org/10.1038/emboj.2008.133

Colton, C.A., Gilbert, D.L., 1987. Production of superoxide anions by a CNS macrophage, the microglia. FEBS Lett. 223, 284–288. https://doi.org/10.1016/0014-5793(87)80305-8

Comi, G., Jeffery, D., Kappos, L., Montalban, X., Boyko, A., Rocca, M.A., Filippi, M., ALLEGRO Study Group, 2012. Placebo-Controlled Trial of Oral Laquinimod for Multiple Sclerosis. N. Engl. J. Med. 366, 1000–1009. https://doi.org/10.1056/NEJMoa1104318

Conforti, P., Besusso, D., Bocchi, V.D., Faedo, A., Cesana, E., Rossetti, G., Ranzani, V., Svendsen, C.N., Thompson, L.M., Toselli, M., Biella, G., Pagani, M., Cattaneo, E., 2018. Faulty neuronal determination and cell

polarization are reverted by modulating HD early phenotypes. Proc. Natl. Acad. Sci. 115, E762–E771. https://doi.org/10.1073/pnas.1715865115
Cong, X., Held, J.M., DeGiacomo, F., Bonner, A., Chen, J.M., Schilling, B., Czerwieniec, G.A., Gibson, B.W., Ellerby, L.M., 2011. Mass Spectrometric Identification of Novel Lysine Acetylation Sites in Huntingtin. Mol. Cell. Proteomics 10, M111.009829. https://doi.org/10.1074/mcp.M111.009829
Connolly, C., Magnusson-Lind, A., Lu, G., Wagner, P.K., Southwell, A.L., Hayden, M.R., Björkqvist, M., Leavitt, B.R., 2016. Enhanced immune response to MMP3 stimulation in microglia expressing mutant huntingtin. Neuroscience 325, 74–88. https://doi.org/10.1016/j.neuroscience.2016.03.031
Crotti, A., Benner, C., Kerman, B.E., Gosselin, D., Lagier-Tourenne, C., Zuccato, C., Cattaneo, E., Gage, F.H., Cleveland, D.W., Glass, C.K., 2014. Mutant Huntingtin promotes autonomous microglia activation via myeloid lineage-determining factors. Nat. Neurosci. 17, 513–21. https://doi.org/10.1038/nn.3668
Cubo, E., Martinez-Horta, S.-I., Santalo, F.S., Descalls, A.M., Calvo, S., Gil-Polo, C., Muñoz, I., Llano, K., Mariscal, N., Diaz, D., Gutierrez, A., Aguado, L., Ramos-Arroyo, M.A., European HD Network, the E.H., 2019. Clinical manifestations of homozygote allele carriers in Huntington disease. Neurology 10.1212/WNL.0000000000007147. https://doi.org/10.1212/WNL.0000000000007147
Cudkowicz, M., 2010. A futility study of minocycline in Huntington's disease. Mov. Disord. 25, 2219–2224. https://doi.org/10.1002/mds.23236
Culver, B.P., DeClercq, J., Dolgalev, I., Yu, M.S., Ma, B., Heguy, A., Tanese, N., 2016. Huntington's Disease Protein Huntingtin Associates with its own mRNA. J. Huntingtons. Dis. 5, 39–51. https://doi.org/10.3233/JHD-150177
Culver, B.P., Savas, J.N., Park, S.K., Choi, J.H., Zheng, S., Zeitlin, S.O., Yates, J.R., Tanese, N., 2012. Proteomic analysis of wild-type and mutant huntingtin-associated proteins in mouse brains identifies unique interactions and involvement in protein synthesis. J. Biol. Chem. 287, 21599–21614. https://doi.org/10.1074/jbc.M112.359307
Cunningham, C.L., Martínez-Cerdeño, V., Noctor, S.C., 2013. Microglia regulate the number of neural precursor cells in the developing cerebral cortex. J. Neurosci. 33, 4216–4233. https://doi.org/10.1523/JNEUROSCI.3441-12.2013
Da Silva, H.B., Fonseca, R., Alvarez, J.M., Lima, M.R.D.I., 2015. IFN- γ Priming Effects on the Maintenance of Effector Memory CD4+ T Cells and on Phagocyte Function: Evidences from Infectious Diseases. J. Immunol. Res. https://doi.org/10.1155/2015/202816
Dagher, N.N., Najafi, A.R., Kayala, K.M.N., Elmore, M.R.P., White, T.E., Medeiros, R., West, B.L., Green, K.N., 2015. Colony-stimulating factor 1 receptor inhibition prevents microglial plaque association and improves cognition in 3xTg-AD mice. J. Neuroinflammation 12, 139. https://doi.org/10.1186/s12974-015-0366-9
Dalmau, I., Finsen, B., Zimmer, J., González, B., Castellano, B., 1998. Development of microglia in the postnatal rat hippocampus. Hippocampus 8, 458–474. https://doi.org/10.1002/(SICI)1098-1063(1998)8:5<458::AID-HIPO6>3.0.CO;2-N
Dalrymple, A., Wild, E.J., Joubert, R., Sathasivam, K., Björkqvist, M., Petersén, Å., Jackson, G.S., Isaacs, J.D., Kristiansen, M., Bates, G.P., Leavitt, B.R.,

Keir, G., Ward, M., Tabrizi, S.J., Edward Wild, O.J., Richard Joubert, O., Sathasivam, K., Bjo, M., Petersén, Å., Jackson, G.S., Isaacs, J.D., Kristiansen, M., Bates, G.P., Leavitt, B.R., Keir, G., Ward, M., Tabrizi, S.J., 2007. Proteomic profiling of plasma in Huntington's disease reveals neuroinflammatory activation and biomarker candidates. J. Proteome Res. 6, 2833–2840. https://doi.org/10.1021/pr0700753

Dantzer, R., O'Connor, J.C., Freund, G.G., Johnson, R.W., Kelley, K.W., 2008. From inflammation to sickness and depression: When the immune system subjugates the brain. Nat. Rev. Neurosci. https://doi.org/10.1038/nrn2297

Das, A., Kim, S.H., Arifuzzaman, S., Yoon, T., Chai, J.C., Lee, Y.S., Park, K.S., Jung, K.H., Chai, Y.G., 2016. Transcriptome sequencing reveals that LPS-triggered transcriptional responses in established microglia BV2 cell lines are poorly representative of primary microglia. J. Neuroinflammation 13. https://doi.org/10.1186/s12974-016-0644-1

Davalos, D., Grutzendler, J., Yang, G., Kim, J. V, Zuo, Y., Jung, S., Littman, D.R., Dustin, M.L., Gan, W.-B., 2005. ATP mediates rapid microglial response to local brain injury in vivo. Nat. Neurosci. 8, 752–758. https://doi.org/10.1038/nn1472

Davies, S.W., Turmaine, M., Cozens, B.A., DiFiglia, M., Sharp, A.H., Ross, C.A., Scherzinger, E., Wanker, E.E., Mangiarini, L., Bates, G.P., 1997. Formation of neuronal intranuclear inclusions underlies the neurological dysfunction in mice transgenic for the HD mutation. Cell 90, 537–548. https://doi.org/10.1016/S0092-8674(00)80513-9

Deckel, A.W., 2001. Nitric oxide and nitric oxide synthase in Huntington's disease. J. Neurosci. Res. 64, 99–107. https://doi.org/10.1002/jnr.1057

Deckel, A.W., Tang, V., Nuttal, D., Gary, K., Elder, R., 2002. Altered neuronal nitric oxide synthase expression contributes to disease progression in Huntington's disease transgenic mice. Brain Res. 939, 76–86. https://doi.org/10.1016/s0006-8993(02)02550-7

Deckel, A.W., Volmer, P., Weiner, R., Gary, K.A., Covault, J., Sasso, D., Schmerler, N., Watts, D., Yan, Z., Abeles, I., 2000. Dietary arginine alters time of symptom onset in Huntington's disease transgenic mice. Brain Res. 875, 187–195. https://doi.org/10.1016/S0006-8993(00)02640-8

Deretic, V., Saitoh, T., Akira, S., 2013. Autophagy in infection, inflammation and immunity. Nat. Publ. Gr. 13. https://doi.org/10.1038/nri3532

DiFiglia, M., Sapp, E., Chase, K.O., Davies, S.W., Bates, G.P., Vonsattel, J.P., Aronin, N., Byers, K., Gilles, F.H., Fung, C., Graveland, G.A., Williams, R.S., DiFiglia, M., Cudkowicz, M., Kowall, N.S., Monte, S.M.D. La, Vonsattel, J.P., Richardson, E.P., Myers, R.H., Duyao, M., Stine, O.C., Aronin, N., Perutz, M.F., Johnson, T., Suzuki, M., Finch, J.T., Stott, K., Blackburn, J.M., Butler, P.J.G., Perutz, M., Perutz, M.F., Kahlen, P., Terre, C., Green, H., Djian, P., Burke, J.R., Li, X.J., Sapp, E., Davies, S.W., DiFiglia, M., Bhide, P.G., Trottier, Y., Sonnenberg, J.L., Macgregor-Leon, P.F., Curran, T., Morgan, J.I., Aronin, N., Chase, K., Sagar, S.M., Sharp, F.R., DiFiglia, M., Scherzinger, E., Goldberg, Y.P., Kalchman, M.A., Cammarata, S., Caponnetto, C., Tabaton, M., Jackson, M., Hedreen, J.C., Peyser, C.E., Folstein, S.E., Ross, C.A., Sahenk, Z., Lasek, R.J., Block-Galarza, J., Reddy, P.S., Housman, D.E., Haltia, M., Somer, H., Palo, J., Johnson, W.G., Funata, N., Brasch, K., Ochs, R.L., Peters, M., Franke, W.W., Kleinschmidt, J.A., 1997. Aggregation of huntingtin in neuronal intranuclear inclusions and dystrophic neurites in brain. Science 277,

1990–3. https://doi.org/10.1126/science.277.5334.1990
DiGiovanni, L.F., Mocle, A.J., Xia, J., Truant, R., 2016. Huntingtin N17 domain is a reactive oxygen species sensor regulating huntingtin phosphorylation and localization. Hum. Mol. Genet. 25, 3937–3945. https://doi.org/10.1093/hmg/ddw234
Ding, X., Ma, M., Teng, J., Teng, R.K.F., Zhou, S., Yin, J., Fonkem, E., Huang, J.H., Wu, E., Wang, X., 2015. Exposure to ALS-FTD-CSF generates TDP-43 aggregates in glioblastoma cells through exosomes and TNTs-like structure. Oncotarget 6, 24178–24191. https://doi.org/10.18632/oncotarget.4680
Douvaras, P., Sun, B., Wang, M., Kruglikov, I., Lallos, G., Zimmer, M., Terrenoire, C., Zhang, B., Gandy, S., Schadt, E., Freytes, D.O., Noggle, S., Fossati, V., 2017. Directed Differentiation of Human Pluripotent Stem Cells to Microglia. Stem cell reports 8, 1516–1524. https://doi.org/10.1016/j.stemcr.2017.04.023
Dragatsis, I., Efstratiadis, A., Zeitlin, S., 1998. Mouse mutant embryos lacking huntingtin are rescued from lethality by wild-type extraembryonic tissues. Development 125, 1529–1539.
Dragatsis, I., Levine, M.S., Zeitlin, S., 2000. Inactivation of Hdh in the brain and testis results in progressive neurodegeneration and sterility in mice. Nat. Genet. 26, 300–306. https://doi.org/10.1038/81593
Drouin-Ouellet, J., Sawiak, S.J., Cisbani, G., Lagacé, M., Kuan, W.L., Saint-Pierre, M., Dury, R.J., Alata, W., St-Amour, I., Mason, S.L., Calon, F., Lacroix, S., Gowland, P.A., Francis, S.T., Barker, R.A., Cicchetti, F., 2015. Cerebrovascular and blood-brain barrier impairments in Huntington's disease: Potential implications for its pathophysiology. Ann. Neurol. https://doi.org/10.1002/ana.24406
Duyao, M.P., Auerbach, A.B., Ryan, A., Persichetti, F., Barnes, G.T., McNeil, S.M., Ge, P., Vonsattel, J.P., Gusella, J.F., Joyner, A.L., 1995. Inactivation of the mouse Huntington's disease gene homolog Hdh. Science 269, 407–10.
Ehrlich, M.E., 2012. Huntington's Disease and the Striatal Medium Spiny Neuron: Cell-Autonomous and Non-Cell-Autonomous Mechanisms of Disease. Neurotherapeutics. https://doi.org/10.1007/s13311-012-0112-2
Ehrnhoefer, Dagmar E., Butland, S.L., Pouladi, M.A., Hayden, M.R., 2009. Mouse models of Huntington disease: variations on a theme. Dis. Model. Mech. 2, 123–129. https://doi.org/10.1242/dmm.002451
Ehrnhoefer, D.E., Butland, S.L., Pouladi, M.A., Hayden, M.R., 2009. Mouse models of Huntington disease: Variations on a theme. DMM Dis. Model. Mech. 2, 123–129. https://doi.org/10.1242/dmm.002451
Elkabes, S., DiCicco-Bloom, E.M., Black, I.B., 1996. Brain microglia/macrophages express neurotrophins that selectively regulate microglial proliferation and function. J. Neurosci. 16, 2508–2521. https://doi.org/10.1523/jneurosci.16-08-02508.1996
Ellrichmann, G., Reick, C., Saft, C., Linker, R.A., 2013. The Role of the Immune System in Huntington's Disease. Clin. Dev. Immunol. 11, 541259. https://doi.org/10.1155/2013/541259
Elmore, M.R.P., Najafi, A.R., Koike, M.A., Dagher, N.N., Spangenberg, E.E., Rice, R.A., Kitazawa, M., Matusow, B., Nguyen, H., West, B.L., Green, K.N., 2014. Colony-stimulating factor 1 receptor signaling is necessary for microglia viability, unmasking a microglia progenitor cell in the adult brain.

Neuron 82, 380–397. https://doi.org/10.1016/j.neuron.2014.02.040
Engelender, S., Sharp, A.H., Colomer, V., Tokito, M.K., Lanahan, A., Worley, P., Holzbaur, E.L.F., Ross, C.A., 1997. Huntingtin-associated protein 1 (HAP1) interacts with the p150Glued subunit of dynactin. Hum. Mol. Genet. 6, 2205–12. https://doi.org/10.1093/hmg/6.13.2205
Espey, M.G., Miranda, K.M., Feelisch, M., Fukuto, J., Grisham, M.B., Vitek, M.P., Wink, D.A., 2000. Mechanisms of cell death governed by the balance between nitrosative and oxidative stress. Ann. N. Y. Acad. Sci. 899, 209–21.
Evans, S.J., Douglas, I., Rawlins, M.D., Wexler, N.S., Tabrizi, S.J., Smeeth, L., 2013. Prevalence of adult Huntington's disease in the UK based on diagnoses recorded in general practice records. J Neurol Neurosurg Psychiatry 84, 1156–1160. https://doi.org/10.1136/jnnp-2012-304636
Evers, M.M., Pepers, B.A., van Deutekom, J.C.T., Mulders, S.A.M., den Dunnen, J.T., Aartsma-Rus, A., van Ommen, G.-J.B., van Roon-Mom, W.M.C., 2011. Targeting Several CAG Expansion Diseases by a Single Antisense Oligonucleotide. PLoS One 6, e24308. https://doi.org/10.1371/journal.pone.0024308
Ferlazzo, M.L., Sonzogni, L., Granzotto, A., Bodgi, L., Lartin, O., Devic, C., Vogin, G., Pereira, S., Foray, N., 2014. Mutations of the Huntington's Disease Protein Impact on the ATM-Dependent Signaling and Repair Pathways of the Radiation-Induced DNA Double-Strand Breaks: Corrective Effect of Statins and Bisphosphonates. Mol. Neurobiol. 49, 1200–1211. https://doi.org/10.1007/s12035-013-8591-7
Ferri, C.P., Prince, M., Brayne, C., Brodaty, H., Fratiglioni, L., Ganguli, M., Hall, K., Hasegawa, K., Hendrie, H., Huang, Y., Jorm, A., Mathers, C., Menezes, P.R., Rimmer, E., Scazufca, M., Alzheimer's Disease International, A.D., 2005. Global prevalence of dementia: a Delphi consensus study. Lancet (London, England) 366, 2112–7. https://doi.org/10.1016/S0140-6736(05)67889-0
Ferrini, F., De Koninck, Y., 2013. Microglia control neuronal network excitability via BDNF signalling. Neural Plast. https://doi.org/10.1155/2013/429815
Floden, A.M., Combs, C.K., 2011. Microglia demonstrate age-dependent interaction with amyloid-β fibrils. J. Alzheimer's Dis. 25, 279–293. https://doi.org/10.3233/JAD-2011-101014
Flower, M., Lomeikaite, V., Ciosi, M., Cumming, S., Morales, F., Lo, K., Hensman Moss, D., Jones, L., Holmans, P., Kraus, P., Hoffman, R., Tobin, A., Borowsky, B., Keenan, S., Whitlock, K.B., Queller, S., Campbell, C., Wang, C., Langbehn, D., Axelson, E., Johnson, H., Acharya, T., Cash, D.M., Frost, C., Jones, R., Jurgens, C., 't Hart, E.P., van der Grond, J., Witjes- Ane, M.-N.N., Roos, R.A.C., Dumas, E.M., van den Bogaard, S.J.A., Stopford, C., Craufurd, D., Callaghan, J., Arran, N., Rosas, D.D., Lee, S., Monaco, W., O'Regan, A., Milchman, C., Frajman, E., Labuschagne, I., Stout, J., Campbell, M., Andrews, S.C., Bechtel, N., Reilmann, R., Bohlen, S., Kennard, C., Berna, C., Hicks, S., Durr, A., Pourchot, C., Bardinet, E., Nigaud, K., Valabrègue, R., Lehericy, S., Marelli, C., Jauffret, C., Justo, D., Leavitt, B., Decolongon, J., Sturrock, A., Coleman, A., Santos, R.D., Patel, A., Gibbard, C., Whitehead, D., Wild, E., Owen, G., Crawford, H., Malone, I., Lahiri, N., Fox, N.C., Hobbs, N.Z., Scahill, R.I., Ordidge, R., Pepple, T., Read, J., Say, M.J., Landwehrmeyer, B., Daidj, F., Bassez, G., Lignier, B., Couppey, F., Delmas, S., Deux, J.-F.,

Hankiewicz, K., Dogan, C., Minier, L., Chevalier, P., Hamadouche, A., Catt, M., van Hees, V., Catt, S., Schwalber, A., Dittrich, J., Kierkegaard, M., Wenninger, S., Schoser, B., Schüller, A., Stahl, K., Künzel, H., Wolff, M., Jellinek, A., Moreno, C.J., Gorman, G., Lochmüller, H., Trenell, M., van Laar, S., Wood, L., Cassidy, S., Newman, J., Charman, S., Steffaneti, R., Taylor, L., Brownrigg, A., Day, S., Atalaia, A., Raaphorst, J., Okkersen, K., van Engelen, B., Nikolaus, S., Cornelissen, Y., van Nimwegen, M., Maas, D., Klerks, E., Bouman, S., Knoop, H., Heskamp, L., Heerschap, A., Rahmadi, R., Groot, P., Heskes, T., Kapusta, K., Glennon, J., Abghari, S., Aschrafi, A., Poelmans, G., Treweek, S., Hogarth, F., Littleford, R., Donnan, P., Hapca, A., Hannah, M., McKenzie, E., Rauchhaus, P., Cumming, S.A., Monckton, D.G., Adam, B., Faber, C., Merkies, I., Monckton, D.G., Tabrizi, S.J., 2019. MSH3 modifies somatic instability and disease severity in Huntington's and myotonic dystrophy type 1. Brain. https://doi.org/10.1093/brain/awz115

Futter, M., Diekmann, H., Schoenmakers, E., Sadiq, O., Chatterjee, K., Rubinsztein, D.C., 2009. Wild-type but not mutant huntingtin modulates the transcriptional activity of liver X receptors. J. Med. Genet. 46, 438–446. https://doi.org/10.1136/jmg.2009.066399

Galpern, W.R., Matthews, R.T., Beal, M.F., Isacson, O., 1996. NGF attenuates 3-nitrotyrosine formation in a 3-NP model of Huntington's disease. Neuroreport 7, 2639–42.

Garriga-Canut, M., Agustin-Pavon, C., Herrmann, F., Sanchez, A., Dierssen, M., Fillat, C., Isalan, M., 2012. Synthetic zinc finger repressors reduce mutant huntingtin expression in the brain of R6/2 mice. Proc. Natl. Acad. Sci. 109, E3136–E3145. https://doi.org/10.1073/pnas.1206506109

Gasteiger, G., D'Osualdo, A., Schubert, D.A., Weber, A., Bruscia, E.M., Hartl, D., 2017. Cellular Innate Immunity: An Old Game with New Players. J. Innate Immun. 9, 111–125. https://doi.org/10.1159/000453397

Gauthier, L.R., Charrin, B.C., Borrell-Pagès, M., Dompierre, J.P., Rangone, H., Cordelières, F.P., De Mey, J., Macdonald, M.E., Leßmann, V., Humbert, S., Saudou, F., Charrin, C., Dompierre, J.P., Borrell-page, M., Cordelie, F.P., Mey, J. De, Macdonald, M.E., Leßmann, V., Humbert, S., Gutenberg-universita, J., 2004. Huntingtin controls neurotrophic support and survival of neurons by enhancing BDNF vesicular transport along microtubules. Cell 118, 127–138. https://doi.org/10.1016/j.cell.2004.06.018

Geissmann, F., Manz, M.G., Jung, S., Sieweke, M.H., Merad, M., Ley, K., 2010. Development of monocytes, macrophages, and dendritic cells. Science 327, 656–61. https://doi.org/10.1126/science.1178331

Germain, P.L., Testa, G., 2017. Taming Human Genetic Variability: Transcriptomic Meta-Analysis Guides the Experimental Design and Interpretation of iPSC-Based Disease Modeling. Stem Cell Reports 8, 1784–1796. https://doi.org/10.1016/j.stemcr.2017.05.012

Gervais, F.G., Singaraja, R., Xanthoudakis, S., Gutekunst, C.-A., Leavitt, B.R., Metzler, M., Hackam, A.S., Tam, J., Vaillancourt, J.P., Houtzager, V., Rasper, D.M., Roy, S., Hayden, M.R., Nicholson, D.W., 2002. Recruitment and activation of caspase-8 by the Huntingtin-interacting protein Hip-1 and a novel partner Hippi. Nat. Cell Biol. 4, 95–105. https://doi.org/10.1038/ncb735

Gibbons, H.M., Dragunow, M., 2006. Microglia induce neural cell death via a proximity-dependent mechanism involving nitric oxide. Brain Res. 1084, 1–

15. https://doi.org/10.1016/j.brainres.2006.02.032
Gil-Mohapel, J., Brocardo, P., Christie, B., 2014. The Role of Oxidative Stress in Huntington's Disease: Are Antioxidants Good Therapeutic Candidates? Curr. Drug Targets 15, 454–468. https://doi.org/10.2174/1389450115666140115113734
Ginhoux, F., Greter, M., Leboeuf, M., Nandi, S., See, P., Gokhan, S., Mehler, M.F., Conway, S.J., Ng, L.G., Stanley, E.R., Samokhvalov, I.M., Merad, M., 2010. Fate mapping analysis reveals that adult microglia derive from primitive macrophages. Science 330, 841–5. https://doi.org/10.1126/science.1194637
Ginhoux, F., Lim, S., Hoeffel, G., Low, D., Huber, T., 2013. Origin and differentiation of microglia. Front. Cell. Neurosci. 7, 45. https://doi.org/10.3389/fncel.2013.00045
Godin, J.D., Colombo, K., Molina-Calavita, M., Keryer, G., Zala, D., Charrin, B.C., Dietrich, P., Volvert, M.-L., Guillemot, F., Dragatsis, I., Bellaiche, Y., Saudou, F., Nguyen, L., Humbert, S., 2010. Huntingtin Is Required for Mitotic Spindle Orientation and Mammalian Neurogenesis. Neuron 67, 392–406. https://doi.org/10.1016/j.neuron.2010.06.027
Godin, J.D., Humbert, S., 2011. Mitotic spindle: Focus on the function of huntingtin. Int. J. Biochem. Cell Biol. 43, 852–856. https://doi.org/10.1016/j.biocel.2011.03.009
Goldmann, T., Wieghofer, P., Jordão, M.J.C., Prutek, F., Hagemeyer, N., Frenzel, K., Amann, L., Staszewski, O., Kierdorf, K., Krueger, M., Locatelli, G., Hochgerner, H., Zeiser, R., Epelman, S., Geissmann, F., Priller, J., Rossi, F.M.V., Bechmann, I., Kerschensteiner, M., Linnarsson, S., Jung, S., Prinz, M., 2016. Origin, fate and dynamics of macrophages at central nervous system interfaces. Nat. Immunol. 17, 797–805. https://doi.org/10.1038/ni.3423
Gomez Perdiguero, E., Klapproth, K., Schulz, C., Busch, K., Azzoni, E., Crozet, L., Garner, H., Trouillet, C., de Bruijn, M.F., Geissmann, F., Rodewald, H.-R., 2014. Tissue-resident macrophages originate from yolk-sac-derived erythro-myeloid progenitors. Nature 518, 547–551. https://doi.org/10.1038/nature13989
Gonitel, R., Moffitt, H., Sathasivam, K., Woodman, B., Detloff, P.J., Faull, R.L.M., Bates, G.P., 2008. DNA instability in postmitotic neurons. Proc. Natl. Acad. Sci. U. S. A. 105, 3467–3472. https://doi.org/10.1073/pnas.0800048105
Gonzalez-Alegre, P., Afifi, A.K., 2006. Clinical characteristics of childhood-onset (juvenile) Huntington disease: report of 12 patients and review of the literature. J. Child Neurol. 21, 223–9. https://doi.org/10.2310/7010.2006.00055
Goodman, A.O.G., Barker, R.A., 2011. Body composition in premanifest Huntington's disease reveals lower bone density compared to controls. PLoS Curr. 3, RRN1214. https://doi.org/10.1371/currents.RRN1214
Goodman, A.O.G., Murgatroyd, P.R., Medina-Gomez, G., Wood, N.I., Finer, N., Vidal-Puig, A.J., Morton, A.J., Barker, R.A., 2008. The metabolic profile of early Huntington ' s disease - a combined human and transgenic mouse study. https://doi.org/10.1016/j.expneurol.2007.12.026
Goold, R., Flower, M., Moss, D.H., Medway, C., Wood-Kaczmar, A., Andre, R., Farshim, P., Bates, G.P., Holmans, P., Jones, L., Tabrizi, S.J., 2019. FAN1 modifies Huntington's disease progression by stabilizing the expanded HTT

CAG repeat. Hum. Mol. Genet. 28, 650–661. https://doi.org/10.1093/hmg/ddy375
Gosselin, D., Skola, D., Coufal, N.G., Holtman, I.R., Schlachetzki, J.C.M., Sajti, E., Jaeger, B.N., O'Connor, C., Fitzpatrick, C., Pasillas, M.P., Pena, M., Adair, A., Gonda, D.D.G., Levy, M.L., Ransohoff, R.M., Gage, F.H., Glass, C.K., O'Connor, C., Fitzpatrick, C., Pasillas, M.P., Pena, M., Adair, A., Gonda, D.D.G., Levy, M.L., Ransohoff, R.M., Gage, F.H., Glass, C.K., 2017. An environment-dependent transcriptional network specifies human microglia identity. Science (80-.). 356, 1248–1259. https://doi.org/10.1126/science.aal3222
Goswami, A., Dikshit, P., Mishra, A., Mulherkar, S., Nukina, N., Ranjan Jana, N., 2006. Oxidative stress promotes mutant huntingtin aggregation and mutant huntingtin-dependent cell death by mimicking proteasomal malfunction. https://doi.org/10.1016/j.bbrc.2006.01.136
Graeber, M.B., Bolasco, G., Pagani, F., Maggi, L., Scianni, M., Panzanelli, P., Giustetto, M., Ferreira, T.A., Guiducci, E., Dumas, L., Ragozzino, D., Gross, C.T., 2010. Changing face of microglia. Science 330, 783–8. https://doi.org/10.1126/science.1190929
Graham, R.K., Deng, Y., Slow, E.J., Haigh, B., Bissada, N., Lu, G., Pearson, J., Shehadeh, J., Bertram, L., Murphy, Z., Warby, S.C., Doty, C.N., Roy, S., Wellington, C.L., Leavitt, B.R., Raymond, L.A., Nicholson, D.W., Hayden, M.R., 2006. Cleavage at the Caspase-6 Site Is Required for Neuronal Dysfunction and Degeneration Due to Mutant Huntingtin. Cell 125, 1179–1191. https://doi.org/10.1016/j.cell.2006.04.026
Gray, M., Shirasaki, D.I., Cepeda, C., André, V.M., Wilburn, B., Lu, X.-H., Tao, J., Yamazaki, I., Li, S.-H., Sun, Y.E., Li, X.-J., Levine, M.S., Yang, X.W., 2008. Full-length human mutant huntingtin with a stable polyglutamine repeat can elicit progressive and selective neuropathogenesis in BACHD mice. J. Neurosci. 28, 6182–95. https://doi.org/10.1523/JNEUROSCI.0857-08.2008
Gresa-Arribas, N., Viéitez, C., Dentesano, G., Serratosa, J., Saura, J., Solà, C., 2012. Modelling neuroinflammation in vitro: a tool to test the potential neuroprotective effect of anti-inflammatory agents. PLoS One 7, e45227. https://doi.org/10.1371/journal.pone.0045227
Greter, M., Lelios, I., Pelczar, P., Hoeffel, G., Price, J., Leboeuf, M., Kündig, T.M., Frei, K., Ginhoux, F., Merad, M., Becher, B., 2012. Stroma-Derived Interleukin-34 Controls the Development and Maintenance of Langerhans Cells and the Maintenance of Microglia. Immunity 37, 1050–1060. https://doi.org/10.1016/j.immuni.2012.11.001
Grimm, S., 2004. The art and design of genetic screens: mammalian culture cells. Nat. Rev. Genet. 5, 179–189. https://doi.org/10.1038/nrg1291
Grondin, R., Kaytor, M.D., Ai, Y., Nelson, P.T., Thakker, D.R., Heisel, J., Weatherspoon, M.R., Blum, J.L., Burright, E.N., Zhang, Z., Kaemmerer, W.F., 2012. Six-month partial suppression of Huntingtin is well tolerated in the adult rhesus striatum. Brain 135, 1197–1209. https://doi.org/10.1093/brain/awr333
Gu, M., Gash, M.T., Mann, V.M., Javoy-Agid, F., Cooper, J.M., Schapira, A.H. V., 1996. Mitochondrial defect in Huntington's disease caudate nucleus. Ann. Neurol. 39, 385–389. https://doi.org/10.1002/ana.410390317
Gu, X., André, V.M., Cepeda, C., Li, S.H., Li, X.J., Levine, M.S., William Yang, X., 2007. Pathological cell-cell interactions are necessary for striatal

pathogenesis in a conditional mouse model of Huntington's disease. Mol. Neurodegener. 2. https://doi.org/10.1186/1750-1326-2-8
Gu, X., Li, C., Wei, W., Lo, V., Gong, S., Li, S.-H.H., Iwasato, T., Itohara, S., Li, X.-J.J., Mody, I., Heintz, N., Yang, X.W., Victor Lo, I., Gong, S., Li, S.-H.H., Lo, V., Gong, S., Li, S.-H.H., Iwasato, T., Itohara, S., Li, X.-J.J., Mody, I., Heintz, N., Yang, X.W., 2005a. Pathological Cell-Cell Interactions Elicited by a Neuropathogenic Form of Mutant Huntingtin Contribute to Cortical Pathogenesis in HD Mice. Neuron 46, 433–444. https://doi.org/10.1016/J.NEURON.2005.03.025
Gu, X., Li, C., Wei, W., Lo, V., Gong, S., Li, S.H., Iwasato, T., Itohara, S., Li, X.J., Mody, I., Heintz, N., Yang, X.W., 2005b. Pathological cell-cell interactions elicited by a neuropathogenic form of mutant huntingtin contribute to cortical pathogenesis in HD mice. Neuron 46, 433–444. https://doi.org/10.1016/j.neuron.2005.03.025
Guerreiro, R., Wojtas, A., Bras, J., Carrasquillo, M., Rogaeva, E., Majounie, E., Cruchaga, C., Sassi, C., Kauwe, J.S.K., Younkin, S., Hazrati, L., Collinge, J., Pocock, J., Lashley, T., Williams, J., Lambert, J.-C., Amouyel, P., Goate, A., Rademakers, R., Morgan, K., Powell, J., St. George-Hyslop, P., Singleton, A., Hardy, J., 2012. TREM2 Variants in Alzheimer's Disease. N. Engl. J. Med. 368, 117–127. https://doi.org/10.1056/nejmoa1211851
Guidetti, P., Bates, G.P., Graham, R.K., Hayden, M.R., Leavitt, B.R., MacDonald, M.E., Slow, E.J., Wheeler, V.C., Woodman, B., Schwarcz, R., 2006. Elevated brain 3-hydroxykynurenine and quinolinate levels in Huntington disease mice. Neurobiol. Dis. 23, 190–197. https://doi.org/10.1016/j.nbd.2006.02.011
Guidetti, P., Luthi-Carter, R.E., Augood, S.J., Schwarcz, R., 2004. Neostriatal and cortical quinolinate levels are increased in early grade Huntington's disease. Neurobiol. Dis. 17, 455–461. https://doi.org/10.1016/j.nbd.2004.07.006
Gunawardena, S., Her, L.-S., Brusch, R.G., Laymon, R.A., Niesman, I.R., Gordesky-Gold, B., Sintasath, L., Bonini, N.M., Goldstein, L.S.B., 2003. Disruption of axonal transport by loss of huntingtin or expression of pathogenic polyQ proteins in Drosophila. Neuron 40, 25–40. https://doi.org/10.1016/S0896-6273(03)00594-4
Guo, Q., Huang, B., Cheng, J., Seefelder, M., Engler, T., Pfeifer, G., Oeckl, P., Otto, M., Moser, F., Maurer, M., Pautsch, A., Baumeister, W., Fernández-Busnadiego, R., Kochanek, S., 2018. The cryo-electron microscopy structure of huntingtin. Nature 555, 117–120. https://doi.org/10.1038/nature25502
Guo, Z., Rudow, G., Pletnikova, O., Codispoti, K.-E., Orr, B.A., Crain, B.J., Duan, W., Margolis, R.L., Rosenblatt, A., Ross, C.A., Troncoso, J.C., 2012. Striatal neuronal loss correlates with clinical motor impairment in Huntington's disease. Mov. Disord. 27, 1379–86. https://doi.org/10.1002/mds.25159
Guo, Z., Shao, L., Feng, X., Reid, K., Marderstein, E., Nakao, A., Geller, D.A., 2003. A critical role for C/EBPbeta binding to the AABS promoter response element in the human iNOS gene. FASEB J. 17, 1718–1720. https://doi.org/10.1096/fj.02-1172fje
Hackam, A.S., Yassa, A.S., Singaraja, R., Metzler, M., Gutekunst, C.A., Gan, L., Warby, S., Wellington, C.L., Vaillancourt, J., Chen, N., Gervais, F.G., Raymond, L., Nicholson, D.W., Hayden, M.R., 2000. Huntingtin interacting

protein 1 induces apoptosis via a novel caspase-dependent death effector domain. J. Biol. Chem. 275, 41299–308. https://doi.org/10.1074/jbc.M008408200
Haenseler, W., Sansom, S.N., Buchrieser, J., Newey, S.E., Moore, C.S., Nicholls, F.J., Chintawar, S., Schnell, C., Antel, J.P., Allen, N.D., Cader, M.Z., Wade-Martins, R., James, W.S., Cowley, S.A., 2017. A Highly Efficient Human Pluripotent Stem Cell Microglia Model Displays a Neuronal-Co-culture-Specific Expression Profile and Inflammatory Response. Stem Cell Reports 8, 1727–1742. https://doi.org/10.1016/j.stemcr.2017.05.017
Halevy, T., Urbach, A., 2014. Comparing ESC and iPSC—Based Models for Human Genetic Disorders. J. Clin. Med. 3, 1146. https://doi.org/10.3390/JCM3041146
Halliday, G.M., McRitchie, D.A., Macdonald, V., Double, K.L., Trent, R.J., McCusker, E., 1998. Regional Specificity of Brain Atrophy in Huntington's Disease. Exp. Neurol. 154, 663–672. https://doi.org/10.1006/exnr.1998.6919
Hammond, T.R., Dufort, C., Dissing-Olesen, L., Giera, S., Young, A., Wysoker, A., Walker, A.J., Gergits, F., Segel, M., Nemesh, J., Marsh, S.E., Saunders, A., Macosko, E., Ginhoux, F., Chen, J., Franklin, R.J.M., Piao, X., McCarroll, S.A., Stevens, B., 2019. Single-Cell RNA Sequencing of Microglia throughout the Mouse Lifespan and in the Injured Brain Reveals Complex Cell-State Changes. Immunity 50, 253-271.e6. https://doi.org/10.1016/j.immuni.2018.11.004
Handley, R.R., Reid, S.J., Patassini, S., Rudiger, S.R., Obolonkin, V., Mclaughlan, C.J., Jacobsen, J.C., Gusella, J.F., Macdonald, M.E., Waldvogel, H.J., Simon Bawden, C., Faull, R.L.M., Snell, R.G., 2016. Metabolic disruption identified in the Huntington's disease transgenic sheep model. Nat. Publ. Gr. https://doi.org/10.1038/srep20681
Hands, S., Sajjad, M.U., Newton, M.J., Wyttenbach, A., 2011. In vitro and in vivo aggregation of a fragment of huntingtin protein directly causes free radical production. J. Biol. Chem. 286, 44512–44520. https://doi.org/10.1074/jbc.M111.307587
Hanisch, U.K., Prinz, M., Angstwurm, K., Häusler, K.G., Kann, O., Kettenmann, H., Weber, J.R., 2001. The protein tyrosine kinase inhibitor AG126 prevents the massive microglial cytokine induction by pneumococcal cell walls. Eur. J. Immunol. 31, 2104–15. https://doi.org/10.1002/1521-4141(200107)31:7<2104::AID-IMMU2104gt;3.0.CO;2-3
Hao, R., Ebadi, M., Pfeiffer, R.F., 1995. Selegiline protects dopaminergic neurons in culture from toxic factor(s) present in the cerebrospinal fluid of patients with Parkinson's disease. Neurosci. Lett. 200, 77–80. https://doi.org/10.1016/0304-3940(95)12113-i
Haremaki, T., Deglincerti, A., Brivanlou, A.H., 2015. Huntingtin is required for ciliogenesis and neurogenesis during early Xenopus development. Dev. Biol. 408, 305–315. https://doi.org/10.1016/j.ydbio.2015.07.013
Harjes, P., Wanker, E.E., 2003. The hunt for huntingtin function: interaction partners tell many different stories. Trends Biochem. Sci. 28, 425–433. https://doi.org/10.1016/S0968-0004(03)00168-3
Häusler, K.G., Prinz, M., Nolte, C., Weber, J.R., Schumann, R.R., Kettenmann, H., Hanisch, U.-K., 2002. Interferon-gamma differentially modulates the release of cytokines and chemokines in lipopolysaccharide- and

pneumococcal cell wall-stimulated mouse microglia and macrophages. Eur. J. Neurosci. 16, 2113–22.
Hawksworth, G.M., 1994. Advantages and Disadvantages of Using Human Cells for Pharmacological and Toxicological Studies. Hum. Exp. Toxicol. 13, 568–573. https://doi.org/10.1177/096032719401300811
Hayden, M.S., Ghosh, S., 2011. NF-κB in immunobiology. Cell Res. 21, 223–44. https://doi.org/10.1038/cr.2011.13
Heneka, M.T., Kummer, M.P., Latz, E., 2014. Innate immune activation in neurodegenerative disease. Nat. Publ. Gr. 14. https://doi.org/10.1038/nri3705
Hensman Moss, D.J., Tabrizi, S.J., Mead, S., Lo, K., Pardiñas, A.F., Holmans, P., Jones, L., Langbehn, D., Coleman, A., Santos, R.D., Decolongon, J., Sturrock, A., Bardinet, E., Ret, C.J., Justo, D., Lehericy, S., Marelli, C., Nigaud, K., Valabrègue, R., van den Bogaard, S. J.A., Dumas, E. M., van der Grond, J., T'Hart, E.P., Jurgens, C., Witjes-Ane, M.N., Arran, N., Callaghan, J., Stopford, C., Frost, C., Jones, R., Hobbs, N., Lahiri, N., Ordidge, R., Owen, G., Pepple, T., Read, J., Say, M., Wild, E., Patel, A., Fox, N.C., Gibbard, C., Malone, I., Crawford, H., Whitehead, D., Keenan, S., Cash, D.M., Berna, C., Bechtel, N., Bohlen, S., Man, A.H., Kraus, P., Axelson, E., Wang, C., Acharya, T., Lee, S., Monaco, W., Campbell, C., Queller, S., Whitlock, K., Campbell, C., Campbell, M., Frajman, E., Milchman, C., O'Regan, A., Labuschagne, I., Stout, J., Landwehrmeyer, B., Craufurd, D., Scahill, R., Hicks, S., Kennard, C., Johnson, H., Tobin, A., Rosas, H.D., Reilmann, R., Borowsky, B., Pourchot, C., Andrews, S.C., Bachoud-Lévi, A.C., Bentivoglio, A.R., Biunno, I., Bonelli, R., Burgunder, J.M., Dunnett, S., Ferreira, J., Handley, O., Heiberg, A., Illmann, T., Landwehrmeyer, G.B., Levey, J., Ramos-Arroyo, M.A., Nielsen, J., Koivisto, S.P., Päivärinta, M., Roos, R.A.C., Sebastián, A. Rojo, Tabrizi, S., Vandenberghe, W., Verellen-Dumoulin, C., Uhrova, T., Wahlström, J., Zaremba, J., Baake, V., Barth, K., Garde, M.B., Betz, S., Bos, R., Callaghan, Jenny, Come, A., Guedes, L.C., Ecker, D., Finisterra, A.M., Fullam, R., Gilling, M., Gustafsson, L., Handley, O.J., Hvalstedt, C., Held, C., Koppers, K., Lamanna, C., Laurà, M., Descals, A.M., Martinez-Horta, S., Mestre, T., Minster, S., Monza, D., Mütze, L., Oehmen, M., Orth, M., Padieu, H., Paterski, L., Peppa, N., Koivisto, S.P., Di Renzo, M., Rialland, A., Røren, N., Šašinková, P., Timewell, E., Townhill, J., Cubillo, P.T., da Silva, W.V., van Walsem, M.R., Whalstedt, C., Witjes-Ané, M.N., Witkowski, G., Wright, A., Zielonka, D., Zielonka, E., Zinzi, P., Bonelli, R.M., Lilek, S., Hecht, K., Herranhof, B., Holl, A., Kapfhammer, H.P., Koppitz, M., Magnet, M., Müller, N., Otti, D., Painold, A., Reisinger, K., Scheibl, M., Schöggl, H., Ullah, J., Braunwarth, E.M., Brugger, F., Buratti, L., Hametner, E.M., Hepperger, C., Holas, C., Hotter, A., Hussl, A., Müller, C., Poewe, W., Seppi, K., Sprenger, F., Wenning, G., Boogaerts, A., Calmeyn, G., Delvaux, I., Liessens, D., Somers, N., Dupuit, M., Minet, C., van Paemel, D., Ribaï, P., Verellen-Dumoulin, C., Boogaerts, A., Vandenberghe, W., van Reijen, D., Klempír, J., Majerová, V., Roth, J., Stárková, I., Hjermind, L.E., Jacobsen, O., Nielsen, J.E., Larsen, I.U., Vinther-Jensen, T., Hiivola, H., Hyppönen, H., Martikainen, K., Tuuha, K., Allain, P., Bonneau, D., Bost, M., Gohier, B., Guérid, M.A., Olivier, A., Prundean, A., Scherer-Gagou, C., Verny, C., Babiloni, B., Debruxelles, S., Duché, C., Goizet, C., Jameau, L., Lafoucrière, D., Spampinato, U., Barthélémy, R., De Bruycker, C., Carette,

M.C.A.S., Defebvre, E.D.L., Delliaux, M., Delval, A., Destee, A., Dujardin, K., Lemaire, M.H., Manouvrier, S., Peter, M., Plomhouse, L., Sablonnière, B., Simonin, C., Thibault-Tanchou, S., Vuillaume, I., Bellonet, M., Berrissoul, H., Blin, S., Courtin, F., Duru, C., Fasquel, V., Godefroy, O., Krystkowiak, P., Mantaux, B., Roussel, M., Wannepain, S., Azulay, J.P., Delfini, M., Eusebio, A., Fluchere, F., Mundler, L., Anheim, M., Julié, C., Boukbiza, O.L., Longato, N., Rudolf, G., Tranchant, C., Zimmermann, M.A., Kosinski, C.M., Milkereit, E., Probst, D., Reetz, K., Sass, C., Schiefer, J., Schlangen, C., Werner, C.J., Gelderblom, H., Priller, J., Prüß, H., Spruth, E.J., Ellrichmann, G., Herrmann, L., Hoffmann, R., Kaminski, B., Kotz, P., Prehn, C., Saft, C., Lange, H., Maiwald, R., Löhle, M., Maass, A., Schmidt, S., Bosredon, C., Storch, A., Wolz, A., Wolz, M., Capetian, P., Lambeck, J., Zucker, B., Boelmans, K., Ganos, C., Heinicke, W., Hidding, U., Lewerenz, J., Münchau, A., Orth, M., Schmalfeld, J., Stubbe, L., Zittel, S., Diercks, G., Dressler, D., Gorzolla, H., Schrader, C., Tacik, P., Ribbat, M., Longinus, B., Bürk, K., Möller, J.C., Rissling, I., Mühlau, M., Peinemann, A., Städtler, M., Weindl, A., Winkelmann, J., Ziegler, C., Bechtel, Natalie, Beckmann, H., Bohlen, Stefan, Hölzner, E., Lange, H., Reilmann, Ralf, Rohm, S., Rumpf, S., Schepers, S., Weber, N., Dose, M., Leythäuser, G., Marquard, R., Raab, T., Wiedemann, A., Barth, K., Buck, A., Connemann, J., Ecker, D., Geitner, C., Held, C., Kesse, A., Landwehrmeyer, Bernhard, Lang, C., Lewerenz, J., Lezius, F., Nepper, S., Niess, A., Orth, M., Schneider, A., Schwenk, D., Süßmuth, S., Trautmann, S., Weydt, P., Cormio, C., Sciruicchio, V., Serpino, C., de Tommaso, M., Capellari, S., Cortelli, P., Galassi, R., Rizzo, G., Poda, R., Scaglione, C., Bertini, E., Ghelli, E., Ginestroni, A., Massaro, F., Mechi, C., Paganini, M., Piacentini, S., Pradella, S., Romoli, A.M., Sorbi, S., Abbruzzese, G., di Poggio, M.B., Ferrandes, G., Mandich, P., Marchese, R., Albanese, A., Di Bella, D., Castaldo, A., Di Donato, S., Gellera, C., Genitrini, S., Mariotti, C., Monza, D., Nanetti, L., Paridi, D., Soliveri, P., Tomasello, C., De Michele, G., Di Maio, L., Massarelli, M., Peluso, S., Roca, A., Russo, C.V., Salvatore, E., Sorrentino, P., Amico, E., Favellato, M., Griguoli, A., Mazzante, I., Petrollini, M., Squitieri, F., D'Alessio, B., Esposito, C., Bentivoglio, R., Frontali, M., Guidubaldi, A., Ialongo, T., Jacopini, G., Piano, C., Romano, S., Soleti, F., Spadaro, M., Zinzi, P., van Hout, M.S.E., Verhoeven, M.E., van Vugt, J.P.P., de Weert, A.M., Bolwijn, J.J.W., Dekker, M., Kremer, B., Leenders, K.L., van Oostrom, J.C.H., van den Bogaard, Simon J.A., Bos, R., Dumas, Eve M., 't Hart, E.P., Roos, R.A.C., Kremer, Berry, Verstappen, C.C.P., Aaserud, O., Jan Frich, C., Heiberg, A., van Walsem, M.R., Wehus, R., Bjørgo, K., Fannemel, M., Gørvell, P.F., Lorentzen, E., Koivisto, S.P., Retterstøl, L., Stokke, B., Bjørnevoll, I., Sando, S.B., Dziadkiewicz, A., Nowak, M., Robowski, P., Sitek, E., Slawek, J., Soltan, W., Szinwelski, M., Blaszcyk, M., Boczarska-Jedynak, M., Ciach-Wysocka, E., Gorzkowska, A., Jasinska-Myga, B., Klodowska-Duda, G., Opala, G., Stompel, D., Banaszkiewicz, K., Bocwinska, D., Bojakowska-Jaremek, K., Dec, M., Krawczyk, M., Rudzinska, M., Szczygiel, E., Szczudlik, A., Wasielewska, A., Wójcik, M., Bryl, A., Ciesielska, A., Klimberg, A., Marcinkowski, J., Samara, H., Sempolowicz, J., Zielonka, D., Gogol, A., Janik, P., Kwiecinski, H., Jamrozik, Z., Antczak, J., Jachinska, K., Krysa, W., Rakowicz, M., Richter, P., Rola, R., Ryglewicz, D., Sienkiewicz-Jarosz, H., Stepniak, I., Sulek, A., Witkowski, G., Zaremba, J., Zdzienicka, E., Zieora-Jakutowicz,

K., Ferreira, J.J., Coelho, M., Guedes, L.C., Mendes, T., Mestre, T., Valadas, A., Andrade, C., Gago, M., Garrett, C., Guerra, M.R., Herrera, C.D., Garcia, P.M., Barbera, M.A., Guia, D.B., Hernanz, L.C., Catena, J.L., Ferrer, P.Q., Sebastián, Ana Rojo, Carruesco, G.T., Bas, J., Busquets, N., Calopa, M., Robert, M.F., Viladrich, C.M., Idiago, J.M.R., Riballo, A.V., Cubo, E., Polo, C.G., Mariscal, N., Rivadeneyra, P.J., Barrero, F., Morales, B., Fenollar, M., García, R.G.R., Ortega, P., Villanueva, C., Alegre, J., Bascuñana, M., Caldentey, J.G., Ventura, M.F., Ribas, G.G., de Yébenes, J.G., Moreno, J.L.L.S., Cubillo, P.T., Alegre, J., Frech, F.A., de Yébenes, J.G., Ruíz, P.J.G., Martínez-Descals, A., Guerrero, R., Artiga, M.J.S., Sánchez, V., Perea, M.F.N., Fortuna, L., Manzanares, S., Reinante, G., Torres, M.M.A., Moreau, L.V., González González, S., Guisasola, L.M., Salvador, C., Martín, E.S.S., Ramirez, I.L., Gorospe, A., Lopera, M.R., Arques, P.N., Rodríguez, M.J.T., Pastor, B.V., Gaston, I., Martinez-Jaurrieta, M.D., Ramos-Arroyo, M.A., Moreno, J.M.G., Lucena, C.M., Damas, F., Cortegana, H.E.P., Peña, J.C., Redondo, L., Carrillo, F., Teresa Cáceres, M., Mir, P., Suarez, M.J.L., Vargas-González, L., Bosca, M.E., Brugada, F.C., Burguera, J.A., Campos, A., Vilaplana, G.C.P., Berglund, P., Constantinescu, R., Fredlund, G., Høsterey-Ugander, U., Linnsand, P., Neleborn-Lingefjärd, L., Wahlström, J., Wentzel, M., Loutfi, G., Olofsson, C., Stattin, E.L., Westman, L., Wikström, B., Burgunder, J.M., Stebler, Y., Kaelin, A., Romero, I., Schüpbach, M., Weber Zaugg, S., Hauer, M., Gonzenbach, R., Jung, H.H., Mihaylova, V., Petersen, J., Jack, R., Matheson, K., Miedzybrodzka, Z., Rae, D., Simpson, S.A., Summers, F., Ure, A., Vaughan, V., Akhtar, S., Crooks, J., Curtis, A., de Souza, J., Piedad, J., Rickards, H., Wright, J., Coulthard, E., Gethin, L., Hayward, B., Sieradzan, K., Wright, A., Armstrong, M., Barker, R.A., O'Keefe, D., Di Pietro, A., Fisher, K., Goodman, A., Hill, S., Kershaw, A., Mason, S., Paterson, N., Raymond, L., Swain, R., Guzman, N.V., Busse, M., Butcher, C., Callaghan, Jenny, Dunnett, S., Clenaghan, C., Fullam, R., Handley, O., Hunt, S., Jones, L., Jones, U., Khalil, H., Minster, S., Owen, M., Price, K., Rosser, A., Townhill, J., Edwards, M., Ho, C., Hughes, T., McGill, M., Pearson, P., Porteous, M., Smith, P., Brockie, P., Foster, J., Johns, N., McKenzie, S., Rothery, J., Thomas, G., Yates, S., Burrows, L., Chu, C., Fletcher, A., Gallantrae, D., Hamer, S., Harding, A., Klöppel, S., Kraus, A., Laver, F., Lewis, M., Longthorpe, M., Markova, I., Raman, A., Robertson, N., Silva, M., Thomson, A., Wild, S., Yardumian, P., Chu, C., Evans, C., Gallentrae, D., Hamer, S., Kraus, A., Markova, I., Raman, A., Chu, C., Hamer, S., Hobson, E., Jamieson, S., Kraus, A., Markova, I., Raman, A., Musgrave, H., Rowett, L., Toscano, J., Wild, S., Yardumian, P., Bourne, C., Clapton, J., Clayton, C., Dipple, H., Freire-Patino, D., Grant, J., Gross, D., Hallam, C., Middleton, J., Murch, A., Thompson, C., Alusi, S., Davies, R., Foy, K., Gerrans, E., Pate, L., Andrews, T., Dougherty, A., Golding, C., Kavalier, F., Laing, H., Lashwood, A., Robertson, D., Ruddy, D., Santhouse, A., Whaite, A., Andrews, T., Bruno, S., Doherty, K., Golding, C., Haider, S., Hensman, D., Lahiri, Nayana, Lewis, M., Novak, M., Patel, Aakta, Robertson, N., Rosser, E., Tabrizi, S., Taylor, R., Warner, T., Wild, Edward, Arran, Natalie, Bek, J., Callaghan, Jenny, Craufurd, David, Fullam, R., Hare, M., Howard, L., Huson, S., Johnson, L., Jones, M., Murphy, H., Oughton, E., Partington-Jones, L., Rogers, D., Sollom, A., Snowden, J., Stopford, Cheryl, Thompson, J., Trender-Gerhard, I., Verstraelen, N.,

Westmoreland, L., Armstrong, R., Dixon, K., Nemeth, A.H., Siuda, G., Valentine, R., Harrison, D., Hughes, M., Parkinson, A., Soltysiak, B., Bandmann, O., Bradbury, A., Gill, P., Fairtlough, H., Fillingham, K., Foustanos, I., Kazoka, M., O'Donovan, K., Peppa, N., Taylor, C., Tidswell, K., Quarrell, O., Burgunder, J.M., Lau, P.N., Pica, E., Tan, L., 2017. Identification of genetic variants associated with Huntington's disease progression: a genome-wide association study. Lancet Neurol. https://doi.org/10.1016/S1474-4422(17)30161-8

Herrera, A.J., Castaño, A., Venero, J.L., Cano, J., Machado, A., 2000. The Single Intranigral Injection of LPS as a New Model for Studying the Selective Effects of Inflammatory Reactions on Dopaminergic System. Neurobiol. Dis. 7, 429–447. https://doi.org/10.1006/NBDI.2000.0289

Hersch, S.M., Gevorkian, S., Marder, K., Moskowitz, C., Feigin, A., Cox, M., Como, P., Zimmerman, C., Lin, M., Zhang, L., Ulug, A.M., Beal, M.F., Matson, W., Bogdanov, M., Ebbel, E., Zaleta, A., Kaneko, Y., Jenkins, B., Hevelone, N., Zhang, H., Yu, H., Schoenfeld, D., Ferrante, R., Rosas, H.D., 2006. Creatine in Huntington disease is safe, tolerable, bioavailable in brain and reduces serum 8OH2'dG. Neurology 66, 250–252. https://doi.org/10.1212/01.wnl.0000194318.74946.b6

Hersch, S.M., Schifitto, G., Oakes, D., Bredlau, A.L., Meyers, C.M., Nahin, R., Rosas, H.Di., 2017. The CREST-E study of creatine for Huntington disease. Neurology 89, 594–601. https://doi.org/10.1212/WNL.0000000000004209

Hickey, M.A., Gallant, K., Gross, G.G., Levine, M.S., Chesselet, M.F., 2005. Early behavioral deficits in R6/2 mice suitable for use in preclinical drug testing. Neurobiol. Dis. 20, 1–11. https://doi.org/10.1016/j.nbd.2005.01.024

Hodge, R.D., Bakken, T.E., Miller, J.A., Smith, K.A., Barkan, E.R., Graybuck, L.T., Close, J.L., Long, B., Johansen, N., Penn, O., Yao, Z., Eggermont, J., Höllt, T., Levi, B.P., Shehata, S.I., Aevermann, B., Beller, A., Bertagnolli, D., Brouner, K., Casper, T., Cobbs, C., Dalley, R., Dee, N., Ding, S.L., Ellenbogen, R.G., Fong, O., Garren, E., Goldy, J., Gwinn, R.P., Hirschstein, D., Keene, C.D., Keshk, M., Ko, A.L., Lathia, K., Mahfouz, A., Maltzer, Z., McGraw, M., Nguyen, T.N., Nyhus, J., Ojemann, J.G., Oldre, A., Parry, S., Reynolds, S., Rimorin, C., Shapovalova, N. V., Somasundaram, S., Szafer, A., Thomsen, E.R., Tieu, M., Quon, G., Scheuermann, R.H., Yuste, R., Sunkin, S.M., Lelieveldt, B., Feng, D., Ng, L., Bernard, A., Hawrylycz, M., Phillips, J.W., Tasic, B., Zeng, H., Jones, A.R., Koch, C., Lein, E.S., 2019. Conserved cell types with divergent features in human versus mouse cortex. Nature 573, 61–68. https://doi.org/10.1038/s41586-019-1506-7

Hoeffel, G., Chen, J., Lavin, Y., Low, D., Almeida, F.F., See, P., Beaudin, A.E., Lum, J., Low, I., Forsberg, E.C., Poidinger, M., Zolezzi, F., Larbi, A., Ng, L.G., Chan, J.K.Y.Y., Greter, M., Becher, B., Samokhvalov, I.M., Merad, M., Ginhoux, F., 2015. C-Myb+ Erythro-Myeloid Progenitor-Derived Fetal Monocytes Give Rise to Adult Tissue-Resident Macrophages. Immunity 42, 665–678. https://doi.org/10.1016/j.immuni.2015.03.011

Hoeffel, G., Ginhoux, F., 2015. Ontogeny of tissue-resident macrophages. Front. Immunol. https://doi.org/10.3389/fimmu.2015.00486

Hollingworth, P., Harold, D., Sims, R., Gerrish, A., Lambert, J.C., Carrasquillo, M.M., Abraham, R., Hamshere, M.L., Pahwa, J.S., Moskvina, V., Dowzell, K., Jones, N., Stretton, A., Thomas, C., Richards, A., Ivanov, D., Widdowson, C., Chapman, J., Lovestone, S., Powell, J., Proitsi, P., Lupton,

M.K., Brayne, C., Rubinsztein, D.C., Gill, M., Lawlor, B., Lynch, A., Brown, K.S., Passmore, P.A., Craig, D., McGuinness, B., Todd, S., Holmes, C., Mann, D., Smith, A.D., Beaumont, H., Warden, D., Wilcock, G., Love, S., Kehoe, P.G., Hooper, N.M., Vardy, E.R.L.C., Hardy, J., Mead, S., Fox, N.C., Rossor, M., Collinge, J., Maier, W., Jessen, F., Rüther, E., Schürmann, B., Heun, R., Kölsch, H., Van Den Bussche, H., Heuser, I., Kornhuber, J., Wiltfang, J., Dichgans, M., Frölich, L., Hampel, H., Gallacher, J., Hüll, M., Rujescu, D., Giegling, I., Goate, A.M., Kauwe, J.S.K., Cruchaga, C., Nowotny, P., Morris, J.C., Mayo, K., Sleegers, K., Bettens, K., Engelborghs, S., De Deyn, P.P., Van Broeckhoven, C., Livingston, G., Bass, N.J., Gurling, H., McQuillin, A., Gwilliam, R., Deloukas, P., Al-Chalabi, A., Shaw, C.E., Tsolaki, M., Singleton, A.B., Guerreiro, R., Mühleisen, T.W., Nöthen, M.M., Moebus, S., Jöckel, K.H., Klopp, N., Wichmann, H.E., Pankratz, V.S., Sando, S.B., Aasly, J.O., Barcikowska, M., Wszolek, Z.K., Dickson, D.W., Graff-Radford, N.R., Petersen, R.C., Van Duijn, C.M., Breteler, M.M.B., Ikram, M.A., Destefano, A.L., Fitzpatrick, A.L., Lopez, O., Launer, L.J., Seshadri, S., Berr, C., Campion, D., Epelbaum, J., Dartigues, J.F., Tzourio, C., Alpérovitch, A., Lathrop, M., Feulner, T.M., Friedrich, P., Riehle, C., Krawczak, M., Schreiber, S., Mayhaus, M., Nicolhaus, S., Wagenpfeil, S., Steinberg, S., Stefansson, H., Stefansson, K., SnÆdal, J., Björnsson, S., Jonsson, P. V., Chouraki, V., Genier-Boley, B., Hiltunen, M., Soininen, H., Combarros, O., Zelenika, D., Delepine, M., Bullido, M.J., Pasquier, F., Mateo, I., Frank-Garcia, A., Porcellini, E., Hanon, O., Coto, E., Alvarez, V., Bosco, P., Siciliano, G., Mancuso, M., Panza, F., Solfrizzi, V., Nacmias, B., Sorbi, S., Bossù, P., Piccardi, P., Arosio, B., Annoni, G., Seripa, D., Pilotto, A., Scarpini, E., Galimberti, D., Brice, A., Hannequin, D., Licastro, F., Jones, L., Holmans, P.A., Jonsson, T., Riemenschneider, M., Morgan, K., Younkin, S.G., Owen, M.J., O'Donovan, M., Amouyel, P., Williams, J., 2011. Common variants at ABCA7, MS4A6A/MS4A4E, EPHA1, CD33 and CD2AP are associated with Alzheimer's disease. Nat. Genet. 43, 429–436. https://doi.org/10.1038/ng.803

Hong, S., Beja-Glasser, V.F., Nfonoyim, B.M., Frouin, A., Li, S., Ramakrishnan, S., Merry, K.M., Shi, Q., Rosenthal, A., Barres, B.A., Lemere, C.A., Selkoe, D.J., Stevens, B., 2016a. Complement and microglia mediate early synapse loss in Alzheimer mouse models. Science (80-.). 352, 712–716. https://doi.org/10.1126/science.aad8373

Hong, S., Dissing-Olesen, L., Stevens, B., 2016b. New insights on the role of microglia in synaptic pruning in health and disease. Curr. Opin. Neurobiol. https://doi.org/10.1016/j.conb.2015.12.004

Hsu, D.C., Katelaris, C.H., 2009. Long-term management of patients taking immunosuppressive drugs. Aust. Prescr. https://doi.org/10.18773/austprescr.2009.035

Hunot, S., Dugas, N., Faucheux, B., Hartmann, A., Tardieu, M., Debré, P., Agid, Y., Dugas, B., Hirsch, E.C., 1999. FcepsilonRII/CD23 is expressed in Parkinson's disease and induces, in vitro, production of nitric oxide and tumor necrosis factor-alpha in glial cells. J. Neurosci. 19, 3440–7. https://doi.org/10.1523/jneurosci.1504-06.2006

Hunter, R., Ojha, U., Bhurtel, S., Bing, G., Choi, D.-Y., 2017. Lipopolysaccharide-induced functional and structural injury of the mitochondria in the nigrostriatal pathway. Neurosci. Res. 114, 62–69.

https://doi.org/10.1016/J.NEURES.2016.09.007
Janeway, C., Travers, P., Walport, M., Shlomick, M., 2001. Immunobiology: The immune system in health and disease. 5th Edition, 5th ed. Garland Science. https://doi.org/10.1111/j.1467-2494.1995.tb00120.x
Janeway, C.A., 1989. Approaching the asymptote? Evolution and revolution in immunology. Cold Spring Harb. Symp. Quant. Biol. 54 Pt 1, 1–13. https://doi.org/10.1101/SQB.1989.054.01.003
Jansen, A.H.P., van Hal, M., op den Kelder, I.C., Meier, R.T., de Ruiter, A.A., Schut, M.H., Smith, D.L., Grit, C., Brouwer, N., Kamphuis, W., Boddeke, H.W.G.M., den Dunnen, W.F.A., van Roon, W.M.C., Bates, G.P., Hol, E.M., Reits, E.A., 2017. Frequency of nuclear mutant huntingtin inclusion formation in neurons and glia is cell-type-specific. Glia 65, 50–61. https://doi.org/10.1002/glia.23050
Jia, H., Wang, Y., Morris, C.D., Jacques, V., Gottesfeld, J.M., Rusche, J.R., Thomas, E.A., 2016. The effects of pharmacological inhibition of histone deacetylase 3 (HDAC3) in Huntington's disease mice. PLoS One 11, e0152498. https://doi.org/10.1371/journal.pone.0152498
Jinno, S., Fleischer, F., Eckel, S., Schmidt, V., Kosaka, T., 2007. Spatial arrangement of microglia in the mouse hippocampus: A stereological study in comparison with astrocytes. Glia 55, 1334–1347. https://doi.org/10.1002/glia.20552
Jones, L., Holmans, P.A., Hamshere, M.L., Harold, D., Moskvina, V., Ivanov, D., Pocklington, A., Abraham, R., Hollingworth, P., Sims, R., Gerrish, A., Pahwa, J.S., Jones, N., Stretton, A., Morgan, A.R., Lovestone, S., Powell, J., Proitsi, P., Lupton, M.K., Brayne, C., Rubinsztein, D.C., Gill, M., Lawlor, B., Lynch, A., Morgan, K., Brown, K.S., Passmore, P.A., Craig, D., Mcguinness, B., Todd, S., Holmes, C., Mann, D., Smith, A.D., Love, S., Kehoe, P.G., Mead, S., Fox, N., Rossor, M., Collinge, J., Maier, W., Jessen, F., Schürmann, B., van den Bussche, H., Heuser, I., Peters, O., Kornhuber, J., Wiltfang, J., Dichgans, M., Frölich, L., Harald, H., Hüll, M., Rujescu, D., Goate, A.M., Kauwe, J.S.K., Cruchaga, C., Nowotny, P., Morris, J.C., Mayo, K., Livingston, G., Bass, N.J., Gurling, H., Mcquillin, A., Gwilliam, R., Deloukas, P., Al-Chalabi, A., Shaw, C.E., Singleton, A.B., Guerreiro, R., Mühleisen, T.W., Nöthen, M.M., Moebus, S., Jöckel, K.H., Klopp, N., Wichmann, H.E., Rüther, E., Carrasquillo, M.M., Pankratz, V.S., Younkin, S.G., Hardy, J., O'Donovan, M.C., Owen, M.J., Williams, J., 2010. Genetic evidence implicates the immune system and cholesterol metabolism in the aetiology of Alzheimer's disease. PLoS One 5. https://doi.org/10.1371/journal.pone.0013950
Jonsson, T., Stefansson, H., Steinberg, S., Jonsdottir, I., Jonsson, P. V, Snaedal, J., Bjornsson, S., Huttenlocher, J., Levey, A.I., Lah, J.J., Rujescu, D., Hampel, H., Giegling, I., Andreassen, O.A., Engedal, K., Ulstein, I., Djurovic, S., Ibrahim-Verbaas, C., Hofman, A., Ikram, M.A., van Duijn, C.M., Thorsteinsdottir, U., Kong, A., Stefansson, K., 2013. Variant of TREM2 associated with the risk of Alzheimer's disease. N. Engl. J. Med. 368, 107–16. https://doi.org/10.1056/NEJMoa1211103
Kaemmerer, W.F., Grondin, R., 2019. The effects of huntingtin-lowering: what do we know so far? Degener. Neurol. Neuromuscul. Dis. Volume 9, 3–17. https://doi.org/10.2147/DNND.S163808
Kennedy, N.J., Kataoka, T., Tschopp, J., Budd, R.C., 1999. Caspase Activation Is Required for T Cell Proliferation. J. Exp. Med. 190, 1891–1896.

https://doi.org/10.1084/jem.190.12.1891
Keryer, G., Pineda, J.R., Liot, G., Kim, J., Dietrich, P., Benstaali, C., Smith, K., Cordelières, F.P., Spassky, N., Ferrante, R.J., Dragatsis, I., Saudou, F., 2011. Ciliogenesis is regulated by a huntingtin-HAP1-PCM1 pathway and is altered in Huntington disease. J. Clin. Invest. 121, 4372–4382. https://doi.org/10.1172/JCI57552
Khoshnan, A., Ko, J., Watkin, E.E., Paige, L.A., Reinhart, P.H., Patterson, P.H., 2004. Activation of the IκB Kinase Complex and Nuclear Factor-κB Contributes to Mutant Huntingtin Neurotoxicity. J. Neurosci. 24, 7999–8008. https://doi.org/10.1523/JNEUROSCI.2675-04.2004
Khoshnan, A., Sabbaugh, A., Calamini, B., Marinero, S.A., Dunn, D.E., Yoo, J.H., Ko, J., Lo, D.C., Patterson, P.H., 2017a. IKKβ and mutant huntingtin interactions regulate the expression of IL-34: implications for microglial-mediated neurodegeneration in HD. Hum. Mol. Genet. 26, 4267–4277. https://doi.org/10.1093/hmg/ddx315
Khoshnan, A., Sabbaugh, A., Calamini, B., Marinero, S.A., Dunn, D.E., Yoo, J.H., Ko, J., Lo, D.C., Patterson, P.H., 2017b. IKKβ and mutant huntingtin interactions regulate the expression of IL-34: Implications for microglial mediated neurodegeneration in HD. Hum. Mol. Genet. 26, 4267–4277. https://doi.org/10.1093/hmg/ddx315
Kieburtz, K., Reilmann, R., Olanow, C.W., 2018. Huntington's disease: Current and future therapeutic prospects. Mov. Disord. 33, 1033–1041. https://doi.org/10.1002/mds.27363
Kierdorf, K., Erny, D., Goldmann, T., Sander, V., Schulz, C., Perdiguero, E.G., Wieghofer, P., Heinrich, A., Riemke, P., Hölscher, C., Müller, D.N., Luckow, B., Brocker, T., Debowski, K., Fritz, G., Opdenakker, G., Diefenbach, A., Biber, K., Heikenwalder, M., Geissmann, F., Rosenbauer, F., Prinz, M., 2013. Microglia emerge from erythromyeloid precursors via Pu.1- and Irf8-dependent pathways. Nat. Neurosci. 16, 273–80. https://doi.org/10.1038/nn.3318
Kim, K., Doi, A., Wen, B., Ng, K., Zhao, R., Cahan, P., Kim, J., Aryee, M.J., Ji, H., Ehrlich, L.I.R., Yabuuchi, A., Takeuchi, A., Cunniff, K.C., Hongguang, H., Mckinney-Freeman, S., Naveiras, O., Yoon, T.J., Irizarry, R.A., Jung, N., Seita, J., Hanna, J., Murakami, P., Jaenisch, R., Weissleder, R., Orkin, S.H., Weissman, I.L., Feinberg, A.P., Daley, G.Q., 2010. Epigenetic memory in induced pluripotent stem cells. Nature 467, 285–290. https://doi.org/10.1038/nature09342
Kim, M.W., Chelliah, Y., Kim, S.W., Otwinowski, Z., Bezprozvanny, I., 2009. Secondary structure of Huntingtin amino-terminal region. Structure 17, 1205–12. https://doi.org/10.1016/j.str.2009.08.002
Kim, W.-G., Mohney, R.P., Wilson, B., Jeohn, G.-H., Liu, B., Hong, J.-S., 2000. Regional Difference in Susceptibility to Lipopolysaccharide-Induced Neurotoxicity in the Rat Brain: Role of Microglia. J. Neurosci. 20, 6309–6316. https://doi.org/10.1523/JNEUROSCI.20-16-06309.2000
Kirkham, P.A., Spooner, G., Rahman, I., Rossi, A.G., 2004. Macrophage phagocytosis of apoptotic neutrophils is compromised by matrix proteins modified by cigarette smoke and lipid peroxidation products. Biochem. Biophys. Res. Commun. 318, 32–37. https://doi.org/10.1016/j.bbrc.2004.04.003
Koguchi, K., Nakatsuji, Y., Okuno, T., Sawada, M., Sakoda, S., 2003. Microglial Cell Cycle-Associated Proteins Control Microglial Proliferation in Vivo and

in Vitro and Are Regulated by GM-CSF and Density-Dependent Inhibition. J. Neurosci. Res. 74, 898–905. https://doi.org/10.1002/jnr.10829
Kovtun, I. V., Liu, Y., Bjoras, M., Klungland, A., Wilson, S.H., McMurray, C.T., 2007. OGG1 initiates age-dependent CAG trinucleotide expansion in somatic cells. Nature 447, 447–452. https://doi.org/10.1038/nature05778
Kraft, A.D., Kaltenbach, L.S., Lo, D.C., Harry, G.J., 2012. Activated microglia proliferate at neurites of mutant huntingtin-expressing neurons. Neurobiol. Aging 33, 621.e17-621.e33. https://doi.org/10.1016/j.neurobiolaging.2011.02.015
Krencik, R., Seo, K., van Asperen, J. V., Basu, N., Cvetkovic, C., Barlas, S., Chen, R., Ludwig, C., Wang, C., Ward, M.E., Gan, L., Horner, P.J., Rowitch, D.H., Ullian, E.M., 2017. Systematic Three-Dimensional Coculture Rapidly Recapitulates Interactions between Human Neurons and Astrocytes. Stem Cell Reports. https://doi.org/10.1016/j.stemcr.2017.10.026
Kumar, H., Kawai, T., Akira, S., 2011. Pathogen Recognition by the Innate Immune System. Int. Rev. Immunol. 30, 16–34. https://doi.org/10.3109/08830185.2010.529976
Kurkowska-Jastrzębska, I., Litwin, T., Joniec, I., Ciesielska, A., Przybyłkowski, A., Członkowski, A., Członkowska, A., 2004. Dexamethasone protects against dopaminergic neurons damage in a mouse model of Parkinson's disease. Int. Immunopharmacol. 4, 1307–1318. https://doi.org/10.1016/J.INTIMP.2004.05.006
Kwan, W., Träger, U., Davalos, D., Chou, A., Bouchard, J., Andre, R., Miller, A.A.A., Weiss, A., Giorgini, F., Cheah, C., Möller, T., Stella, N., Akassoglou, K., Tabrizi, S.J., Muchowski, P.J., Sassone, J., Colciago, C., Cislaghi, G., Silani, V., Ciammola, A., Burg, J. van der, Bjorkqvist, M., Brundin, P., Hult, S., Bjorkqvist, M., Propert, D., Lodi, R., Aziz, N., Burg, J. van der, Landwehrmeyer, G., Brundin, P., Stijnen, T., Roos, R., Moscovitch-Lopatin, M., Leblhuber, F., Dalrymple, A., Bjorkqvist, M., Wild, E., Anderson, A., Roncaroli, F., Hodges, A., Deprez, M., Turkheimer, F., Borovecki, F., Runne, H., Kwan, W., Sapp, E., Vonsattel, J., Myers, R., Stevens, T., Ferrante, R., Bird, E., Richardson, E., Simmons, D., Casale, M., Alcon, B., Pham, N., Narayan, N., Lynch, G., Lotharius, J., Tai, Y., Tai, Y., Politis, M., Luster, A., Alon, R., Andrian, U. von, Madri, J., Graesser, D., Stossel, T., Jones, G., Inoue, K., Koizumi, S., Davalos, D., Nimmerjahn, A., Kirchhoff, F., Helmchen, F., Wake, H., Moorhouse, A., Jinno, S., Kohsaka, S., Nabekura, J., Kurihara, T., Warr, G., Loy, J., Bravo, R., Blundell, M., Worth, A., Bouma, G., Thrasher, A., Slow, E., Gray, M., Blasi, E., Barluzzi, R., Bocchini, V., Mazzolla, R., Bistoni, F., Haynes, S., Irino, Y., Nakamura, Y., Inoue, K., Kohsaka, S., Ohsawa, K., Miller, A.A.A., Stella, N., McKercher, S., Ransohoff, R., Cardona, A., Ginhoux, F., Boillee, S., Ohsawa, K., Imai, Y., Kanazawa, H., Sasaki, Y., Kohsaka, S., Imai, Y., Kohsaka, S., Dawe, H., Minamide, L., Bamburg, J., Cramer, L., Wang, Y., Shibasaki, F., Mizuno, K., Munsie, L., Ma, L., Morton, A., Nicholson, L., Lynch, G., Reis, S., Myre, M., Lumsden, A., Thompson, M., Wasco, W., Macdonald, M., Gusella, J., Pascual, O., Achour, S. Ben, Rostaing, P., Triller, A., Bessis, A., Cardona, A., Zwilling, D., Goodman, J., Van, M., Gopinath, S., Robertson, C., Chaparro-Huerta, V., Rivera-Cervantes, M., Flores-Soto, M., Gomez-Pinedo, U., Beas-Zarate, C., Rogers, J., Rampersad, R., Ishida, Y., Gao, J., Murphy, P., Boring, L., Christensen, P.,

Lanska, D., Lanska, M., Lavine, L., Schoenberg, B., Herring, A., Koh, W., Kaminski, N., Ehrhart, J., Mukhopadhyay, S., Palazuelos, J., Bouchar, J., Etzioni, A., Jung, S., Balcaitis, S., Weinstein, J., Li, S., Chamberlain, J., Moller, T., Saederup, N., Benn, C., Fox, H., Bates, G., 2012. Mutant huntingtin impairs immune cell migration in Huntington disease. J. Clin. Invest. 122, 4737–47. https://doi.org/10.1172/JCI64484.)

Labbadia, J., Cunliffe, H., Weiss, A., Katsyuba, E., Sathasivam, K., Seredenina, T., Woodman, B., Moussaoui, S., Frentzel, S., Luthi-Carter, R., Paganetti, P., Bates, G.P., 2011. Altered chromatin architecture underlies progressive impairment of the heat shock response in mouse models of Huntington disease. J. Clin. Invest. 121, 3306–3319. https://doi.org/10.1172/JCI57413

Labbadia, J., Morimoto, R.I., 2013. Huntington's disease: underlying molecular mechanisms and emerging concepts. Trends Biochem. Sci. 38, 378–85. https://doi.org/10.1016/j.tibs.2013.05.003

Labbadia, J., Novoselov, S.S., Bett, J.S., Weiss, A., Paganetti, P., Bates, G.P., Cheetham, M.E., 2012. Suppression of protein aggregation by chaperone modification of high molecular weight complexes. Brain 135, 1180–1196. https://doi.org/10.1093/brain/aws022

Lacy, P., Stow, J.L., 2011. Cytokine release from innate immune cells: association with diverse membrane trafficking pathways. Blood 118, 9–18. https://doi.org/10.1182/blood-2010-08-265892

Lambert, J.-C., Grenier-Boley, B., Chouraki, V., Heath, S., Zelenika, D., Fievet, N., Hannequin, D., Pasquier, F., Hanon, O., Brice, A., Epelbaum, J., Berr, C., Dartigues, J.-F., Tzourio, C., Campion, D., Lathrop, M., Amouyel, P., 2010. Implication of the Immune System in Alzheimer's Disease: Evidence from Genome-Wide Pathway Analysis. J. Alzheimer's Dis. 20, 1107–1118. https://doi.org/10.3233/JAD-2010-100018

Lambert, J.C., Heath, S., Even, G., Campion, D., Sleegers, K., Hiltunen, M., Combarros, O., Zelenika, D., Bullido, M.J., Tavernier, B., Letenneur, L., Bettens, K., Berr, C., Pasquier, F., Fiévet, N., Barberger-Gateau, P., Engelborghs, S., De Deyn, P., Mateo, I., Franck, A., Helisalmi, S., Porcellini, E., Hanon, O., De Pancorbo, M.M., Lendon, C., Dufouil, C., Jaillard, C., Leveillard, T., Alvarez, V., Bosco, P., Mancuso, M., Panza, F., Nacmias, B., Boss, P., Piccardi, P., Annoni, G., Seripa, D., Galimberti, D., Hannequin, D., Licastro, F., Soininen, H., Ritchie, K., Blanché, H., Dartigues, J.F., Tzourio, C., Gut, I., Van Broeckhoven, C., Alpérovitch, A., Lathrop, M., Amouyel, P., Arosio, B., Coto, E., Zompo, M. Del, Deramecourt, V., Epelbaum, J., Forti, P., Brice, A., Ferri, R., Scarpini, E., Siciliano, G., Solfrizzi, V., Sorbi, S., Spalletta, G., Ravaglia, G., Sahel, J., Valdivieso, F., Vepsäläinen, S., Pilotto, A., 2009. Genome-wide association study identifies variants at CLU and CR1 associated with Alzheimer's disease. Nat. Genet. 41, 1094–1099. https://doi.org/10.1038/ng.439

Lambert, J.C., Ibrahim-Verbaas, C.A., Harold, D., Naj, A.C., Sims, R., Bellenguez, C., Jun, G., DeStefano, A.L., Bis, J.C., Beecham, G.W., Grenier-Boley, B., Russo, G., Thornton-Wells, T.A., Jones, N., Smith, A. V, Chouraki, V., Thomas, C., Ikram, M.A., Zelenika, D., Vardarajan, B.N., Kamatani, Y., Lin, C.F., Gerrish, A., Schmidt, H., Kunkle, B., Fiévet, N., Amouyel, P., Pasquier, F., Deramecourt, V., De Bruijn, R.F.A.G., Amin, N., Hofman, A., Van Duijn, C.M., Dunstan, M.L., Hollingworth, P., Owen, M.J., O'Donovan, M.C., Jones, L., Holmans, P.A., Moskvina, V., Williams, J., Baldwin, C., Farrer, L.A., Choi, S.H., Lunetta, K.L., Fitzpatrick, A.L., Harris,

T.B., Psaty, B.M., Gilbert, J.R., Hamilton-Nelson, K.L., Martin, E.R., Pericak-Vance, M.A., Haines, J.L., Gudnason, V., Jonsson, P. V, Eiriksdottir, G., Bihoreau, M.T., Lathrop, M., Valladares, O., Cantwell, L.B., Wang, L.S., Schellenberg, G.D., Ruiz, A., Boada, M., Reitz, C., Mayeux, R., Ramirez, A., Maier, W., Hanon, O., Kukull, W.A., Buxbaum, J.D., Campion, D., Wallon, D., Hannequin, D., Crane, P.K., Larson, E.B., Becker, T., Cruchaga, C., Goate, A.M., Craig, D., Johnston, J.A., Mc-Guinness, B., Todd, S., Passmore, P., Berr, C., Ritchie, K., Lopez, O.L., De Jager, P.L., Evans, D., Lovestone, S., Proitsi, P., Powell, J.F., Letenneur, L., Barberger-Gateau, P., Dufouil, C., Dartigues, J.F., Morón, F.J., Rubinsztein, D.C., St. George-Hyslop, P., Sleegers, K., Bettens, K., Van Broeckhoven, C., Huentelman, M.J., Gill, M., Brown, K., Morgan, K., Kamboh, M.I., Keller, L., Fratiglioni, L., Green, R., Myers, A.J., Love, S., Rogaeva, E., Gallacher, J., Bayer, A., Clarimon, J., Lleo, A., Tsuang, D.W., Yu, L., Bennett, D.A., Tsolaki, M., Bossù, P., Spalletta, G., Collinge, J., Mead, S., Sorbi, S., Nacmias, B., Sanchez-Garcia, F., Deniz Naranjo, M.C., Fox, N.C., Hardy, J., Bosco, P., Clarke, R., Brayne, C., Galimberti, D., Mancuso, M., Matthews, F., Moebus, S., Mecocci, P., Del Zompo, M., Hampel, H., Pilotto, A., Bullido, M., Panza, F., Caffarra, P., Mayhaus, M., Pichler, S., Gu, W., Riemenschneider, M., Lannfelt, L., Ingelsson, M., Hakonarson, H., Carrasquillo, M.M., Zou, F., Younkin, S.G., Beekly, D., Alvarez, V., Coto, E., Razquin, C., Pastor, P., Mateo, I., Combarros, O., Faber, K.M., Foroud, T.M., Soininen, H., Hiltunen, M., Blacker, D., Mosley, T.H., Graff, C., Holmes, C., Montine, T.J., Rotter, J.I., Brice, A., Nalls, M.A., Kauwe, J.S.K., Boerwinkle, E., Schmidt, R., Rujescu, D., Tzourio, C., Nöthen, M.M., Launer, L.J., Seshadri, S., 2013. Meta-analysis of 74,046 individuals identifies 11 new susceptibility loci for Alzheimer's disease. Nat. Genet. 45, 1452–1458. https://doi.org/10.1038/ng.2802

Lamkanfi, M., Dixit, V.M., 2014. Mechanisms and Functions of Inflammasomes. Cell 157, 1013–1022. https://doi.org/10.1016/j.cell.2014.04.007

Langbehn, D.R., Hayden, M.R., Paulsen, J.S., 2010. CAG-repeat length and the age of onset in Huntington disease (HD): A review and validation study of statistical approaches. Am. J. Med. Genet. Part B Neuropsychiatr. Genet. 153B, 397–408. https://doi.org/10.1002/ajmg.b.30992

Lanska, D.J., Lavine, L., Lanska, M.J., Schoenberg, B.S., 1988. Huntington's disease mortality in the United States. Neurology 38, 769–72. https://doi.org/10.1212/WNL.38.5.769

Lara-Marquez, M.L., Mehta, V., Michalsky, M.P., Fleming, J.B., Besner, G.E., 2002. Heparin-Binding EGF-Like Growth Factor Down Regulates Proinflammatory Cytokine-Induced Nitric Oxide and Inducible Nitric Oxide Synthase Production in Intestinal Epithelial Cells. Nitric Oxide 6, 142–152. https://doi.org/10.1006/niox.2001.0393

Leavitt, B.R., Van Raamsdonk, J.M., Shehadeh, J., Fernandes, H., Murphy, Z., Graham, R.K., Wellington, C.L., Raymond, L.A., Hayden, M.R., Raamsdonk, J.M., Shehadeh, J., Fernandes, H., Murphy, Z., Graham, R.K., Wellington, C.L., Hayden, M.R., 2006. Wild-type huntingtin protects neurons from excitotoxicity. J. Neurochem. 96, 1121–1129. https://doi.org/10.1111/j.1471-4159.2005.03605.x

Leavitt, B.R.B., Guttman, J.A., Hodgson, J.G.J., Kimel, G.H., Singaraja, R., Vogl, A.W., Hayden, M.M.R., Andrew, S., Goldberg, Y., Kremer, B., Telenius, H., Theilmann, J., Adam, S., Starr, E., Squitieri, F., Lin, B.,

Kalchman, M., Graham, R., Hayden, M.M.R., Bao, J., Sharp, A., Wagster, M., Becher, M., Schilling, G., Ross, C.C., Dawson, V., Dawson, T., Becher, M., Kotzuk, J., Sharp, A., Davies, S., Bates, G., Price, D., Ross, C.C., Burke, J., Enghild, J., Martin, M., Jou, Y.-S., Myers, R., Roses, A., Vance, J., Strittmatter, W., Cooper, J., Schilling, G., Peters, M., Herring, W., Sharp, A., Kaminsky, Z., Masone, J., Khan, F., Delanoy, M., Borschelt, D., Dawson, V., Dawson, T., Ross, C.C., Davies, S., Turmaine, M., Cozens, B., DiFiglia, M., Sharp, A., Ross, C.C., Scherzinger, E., Wanker, E., Mangiarini, L., Bates, G., DiFiglia, M., Sapp, E., Chase, K., Davies, S., Bates, G., Vonsattel, J.-P., Aronin, N., Dragatsis, I., Levine, M., Zeitlin, S., Duyao, M., Auerbach, A., Ryan, A., Persichetti, F., Barnes, G., McNeil, S., Kowell, N., Ge, P., Vonsattel, J.-P., Gusella, J.J., Joyner, A., MacDonald, M., Goldberg, Y., Nicholson, D., Rasper, D., Kalchman, M., Koide, H., Graham, R., Bromm, M., Kazemi-Esfajani, P., Thornberry, N., Vaillancourt, J., Hayden, M.M.R., Gutekunst, C., Li, S.-H.S., Yi, H., Mulroy, J., Kuemmerle, S., Jones, R., Rye, D., Ferrante, R., Hersch, S., Li, X.-J.X., Hackam, A., Singaraja, R., Wellington, C., Metzler, M., McCutcheon, K., Zhang, T., Kalchman, M., Hayden, M.M.R., Hodgson, J.G.J., Agopyan, N., Gutekunst, C., Leavitt, B.R.B., LePiane, F., Singaraja, R., Smith, D., Bissada, N., McCutcheon, K., Nasir, J., Jamot, L., Li, X.-J.X., Stevens, M.M., Rosemond, E., Roder, J., Phillips, A., Rubin, E., Hersch, S., Hayden, M.M.R., Hodgson, J.G.J., Smith, D., McCutcheon, K., Koide, H., Nishiyama, K., Dinulos, M., Stevens, M.M., Bissada, N., Nasir, J., Kanazawa, I., Disteche, C., Rubin, E., Hayden, M.M.R., Group, H.D.C.R., Kalchman, M., Graham, R., Xia, G., Koide, H., Hodgson, J.G.J., Goldberg, Y., Gietz, R., Pickart, C., Hayden, M.M.R., Kalchman, M., Koide, H., McCutcheon, K., Graham, R., Nichol, K., Nishiyama, K., Kasemi-Esfarjani, P., Lynn, F., Wellington, C., Metzler, M., Goldberg, Y., Kanazawa, I., Gietz, R., Hayden, M.M.R., Li, H., Li, S.-H.S., Johnston, H., Shelbourne, P., Li, X.-J.X., Li, X.-J.X., Sharp, A., Nucifora, F., Schilling, G., Lanahan, A., Worely, P., Snyder, S., Ross, C.C., Lin, B., Nasir, J., MacDonald, H., Hutchison, G., Graham, R., Rommens, J., Hayden, M.M.R., MacDonald, M., Gusella, J.J., Martindale, D., Hackam, A., Weiczorek, A., Ellerby, L., Wellington, C., McCutcheon, K., Singaraja, R., Kazemi-Esfarjani, P., Devon, R., Bredesen, D., Tufaro, F., Hayden, M.M.R., Nasir, J., Floresco, S., O'Kusky, J., Diewert, V., Richman, J., Zeisler, J., Borowski, A., Marth, J., Phillips, A., Hayden, M.M.R., O'Kusky, J., Nasir, J., Cicchetti, F., Parent, A., Hayden, M.M.R., Rigamonti, D., Bauer, J., De-Fraja, C., Conti, L., Sipione, S., Sciorati, C., Clementi, E., Hackam, A., Hayden, M.M.R., Li, Y., Cooper, J., Ross, C.C., Govoni, S., Vincenz, C., Cattaneo, E., Sandou, F., Finkbinder, S., Devys, D., Greenberg, M., Schilling, G., Becher, M., Sharp, A., Jinnah, H., Duan, K., Kotzuk, J., Slunt, H., Ratovitski, T., Cooper, J., Jenkins, N., Copeland, N., Price, D., Ross, C.C., Borschelt, D., Sharp, A., Ross, C.C., Sisoda, S., Wanker, E., Rovira, C., Scherzinger, E., Hasenbank, R., Walter, S., Tait, D., Colicelli, J., Lehrach, H., Wellington, C., Ellerby, L., Hackam, A., Margolis, R., Trifiro, M., Singaraja, R., McCutcheon, K., Salvesen, G., Propp, S., Bromm, M., Rowland, K., Zhang, T., Rasper, D., Roy, S., Thornberry, N., Pinsky, L., Kakisuka, A., Ross, C.C., Nicholson, D., Bredesen, D., Hayden, M.M.R., Wellington, C., Singaraja, R., Ellerby, L., Savill, J., Roy, S., Leavitt, B.R.B., Cattaneo, E., Hackam, A., Sharp, A., Thornberry, N., Nicholson, D., Bredesen, D., Hayden, M.M.R., Wheeler, V.,

White, J., Gutekunst, C., Vrbanac, V., Weaver, M., Li, X.-J.X., Li, S.-H.S., Yi, H., Vonsattel, J.-P., Gusella, J.J., Hersch, S., Auerbach, W., Joyner, A., MacDonald, M., White, J., Auerbach, W., Duyao, M., Vonsattel, J.-P., Gusella, J.J., Joyner, A., MacDonald, M., Zeitlin, S., Liu, J., Chapman, D., Papaioannou, V., Esfratiadis, A., 2001. Wild-Type Huntingtin Reduces the Cellular Toxicity of Mutant Huntingtin In Vivo. Am. J. Hum. Genet. 68, 313–324. https://doi.org/10.1086/318207

Lee, J.-M., Wheeler, V.C., Chao, M.J., Vonsattel, J.P.G., Pinto, R.M., Lucente, D., Abu-Elneel, K., Ramos, E.M., Mysore, J.S., Gillis, T., MacDonald, M.E., Gusella, J.F., Harold, D., Stone, T.C., Escott-Price, V., Han, J., Vedernikov, A., Holmans, P., Jones, L., Kwak, S., Mahmoudi, M., Orth, M., Landwehrmeyer, G.B., Paulsen, J.S., Dorsey, E.R., Shoulson, I., Myers, R.H., 2015. Identification of Genetic Factors that Modify Clinical Onset of Huntington's Disease. Cell 162, 516–526. https://doi.org/10.1016/j.cell.2015.07.003

Lee, J., Kosaras, B., Del Signore, S.J., Cormier, K., McKee, A., Ratan, R.R., Kowall, N.W., Ryu, H., 2011. Modulation of lipid peroxidation and mitochondrial function improves neuropathology in Huntington's disease mice. Acta Neuropathol. 121, 487–498. https://doi.org/10.1007/s00401-010-0788-5

Lee, J.M., Correia, K., Loupe, J., Kim, K.H., Barker, D., Hong, E.P., Chao, M.J., Long, J.D., Lucente, D., Vonsattel, J.P.G., Pinto, R.M., Abu Elneel, K., Ramos, E.M., Mysore, J.S., Gillis, T., Wheeler, V.C., MacDonald, M.E., Gusella, J.F., McAllister, B., Massey, T., Medway, C., Stone, T.C., Hall, L., Jones, L., Holmans, P., Kwak, S., Ehrhardt, A.G., Sampaio, C., Ciosi, M., Maxwell, A., Chatzi, A., Monckton, D.G., Orth, M., Landwehrmeyer, G.B., Paulsen, J.S., Dorsey, E.R., Shoulson, I., Myers, R.H., 2019. CAG Repeat Not Polyglutamine Length Determines Timing of Huntington's Disease Onset. Cell 178, 887-900.e14. https://doi.org/10.1016/j.cell.2019.06.036

Lee, J.M., Wheeler, V.C., Chao, M.J., Vonsattel, J.P.G., Pinto, R.M., Lucente, D., Abu-Elneel, K., Ramos, E.M., Mysore, J.S., Gillis, T., MacDonald, M.E., Gusella, J.F., Harold, D., Stone, T.C., Escott-Price, V., Han, J., Vedernikov, A., Holmans, P., Jones, L., Kwak, S., Mahmoudi, M., Orth, M., Landwehrmeyer, G.B., Paulsen, J.S., Dorsey, E.R., Shoulson, I., Myers, R.H., 2015. Identification of Genetic Factors that Modify Clinical Onset of Huntington's Disease. Cell 162, 516–526. https://doi.org/10.1016/j.cell.2015.07.003

Lee, J.W., Lee, Y.K., Yuk, D.Y., Choi, D.Y., Ban, S.B., Oh, K.W., Hong, J.T., 2008. Neuro-inflammation induced by lipopolysaccharide causes cognitive impairment through enhancement of beta-amyloid generation. J. Neuroinflammation 5, 37. https://doi.org/10.1186/1742-2094-5-37

Lee, S.W., Park, H.J., Im, W., Kim, M., Hong, S., 2018. Repeated immune activation with low-dose lipopolysaccharide attenuates the severity of Huntington's disease in R6/2 transgenic mice. Animal Cells Syst. (Seoul). 22, 219–226. https://doi.org/10.1080/19768354.2018.1473291

Leschik, J., Eckenstaler, R., Nieweg, K., Lichtenecker, P., Brigadski, T., Gottmann, K., Lessmann, V., Lutz, B., 2013. Embryonic stem cells stably expressing BDNF-GFP exhibit a BDNF-release-dependent enhancement of neuronal differentiation. J. Cell Sci. 126, 5062–5073. https://doi.org/10.1242/jcs.135384

Lewis, E.A., Smith, G.A., 2016. Using Drosophila models of Huntington's

disease as a translatable tool. J. Neurosci. Methods 265, 89–98. https://doi.org/10.1016/j.jneumeth.2015.07.026
Li, H., Jiang, H., Zhang, B., Feng, J., 2018. Modeling Parkinson's Disease Using Patient-specific Induced Pluripotent Stem Cells. J. Parkinsons. Dis. 8, 479–493. https://doi.org/10.3233/JPD-181353
Li, J., Ramenaden, E.R., Peng, J., Koito, H., Volpe, J.J., Rosenberg, P.A., 2008. Tumor Necrosis Factor Mediates Lipopolysaccharide-Induced Microglial Toxicity to Developing Oligodendrocytes When Astrocytes Are Present. J. Neurosci. 28, 5321–5330. https://doi.org/10.1523/jneurosci.3995-07.2008
Li, Q., Barres, B.A., 2018. Microglia and macrophages in brain homeostasis and disease. Nat. Rev. Immunol. https://doi.org/10.1038/nri.2017.125
Li, S.-H., Cheng, A.L., Zhou, H., Lam, S., Rao, M., Li, H., Li, X.-J., 2002. Interaction of Huntington Disease Protein with Transcriptional Activator Sp1. Mol. Cell. Biol. 22, 1277–1287. https://doi.org/10.1128/mcb.22.5.1277-1287.2002
Li, S.-H., Gutekunst, C.-A., Hersch, S.M., Li, X.-J., 2018. Interaction of Huntingtin-Associated Protein with Dynactin P150 Glued. J. Neurosci. 18, 1261–1269. https://doi.org/10.1523/jneurosci.18-04-01261.1998
Li, S.-H., Schilling, G., Young, W.S., Li, X.-., Margolis, R.L., Stine, O.C., Wagster, M.V., Abbott, M.H., Franz, M.L., Ranen, N.G., Folstein, S.E., Hedreen, J.C., Ross, C.A., 1993. Huntington's disease gene (IT15) is widely expressed in human and rat tissues. Neuron 11, 985–993. https://doi.org/10.1016/0896-6273(93)90127-D
Li, X., Sapp, E., Valencia, A., Kegel, K.B., Qin, Z.H., Alexander, J., Masso, N., Reeves, P., Ritch, J.J., Zeitlin, S., Aronin, N., DiFiglia, M., 2008. A function of huntingtin in guanine nucleotide exchange on Rabll. Neuroreport 19, 1643–1647. https://doi.org/10.1097/WNR.0b013e328315cd4c
Li, X., Sapp, E., Valencia, A., Qin, Z.-H., Kegel, K.B., Yoder, J., Comer-Tierney, L.A., Esteves, M., Alexander, J., Masso, N., Sobin, L., DiFiglia, M., Standley, C., Bellve, K., Tuft, R., Lifshitz, L., Fogarty, K., Chase, K., Aronin, N., 2009. Mutant huntingtin impairs vesicle formation from recycling endosomes by interfering with Rab11 activity. Mol. Cell. Biol. 29, 6106–6116. https://doi.org/10.1128/MCB.00420-09
Li, X.J., Li, S.H., Sharp, A.H., Nucifora, F.C., Schilling, G., Lanahan, A., Worley, P., Snydert, S.H., Ross, C.A., 1995. A huntingtin-associated protein enriched in brain with implications for pathology. Nature 378, 398–402. https://doi.org/10.1038/378398a0
Liddelow, S.A., Guttenplan, K.A., Clarke, L.E., Bennett, F.C., Bohlen, C.J., Schirmer, L., Bennett, M.L., Münch, A.E., Chung, W.-S., Peterson, T.C., Wilton, D.K., Frouin, A., Napier, B.A., Panicker, N., Kumar, M., Buckwalter, M.S., Rowitch, D.H., Dawson, V.L., Dawson, T.M., Stevens, B., Barres, B.A., 2017. Neurotoxic reactive astrocytes are induced by activated microglia. Nature 541, 481–487. https://doi.org/10.1038/nature21029
Lin, C.-H., Tallaksen-Greene, S., Chien, W.-M., Cearley, J.A., Jackson, W.S., Crouse, A.B., Ren, S., Li, X.-J., Albin, R.L., Detloff, P.J., 2001. Neurological abnormalities in a knock-in mouse model of Huntington's disease. Hum. Mol. Genet. 10, 137–144. https://doi.org/10.1093/hmg/10.2.137
Lione, L.A., Carter, R.J., Hunt, M.J., Bates, G.P., Morton, A.J., Dunnett, S.B., 1999. Selective discrimination learning impairments in mice expressing the human Huntington's disease mutation. J. Neurosci. 19, 10428–37.
Liot, G., Zala, D., Pla, P., Mottet, G., Piel, M., Saudou, F., 2013. Mutant

Huntingtin alters retrograde transport of TrkB receptors in striatal dendrites. J. Neurosci. 33, 6298–309. https://doi.org/10.1523/JNEUROSCI.2033-12.2013
Liu, C., Chyr, J., Zhao, W., Xu, Y., Ji, Z., Tan, H., Soto, C., Zhou, X., 2018. Genome-wide association and mechanistic studies indicate that immune response contributes to Alzheimer's disease development. Front. Genet. https://doi.org/10.3389/fgene.2018.00410
Liu, T., Zhang, L., Joo, D., Sun, S.-C., 2017. NF-κB signaling in inflammation. Signal Transduct. Target. Ther. 2, 17023. https://doi.org/10.1038/sigtrans.2017.23
Liu, W., Kennington, L.A., Rosas, H.D., Hersch, S., Cha, J.-H., Zamore, P.D., Aronin, N., 2008. Linking SNPs to CAG repeat length in Huntington's disease patients. Nat. Methods 5, 951–953. https://doi.org/10.1038/nmeth.1261
Lobo, A., Launer, L.J., Fratiglioni, L., Andersen, K., Di Carlo, A., Breteler, M.M., Copeland, J.R., Dartigues, J.F., Jagger, C., Martinez-Lage, J., Soininen, H., Hofman, A., 2000. Prevalence of dementia and major subtypes in Europe: A collaborative study of population-based cohorts. Neurologic Diseases in the Elderly Research Group. Neurology 54, S4-9.
Lombardi, M.S., Jaspers, L., Spronkmans, C., Gellera, C., Taroni, F., Di Maria, E., Donato, S. Di, Kaemmerer, W.F., 2009. A majority of Huntington's disease patients may be treatable by individualized allele-specific RNA interference. Exp. Neurol. 217, 312–319. https://doi.org/10.1016/j.expneurol.2009.03.004
Long, J.D., Lee, J.-M., Aylward, E.H., Gillis, T., Mysore, J.S., Abu Elneel, K., Chao, M.J., Paulsen, J.S., MacDonald, M.E., Gusella, J.F., 2018. Genetic Modification of Huntington Disease Acts Early in the Prediagnosis Phase. Am. J. Hum. Genet. 103, 349–357. https://doi.org/10.1016/j.ajhg.2018.07.017
López-Sendón Moreno, J.L., García Caldentey, J., Trigo Cubillo, P., Ruiz Romero, C., García Ribas, G., Alonso Arias, M.A.A., García de Yébenes, M.J., Tolón, R.M., Galve-Roperh, I., Sagredo, O., Valdeolivas, S., Resel, E., Ortega-Gutierrez, S., García-Bermejo, M.L., Fernández Ruiz, J., Guzmán, M., García de Yébenes Prous, J., 2016. A double-blind, randomized, cross-over, placebo-controlled, pilot trial with Sativex in Huntington's disease. J. Neurol. 263, 1390–1400. https://doi.org/10.1007/s00415-016-8145-9
Lowry, W.E., Richter, L., Yachechko, R., Pyle, A.D., Tchieu, J., Sridharan, R., Clark, A.T., Plath, K., 2008. Generation of human induced pluripotent stem cells from dermal fibroblasts. Proc. Natl. Acad. Sci. 105, 2883–2888. https://doi.org/10.1073/pnas.0711983105
Lucin, K.M., Wyss-Coray, T., 2009. Immune activation in brain aging and neurodegeneration: too much or too little? Neuron 64, 110–22. https://doi.org/10.1016/j.neuron.2009.08.039
Luheshi, N.M., Kovács, K.J., Lopez-Castejon, G., Brough, D., Denes, A., 2011. Interleukin-1α expression precedes IL-1β after ischemic brain injury and is localised to areas of focal neuronal loss and penumbral tissues. J. Neuroinflammation 8, 186. https://doi.org/10.1186/1742-2094-8-186
Ma, B., Savas, J.N., Yu, M.S., Culver, B.P., Chao, M. V., Tanese, N., 2011. Huntingtin mediates dendritic transport of β-actin mRNA in rat neurons. Sci. Rep. 1, 140. https://doi.org/10.1038/srep00140

Ma, H., Morey, R., O'Neil, R.C., He, Y., Daughtry, B., Schultz, M.D., Hariharan, M., Nery, J.R., Castanon, R., Sabatini, K., Thiagarajan, R.D., Tachibana, M., Kang, E., Tippner-Hedges, R., Ahmed, R., Gutierrez, N.M., Van Dyken, C., Polat, A., Sugawara, A., Sparman, M., Gokhale, S., Amato, P., P.Wolf, D., Ecker, J.R., Laurent, L.C., Mitalipov, S., 2014. Abnormalities in human pluripotent cells due to reprogramming mechanisms. Nature 511, 177–183. https://doi.org/10.1038/nature13551

Mahé, C., Loetscher, E., Dev, K.K., Bobirnac, I., Otten, U., Schoeffter, P., 2005. Serotonin 5-HT7 receptors coupled to induction of interleukin-6 in human microglial MC-3 cells. Neuropharmacology. https://doi.org/10.1016/j.neuropharm.2005.01.025

Maiuri, T., Mocle, A.J., Hung, C.L., Xia, J., van Roon-Mom, W.M.C., Truant, R., 2016. Huntingtin is a scaffolding protein in the ATM oxidative DNA damage response complex. Hum. Mol. Genet. 26, ddw395. https://doi.org/10.1093/hmg/ddw395

Mangiarini, L., Sathasivam, K., Seller, M., Cozens, B., Harper, A., Hetherington, C., Lawton, M., Trottier, Y., Lehrach, H., Davies, S.W., Bates, G.P., 1996. Exon I of the HD gene with an expanded CAG repeat is sufficient to cause a progressive neurological phenotype in transgenic mice. Cell 87, 493–506. https://doi.org/10.1016/S0092-8674(00)81369-0

Marcora, E., Kennedy, M.B., 2010. The Huntington's disease mutation impairs Huntingtin's role in the transport of NF-??B from the synapse to the nucleus. Hum. Mol. Genet. 19, 4373–4384. https://doi.org/10.1093/hmg/ddq358

Marín-Teva, J.L., Cuadros, M.A., Martín-Oliva, D., Navascués, J., 2012. Microglia and neuronal cell death. Neuron Glia Biol. https://doi.org/10.1017/S1740925X12000014

Martin, D.D.O., Ladha, S., Ehrnhoefer, D.E., Hayden, M.R., 2015. Autophagy in Huntington disease and huntingtin in autophagy. Trends Neurosci. https://doi.org/10.1016/j.tins.2014.09.003

Martinez, F.O., Gordon, S., 2014. The M1 and M2 paradigm of macrophage activation: time for reassessment. F1000Prime Rep. 6, 13. https://doi.org/10.12703/P6-13

Massey, T.H., Jones, L., 2018. The central role of DNA damage and repair in CAG repeat diseases. Dis. Model. Mech. 11. https://doi.org/10.1242/dmm.031930

McAdam, E., Haboubi, H.N., Forrester, G., Eltahir, Z., Spencer-Harty, S., Davies, C., Griffiths, A.P., Baxter, J.N., Jenkins, G.J.S., 2012. Inducible Nitric Oxide Synthase (iNOS) and Nitric Oxide (NO) are Important Mediators of Reflux-induced Cell Signalling in Esophageal Cells. Carcinogenesis 33, 2035–2043. https://doi.org/10.1093/carcin/bgs241

McBride, J.L., Pitzer, M.R., Boudreau, R.L., Dufour, B., Hobbs, T., Ojeda, S.R., Davidson, B.L., 2011. Preclinical safety of RNAi-mediated HTT suppression in the rhesus macaque as a potential therapy for Huntington's disease. Mol. Ther. 19, 2152–2162. https://doi.org/10.1038/mt.2011.219

McClory, H., Williams, D., Sapp, E., Gatune, L.W., Wang, P., DiFiglia, M., Li, X., 2014. Glucose transporter 3 is a rab11-dependent trafficking cargo and its transport to the cell surface is reduced in neurons of CAG140 Huntington's disease mice. Acta Neuropathol. Commun. https://doi.org/10.1186/s40478-014-0178-7

McColgan, P., Seunarine, K.K., Gregory, S., Razi, A., Papoutsi, M., Long, J.D.,

Mills, J.A., Johnson, E., Durr, A., Roos, R.A.C.A.A.C., Leavitt, B.R., Stout, J.C., Scahill, R.I., Clark, C.A., Rees, G., Tabrizi, S.J., Investigators, the T.-O.H., Durr, A., Scahill, R.I., Roos, R.A.C.A.A.C., McColgan, P., Mills, J.A., Papoutsi, M., Johnson, E., Tabrizi, S.J., Investigators, the T.-O.H., Clark, C.A., Gregory, S., Rees, G., Long, J.D., Seunarine, K.K., Gregory, S., Razi, A., Papoutsi, M., Long, J.D., Mills, J.A., Johnson, E., Durr, A., Roos, R.A.C.A.A.C., Leavitt, B.R., Stout, J.C., Scahill, R.I., Clark, C.A., Rees, G., Tabrizi, S.J., Investigators, the T.-O.H., 2017. Topological length of white matter connections predicts their rate of atrophy in premanifest Huntington's disease. JCI Insight 2. https://doi.org/10.1172/jci.insight.92641

McColgan, P., Tabrizi, S.J., 2018. Huntington's disease: a clinical review. Eur. J. Neurol. 25, 24–34. https://doi.org/10.1111/ene.13413

McCoy, M.K., Ruhn, K.A., Martinez, T.N., McAlpine, F.E., Blesch, A., Tansey, M.G., 2008. Intranigral Lentiviral Delivery of Dominant-negative TNF Attenuates Neurodegeneration and Behavioral Deficits in Hemiparkinsonian rats. Mol. Ther. 16, 1572–1579. https://doi.org/10.1038/MT.2008.146

McGeer, P.L., Itagaki, S., Tago, H., McGeer, E.G., 1988. Occurrence of HLA-DR Reactive Microglia in Alzheimer's Disease. Ann. N. Y. Acad. Sci. 540, 319–323. https://doi.org/10.1111/j.1749-6632.1988.tb27086.x

McGuire, J.R., Rong, J., Li, S.H., Li, X.J., 2006. Interaction of Huntingtin-associated protein-1 with kinesin light chain: Implications in intracellular trafficking in neurons. J. Biol. Chem. 281, 3552–3559. https://doi.org/10.1074/jbc.M509806200

McKinstry, S.U., Karadeniz, Y.B., Worthington, A.K., Hayrapetyan, V.Y., Ozlu, M.I., Serafin-Molina, K., Risher, W.C., Ustunkaya, T., Dragatsis, I., Zeitlin, S., Yin, H.H., Eroglu, C., 2014. Huntingtin Is Required for Normal Excitatory Synapse Development in Cortical and Striatal Circuits. J. Neurosci. 34, 9455–9472. https://doi.org/10.1523/JNEUROSCI.4699-13.2014

Medzhitov, R., Janeway, C., 2000. Innate Immunity. N. Engl. J. Med. 343, 338–344. https://doi.org/10.1056/NEJM200008033430506

Medzhitov, R., Janeway, C.A., 1997. Innate immunity: the virtues of a nonclonal system of recognition. Cell 91, 295–8. https://doi.org/10.1016/S0092-8674(00)80412-2

Mehrabi, N.F., Waldvogel, H.J., Tippett, L.J., Hogg, V.M., Synek, B.J., Faull, R.L.M., 2016. Symptom heterogeneity in Huntington's disease correlates with neuronal degeneration in the cerebral cortex. Neurobiol. Dis. https://doi.org/10.1016/j.nbd.2016.08.015

Melief, J., Sneeboer, M.A.M., Litjens, M., Ormel, P.R., Palmen, S.J.M.C., Huitinga, I., Kahn, R.S., Hol, E.M., de Witte, L.D., 2016. Characterizing primary human microglia: A comparative study with myeloid subsets and culture models. Glia 64, 1857–1868. https://doi.org/10.1002/glia.23023

Mestas, J., Hughes, C.C.W., 2004. Of Mice and Not Men: Differences between Mouse and Human Immunology. J. Immunol. 172, 2731–2738. https://doi.org/10.4049/jimmunol.172.5.2731

Metzler, M., Chen, N., Helgason, C.D., Graham, R.K., Nichol, K., McCutcheon, K., Nasir, J., Humphries, R.K., Raymond, L.A., Hayden, M.R., 1999. Life Without Huntingtin. Normal Differentiation into FunctionalNeurons. J. Neurochem. 72, 1009–1018. https://doi.org/10.1046/j.1471-4159.1999.0721009.x

Mievis, S., Levivier, M., Communi, D., Vassart, G., Brotchi, J., Ledent, C., Blum,

D., 2007. Lack of minocycline efficiency in genetic models of Huntington's disease. Neuromolecular Med. 9, 47–54.
Mihm, M.J., Amann, D.M., Schanbacher, B.L., Altschuld, R.A., Bauer, J.A., Hoyt, K.R., 2007. Cardiac dysfunction in the R6/2 mouse model of Huntington's disease. Neurobiol. Dis. 25, 297–308. https://doi.org/10.1016/j.nbd.2006.09.016
Miller, J.R., Lo, K.K., Andre, R., Moss, D.J.H., Träger, U., Stone, T.C., Jones, L., Holmans, P., Plagnol, V., Tabrizi, S.J., 2016. RNA-Seq of Huntington's Disease Patient Myeloid Cells Reveals Innate Transcriptional Dysregulation Associated With Proinflammatory Pathway Activation. Hum. Mol. Genet. 0, ddw142. https://doi.org/10.1093/hmg/ddw142
Miller, J.R.C., Pfister, E.L., Liu, W., Andre, R., Träger, U., Kennington, L.A., Lo, K., Dijkstra, S., Macdonald, D., Ostroff, G., Aronin, N., Tabrizi, S.J., 2017. Allele-Selective Suppression of Mutant Huntingtin in Primary Human Blood Cells. Sci. Rep. 7, 46740. https://doi.org/10.1038/srep46740
Minocha, S., Valloton, D., Arsenijevic, Y., Cardinaux, J.R., Guidi, R., Hornung, J.P., Lebrand, C., 2017. Nkx2.1 regulates the generation of telencephalic astrocytes during embryonic development. Sci. Rep. 7. https://doi.org/10.1038/srep43093
Mogi, M., Harada, M., Riederer, P., Narabayashi, H., Fujita, K., Nagatsu, T., 1994. Tumor necrosis factor-α (TNF-α) increases both in the brain and in the cerebrospinal fluid from parkinsonian patients. Neurosci. Lett. 165, 208–210. https://doi.org/10.1016/0304-3940(94)90746-3
Monier, A., Evrard, P., Gressens, P., Verney, C., 2006. Distribution and differentiation of microglia in the human encephalon during the first two trimesters of gestation. J. Comp. Neurol. 499, 565–582. https://doi.org/10.1002/cne.21123
Morrison, P., Harding-Lester, S., Bradley, A., 2011. Uptake of Huntington disease predictive testing in a complete population. Clin. Genet. 80, 281–286. https://doi.org/10.1111/j.1399-0004.2010.01538.x
Muffat, J., Li, Y., Yuan, B., Mitalipova, M., Omer, A., Corcoran, S., Bakiasi, G., Tsai, L.-H., Aubourg, P., Ransohoff, R.M., Jaenisch, R., 2016. Efficient derivation of microglia-like cells from human pluripotent stem cells. Nat. Med. 22, 1358–1367. https://doi.org/10.1038/nm.4189
Munsie, L., Caron, N., Atwal, R.S., Marsden, I., Wild, E.J., Bamburg, J.R., Tabrizi, S.J., Truant, R., 2011. Mutant huntingtin causes defective actin remodeling during stress: Defining a new role for transglutaminase 2 in neurodegenerative disease. Hum. Mol. Genet. 20, 1937–1951. https://doi.org/10.1093/hmg/ddr075
Murphy, K.P., Carter, R.J., Lione, L.A., Mangiarini, L., Mahal, A., Bates, G.P., Dunnett, S.B., Morton, A.J., 2000. Abnormal synaptic plasticity and impaired spatial cognition in mice transgenic for exon 1 of the human Huntington's disease mutation. J. Neurosci. 20, 5115–23. https://doi.org/10.1523/JNEUROSCI.20-13-05115.2000
Murray, C.L., Skelly, D.T., Cunningham, C., 2011. Exacerbation of CNS inflammation and neurodegeneration by systemic LPS treatment is independent of circulating IL-1β and IL-6. J. Neuroinflammation 8, 50. https://doi.org/10.1186/1742-2094-8-50
Myers, R.H., 2004. Huntington's disease genetics. NeuroRx 1, 255–62. https://doi.org/10.1602/neurorx.1.2.255
Myre, M.A., Lumsden, A.L., Thompson, M.N., Wasco, W., MacDonald, M.E.,

Gusella, J.F., 2011. Deficiency of Huntingtin Has Pleiotropic Effects in the Social Amoeba Dictyostelium discoideum. PLoS Genet. 7, e1002052. https://doi.org/10.1371/journal.pgen.1002052

Naj, A.C., Jun, G., Beecham, G.W., Wang, L.S., Vardarajan, B.N., Buros, J., Gallins, P.J., Buxbaum, J.D., Jarvik, G.P., Crane, P.K., Larson, E.B., Bird, T.D., Boeve, B.F., Graff-Radford, N.R., De Jager, P.L., Evans, D., Schneider, J.A., Carrasquillo, M.M., Ertekin-Taner, N., Younkin, S.G., Cruchaga, C., Kauwe, J.S.K., Nowotny, P., Kramer, P., Hardy, J., Huentelman, M.J., Myers, A.J., Barmada, M.M., Demirci, F.Y., Baldwin, C.T., Green, R.C., Rogaeva, E., George-Hyslop, P.S., Arnold, S.E., Barber, R., Beach, T., Bigio, E.H., Bowen, J.D., Boxer, A., Burke, J.R., Cairns, N.J., Carlson, C.S., Carney, R.M., Carroll, S.L., Chui, H.C., Clark, D.G., Corneveaux, J., Cotman, C.W., Cummings, J.L., Decarli, C., Dekosky, S.T., Diaz-Arrastia, R., Dick, M., Dickson, D.W., Ellis, W.G., Faber, K.M., Fallon, K.B., Farlow, M.R., Ferris, S., Frosch, M.P., Galasko, D.R., Ganguli, M., Gearing, M., Geschwind, D.H., Ghetti, B., Gilbert, J.R., Gilman, S., Giordani, B., Glass, J.D., Growdon, J.H., Hamilton, R.L., Harrell, L.E., Head, E., Honig, L.S., Hulette, C.M., Hyman, B.T., Jicha, G.A., Jin, L.W., Johnson, N., Karlawish, J., Karydas, A., Kaye, J.A., Kim, R., Koo, E.H., Kowall, N.W., Lah, J.J., Levey, A.I., Lieberman, A.P., Lopez, O.L., MacK, W.J., Marson, D.C., Martiniuk, F., Mash, D.C., Masliah, E., McCormick, W.C., McCurry, S.M., McDavid, A.N., McKee, A.C., Mesulam, M., Miller, B.L., Miller, C.A., Miller, J.W., Parisi, J.E., Perl, D.P., Peskind, E., Petersen, R.C., Poon, W.W., Quinn, J.F., Rajbhandary, R.A., Raskind, M., Reisberg, B., Ringman, J.M., Roberson, E.D., Rosenberg, R.N., Sano, M., Schneider, L.S., Seeley, W., Shelanski, M.L., Slifer, M.A., Smith, C.D., Sonnen, J.A., Spina, S., Stern, R.A., Tanzi, R.E., Trojanowski, J.Q., Troncoso, J.C., Van Deerlin, V.M., Vinters, H. V, Vonsattel, J.P., Weintraub, S., Welsh-Bohmer, K.A., Williamson, J., Woltjer, R.L., Cantwell, L.B., Dombroski, B.A., Beekly, D., Lunetta, K.L., Martin, E.R., Kamboh, M.I., Saykin, A.J., Reiman, E.M., Bennett, D.A., Morris, J.C., Montine, T.J., Goate, A.M., Blacker, D., Tsuang, D.W., Hakonarson, H., Kukull, W.A., Foroud, T.M., Haines, J.L., Mayeux, R., Pericak-Vance, M.A., Farrer, L.A., Schellenberg, G.D., 2011. Common variants at MS4A4/MS4A6E, CD2AP, CD33 and EPHA1 are associated with late-onset Alzheimer's disease. Nat. Genet. 43, 436–443. https://doi.org/10.1038/ng.801

Nakagawa, Y., Chiba, K., 2014. Role of microglial M1/M2 polarization in relapse and remission of psychiatric disorders and diseases. Pharmaceuticals. https://doi.org/10.3390/ph7121028

Nakanishi, H., 2003. Microglial Functions and Proteases. Mol. Neurobiol. 27, 163–176. https://doi.org/10.1385/MN:27:2:163

Nasir, J., Floresco, S.B., O'Kusky, J.R., Diewert, V.M., Richman, J.M., Zeisler, J., Borowski, A., Marth, J.D., Phillips, A.G., Hayden, M.R., 1995. Targeted disruption of the Huntington's disease gene results in embryonic lethality and behavioral and morphological changes in heterozygotes. Cell 81, 811–823. https://doi.org/10.1016/0092-8674(95)90542-1

Nath, S., Munsie, L.N., Truant, R., 2015. A huntingtin-mediated fast stress response halting endosomal trafficking is defective in Huntington's disease. Hum. Mol. Genet. 24, 450–462. https://doi.org/10.1093/hmg/ddu460

Nayak, D., Roth, T.L., McGavern, D.B., 2014. Microglia Development and Function. Annu. Rev. Immunol. 32, 367–402.

https://doi.org/10.1146/annurev-immunol-032713-120240
Neumann, H., Kotter, M.R., Franklin, R.J.M., 2009. Debris clearance by microglia: An essential link between degeneration and regeneration. Brain. https://doi.org/10.1093/brain/awn109
Neuwald, A.F., Hirano, T., 2000. HEAT repeats associated with condensins, cohesins, and other complexes involved in chromosome-related functions. Genome Res. 10, 1445–52. https://doi.org/10.1101/GR.147400
Nguyen, M.D., 2004. Exacerbation of Motor Neuron Disease by Chronic Stimulation of Innate Immunity in a Mouse Model of Amyotrophic Lateral Sclerosis. J. Neurosci. 24, 1340–1349. https://doi.org/10.1523/JNEUROSCI.4786-03.2004
Nimmerjahn, A., Kirchhoff, F., Helmchen, F., 2005. Resting microglial cells are highly dynamic surveillants of brain parenchyma in vivo. Science 308, 1314–8. https://doi.org/10.1126/science.1110647
Nishino, H., HIDA, H., KUMAZAKI, M., SHIMANO, Y., NAKAJIMA, K., SHIMIZU, H., OOIWA, T., BABA, H., 2000. The Striatum Is the Most Vulnerable Region in the Brain to Mitochondrial Energy Compromise: A Hypothesis to Explain Its Specific Vulnerability. J. Neurotrauma 17, 251–260. https://doi.org/10.1089/neu.2000.17.251
Njie, e. M.G., Boelen, E., Stassen, F.R., Steinbusch, H.W.M., Borchelt, D.R., Streit, W.J., 2012. Ex vivo cultures of microglia from young and aged rodent brain reveal age-related changes in microglial function. Neurobiol. Aging 33, 195.e1-195.e12. https://doi.org/10.1016/j.neurobiolaging.2010.05.008
Noda, M., Nakanishi, H., Nabekura, J., Akaike, N., 2000. AMPA–Kainate Subtypes of Glutamate Receptor in Rat Cerebral Microglia. J. Neurosci. https://doi.org/10.1523/jneurosci.20-01-00251.2000
Norden, D.M., Godbout, J.P., 2013. Microglia of the aged brain: Primed to be activated and resistant to regulation. Neuropathol. Appl. Neurobiol. https://doi.org/10.1111/j.1365-2990.2012.01306.x
Norflus, F., Nanje, A., Gutekunst, C.-A., Shi, G., Cohen, J., Bejarano, M., Fox, J., Ferrante, R.J., Hersch, S.M., 2004. Anti-inflammatory treatment with acetylsalicylate or rofecoxib is not neuroprotective in Huntington's disease transgenic mice. Neurobiol. Dis. 17, 319–325. https://doi.org/10.1016/j.nbd.2004.07.011
Norris, P.J., Waldvogel, H.J., Faull, R.L., Love, D.R., Emson, P.C., 1996. Decreased neuronal nitric oxide synthase messenger RNA and somatostatin messenger RNA in the striatum of Huntington's disease. Neuroscience 72, 1037–47.
Novak, M.J.U., Seunarine, K.K., Gibbard, C.R., Hobbs, N.Z., Scahill, R.I., Clark, C.A., Tabrizi, S.J., 2014. White matter integrity in premanifest and early Huntington's disease is related to caudate loss and disease progression. Cortex 52, 98–112. https://doi.org/10.1016/j.cortex.2013.11.009
Novak, M.J.U., Tabrizi, S.J., 2010. Huntington's disease. BMJ 340.
O'Kusky, J.R., Nasir, J., Cicchetti, F., Parent, A., Hayden, M.R., 1999. Neuronal degeneration in the basal ganglia and loss of pallido-subthalamic synapses in mice with targeted disruption of the Huntington's disease gene. Brain Res. 818, 468–479. https://doi.org/10.1016/S0006-8993(98)01312-2
O'Neill, L.A.J., Golenbock, D., Bowie, A.G., 2013. The history of Toll-like receptors - redefining innate immunity. Nat. Rev. Immunol. 13, 453–60. https://doi.org/10.1038/nri3446

Ochaba, J., Lukacsovich, T., Csikos, G., Zheng, S., Margulis, J., Salazar, L., Mao, K., Lau, A.L., Yeung, S.Y., Humbert, S., Saudou, F., Klionsky, D.J., Finkbeiner, S., Zeitlin, S.O., Marsh, J.L., Housman, D.E., Thompson, L.M., Steffan, J.S., 2014. Potential function for the Huntingtin protein as a scaffold for selective autophagy. Proc. Natl. Acad. Sci. 111, 16889–16894. https://doi.org/10.1073/pnas.1420103111

Ooi, J., Langley, S.R., Xu, X., Utami, K.H., Sim, B., Huang, Y., Harmston, N.P., Tay, Y.L., Ziaei, A., Zeng, R., Low, D., Aminkeng, F., Sobota, R.M., Ginhoux, F., Petretto, E., Pouladi, M.A., 2019. Unbiased Profiling of Isogenic Huntington Disease hPSC-Derived CNS and Peripheral Cells Reveals Strong Cell-Type Specificity of CAG Length Effects. Cell Rep. 26, 2494-2508.e7. https://doi.org/10.1016/j.celrep.2019.02.008

Ortega, Z., Díaz-Hernández, M., Maynard, C.J., Hernández, F., Dantuma, N.P., Lucas, J.J., 2010. Acute polyglutamine expression in inducible mouse model unravels ubiquitin/proteasome system impairment and permanent recovery attributable to aggregate formation. J. Neurosci. 30, 3675–3688. https://doi.org/10.1523/JNEUROSCI.5673-09.2010

Owen, D.R.J., Matthews, P.M., 2011. Imaging Brain Microglial Activation Using Positron Emission Tomography and Translocator Protein-Specific Radioligands, in: International Review of Neurobiology. Academic Press Inc., pp. 19–39. https://doi.org/10.1016/B978-0-12-387718-5.00002-X

Owen, J., 2012. Kuby Immunology. Kuby Immunol. 6, 574. https://doi.org/10.1016/S0076-6879(09)04815-0

Palis, J., Robertson, S., Kennedy, M., Wall, C., Keller, G., 1999. Development of erythroid and myeloid progenitors in the yolk sac and embryo proper of the mouse. Development 126, 5073–5084.

Pallos, J., Bodai, L., Lukacsovich, T., Purcell, J.M., Steffan, J.S., Thompson, L.M., Marsh, J.L., 2008. Inhibition of specific HDACs and sirtuins suppresses pathogenesis in a Drosophila model of Huntington's disease. Hum. Mol. Genet. 17, 3767–3775. https://doi.org/10.1093/hmg/ddn273

Pandya, H., Shen, M.J., Ichikawa, D.M., Sedlock, A.B., Choi, Y., Johnson, K.R., Kim, G., Brown, M.A., Elkahloun, A.G., Maric, D., Sweeney, C.L., Gossa, S., Malech, H.L., McGavern, D.B., Park, J.K., 2017. Differentiation of human and murine induced pluripotent stem cells to microglia-like cells. Nat. Neurosci. 20, 753–759. https://doi.org/10.1038/nn.4534

Paolicelli, R.C., Bolasco, G., Pagani, F., Maggi, L., Scianni, M., Panzanelli, P., Giustetto, M., Ferreira, T.A., Guiducci, E., Dumas, L., Ragozzino, D., Gross, C.T., 2011. Synaptic pruning by microglia is necessary for normal brain development. Science 333, 1456–8. https://doi.org/10.1126/science.1202529

Paraskevopoulou, F., Herman, M.A., Rosenmund, C., 2019. Glutamatergic Innervation onto Striatal Neurons Potentiates GABAergic Synaptic Output. J. Neurosci. 39, 4448–4460. https://doi.org/10.1523/jneurosci.2630-18.2019

Park, I.-H., Arora, N., Huo, H., Maherali, N., Ahfeldt, T., Shimamura, A., Lensch, M.W., Cowan, C., Hochedlinger, K., Daley, G.Q., 2008. Disease-specific induced pluripotent stem cells. Cell 134, 877–86. https://doi.org/10.1016/j.cell.2008.07.041

Park, L.C.., Zhang, H., Gibson, G.E., 2001. Co-culture with astrocytes or microglia protects metabolically impaired neurons. Mech. Ageing Dev. 123, 21–27. https://doi.org/10.1016/S0047-6374(01)00336-0

Parsons, M.P., Kang, R., Buren, C., Dau, A., Southwell, A.L., Doty, C.N., Sanders, S.S., Hayden, M.R., Raymond, L.A., 2014. Bidirectional Control of Postsynaptic Density-95 (PSD-95) Clustering by Huntingtin. J. Biol. Chem. 289, 3518–3528. https://doi.org/10.1074/jbc.M113.513945

Pattison, J.S., Sanbe, A., Maloyan, A., Osinska, H., Klevitsky, R., Robbins, J., 2008. Cardiomyocyte expression of a polyglutamine preamyloid oligomer causes heart failure. Circulation 117, 2743–51. https://doi.org/10.1161/CIRCULATIONAHA.107.750232

Pavese, N., Gerhard, A., Tai, Y.F., Ho, A.K., Turkheimer, F., Barker, R.A., Brooks, D.J., Piccini, P., 2006. Microglial activation correlates with severity in Huntington disease: A clinical and PET study. Neurology 66, 1638–1643. https://doi.org/10.1212/01.wnl.0000222734.56412.17

Pérez-Severiano, F., Escalante, B., Ríos, C., 1998. Nitric oxide synthase inhibition prevents acute quinolinate-induced striatal neurotoxicity. Neurochem. Res. 23, 1297–302.

Pérez-Severiano, F., Escalante, B., Vergara, P., Ríos, C., Segovia, J., 2002. Age-dependent changes in nitric oxide synthase activity and protein expression in striata of mice transgenic for the Huntington's disease mutation. Brain Res. 951, 36–42. https://doi.org/10.1016/S0006-8993(02)03102-5

Pérez-Severiano, F., Ríos, C., Segovia, J., 2000. Striatal oxidative damage parallels the expression of a neurological phenotype in mice transgenic for the mutation of Huntington's disease. Brain Res. 862, 234–237. https://doi.org/10.1016/S0006-8993(00)02082-5

Pérez-Severiano, F., Santamaría, A., Pedraza-Chaverri, J., Medina-Campos, O.N., Ríos, C., Segovia, J., 2004. Increased Formation of Reactive Oxygen Species, but No Changes in Glutathione Peroxidase Activity, in Striata of Mice Transgenic for the Huntington's Disease Mutation. Neurochem. Res. 29, 729–733. https://doi.org/10.1023/B:NERE.0000018843.83770.4b

Perl, D.P., 2010. Neuropathology of Alzheimer's disease. Mt. Sinai J. Med. 77, 32–42. https://doi.org/10.1002/msj.20157

Perlmutter, L.S., Scott, S.A., Barrón, E., Chui, H.C., 1992. MHC class II-positive microglia in human brain: Association with alzheimer lesions. J. Neurosci. Res. 33, 549–558. https://doi.org/10.1002/jnr.490330407

Petkau, T.L., Hill, A., Connolly, C., Lu, G., Wagner, P., Kosior, N., Blanco, J., Leavitt, B.R., 2019. Mutant huntingtin expression in microglia is neither required nor sufficient to cause the Huntington's disease-like phenotype in BACHD mice. Hum. Mol. Genet. https://doi.org/10.1093/hmg/ddz009

Petrik, D., Yun, S., Latchney, S.E., Kamrudin, S., LeBlanc, J.A., Bibb, J.A., Eisch, A.J., 2013. Early Postnatal In Vivo Gliogenesis From Nestin-Lineage Progenitors Requires Cdk5. PLoS One 8. https://doi.org/10.1371/journal.pone.0072819

Peyser, C.E., Folstein, M., Chase, G.A., Starkstein, S., Brandt, J., Cockrell, J.R., Bylsma, F., Coyle, J.T., McHugh, P.R., Folstein, S.E., 1995. Trial of d-α-tocopherol in Huntington's disease. Am. J. Psychiatry 152, 1771–1775. https://doi.org/10.1176/ajp.152.12.1771

Pfister, E.L., Kennington, L., Straubhaar, J., Wagh, S., Liu, W., DiFiglia, M., Landwehrmeyer, B., Vonsattel, J.P., Zamore, P.D., Aronin, N., 2009. Five siRNAs Targeting Three SNPs May Provide Therapy for Three-Quarters of Huntington's Disease Patients. Curr. Biol. 19, 774–778. https://doi.org/10.1016/j.cub.2009.03.030

Phillips, O., Squitieri, F., Sanchez-Castaneda, C., Elifani, F., Caltagirone, C., Sabatini, U., Di Paola, M., 2014. Deep white matter in Huntington's disease. PLoS One 9, e109676. https://doi.org/10.1371/journal.pone.0109676
Phillips, O.R., Joshi, S.H., Squitieri, F., Sanchez-Castaneda, C., Narr, K., Shattuck, D.W., Caltagirone, C., Sabatini, U., Di Paola, M., 2016. Major superficial white matter abnormalities in Huntington's disease. Front. Neurosci. https://doi.org/10.3389/fnins.2016.00197
Pitts, A., Dailey, K., Newington, J.T., Chien, A., Arseneault, R., Cann, T., Thompson, L.M., Cumming, R.C., 2012. Dithiol-based compounds maintain expression of antioxidant protein peroxiredoxin 1 that counteracts toxicity of mutant huntingtin. J. Biol. Chem. 287, 22717–22729. https://doi.org/10.1074/jbc.M111.334565
Pocock, J.M., Kettenmann, H., Liu, H., Leak, R.K., Hu, X., 2016. Neurotransmitter receptors on microglia. Stroke Vasc. Neurol. 1, 52–58. https://doi.org/10.1016/j.tins.2007.07.007
Politis, M., Lahiri, N., Niccolini, F., Su, P., Wu, K., Giannetti, P., Scahill, R.I., Turkheimer, F.E., Tabrizi, S.J., Piccini, P., 2015. Increased central microglial activation associated with peripheral cytokine levels in premanifest Huntington's disease gene carriers. Neurobiol. Dis. 83, 115–121. https://doi.org/10.1016/j.nbd.2015.08.011
Politis, M., Pavese, N., Tai, Y.F., Kiferle, L., Mason, S.L., Brooks, D.J., Tabrizi, S.J., Barker, R.A., Piccini, P., 2011. Microglial activation in regions related to cognitive function predicts disease onset in Huntington's disease: A multimodal imaging study. Hum. Brain Mapp. 32, 258–270. https://doi.org/10.1002/hbm.21008
Possel, H., Noack, H., Putzke, J., Wolf, G., Sies, H., 2000. Selective upregulation of inducible nitric oxide synthase (iNOS) by lipopolysaccharide (LPS) and cytokines in microglia: In vitro and in vivo studies. Glia 32, 51–59. https://doi.org/10.1002/1098-1136(200010)32:1<51::AID-GLIA50>3.0.CO;2-4
Pouladi, M.A., Morton, A.J., Hayden, M.R., 2013. Choosing an animal model for the study of Huntington's disease, Nature Reviews Neuroscience. Nature Publishing Group. https://doi.org/10.1038/nrn3570
Power, D., Srinivasan, S., Gunawardena, S., 2012. In-vivo evidence for the disruption of Rab11 vesicle transport by loss of huntingtin. Neuroreport 23, 970–977. https://doi.org/10.1097/WNR.0b013e328359d990
Prasad, A., Manivannan, J., Loong, D.T.B., Chua, S.M., Gharibani, P.M., All, A.H., 2016. A review of induced pluripotent stem cell, direct conversion by trans-differentiation, direct reprogramming and oligodendrocyte differentiation. Regen. Med. https://doi.org/10.2217/rme.16.5
Qiu, C., Kivipelto, M., von Strauss, E., 2009. Epidemiology of Alzheimer's disease: occurrence, determinants, and strategies toward intervention. Dialogues Clin. Neurosci. 11, 111–28.
Quarrell, O.W., Nance, M.A., Nopoulos, P., Paulsen, J.S., Smith, J.A., Squitieri, F., 2013. Managing juvenile Huntington's disease. Neurodegener. Dis. Manag. 3, 267–276. https://doi.org/10.2217/nmt.13.18
Quarrell, O.W.J., Nance, M.A., Nopoulos, P., Paulsen, J.S., Smith, J.A., Squitieri, F., 2013. Managing juvenile Huntington's disease. Neurodegener. Dis. Manag. 3. https://doi.org/10.2217/nmt.13.18
Radford, R.A., Morsch, M., Rayner, S.L., Cole, N.J., Pountney, D.L., Chung,

R.S., 2015. The established and emerging roles of astrocytes and microglia in amyotrophic lateral sclerosis and frontotemporal dementia. Front. Cell. Neurosci. https://doi.org/10.3389/fncel.2015.00414
Rando, T.A., Chang, H.Y., 2012. Aging, rejuvenation, and epigenetic reprogramming: resetting the aging clock. Cell 148, 46–57. https://doi.org/10.1016/j.cell.2012.01.003
Ranen, N.G., Peyser, C.E., Coyle, J.T., Bylsma, F.W., Sherr, M., Day, L., Folstein, M.F., Brandt, J., Ross, C.A., Folstein, S.E., 1996. A controlled trial of idebenone in Huntington's disease. Mov. Disord. 11, 549–554. https://doi.org/10.1002/mds.870110510
Ransohoff, R.M., Brown, M.A., 2012. Innate immunity in the central nervous system. J. Clin. Invest. 122, 1164–71. https://doi.org/10.1172/JCI58644
Rao, D.S., Chang, J.C., Kumar, P.D., Mizukami, I., Smithson, G.M., Bradley, S. V., Parlow, A.F., Ross, T.S., 2002. Huntingtin Interacting Protein 1 Is a Clathrin Coat Binding Protein Required for Differentiation of late Spermatogenic Progenitors. Mol. Cell. Biol. 21, 7796–7806. https://doi.org/10.1128/mcb.21.22.7796-7806.2001
Rawlins, M.D., Wexler, N.S., Wexler, A.R., Tabrizi, S.J., Douglas, I., Evans, S.J.W., Smeeth, L., 2016. The prevalence of huntington's disease. Neuroepidemiology. https://doi.org/10.1159/000443738
Rebec, G. V, Barton, S.J., Ennis, M.D., 2002. Dysregulation of ascorbate release in the striatum of behaving mice expressing the Huntington's disease gene. J. Neurosci. 22, RC202.
Renna, M., Jimenez-Sanchez, M., Sarkar, S., Rubinsztein, D.C., 2010. Chemical Inducers of Autophagy That Enhance the Clearance of Mutant Proteins in Neurodegenerative Diseases. J. Biol. Chem. 285, 11061–11067. https://doi.org/10.1074/jbc.R109.072181
Rigamonti, D., Bauer, J.H., De-Fraja, C., Conti, L., Sipione, S., Sciorati, C., Clementi, E., Hackam, A., Hayden, M.R., Li, Y., Cooper, J.K., Ross, C.A., Govoni, S., Vincenz, C., Cattaneo, E., 2000. Wild-type huntingtin protects from apoptosis upstream of caspase-3. J. Neurosci. 20, 3705–13. https://doi.org/20/10/3705 [pii]
Rigamonti, D., Sipione, S., Goffredo, D., Zuccato, C., Fossale, E., Cattaneo, E., 2001. Huntingtin's neuroprotective activity occurs via inhibition of procaspase-9 processing. J. Biol. Chem. 276, 14545–8. https://doi.org/10.1074/jbc.C100044200
Rikani, A.A., Choudhry, Z., Choudhry, A.M., Rizvi, N., Ikram, H., Mobassarah, N.J., Tulli, S., 2014. The mechanism of degeneration of striatal neuronal subtypes in Huntington disease. Ann. Neurosci. 21, 112–4. https://doi.org/10.5214/ans.0972.7531.210308
Rodrigues, F.B., Byrne, L., McColgan, P., Robertson, N., Tabrizi, S.J., Leavitt, B.R., Zetterberg, H., Wild, E.J., 2016. Cerebrospinal fluid total tau concentration predicts clinical phenotype in Huntington's disease. J. Neurochem. 139, 22–25. https://doi.org/10.1111/jnc.13719
Rong, J., McGuire, J.R., Fang, Z.-H., Sheng, G., Shin, J.-Y., Li, S.-H., Li, X.-J., 2006. Regulation of Intracellular Trafficking of Huntingtin-Associated Protein-1 Is Critical for TrkA Protein Levels and Neurite Outgrowth. J. Neurosci. 26, 6019–6030. https://doi.org/10.1523/JNEUROSCI.1251-06.2006
Roqué, P.J., Costa, L.G., 2017. Co-Culture of Neurons and Microglia. Curr. Protoc. Toxicol. https://doi.org/10.1002/cptx.32

Rosas, H.D., Hevelone, N.D., Zaleta, A.K., Greve, D.N., Salat, D.H., Fischl, B., 2005. Regional cortical thinning in preclinical Huntington disease and its relationship to cognition. Neurology 65, 745–747. https://doi.org/10.1212/01.wnl.0000174432.87383.87

Rosas, H.D., Salat, D.H., Lee, S.Y., Zaleta, A.K., Pappu, V., Fischl, B., Greve, D., Hevelone, N., Hersch, S.M., 2008. Cerebral cortex and the clinical expression of Huntington's disease: complexity and heterogeneity. Brain 131, 1057–68. https://doi.org/10.1093/brain/awn025

Ross, C.A., Aylward, E.H., Wild, E.J., Langbehn, D.R., Long, J.D., Warner, J.H., Scahill, R.I., Leavitt, B.R., Stout, J.C., Paulsen, J.S., Reilmann, R., Unschuld, P.G., Wexler, A., Margolis, R.L., Tabrizi, S.J., 2014. Huntington disease: Natural history, biomarkers and prospects for therapeutics, Nature Reviews Neurology. Nature Publishing Group. https://doi.org/10.1038/nrneurol.2014.24

Ross, C.A., Tabrizi, S.J., 2011. Huntington's disease: From molecular pathogenesis to clinical treatment. Lancet Neurol. https://doi.org/10.1016/S1474-4422(10)70245-3

Rubinsztein, D.C., Carmichael, J., 2003. Huntington's disease: molecular basis of neurodegeneration. Expert Rev. Mol. Med. 5, 1–21. https://doi.org/10.1017/S1462399403006549

Rui, Y.-N., Xu, Z., Patel, B., Chen, Z., Chen, D., Tito, A., David, G., Sun, Y., Stimming, E.F., Bellen, H.J., Cuervo, A.M., Zhang, S., 2015. Huntingtin functions as a scaffold for selective macroautophagy. Nat. Cell Biol. 17, 262–275. https://doi.org/10.1038/ncb3101

Ruzo, A., Croft, G.F., Metzger, J.J., Galgoczi, S., Gerber, L.J., Pellegrini, C., Wang, H., Fenner, M., Tse, S., Marks, A., Nchako, C., Brivanlou, A.H., 2018. Chromosomal instability during neurogenesis in Huntington's disease. Development 145, dev156844. https://doi.org/10.1242/dev.156844

Ryu, H., Lee, J., Hagerty, S.W., Soh, B.Y., McAlpin, S.E., Cormier, K.A., Smith, K.M., Ferrante, R.J., 2006. ESET/SETDB1 gene expression and histone H3 (K9) trimethylation in Huntington's disease. Proc. Natl. Acad. Sci. U. S. A. 103, 19176–81. https://doi.org/10.1073/pnas.0606373103

Sadri-Vakili, G., Bouzou, B., Benn, C.L., Kim, M.O., Chawla, P., Overland, R.P., Glajch, K.E., Xia, E., Qiu, Z., Hersch, S.M., Clark, T.W., Yohrling, G.J., Cha, J.H.J., 2007. Histones associated with downregulated genes are hypo-acetylated in Huntington's disease models. Hum. Mol. Genet. 16, 1293–1306. https://doi.org/10.1093/hmg/ddm078

Sadri-Vakili, G., Cha, J.-H.J., 2006. Mechanisms of disease: Histone modifications in Huntington's disease. Nat. Clin. Pract. Neurol. 2, 330–338. https://doi.org/10.1038/ncpneuro0199

Salichs, E., Ledda, A., Mularoni, L., Albà, M.M., de la Luna, S., 2009. Genome-wide analysis of histidine repeats reveals their role in the localization of human proteins to the nuclear speckles compartment. PLoS Genet. 5, e1000397. https://doi.org/10.1371/journal.pgen.1000397

Samaraweera, S.E., O'Keefe, L. V., Price, G.R., Venter, D.J., Richards, R.I., 2013. Distinct roles for toll and autophagy pathways in double-stranded RNA toxicity in a drosophila model of expanded repeat neurodegenerative diseases. Hum. Mol. Genet. 22, 2811–2819. https://doi.org/10.1093/hmg/ddt130

San Gil, R., Ooi, L., Yerbury, J.J., Ecroyd, H., 2017. The heat shock response in neurons and astroglia and its role in neurodegenerative diseases. Mol.

Neurodegener. 12, 65. https://doi.org/10.1186/s13024-017-0208-6
Sánchez-Pernaute, R., Ferree, A., Cooper, O., Yu, M., Brownell, A.-L., Isacson, O., 2004. Selective COX-2 inhibition prevents progressive dopamine neuron degeneration in a rat model of Parkinson's disease. J. Neuroinflammation 1, 6. https://doi.org/10.1186/1742-2094-1-6
Santamaría, A., Pérez-Severiano, F., Rodríguez-Martínez, E., Maldonado, P.D., Pedraza-Chaverri, J., Ríos, C., Segovia, J., 2001. Comparative analysis of superoxide dismutase activity between acute pharmacological models and a transgenic mouse model of Huntington's disease. Neurochem. Res. 26, 419–424. https://doi.org/10.1023/A:1010911417383
Sapp, E., Kegel, K.B., Aronin, N., Hashikawa, T., Uchiyama, Y., Tohyama, K., Bhide, P.G., Vonsattel, J.P., Difiglia, M., Vonsattel, J.P., Difiglia, M., Vonsattel, J.P., Myers, R., Stevens, T., Sotrel, A., Paskevich, P., Kiely, D., Rajkowska, F., Selemon, L., Goldman-Rakic, P., Myers, R., Vonsattel, J.P., Paskevich, P., Kreutzberg, G., Andersson, P., Perry, V., Gordon, S., Spielmeyer, W., Rio-Hortega, P. Del, Batchelor, P., Liberatore, G., Wong, J., McGeer, P., Iagaki, S., Boyes, B., McGeer, E., Paulus, W., Bancher, C., Jellinger, K., Muhleisen, H., Gehrmann, J., Meyermann, R., Langston, J., Forno, L., Tetrud, J., Rogers, J., Cooper, N., Webster, S., Obanion, J., Finch, C., Popovic, M., Caballero-Bleda, M., Puelles, L., Popovic, N., Velazquez, P., Cribbs, D., Poulos, T., Tenner, A., Watson, M., Roher, A., Kim, K., Weldon, D., Rogers, S., Ghilardi, J., Combs, C., Johnson, D., Cannady, S., Lehrmann, E., Molinari, A., Speciale, C., Schwarcz, R., Safer, D., Elzinga, M., Nachmias, V., Sanders, M., Goldstein, A., Wang, Y., Tohyama, K., Morita, T., Sato, N., Graeber, M., Bise, K., Mehraein, P., Difiglia, M., Sapp, E., Chase, K., Sapp, E., Schwarz, C., Chase, K., Yamamoto, M., Yamagishi, T., Yaginuma, H., Gondo, H., Kudo, J., White, J., Difiglia, M., Sapp, E., Chase, K., Safer, D., Sosnick, T., Elzinga, M., Cassimeris, L., Safer, D., Nachmias, V., Zigmond, S., Radewicz, K., Garey, L., Gentleman, S., Reynolds, R., Sapp, E., Penney, J., Young, A., Zalneraitis, E., Landis, D., Richardson, E., Selkoe, D., Jackson, M., Gentleman, G., Ward, L., Reiner, A., Albin, R., Anderson, K., Sapp, E., Ge, P., Aizawa, H., Dunlap, C., Monte, S.D. La, Vonsattel, J.P., Richardson, E., Avellino, A., Hart, D., Dailey, A., Mitchell, J., Sundstrom, L., Wheal, H., Gehrmann, J., Schoen, S., Kreutzberg, G., Alzheimer, A., Korematsu, K., Goto, S., Nagahir, S., Stichel, C., Muller, H., Neumann, H., Wekerle, H., Davies, S., Turmain, M., Cozens, B., Faber, P., Barnes, G., Srinidhi, J., Lee, D., Goldberg, A., Moulder, K., Onodera, O., Burke, J., Tan, J., Town, T., Paris, D., Graveland, G., Williams, R., Difiglia, M., Sotrel, A., Williams, R., Kaufmann, W., Myers, R., Lin, S., Morrison, B., Yamamoto, M., Shoda, A., Minamino, N., Leonard, D., Ziff, E., Greene, L., Carpintero, P., Anadon, R., Diaz-Regueira, S., Gomez-Marquez, J., Ballweber, E., Hannappel, E., Huff, T., Mannherz, H., Stewart, W., Kawas, C., Corrada, M., Metter, E., Mackenzie, I., Munoz, D., 2001. Early and progressive accumulation of reactive microglia in the Huntington disease brain. J. Neuropathol. Exp. Neurol. 60, 161–72. https://doi.org/10.1093/jnen/60.2.161
Saunders, A., Macosko, E.Z., Wysoker, A., Goldman, M., Krienen, F.M., de Rivera, H., Bien, E., Baum, M., Bortolin, L., Wang, S., Goeva, A., Nemesh, J., Kamitaki, N., Brumbaugh, S., Kulp, D., McCarroll, S.A., 2018. Molecular Diversity and Specializations among the Cells of the Adult Mouse Brain. Cell 174, 1015-1030.e16. https://doi.org/10.1016/j.cell.2018.07.028

Schafer, D.P., Stevens, B., 2015. Microglia function in central nervous system development and plasticity. Cold Spring Harb. Perspect. Biol. 7. https://doi.org/10.1101/cshperspect.a020545
Schafer, D.P., Stevens, B., 2010. Synapse elimination during development and disease: immune molecules take centre stage. Biochem. Soc. Trans. 38, 476–481. https://doi.org/10.1042/BST0380476
Schapansky, J., Nardozzi, J.D., Lavoie, M.J., 2015. The complex relationships between microglia, alpha-synuclein, and LRRK2 in Parkinson's disease. Neuroscience. https://doi.org/10.1016/j.neuroscience.2014.09.049
Schiess, M.C., Barnes, J.L., Ellmore, T.M., Poindexter, B.J., Dinh, K., Bick, R.J., 2010. CSF from Parkinson disease Patients Differentially Affects Cultured Microglia and Astrocytes. BMC Neurosci. 11. https://doi.org/10.1186/1471-2202-11-151
Schoonbroodt, S., Ferreira, V., Best-Belpomme, M., Boelaert, J.R., Legrand-Poels, S., Korner, M., Piette, J., 2000. Crucial role of the amino-terminal tyrosine residue 42 and the carboxyl-terminal PEST domain of I kappa B alpha in NF-kappa B activation by an oxidative stress. J. Immunol. 164, 4292–300. https://doi.org/10.4049/jimmunol.164.8.4292
Schroder, K., 2003. Interferon- : an overview of signals, mechanisms and functions. J. Leukoc. Biol. 75, 163–189. https://doi.org/10.1189/jlb.0603252
Schwarcz, R., Whetsell, W.O., Mangano, R.M., 1983. Quinolinic acid: An endogenous metabolite that produces axon-sparing lesions in rat brain. Science (80-.). 219, 316–318. https://doi.org/10.1126/science.6849138
Schwartz, M.P., Hou, Z., Propson, N.E., Zhang, J., Engstrom, C.J., Costa, V.S., Jiang, P., Nguyen, B.K., Bolin, J.M., Daly, W., Wang, Y., Stewart, R., Page, C.D., Murphy, W.L., Thomson, J.A., 2015. Human pluripotent stem cell-derived neural constructs for predicting neural toxicity. Proc. Natl. Acad. Sci. 112, 12516–12521. https://doi.org/10.1073/PNAS.1516645112
Shapouri-Moghaddam, A., Mohammadian, S., Vazini, H., Taghadosi, M., Esmaeili, S.-A., Mardani, F., Seifi, B., Mohammadi, A., Afshari, J.T., Sahebkar, A., 2018. Macrophage plasticity, polarization, and function in health and disease. https://doi.org/10.1002/jcp.26429
Shen, H., Kan, J.L.C., Green, M.R., 2004. Arginine-Serine-Rich Domains Bound at Splicing Enhancers Contact the Branchpoint to Promote Prespliceosome Assembly. Mol. Cell 13, 367–376. https://doi.org/10.1016/S1097-2765(04)00025-5
Shiga, Y., Tanaka-Matakatsu, M., Hayashi, S., Conti, L., Sipione, S., Sciorati, C., Clementi, E., Hackam, A., Hayden, M., Li, Y., 1996. A nuclear GFP/beta-galactosidase fusion protein as a marker for morphogenesis in living Drosophila. Dev. Growth Differ. 38, 99–106. https://doi.org/10.1046/j.1440-169X.1996.00012.x
Shin, J.-Y., Fang, Z.-H., Yu, Z.-X., Wang, C.-E., Li, S.-H., Li, X.-J., 2005. Expression of mutant huntingtin in glial cells contributes to neuronal excitotoxicity. J. Cell Biol. 171, 1001–12. https://doi.org/10.1083/jcb.200508072
Shobin, E., Bowley, M.P., Estrada, L.I., Heyworth, N.C., Orczykowski, M.E., Eldridge, S.A., Calderazzo, S.M., Mortazavi, F., Moore, T.L., Rosene, D.L., 2017. Microglia activation and phagocytosis: relationship with aging and cognitive impairment in the rhesus monkey. GeroScience 39, 199–220. https://doi.org/10.1007/s11357-017-9965-y
Sieradzan, K. a, Mechan, a O., Jones, L., Wanker, E.E., Nukina, N., Mann,

D.M., 1999. Huntington's disease intranuclear inclusions contain truncated, ubiquitinated huntingtin protein. Exp. Neurol. 156, 92–99. https://doi.org/10.1006/exnr.1998.7005
Silvestroni, A., Faull, R.L.M., Strand, A.D., Möllera, T., 2009. Distinct neuroinflammatory profile in post-mortem human Huntington's disease. Neuroreport 20, 1098–1103. https://doi.org/10.1097/WNR.0b013e32832e34ee
Simmons, D.A., 2017. Modulating Neurotrophin Receptor Signaling as a Therapeutic Strategy for Huntington's Disease. J. Huntingtons. Dis. 6, 303–325. https://doi.org/10.3233/JHD-170275
Singaraja, R.R., Hadano, S., Metzler, M., Givan, S., Wellington, C.L., Warby, S., Yanai, A., Gutekunst, C.-A., Leavitt, B.R., Yi, H., Fichter, K., Gan, L., McCutcheon, K., Chopra, V., Michel, J., Hersch, S.M., Ikeda, J.-E., Hayden, M.R., 2002. HIP14, a novel ankyrin domain-containing protein, links huntingtin to intracellular trafficking and endocytosis. Hum. Mol. Genet. 11, 2815–2828. https://doi.org/10.1093/hmg/11.23.2815
Singhrao, S.K., Neal, J.W., Morgan, B.P., Gasque, P., 1999. Increased complement biosynthesis by microglia and complement activation on neurons in Huntington's disease. Exp. Neurol. 159, 362–376. https://doi.org/10.1006/exnr.1999.7170
Skorokhod, O.A., Schwarzer, E., Ceretto, M., Arese, P., 2007. Malarial pigment haemozoin, IFN-gamma, TNF-alpha, IL-1beta and LPS do not stimulate expression of inducible nitric oxide synthase and production of nitric oxide in immuno-purified human monocytes. Malar. J. 6, 73. https://doi.org/10.1186/1475-2875-6-73
Slow, E.J., van Raamsdonk, J., Rogers, D., Coleman, S.H., Graham, R.K., Deng, Y., Oh, R., Bissada, N., Hossain, S.M., Yang, Y.-Z., Li, X.-J., Simpson, E.M., Gutekunst, C.-A., Leavitt, B.R., Hayden, M.R., 2003. Selective striatal neuronal loss in a YAC128 mouse model of Huntington disease. Hum. Mol. Genet. 12, 1555–1567. https://doi.org/10.1093/hmg/ddg169
Smith, A.M., Dragunow, M., 2014. The human side of microglia. Trends Neurosci. https://doi.org/10.1016/j.tins.2013.12.001
Smith, D.L., Woodman, B., Mahal, A., Sathasivam, K., Ghazi-Noori, S., Lowden, P.A.S., Bates, G.P., Hockly, E., 2003. Minocycline and doxycycline are not beneficial in a model of Huntington's disease. Ann. Neurol. 54, 186–196. https://doi.org/10.1002/ana.10614
Smith, M.R., Syed, A., Lukacsovich, T., Purcell, J., Barbaro, B.A., Worthge, S.A., Wei, S.R., Pollio, G., Magnoni, L., Scali, C., Massai, L., Franceschini, D., Camarri, M., Gianfriddo, M., Diodato, E., Thomas, R., Gokce, O., Tabrizi, S.J.J., Caricasole, A., Landwehrmeyer, B., Menalled, L., Murphy, C., Ramboz, S., Luthi-Carter, R., Westerberg, G., Marsh, J.L., 2014. A potent and selective sirtuin 1 inhibitor alleviates pathology in multiple animal and cell models of huntington's disease. Hum. Mol. Genet. 23, 2995–3007. https://doi.org/10.1093/hmg/ddu010
Smith, R., Bacos, K., Fedele, V., Soulet, D., Walz, H.A., Obermüller, S., Lindqvist, A., Björkqvist, M., Klein, P., Önnerfjord, P., Brundin, P., Mulder, H., Li, J.Y., 2009. Mutant huntingtin interacts with β-tubulin and disrupts vesicular transport and insulin secretion. Hum. Mol. Genet. 18, 3942–3954. https://doi.org/10.1093/hmg/ddp336
Solary, E., Droin, N., 2014. The emerging specificities of interleukin-34. J.

Leukoc. Biol. 95, 3–5. https://doi.org/10.1189/jlb.0813466
Sontag, E.M., Joachimiak, L.A., Tan, Z., Tomlinson, A., Housman, D.E., Glabe, C.G., Potkin, S.G., Frydman, J., Thompson, L.M., 2013. Exogenous delivery of chaperonin subunit fragment ApiCCT1 modulates mutant Huntingtin cellular phenotypes. Proc. Natl. Acad. Sci. 110, 3077–3082. https://doi.org/10.1073/pnas.1222663110
Squitieri, F., Cannella, M., Sgarbi, G., Maglione, V., Falleni, A., Lenzi, P., Baracca, A., Cislaghi, G., Saft, C., Ragona, G., Russo, M.A., Thompson, L.M., Solaini, G., Fornai, F., 2006. Severe ultrastructural mitochondrial changes in lymphoblasts homozygous for Huntington disease mutation. Mech. Ageing Dev. 127, 217–220. https://doi.org/10.1016/J.MAD.2005.09.010
Squitieri, F., Gellera, C., Cannella, M., Mariotti, C., Cislaghi, G., Rubinsztein, D.C., Almqvist, E.W., Turner, D., Bachoud-Lévi, A.C., Simpson, S.A., Delatycki, M., Maglione, V., Hayden, M.R., Di Donato, S., 2003. Homozygosity for CAG mutation in Huntington disease is associated with a more severe clinical course. Brain 126, 946–955. https://doi.org/10.1093/brain/awg077
Staal, R.G.W., Moller, T., 2014. Neuroinflammation in Huntington's disease, in: Neuroinflammation and Neurodegeneration. Springer Vienna, pp. 179–197. https://doi.org/10.1007/978-1-4939-1071-7_10
Stack, E.C., Matson, W.R., Ferrante, R.J., 2008. Evidence of Oxidant Damage in Huntington's Disease: Translational Strategies Using Antioxidants. Ann. N. Y. Acad. Sci. 1147, 79–92. https://doi.org/10.1196/annals.1427.008
Steffan, J.S., Bodai, L., Pallos, J., Poelman, M., McCampbell, A., Apostol, B.L., Kazantsev, A., Schmidt, E., Zhu, Y.Z., Greenwald, M., Kurokawa, R., Housman, D.E., Jackson, G.R., Marsh, J.L., Thompson, L.M., 2001. Histone deacetylase inhibitors arrest polyglutamine-dependent neurodegeneration in Drosophila. Nature 413, 739–743. https://doi.org/10.1038/35099568
Steffan, J.S., Kazantsev, A., Spasic-Boskovic, O., Greenwald, M., Zhu, Y.-Z.Z., Gohler, H., Wanker, E.E., Bates, G.P., Housman, D.E., Thompson, L.M., 2000. The Huntington's disease protein interacts with p53 and CREB-binding protein and represses transcription. Proc Natl Acad Sci USA 97, 6763–6768. https://doi.org/10.1073/pnas.100110097
Stenmark, H., Olkkonen, V.M., 2001. The Rab GTPase family. Genome Biol. 2, reviews3007.1. https://doi.org/10.1186/gb-2001-2-5-reviews3007
Stevens, B., Allen, N.J., Vazquez, L.E., Howell, G.R., Christopherson, K.S., Nouri, N., Micheva, K.D., Mehalow, A.K., Huberman, A.D., Stafford, B., Sher, A., Litke, A.M., Lambris, J.D., Smith, S.J., John, S.W.M., Barres, B.A., 2007. The Classical Complement Cascade Mediates CNS Synapse Elimination. Cell 131, 1164–1178. https://doi.org/10.1016/j.cell.2007.10.036
Stiles, D.K., Zhang, Z., Ge, P., Nelson, B., Grondin, R., Ai, Y., Hardy, P., Nelson, P.T., Guzaev, A.P., Butt, M.T., Charisse, K., Kosovrasti, V., Tchangov, L., Meys, M., Maier, M., Nechev, L., Manoharan, M., Kaemmerer, W.F., Gwost, D., Stewart, G.R., Gash, D.M., Sah, D.W.Y., 2012. Widespread suppression of huntingtin with convection-enhanced delivery of siRNA. Exp. Neurol. 233, 463–471. https://doi.org/10.1016/j.expneurol.2011.11.020
Strehlow, A.N.T., Li, J.Z., Myers, R.M., 2007. Wild-type huntingtin participates in protein trafficking between the Golgi and the extracellular space. Hum. Mol.

Genet. 16, 391–409. https://doi.org/10.1093/hmg/ddl467
Subramanian, A., Tamayo, P., Mootha, V.K., Mukherjee, S., Ebert, B.L., Gillette, M.A., Paulovich, A., Pomeroy, S.L., Golub, T.R., Lander, E.S., Mesirov, J.P., 2005. Gene set enrichment analysis: A knowledge-based approach for interpreting genome-wide expression profiles. Proc. Natl. Acad. Sci. https://doi.org/10.1073/pnas.0506580102
Szekely, C.A., Town, T., Zandi, P.P., 2007. NSAIDs for the chemoprevention of Alzheimer's disease. Subcell. Biochem. 42, 229–48.
Tabrizi, S.J., Leavitt, B.R., Landwehrmeyer, G.B., Wild, E.J., Saft, C., Barker, R.A., Blair, N.F., Craufurd, D., Priller, J., Rickards, H., Rosser, A., Kordasiewicz, H.B., Czech, C., Swayze, E.E., Norris, D.A., Baumann, T., Gerlach, I., Schobel, S.A., Paz, E., Smith, A. V., Bennett, C.F., Lane, R.M., 2019. Targeting Huntingtin Expression in Patients with Huntington's Disease. N. Engl. J. Med. 380, 2307–2316. https://doi.org/10.1056/nejmoa1900907
Tabrizi, S.J., Workman, J., Hart, P.E., Mangiarini, L., Mahal, A., Bates, G., Cooper, J.M., Schapira, A.H., 2000. Mitochondrial dysfunction and free radical damage in the Huntington R6/2 transgenic mouse. Ann. Neurol. 47, 80–6.
Tai, Y.F., Pavese, N., Gerhard, A., Tabrizi, S.J., Barker, R.A., Brooks, D.J., Piccini, P., 2007. Microglial activation in presymptomatic Huntington's disease gene carriers. Brain 130, 1759–1766. https://doi.org/10.1093/brain/awm044
Takada, Y., Mukhopadhyay, A., Kundu, G.C., Mahabeleshwar, G.H., Singh, S., Aggarwal, B.B., 2003. Hydrogen peroxide activates NF-kappa B through tyrosine phosphorylation of I kappa B alpha and serine phosphorylation of p65: evidence for the involvement of I kappa B alpha kinase and Syk protein-tyrosine kinase. J. Biol. Chem. 278, 24233–41. https://doi.org/10.1074/jbc.M212389200
Takahashi, K., Tanabe, K., Ohnuki, M., Narita, M., Ichisaka, T., Tomoda, K., Yamanaka, S., 2007. Induction of Pluripotent Stem Cells from Adult Human Fibroblasts by Defined Factors. Cell 131, 861–872. https://doi.org/10.1016/j.cell.2007.11.019
Takano, H., Gusella, J., 2002. The predominantly HEAT-like motif structure of huntingtin and its association and coincident nuclear entry with dorsal, an NF-kB/Rel/dorsal family transcription factor. BMC Neurosci. 3, 15. https://doi.org/10.1186/1471-2202-3-15
Tarique, A.A., Logan, J., Thomas, E., Holt, P.G., Sly, P.D., Fantino, E., 2015. Phenotypic, Functional, and Plasticity Features of Classical and Alternatively Activated Human Macrophages. Am. J. Respir. Cell Mol. Biol. 53, 676–688. https://doi.org/10.1165/rcmb.2015-0012OC
Taylor, M.W., Feng, G.S., 1991. Relationship between interferon-γ, indoleamine 2,3-dioxygenase, and tryptophan catabolism. FASEB J. 5, 2516–2522. https://doi.org/10.1096/fasebj.5.11.1907934
The Huntington Disease Collaborative Research Group, Macdonald, M.E., Ambrose, C.M., Duyao, M.P., Myers, R.H., Lin, C., Srinidhi, L., Barnes, G., Taylor, S.A., James, M., Groat, N., Macfarlane, H., Jenkins, B., Anderson, M.A., Wexler, N.S., Gusella, J.F., Riba-ramirer, L., Shah, M., Stanton, V.P., Strobel, S.A., Draths, K.M., Wales, J.L., Dervan, P., Housman, D.E., Fielder, T., Wasmuth, J.J., Tagle, D., Valdes, J., Elmer, L., Allard, M., Castilla, L., Swaroop, M., Blanchard, K., Bates, G.P., Baxendale, S.,

Hummerich, H., Kirby, S., North, M., Youngman, S., Mott, R., Zehetner, G., Sedlacek, Z., Snell, R., Holloway, T., Gillespie, K., Datson, N., Shaw, D., Harper, P.S., 1993. A Novel Gene Containing a Trinucleotide That Is Expanded and Unstable on Huntington ' s Disease Chromosomes. Cell 72, 971–983. https://doi.org/10.1016/0092-8674(93)90585-E

Thompson, L.M., Aiken, C.T., Kaltenbach, L.S., Agrawal, N., Illes, K., Khoshnan, A., Martinez-Vincente, M., Arrasate, M., O'Rourke, J.G., Khashwji, H., Lukacsovich, T., Zhu, Y.Z., Lau, A.L., Massey, A., Hayden, M.R., Zeitlin, S.O., Finkbeiner, S., Green, K.N., LaFerla, F.M., Bates, G., Huang, L., Patterson, P.H., Lo, D.C., Cuervo, A.M., Marsh, J.L., Steffan, J.S., 2009. IKK phosphorylates Huntingtin and targets it for degradation by the proteasome and lysosome. J. Cell Biol. 187, 1083–1099. https://doi.org/10.1083/jcb.200909067

Tourette, C., Li, B., Bell, R., O'Hare, S., Kaltenbach, L.S., Mooney, S.D., Hughes, R.E., 2014. A Large Scale Huntingtin Protein Interaction Network Implicates Rho GTPase Signaling Pathways in Huntington Disease. J. Biol. Chem. 289, 6709–6726. https://doi.org/10.1074/jbc.M113.523696

Trager, U., Andre, R., Lahiri, N., Magnusson-Lind, A., Weiss, A., Grueninger, S., McKinnon, C., Sirinathsinghji, E., Kahlon, S., Pfister, E.L., Moser, R., Hummerich, H., Antoniou, M., Bates, G.P., Luthi-Carter, R., Lowdell, M.W., Bjorkqvist, M., Ostroff, G.R., Aronin, N., Tabrizi, S.J., 2014. HTT-lowering reverses Huntington's disease immune dysfunction caused by NF B pathway dysregulation. Brain 137, 819–833. https://doi.org/10.1093/brain/awt355

Träger, U., Andre, R., Magnusson-Lind, A., Miller, J.R.C., Connolly, C., Weiss, A., Grueninger, S., Silajdžić, E., Smith, D.L., Leavitt, B.R., Bates, G.P., Björkqvist, M., Tabrizi, S.J., 2015. Characterisation of immune cell function in fragment and full-length Huntington's disease mouse models. Neurobiol. Dis. 73, 388–98. https://doi.org/10.1016/j.nbd.2014.10.012

Träger, Ulrike, Andre, Ralph, Lahiri, Nayana, Magnusson-Lind, A., Weiss, Andreas, Grueninger, Stephan, McKinnon, C., Sirinathsinghji, E., Kahlon, S., Pfister, E.L., Moser, R., Hummerich, H., Antoniou, M., Bates, G.P., Luthi-Carter, R., Lowdell, M.W., Björkqvist, Maria, Ostroff, G.R., Aronin, Neil, Tabrizi, S.J., Ajami, B., Bennett, J., Krieger, C., Tetzlaff, W., Rossi, F., Alciato, F., Sainaghi, P., Sola, D., Castello, L., Avanzi, G., Alderson, M., Armitage, R., Tough, T., Strockbine, L., Fanslow, W., Spriggs, M., Anderson, A., Cummings, B., Cotman, C., Andrew, S., Goldberg, Y., Kremer, B., Telenius, H., Theilmann, J., Adam, S., Aouadi, M., Tesz, G., Nicoloro, S., Wang, M., Chouinard, M., Soto, E., Baldo, B., Paganetti, P., Grueninger, S., Marcellin, D., Kaltenbach, L., Lo, D., Beinke, S., Ley, S., Benn, C., Sun, T., Sadri-Vakili, G., McFarland, K., DiRocco, D., Yohrling, G., Björkqvist, M., Wild, EJ., Thiele, J., Silvestroni, A., Andre, R., Lahiri, N., Bouchard, J., Truong, J., Bouchard, K., Dunkelberger, D., Desrayaud, S., Moussaoui, S., Brinkman, R., Mezei, M., Theilmann, J., Almqvist, E., Hayden, MR., Brück, W., Pförtner, R., Pham, T., Zhang, J., Hayardeny, L., Piryatinsky, V., Colin, E., Régulier, E., Perrin, V., Dürr, A., Brice, A., Aebischer, P., Comi, G., Jeffery, D., Kappos, L., Montalban, X., Boyko, A., Rocca, M., Dalrymple, A., Wild, EJ., Joubert, R., Sathasivam, K., Björkqvist, M., Petersén, A., DiFiglia, M., Sena-Esteves, M., Chase, K., Sapp, E., Pfister, E., Sass, M., Fan, J., Gladding, C., Wang, L., Zhang, L., Kaufman, A., Milnerwood, A., Gauthier, L., Charrin, B., Borrell-Pagès, M.,

Dompierre, J., Rangone, H., Cordelières, F., Gordon, S., Taylor, P., Grewal, I., Flavell, R., Gross, S., Piwnica-Worms, D., Guerreiro, R., Wojtas, A., Bras, J., Carrasquillo, M., Rogaeva, E., Majounie, E., Harold, D., Abraham, R., Hollingworth, P., Sims, R., Gerrish, A., Hamshere, M., Hayden, MS., Ghosh, S., Hodges, A., Strand, A., Aragaki, A., Kuhn, A., Sengstag, T., Hughes, G., Hsiao, H., Chen, Y., Chen, H., Tu, P., Chern, Y., Hunot, S., Brugg, B., Ricard, D., Michel, P., Muriel, M., Ruberg, M., Israël, A., Kaltschmidt, B., Uherek, M., Volk, B., Baeuerle, P., Kaltschmidt, C., Khoshnan, A., Ko, J., Watkin, E., Paige, L., Reinhart, P., Patterson, P., Khoshnan, A., Patterson, P., Kwan, W., Magnusson, A., Chou, A., Adame, A., Carson, M., Kohsaka, S., Kwan, W., Träger, U., Davalos, D., Chou, A., Bouchard, J., Andre, R., Lacy, P., Stow, J., Lambert, J., Heath, S., Even, G., Campion, D., Sleegers, K., Hiltunen, M., Li, S., Schilling, G., Young, W., Li, X., Margolis, R., Stine, O., Maguire, O., Collins, C., O'Loughlin, K., Miecznikowski, J., Minderman, H., Mattson, M., Meffert, M., Miyamoto, S., Munsie, L., Caron, N., Atwal, R., Marsden, I., Wild, EJ., Bamburg, J., Nucifora, F., Sasaki, M., Peters, M., Huang, H., Cooper, J., Yamada, M., O'Neill, L., Kaltschmidt, C., Perrin, V., Dufour, N., Raoul, C., Hassig, R., Brouillet, E., Aebischer, P., Rajesh, M., Mukhopadhyay, P., Bátkai, S., Haskó, G., Liaudet, L., Huffman, J., Ransohoff, R., Perry, V., Sah, D., Aronin, N., Sapp, E., Kegel, K., Aronin, N., Hashikawa, T., Uchiyama, Y., Tohyama, K., Simard, A., Rivest, S., Soulet, D., Cicchetti, F., Steffan, J., Steffan, J., Kazantsev, A., Spasic-Boskovic, O., Greenwald, M., Zhu, Y., Gohler, H., Sundström, C., Nilsson, K., Tai, Y., Pavese, N., Gerhard, A., Tabrizi, S., Barker, R., Brooks, D., Teng, F., Tang, B., Group, T.H.D.C.R., Thompson, L., Aiken, C., Kaltenbach, L., Agrawal, N., Illes, K., Khoshnan, A., Tobinick, E., Gross, H., Weinberger, A., Cohen, H., Burg, J. van der, Björkqvist, M., Brundin, P., Weiss, A., Träger, U., Wild, EJ., Grueninger, S., Farmer, R., Landles, C., Wexler, N., Lorimer, J., Porter, J., Gomez, F., Moskowitz, C., Shackell, E., Wild, E., Magnusson, A., Lahiri, N., Krus, U., Orth, M., Tabrizi, S., Zwilling, D., Huang, S., Sathyasaikumar, K., Notarangelo, F., Guidetti, P., Wu, H., 2014. HTT-lowering reverses Huntington's disease immune dysfunction caused by NFκB pathway dysregulation. Brain 137, 819–33. https://doi.org/10.1093/brain/awt355

Travessa, A.M., Rodrigues, F.B., Mestre, T.A., Ferreira, J.J., 2017. Fifteen Years of Clinical Trials in Huntington's Disease: A Very Low Clinical Drug Development Success Rate. J. Huntingtons. Dis. 6, 157–163. https://doi.org/10.3233/JHD-170245

Tremblay, M.-È., Lowery, R.L., Majewska, A.K., 2010. Microglial Interactions with Synapses Are Modulated by Visual Experience. PLoS Biol. 8, e1000527. https://doi.org/10.1371/journal.pbio.1000527

Tremblay, M.È., Majewska, A.K., 2011. A role for microglia in synaptic plasticity? Commun. Integr. Biol. 4, 220–222. https://doi.org/10.4161/cib.4.2.14506

Twelvetrees, A.E., Yuen, E.Y., Arancibia-Carcamo, I.L., MacAskill, A.F., Rostaing, P., Lumb, M.J., Humbert, S., Triller, A., Saudou, F., Yan, Z., Kittler, J.T., 2010. Delivery of GABAARs to Synapses Is Mediated by HAP1-KIF5 and Disrupted by Mutant Huntingtin. Neuron 65, 53–65. https://doi.org/10.1016/j.neuron.2009.12.007

Ueno, M., Fujita, Y., Tanaka, T., Nakamura, Y., Kikuta, J., Ishii, M., Yamashita, T., 2013. Layer v cortical neurons require microglial support for survival

during postnatal development. Nat. Neurosci. 16, 543–551. https://doi.org/10.1038/nn.3358
Valdeolivas, S., Sagredo, O., Delgado, M., Pozo, M.A., Fernández-Ruiz, J., 2017. Effects of a sativex-like combination of phytocannabinoids on disease progression in R6/2 mice, an experimental model of huntington's disease. Int. J. Mol. Sci. 18. https://doi.org/10.3390/ijms18040684
van der Burg, J.M., Björkqvist, M., Brundin, P., 2009. Beyond the brain: widespread pathology in Huntington's disease. Lancet Neurol. 8, 765–774. https://doi.org/10.1016/S1474-4422(09)70178-4
Van Raamsdonk, J.M., Murphy, Z., Selva, D.M., Hamidizadeh, R., Pearson, J., Petersén, Åsa, Björkqvist, M., Muir, C., Mackenzie, I.R., Hammond, G.L., Vogl, A.W., Hayden, M.R., Leavitt, B.R., 2007. Testicular degeneration in Huntington disease. Neurobiol. Dis. 26, 512–520. https://doi.org/10.1016/j.nbd.2007.01.006
Van Raamsdonk, J.M., Pearson, J., Murphy, Z., Hayden, M.R., Leavitt, B.R., 2006. Wild-type huntingtin ameliorates striatal neuronal atrophy but does not prevent other abnormalities in the YAC128 mouse model of Huntington disease. BMC Neurosci. 7, 80. https://doi.org/10.1186/1471-2202-7-80
Van Raamsdonk, J.M., Pearson, J., Rogers, D.A., Bissada, N., Vogl, A.W., Hayden, M.R., Leavitt, B.R., 2005. Loss of wild-type huntingtin influences motor dysfunction and survival in the YAC128 mouse model of Huntington disease. Hum. Mol. Genet. 14, 1379–1392. https://doi.org/10.1093/hmg/ddi147
Van Wilgenburg, B., Browne, C., Vowles, J., Cowley, S.A., 2013. Efficient, Long Term Production of Monocyte-Derived Macrophages from Human Pluripotent Stem Cells under Partly-Defined and Fully-Defined Conditions. PLoS One 8. https://doi.org/10.1371/journal.pone.0071098
Velier, J., Kim, M., Schwarz, C., Kim, T.W., Sapp, E., Chase, K., Aronin, N., DiFiglia, M., 1998. Wild-Type and Mutant Huntingtins Function in Vesicle Trafficking in the Secretory and Endocytic Pathways. Exp. Neurol. 152, 34–40. https://doi.org/10.1006/exnr.1998.6832
Venneti, S., Lopresti, B.J., Wiley, C.A., 2006. The peripheral benzodiazepine receptor (Translocator protein 18 kDa) in microglia: From pathology to imaging. Prog. Neurobiol. https://doi.org/10.1016/j.pneurobio.2006.10.002
Veres, A., Gosis, B.S., Ding, Q., Collins, R., Ragavendran, A., Brand, H., Erdin, S., Cowan, C.A., Talkowski, M.E., Musunuru, K., 2014. Low Incidence of Off-Target Mutations in Individual CRISPR-Cas9 and TALEN Targeted Human Stem Cell Clones Detected by Whole-Genome Sequencing. Cell Stem Cell 15, 27–30. https://doi.org/10.1016/J.STEM.2014.04.020
Verlinsky, Y., Strelchenko, N., Kukharenko, V., Rechitsky, S., Verlinsky, O., Galat, V., Kuliev, A., 2005. Human embryonic stem cell lines with genetic disorders. Reprod. Biomed. Online 10, 105–110. https://doi.org/10.1016/S1472-6483(10)60810-3
Vlad, S.C., Miller, D.R., Kowall, N.W., Felson, D.T., 2008. Protective effects of NSAIDs on the development of Alzheimer disease. Neurology 70, 1672–7. https://doi.org/10.1212/01.wnl.0000311269.57716.63
Volpato, V., Smith, J., Sandor, C., Ried, J.S., Baud, A., Handel, A., Newey, S.E., Wessely, F., Attar, M., Whiteley, E., Chintawar, S., Verheyen, A., Barta, T., Lako, M., Armstrong, L., Muschet, C., Artati, A., Cusulin, C., Christensen, K., Patsch, C., Sharma, E., Nicod, J., Brownjohn, P., Stubbs, V., Heywood, W.E., Gissen, P., De Filippis, R., Janssen, K., Reinhardt, P.,

Adamski, J., Royaux, I., Peeters, P.J., Terstappen, G.C., Graf, M., Livesey, F.J., Akerman, C.J., Mills, K., Bowden, R., Nicholson, G., Webber, C., Cader, M.Z., Lakics, V., 2018. Reproducibility of Molecular Phenotypes after Long-Term Differentiation to Human iPSC-Derived Neurons: A Multi-Site Omics Study. Stem Cell Reports 11, 897–911. https://doi.org/10.1016/j.stemcr.2018.08.013

von Hörsten, S., Schmitt, I., Nguyen, H.P., Holzmann, C., Schmidt, T., Walther, T., Bader, M., Pabst, R., Kobbe, P., Krotova, J., Stiller, D., Kask, A., Vaarmann, A., Rathke-Hartlieb, S., Schulz, J.B., Grasshoff, U., Bauer, I., Vieira-Saecker, A.M.M., Paul, M., Jones, L., Lindenberg, K.S., Landwehrmeyer, B., Bauer, A., Li, X.-J., Riess, O., 2003. Transgenic rat model of Huntington's disease. Hum. Mol. Genet. 12, 617–24.

Vonsattel, J.P., DiFiglia, M., 1998. Huntington Disease. J. Neuropathol. Exp. Neurol.

Waelter, S., Scherzinger, E., Hasenbank, R., Nordhoff, E., Lurz, R., Goehler, H., Gauss, C., Sathasivam, K., Bates, G.P., Lehrach, H., Wanker, E.E., 2001. The huntingtin interacting protein HIP1 is a clathrin and alpha-adaptin-binding protein involved in receptor-mediated endocytosis. Hum. Mol. Genet. 10, 1807–1817. https://doi.org/10.1093/hmg/10.17.1807

Wake, H., Moorhouse, A.J., Jinno, S., Kohsaka, S., Nabekura, J., 2009. Resting Microglia Directly Monitor the Functional State of Synapses In Vivo and Determine the Fate of Ischemic Terminals. https://doi.org/10.1523/JNEUROSCI.4363-08.2009

Wang, G., Liu, X., Gaertig, M.A., Li, S., Li, X.-J., 2016. Ablation of huntingtin in adult neurons is nondeleterious but its depletion in young mice causes acute pancreatitis. Proc. Natl. Acad. Sci. U. S. A. 113, 3359–64. https://doi.org/10.1073/pnas.1524575113

Wang, J.Q., Chen, Qian, Wang, X., Wang, Q.C., Wang, Y., Cheng, H.P., Guo, C., Sun, Q., Chen, Quan, Tang, T.S., 2013. Dysregulation of mitochondrial calcium signaling and superoxide flashes cause mitochondrial genomic DNA damage in Huntington disease. J. Biol. Chem. 288, 3070–3084. https://doi.org/10.1074/jbc.M112.407726

Wang, W., Duan, W., Igarashi, S., Morita, H., Nakamura, M., Ross, C.A., 2005. Compounds blocking mutant huntingtin toxicity identified using a Huntington's disease neuronal cell model. Neurobiol. Dis. 20, 500–508. https://doi.org/10.1016/J.NBD.2005.03.026

Waterman-Storer, C.M., Karki, S.B., Kuznetsov, S.A., Tabb, J.S., Weiss, D.G., Langford, G.M., Holzbaur, E.L.F., 2002. The interaction between cytoplasmic dynein and dynactin is required for fast axonal transport. Proc. Natl. Acad. Sci. 94, 12180–12185. https://doi.org/10.1073/pnas.94.22.12180

Wei, Z., Kale, S., El Fatimy, R., Rabinovsky, R., Krichevsky, A.M., 2019. Co-cultures of Glioma Stem Cells and Primary Neurons, Astrocytes, Microglia, and Endothelial Cells for Investigation of Intercellular Communication in the Brain. Front. Neurosci. 13, 361. https://doi.org/10.3389/fnins.2019.00361

Weiss, A., Träger, U., Wild, E.J., Grueninger, S., Farmer, R., Landles, C., Scahill, R.I., Lahiri, N., Haider, S., Macdonald, D., Frost, C., Bates, G.P., Bilbe, G., Kuhn, R., Andre, R., Tabrizi, S.J., 2012. Brief report Mutant huntingtin fragmentation in immune cells tracks Huntington ' s disease progression. J. Clin. Invest. 122, 3731–3736. https://doi.org/10.1172/JCI64565.at

White, J.A., Anderson, E., Zimmerman, K., Zheng, K.H., Rouhani, R., Gunawardena, S., 2015. Huntingtin differentially regulates the axonal transport of a sub-set of Rab-containing vesicles in vivo. Hum. Mol. Genet. 24, 7182–7195. https://doi.org/10.1093/hmg/ddv415

White, J.K., Auerbach, W., Duyao, M.P., Vonsattel, J.-P., Gusella, J.F., Joyner, A.L., MacDonald, M.E., 1997. Huntingtin is required for neurogenesis and is not impaired by the Huntington's disease CAG expansion. Nat. Genet. 17, 404–410. https://doi.org/10.1038/ng1297-404

Wink, D.A., Vodovotz, Y., Grisham, M.B., DeGraff, W., Cook, J.C., Pacelli, R., Krishna, M., Mitchell, J.B., 1999. Antioxidant effects of nitric oxide. Methods Enzymol. 301, 413–24.

Wong, Y.C., Holzbaur, E.L.F., 2014. The Regulation of Autophagosome Dynamics by Huntingtin and HAP1 Is Disrupted by Expression of Mutant Huntingtin, Leading to Defective Cargo Degradation. J. Neurosci. 34, 1293–1305. https://doi.org/10.1523/JNEUROSCI.1870-13.2014

Woodman, B., Butler, R., Landles, C., Lupton, M.K., Tse, J., Hockly, E., Moffitt, H., Sathasivam, K., Bates, G.P., 2007. The HdhQ150/Q150 knock-in mouse model of HD and the R6/2 exon 1 model develop comparable and widespread molecular phenotypes. Brain Res. Bull. 72, 83–97. https://doi.org/10.1016/j.brainresbull.2006.11.004

Wright, G.E.B., Collins, J.A., Kay, C., McDonald, C., Dolzhenko, E., Xia, Q., Bečanović, K., Drögemöller, B.I., Semaka, A., Nguyen, C.M., Trost, B., Richards, F., Bijlsma, E.K., Squitieri, F., Ross, C.J.D., Scherer, S.W., Eberle, M.A., Yuen, R.K.C., Hayden, M.R., 2019. Length of Uninterrupted CAG, Independent of Polyglutamine Size, Results in Increased Somatic Instability, Hastening Onset of Huntington Disease. Am. J. Hum. Genet. 104, 1116–1126. https://doi.org/10.1016/j.ajhg.2019.04.007

Wyss-Coray, T., Rogers, J., 2012. Inflammation in Alzheimer disease-a brief review of the basic science and clinical literature. Cold Spring Harb. Perspect. Med. 2, a006346. https://doi.org/10.1101/cshperspect.a006346

Wyttenbach, A., Sauvageot, O., Carmichael, J., Diaz-Latoud, C., Arrigo, A.-P., Rubinsztein, D.C., 2002. Heat shock protein 27 prevents cellular polyglutamine toxicity and suppresses the increase of reactive oxygen species caused by huntingtin. Hum. Mol. Genet. 11, 1137–1151. https://doi.org/10.1093/hmg/11.9.1137

Xiao, H., Jeang, K.T., 1998. Glutamine-rich domains activate transcription in yeast Saccharomyces cerevisiae. J. Biol. Chem. 273, 22873–6. https://doi.org/10.1074/JBC.273.36.22873

Xu, X., Tay, Y., Sim, B., Yoon, S.-I., Huang, Y., Ooi, J., Utami, K.H., Ziaei, A., Ng, B., Radulescu, C., Low, D., Ng, A.Y.J., Loh, M., Venkatesh, B., Ginhoux, F., Augustine, G.J., Pouladi, M.A., 2017. Reversal of Phenotypic Abnormalities by CRISPR/Cas9-Mediated Gene Correction in Huntington Disease Patient-Derived Induced Pluripotent Stem Cells. Stem cell reports 8, 619–633. https://doi.org/10.1016/j.stemcr.2017.01.022

Yagi, T., Ito, D., Okada, Y., Akamatsu, W., Nihei, Y., Yoshizaki, T., Yamanaka, S., Okano, H., Suzuki, N., 2011. Modeling familial Alzheimer's disease with induced pluripotent stem cells. Hum. Mol. Genet. 20, 4530–4539. https://doi.org/10.1093/hmg/ddr394

Yanagimachi, M.D., Niwa, A., Tanaka, T., Honda-Ozaki, F., Nishimoto, S., Murata, Y., Yasumi, T., Ito, J., Tomida, S., Oshima, K., Asaka, I., Goto, H., Heike, T., Nakahata, T., Saito, M.K., 2013. Robust and Highly-Efficient

Differentiation of Functional Monocytic Cells from Human Pluripotent Stem Cells under Serum- and Feeder Cell-Free Conditions. PLoS One 8, 1–9. https://doi.org/10.1371/journal.pone.0059243
Yanai, A., Huang, K., Kang, R., Singaraja, R.R., Arstikaitis, P., Gan, L., Orban, P.C., Mullard, A., Cowan, C.M., Raymond, L.A., Drisdel, R.C., Green, W.N., Ravikumar, B., Rubinsztein, D.C., El-Husseini, A., Hayden, M.R., 2006. Palmitoylation of huntingtin by HIP14 is essential for its trafficking and function. Nat. Neurosci. 9, 824–31. https://doi.org/10.1038/nn1702
Yang, J., Zhang, L., Yu, C., Yang, X.-F., Wang, H., 2014. Monocyte and macrophage differentiation: circulation inflammatory monocyte as biomarker for inflammatory diseases. Biomark. Res. 2, 1. https://doi.org/10.1186/2050-7771-2-1
Yang, X.W., Cepeda, C., Li, S.-H., André, V.M., Levine, M.S., Li, X.-J., Gu, X., 2007. Pathological cell-cell interactions are necessary for striatal pathogenesis in a conditional mouse model of Huntington's disease. Mol. Neurodegener. 2, 8. https://doi.org/10.1186/1750-1326-2-8
Yi Teo, R.T., Hong, X., Yu-Taeger, L., Huang, Y., Tan, L.J., Xie, Y., To, X.V., Guo, L., Rajendran, R., Novati, A., Calaminus, C., Riess, O., Hayden, M.R., Nguyen, H.P., Chuang, K.H., Pouladi, M.A., 2016. Structural and molecular myelination deficits occur prior to neuronal loss in the YAC128 and BACHD models of Huntington disease. Hum. Mol. Genet. 25, 2621–2632. https://doi.org/10.1093/hmg/ddw122
Yoo, A.S., Sun, A.X., Li, L., Shcheglovitov, A., Portmann, T., Li, Y., Lee-Messer, C., Dolmetsch, R.E., Tsien, R.W., Crabtree, G.R., 2011. MicroRNA-mediated conversion of human fibroblasts to neurons. Nature 476, 228–231. https://doi.org/10.1038/nature10323
Yu, J., Vodyanik, M.A., Smuga-Otto, K., Antosiewicz-Bourget, J., Frane, J.L., Tian, S., Nie, J., Jonsdottir, G.A., Ruotti, V., Stewart, R., Slukvin, I.I., Thomson, J.A., 2007. Induced Pluripotent Stem Cell Lines Derived from Human Somatic Cells. Science (80-.). 318, 1917–1920. https://doi.org/10.1126/science.1151526
Zeitlin, S., Liu, J.P., Chapman, D.L., Papaioannou, V.E., Efstratiadis, A., 1995. Increased apoptosis and early embryonic lethality in mice nullizygous for the Huntington's disease gene homologue. Nat. Genet. 11, 155–163. https://doi.org/10.1038/ng1095-155
Zhang, H., Das, S., Li, Q.Z., Dragatsis, I., Repa, J., Zeitlin, S., Hajnóczky, G., Bezprozvanny, I., 2008. Elucidating a normal function of huntingtin by functional and microarray analysis of huntingtin-null mouse embryonic fibroblasts. BMC Neurosci. 9, 38. https://doi.org/10.1186/1471-2202-9-38
Zhang, N., An, M.C., Montoro, D., Ellerby, L.M., 2010. Characterization of Human Huntington's Disease Cell Model from Induced Pluripotent Stem Cells. PLoS Curr. 2, RRN1193. https://doi.org/10.1371/currents.RRN1193
Zhang, S., Sakuma, M., Deora, G.S., Levy, C.W., Klausing, A., Breda, C., Read, K.D., Edlin, C.D., Ross, B.P., Wright Muelas, M., Day, P.J., O'Hagan, S., Kell, D.B., Schwarcz, R., Leys, D., Heyes, D.J., Giorgini, F., Scrutton, N.S., 2019. A brain-permeable inhibitor of the neurodegenerative disease target kynurenine 3-monooxygenase prevents accumulation of neurotoxic metabolites. Commun. Biol. 2, 271. https://doi.org/10.1038/s42003-019-0520-5
Zhang, Wei, Wang, T., Pei, Z., Miller, D.S., Wu, X., Block, M.L., Wilson, B., Zhang, Wanqin, Zhou, Y., Hong, J.-S., Zhang, J., 2005. Aggregated α-

synuclein activates microglia: a process leading to disease progression in Parkinson's disease. FASEB J. 19, 533–542. https://doi.org/10.1096/fj.04-2751com
Zhang, X.-H., Tee, L.Y., Wang, X.-G., Huang, Q.-S., Yang, S.-H., 2015. Off-target Effects in CRISPR/Cas9-mediated Genome Engineering. Mol. Ther. - Nucleic Acids 4, e264. https://doi.org/10.1038/MTNA.2015.37
Zhang, Y., Engelman, J., Friedlander, R.M., 2009. Allele-specific silencing of mutant Huntington's disease gene. J. Neurochem. 108, 82–90. https://doi.org/10.1111/j.1471-4159.2008.05734.x
Zhang, Y., Li, M., Drozda, M., Chen, M., Ren, S., Mejia Sanchez, R.O., Leavitt, B.R., Cattaneo, E., Ferrante, R.J., Hayden, M.R., Friedlander, R.M., Sanchez, R.O.M., Leavitt, B.R., Cattaneo, E., Ferrante, R.J., Hayden, M.R., Friedlander, R.M., 2003. Depletion of wild-type huntingtin in mouse models of neurologic diseases. J. Neurochem. 87, 101–106. https://doi.org/10.1046/j.1471-4159.2003.01980.x
Ziegler-Heitbrock, L., 2007. The CD14+ CD16+ blood monocytes: their role in infection and inflammation. J. Leukoc. Biol. 81, 584–92. https://doi.org/10.1189/jlb.0806510
Zuccato, C., Cattaneo, E., 2007. Role of brain-derived neurotrophic factor in Huntington's disease. Prog. Neurobiol. https://doi.org/10.1016/j.pneurobio.2007.01.003
Zuccato, C., Ciammola, A., Rigamonti, D., Leavitt, B.R., Goffredo, D., Conti, L., MacDonald, M.E., Timmusk, T., Sipione, S., Cattaneo, E., 2001. Loss of Huntingtin-Mediated BDNF Gene Transcription in Huntington ' s Disease 293, 493–498. https://doi.org/10.1126/science.1059581
Zuccato, C., Tartari, M., Crotti, A., Goffredo, D., Valenza, M., Conti, L., Cataudella, T., Leavitt, B.R., Hayden, M.R., Timmusk, T., Rigamonti, D., Cattaneo, E., 2003. Huntingtin interacts with REST/NRSF to modulate the transcription of NRSE-controlled neuronal genes. Nat. Genet. 35, 76–83. https://doi.org/10.1038/ng1219
Zwilling, D., Huang, S.Y., Sathyasaikumar, K. V., Notarangelo, F.M., Guidetti, P., Wu, H.Q., Lee, J., Truong, J., Andrews-Zwilling, Y., Hsieh, E.W., Louie, J.Y., Wu, T., Scearce-Levie, K., Patrick, C., Adame, A., Giorgini, F., Moussaoui, S., Laue, G., Rassoulpour, A., Flik, G., Huang, Y., Muchowski, J.M., Masliah, E., Schwarcz, R., Muchowski, P.J., 2011. Kynurenine 3-monooxygenase inhibition in blood ameliorates neurodegeneration. Cell 145, 863–874. https://doi.org/10.1016/j.cell.2011.05.020